Saas Fee 39

Magnetic Fields in the Atmospheres of the Sun and Stars

Sami K. Solanki

Max Planck Institute for Solar System Research

Before starting...

Concentrate on observations: only few equations
Will use cgs units

Many people have contributed tremendously with material, advice etc. Without their help this lecture would never have been possible. Only some are named here:

Svetlana Berdyugina, Juan-Manuel Borrero, Paul Charbonneau, Stefan Dreizler, Mark Giampapa, Andreas Lagg, John Landstreet, Theresa Luftinger, Coralie Neiner, Hardi Peter, Ansgar Reiners, Manfred Schüssler, Greg Wade

Thank you!

Table of contents

Introduction

The Sun in White Light

Gas at 5800 K

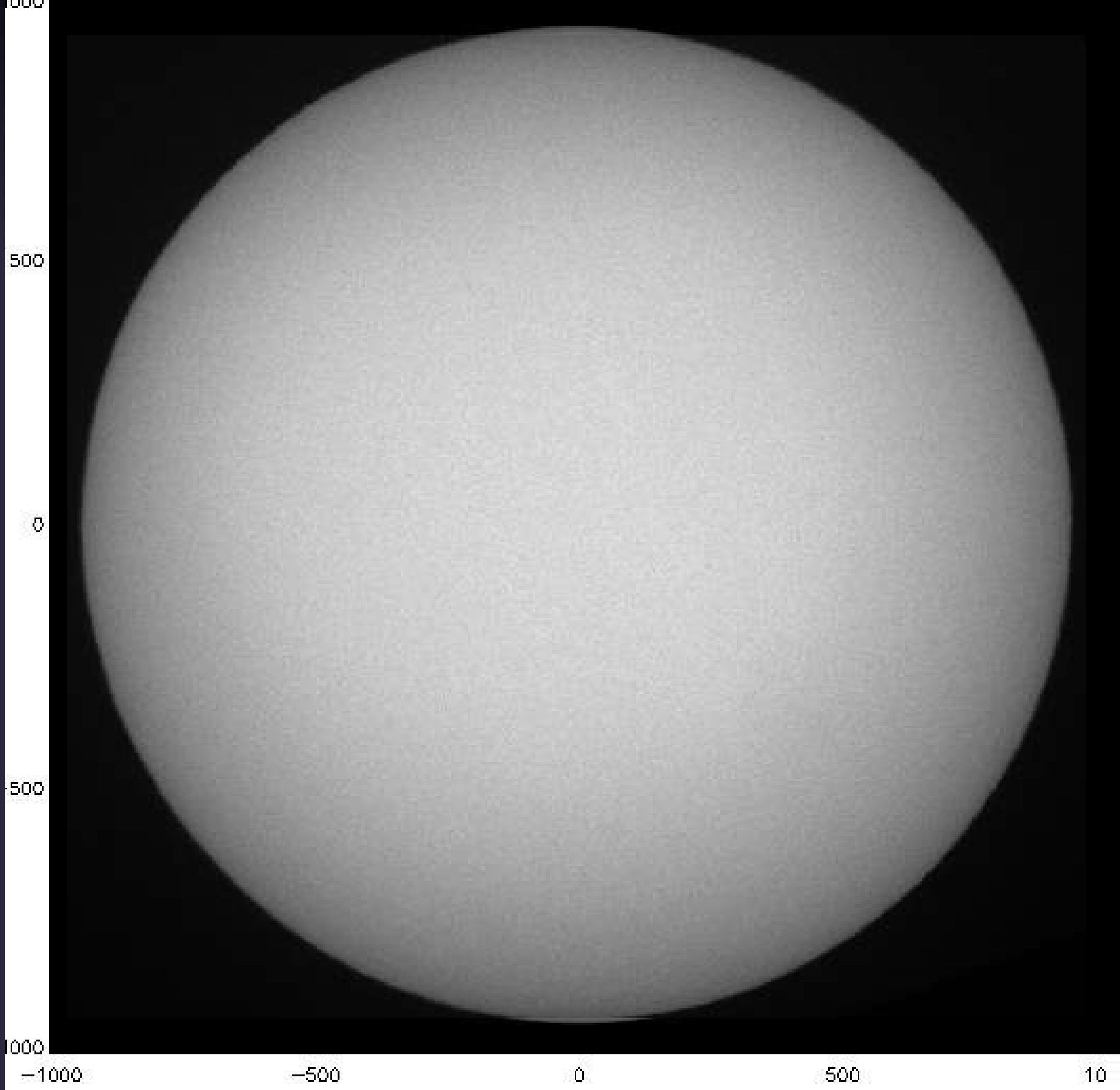

The Dynamic Sun

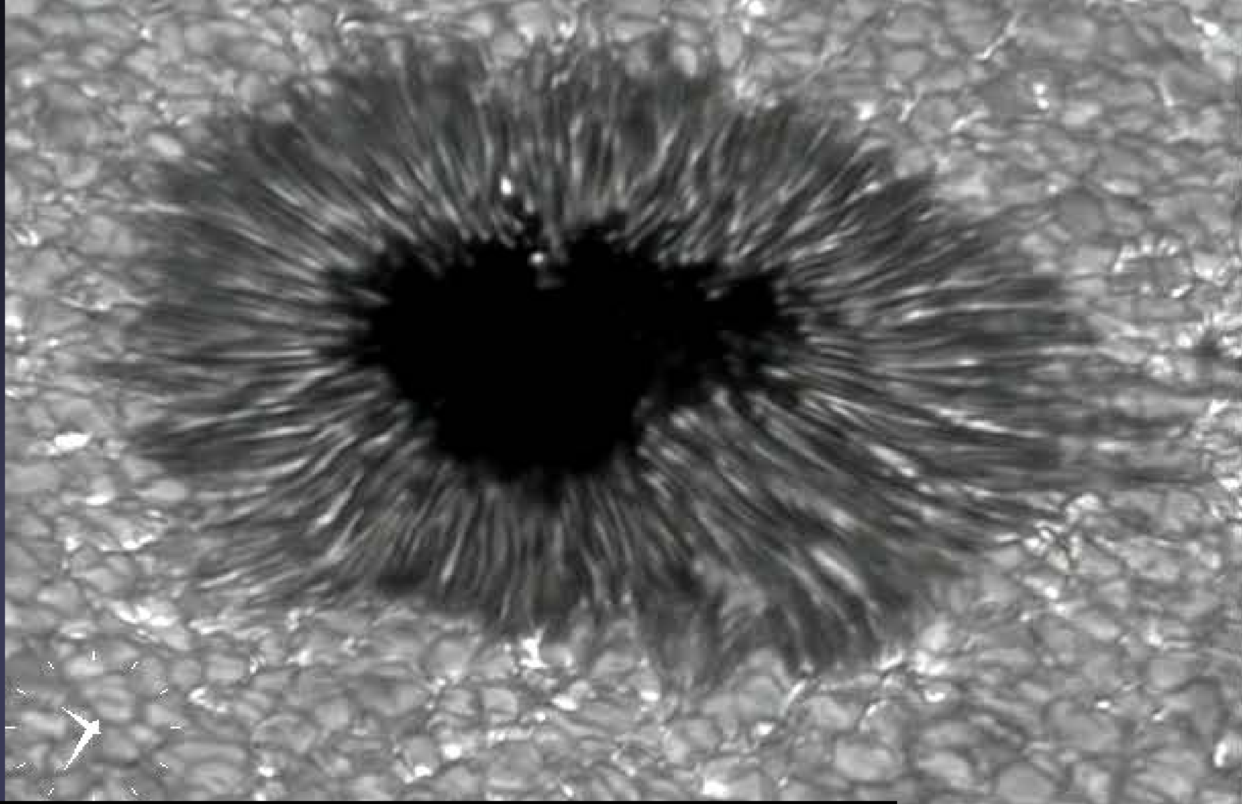

Prominence

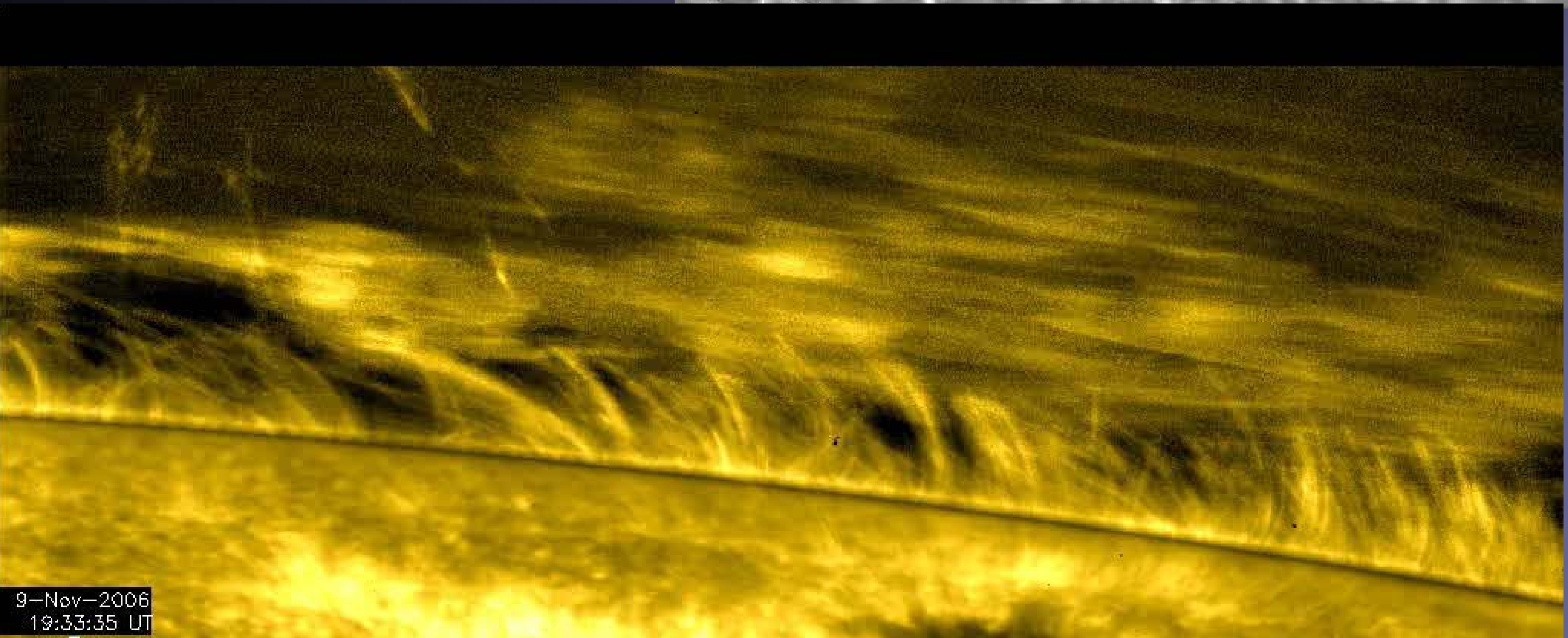

Sunspot

The Violent Sun

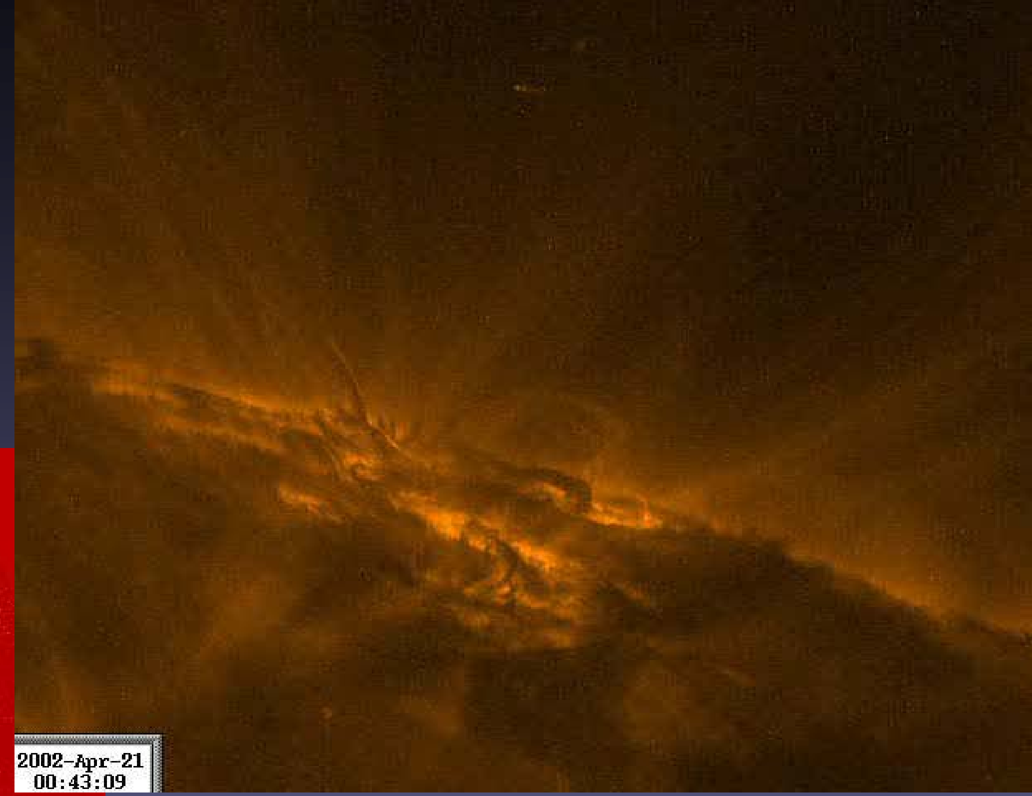

Flare

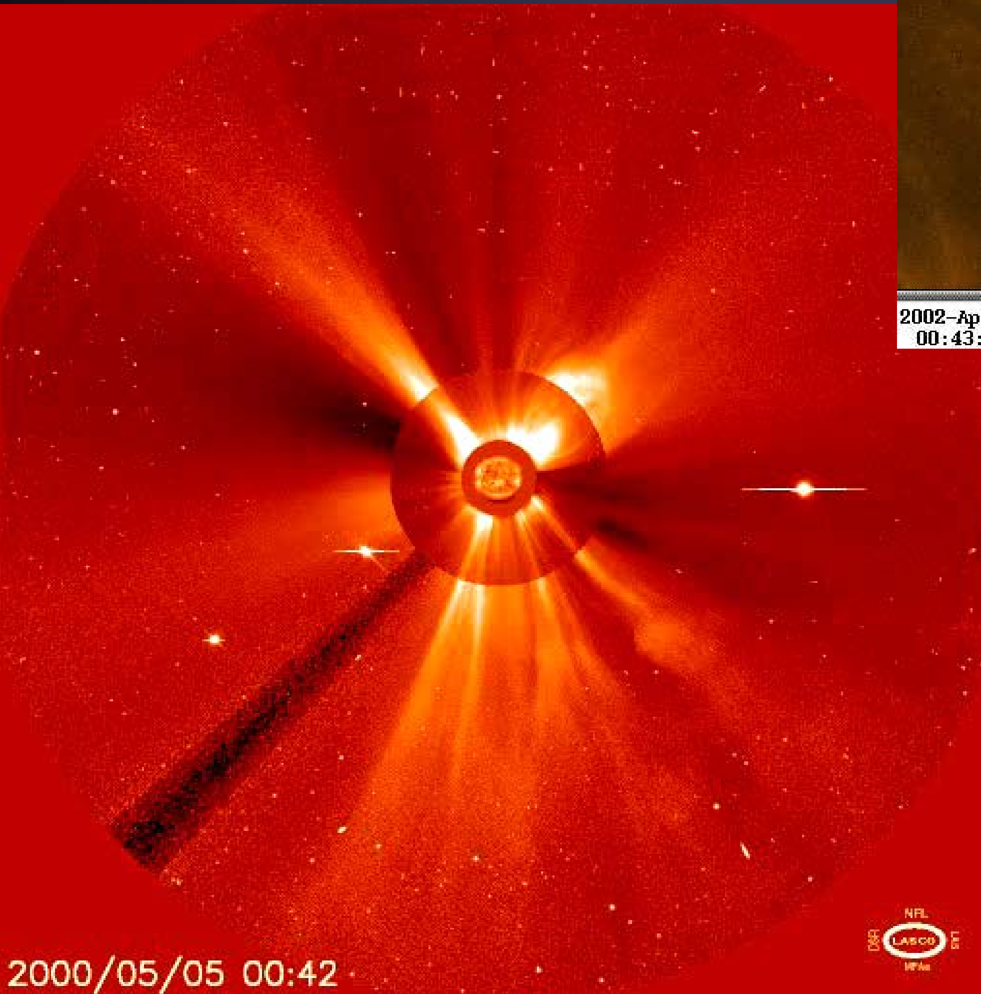

Solar wind
and coronal
mass ejections

The source of the Sun's activity is the magnetic field

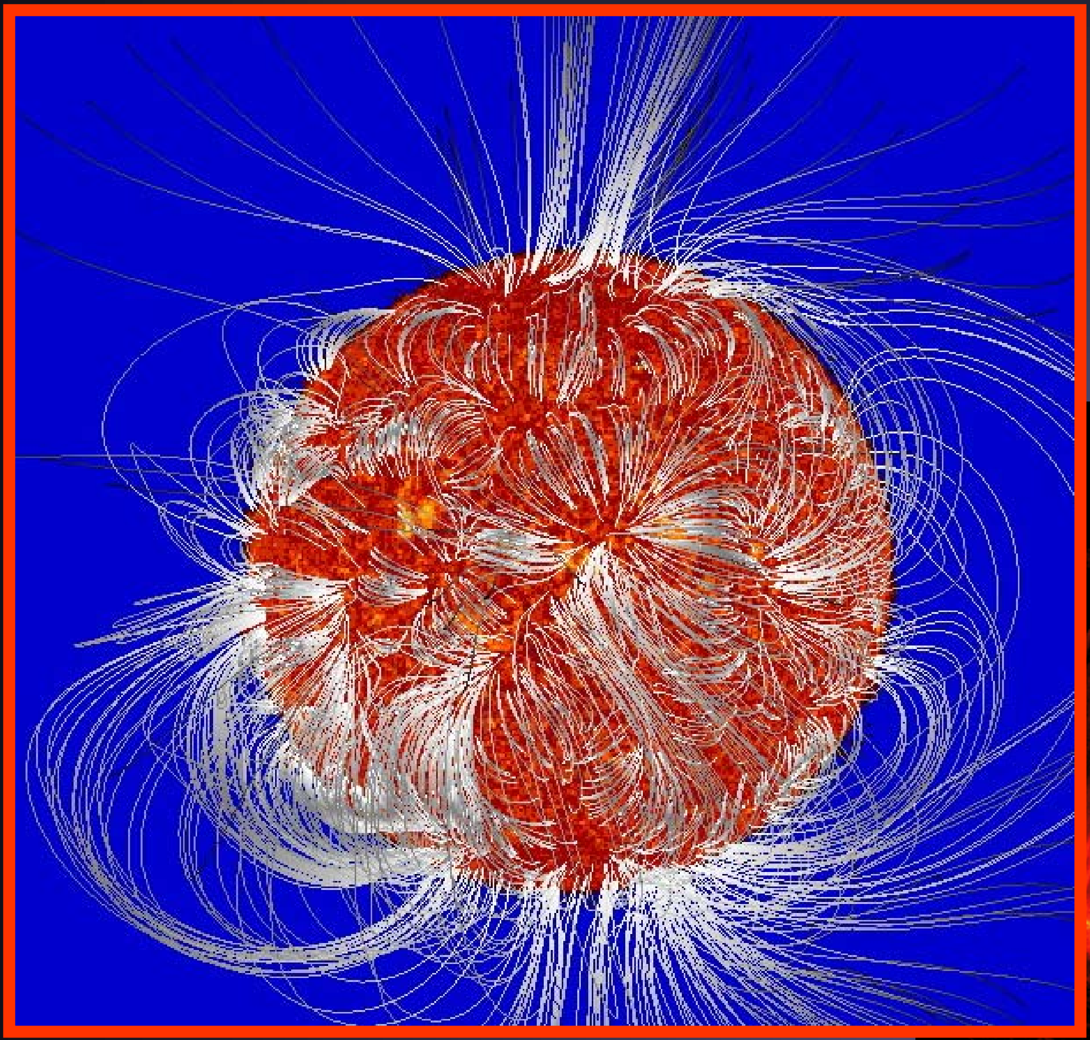

Wiegelmann 2004

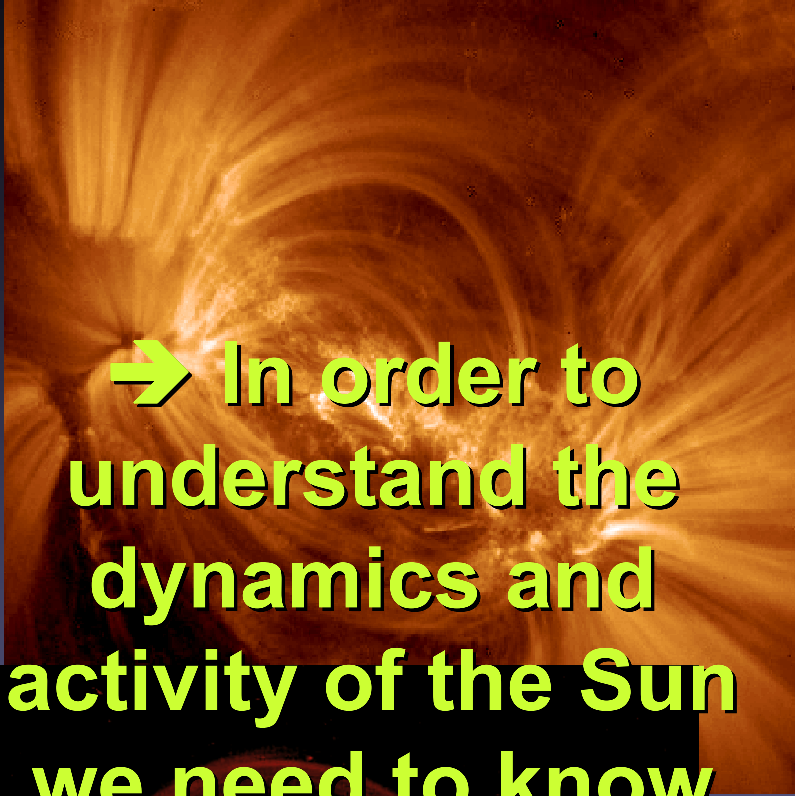

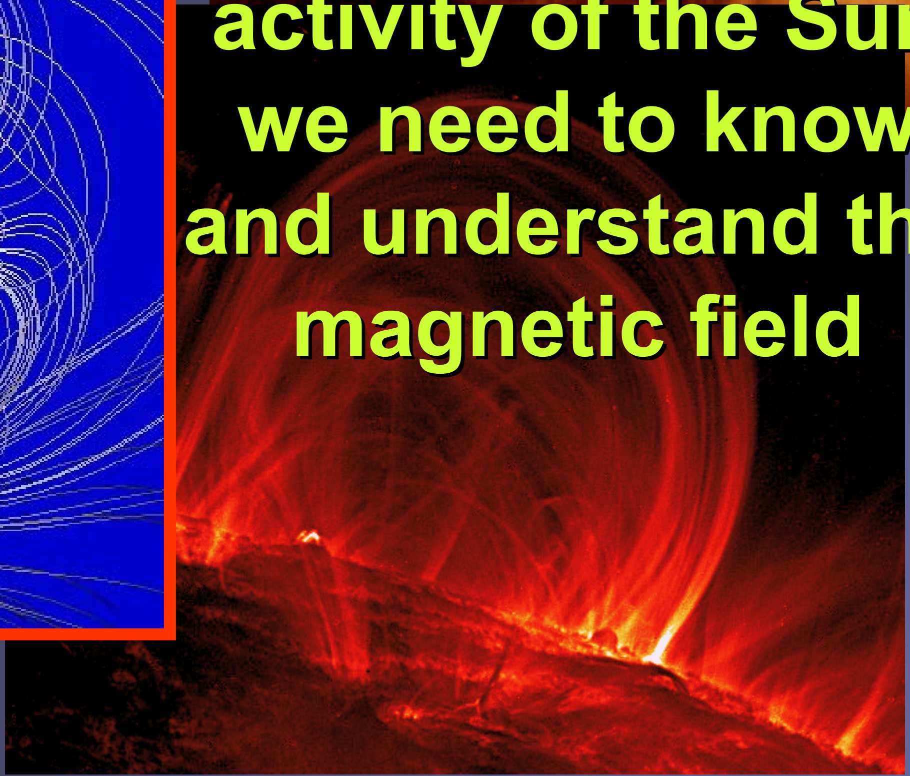

➔ **In order to understand the dynamics and activity of the Sun we need to know and understand the magnetic field**

Stellar magnetic fields

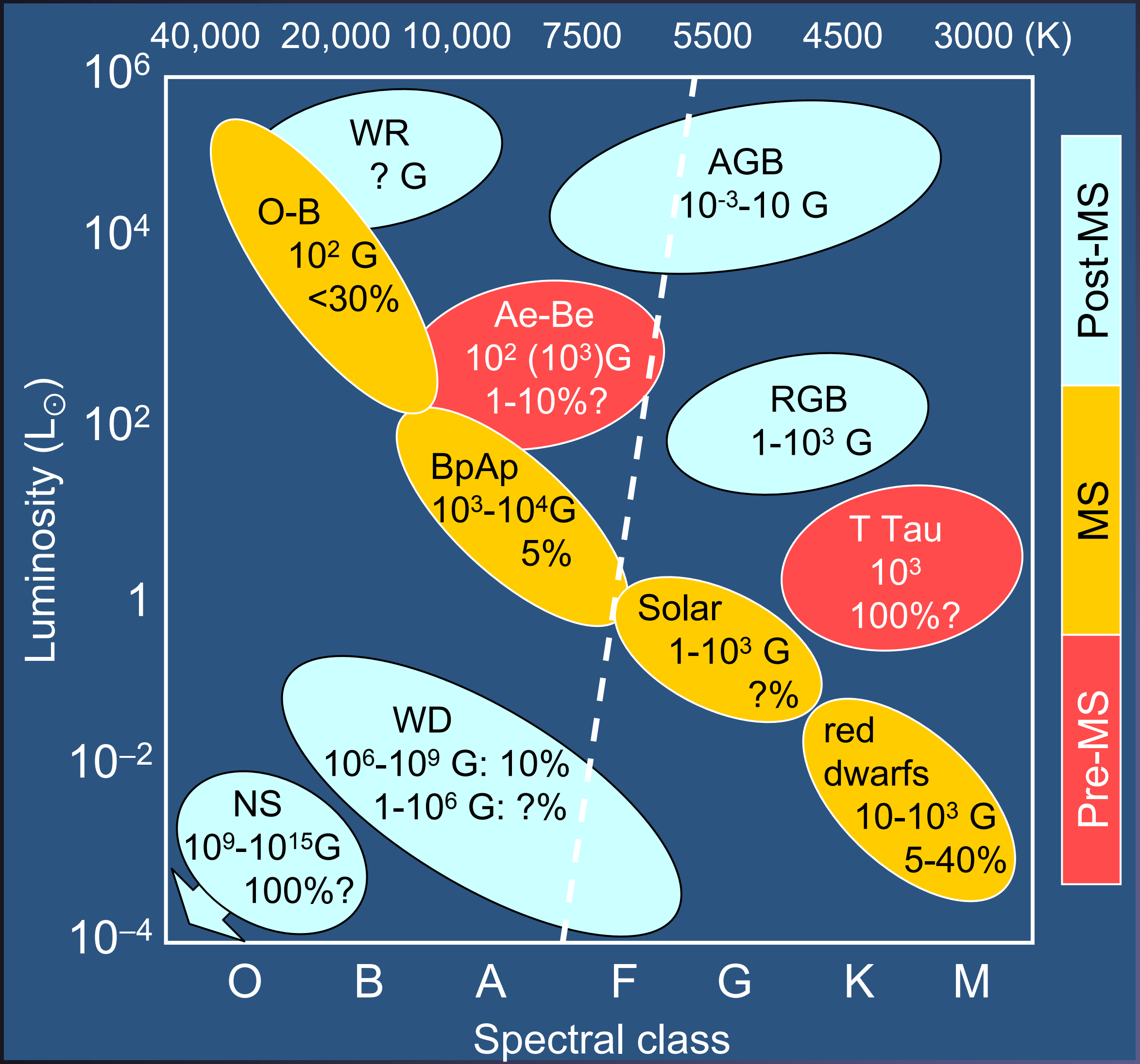

Magnetic fields are found on stars throughout the HR-diagram

Often they produce activity on the star or influence its evolution (e.g. of stellar rotation)

Berdyugina 2008

Basics of polarimetry and the measurement of solar magnetic fields

Methods of solar magnetic field measurement

- Direct methods:
  - Zeeman effect → polarized radiation
  - Hanle effect → polarized radiation
  - Gyroresonance and Bremsstrahlung → polarized radiation (in radio range)
- Indirect methods: Proxies
  - Bright or dark features in photosphere (sunspots, G-band bright points)
  - Ca II H and K plage
  - Fibrils seen in chromospheric lines, e.g. Hα
  - Coronal loops seen in EUV or X-radiation

Atom in magnetic field

- Consider the Hamiltonian of an atom in a magnetic field (Gaussian cgs units; atom in L-S coupling)

$$H = -\frac{\hbar}{2m}\nabla^2 + V(r) + \xi(r)\mathbf{L}\cdot\mathbf{S} + \left(-\frac{e}{2mc}\mathbf{B}\cdot(\mathbf{L}+2\mathbf{S}) + \frac{e^2}{8mc^2}(Br\sin\theta)^2\right)$$

- First 3 terms are kinetic energy, electronic potential, spin-orbit coupling with $\xi(r) = 1/(2m^2c^2r)(dV/dr)$
- Last two terms are magnetic energy terms derived from magnetic vector potential
- For fields up to B~10 MG (1 kT), magnetic terms are small compared to Coulomb potential. Fine structure and field treated by perturbation theory

Following J. Landstreet

Magnetic field regimes

$$H=-\frac{\hbar}{2m}\nabla^2+V(r)+\xi(r)\mathbf{L}\cdot\mathbf{S}+\left(-\frac{e}{2mc}\mathbf{B}\cdot(\mathbf{L}+2\mathbf{S})+\frac{e^2}{8mc^2}(Br\sin\theta)^2\right)$$

- Perturbation theory regimes:
  - Quadratic magnetic term << linear term << spin-orbit term: (linear) Zeeman effect
  - Quadratic magnetic term << spin-orbit term << linear term: Paschen-Back effect
  - Spin-orbit term << linear term << quadratic magnetic term: quadratic Zeeman effect

For Sun

- Schiff 1955, Quantum Mechanics, Chapts. 23 & 39

Following J. Landstreet

(Linear) Zeeman effect

- In weak-field (Zeeman) limit, atomic energy level is only slightly perturbed by $(e/2mc)\mathbf{B}\cdot(\mathbf{L}+2\,\mathbf{S})$
- In L-S coupling (light atoms), J and M_J are good quantum numbers. Magnetic moment of atom is aligned with $\mathbf{J}$. Energy shift of level is proportional to $\mathbf{B}\cdot\mathbf{J}$, so there are $2J+1$ different magnetic sublevels

$$E_i = E_{i\,0} + g_i\,(e\hbar/2mc)\,B\,M_J = E_{i\,0} + \mu_0\,g_i\,M_J\,B$$

where

$$g_i = 1 + [\,J\,(\,J+1) + S\,(S+1) - L(\,L+1)]/\,[2\,J\,(\,J+1)\,]$$

is the (dimensionless) Landé factor (L-S coupling)

Zeeman splitting of atomic levels & lines

- Transitions between Zeeman split upper and lower atomic levels lead to spectral lines that are split in wavelength
- Transitions are allowed between levels with $\Delta J = 0, \pm 1$ & $\Delta M_J = 0\ (\pi), \pm 1\ (\sigma_b, \sigma_r)$ (for the most common types of transitions: electric dipole radiation)

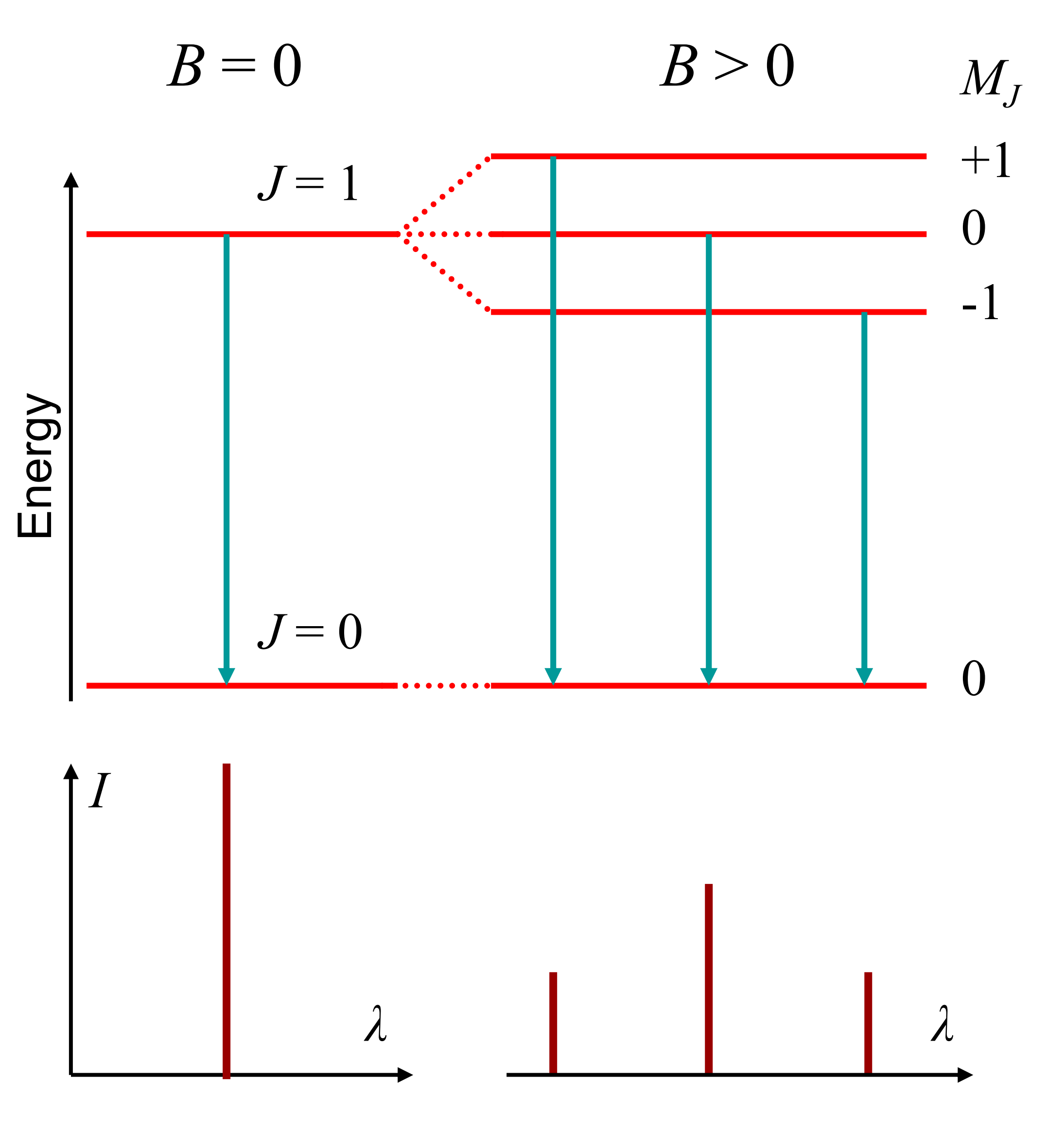

Splitting patterns of lines

G. Mathys

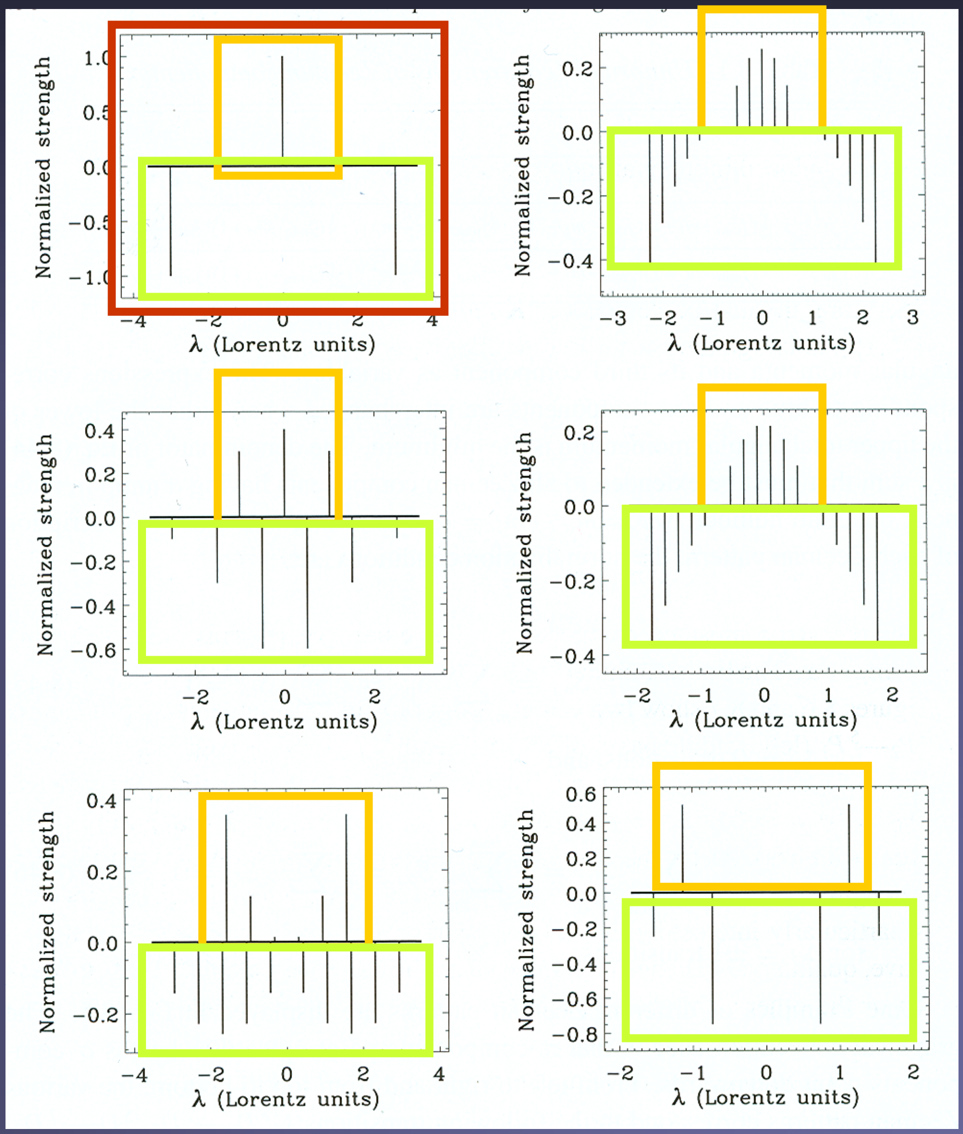

- Depending on g of the upper and lower levels, the spectral line shows different splitting patterns
- Positive: π components: $\Delta M_J = 0$
- Negative: σ components: $\Delta M_J = \pm 1$
- Top left: normal Zeeman effect (rare)
- Rest: anomalous Zeeman effect (usual)

Zeeman effect observed

- First measurement of a cosmic magnetic field, in a sunspot, was carried out 1908 by G.E. Hale
- On Sun: Zeeman effect changes spectral shape of a spectral line (subtle in most lines outside sunspots)
- Zeeman effect also introduces a unique polarisation signature

→ Measurement of polarization is central to measuring solar magnetic fields

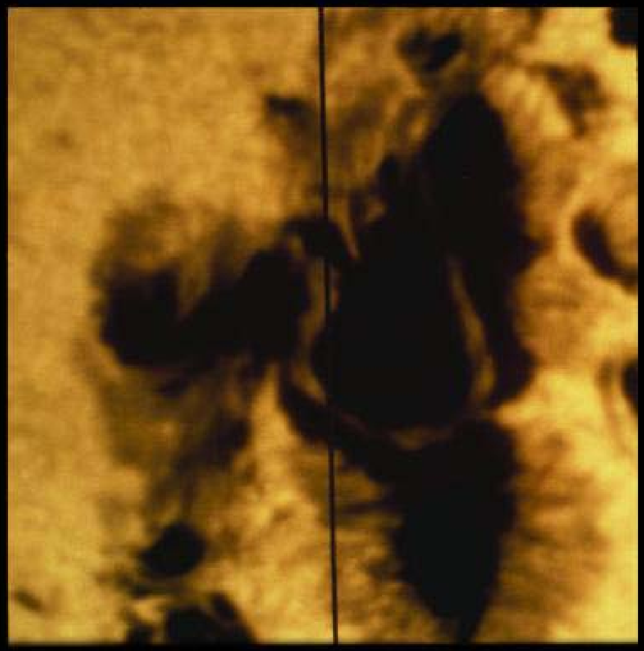

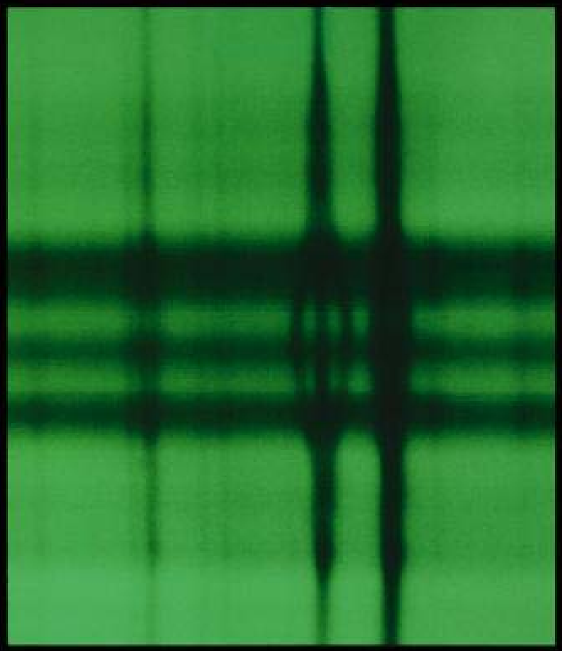

Polarized radiation

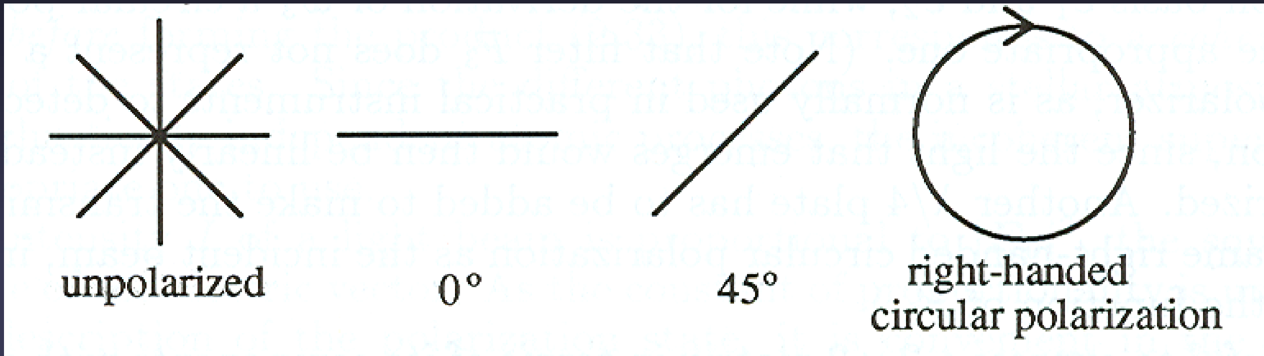

- Polarized radiation is described by the 4 Stokes parameters: *I*, *Q*, *U* and *V*
- I = total intensity $= I_{\rm lin}(0^{\rm o}) + I_{\rm lin}(90^{\rm o}) = I_{\rm lin}(45^{\rm o}) + I_{\rm lin}(135^{\rm o}) = I_{circ}(\text{right}) + I_{\rm circ}(\text{left})$
- $Q = I_{\rm lin}(0^{\rm o})$ - $I_{\rm lin}(90^{\rm o})$
- $U = I_{\rm lin}(45^{\rm o})$ - $I_{\rm lin}(135^{\rm o})$
- $V = I_{\rm circ}(\text{right})$ - $I_{\rm circ}(\text{left})$
- Note: Stokes parameters are sums and differences of intensities, i.e. they are directly measurable

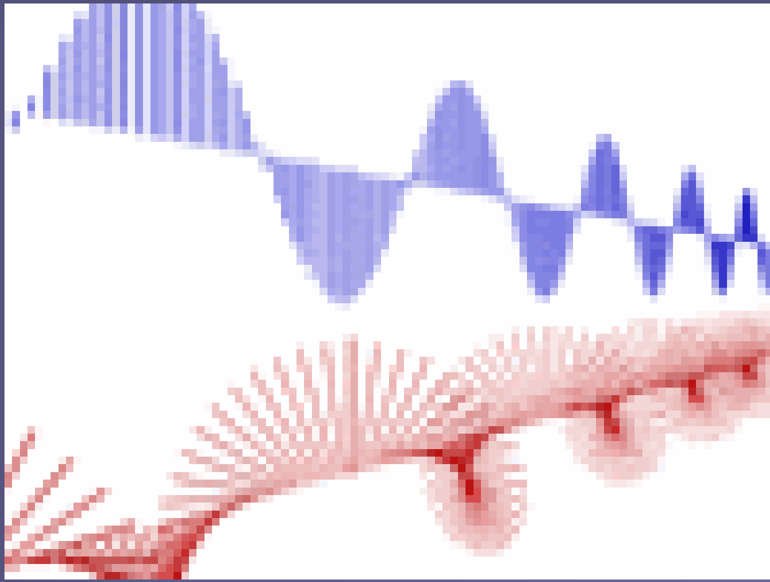

Polarization and Zeeman effect

Longitudinal Zeeman Effect

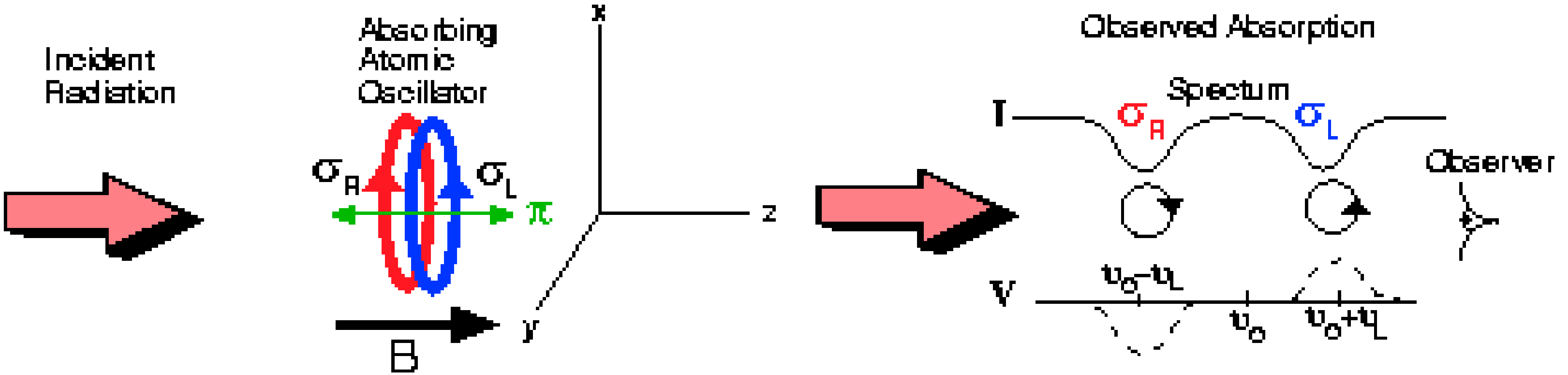

Transverse Zeeman Effect

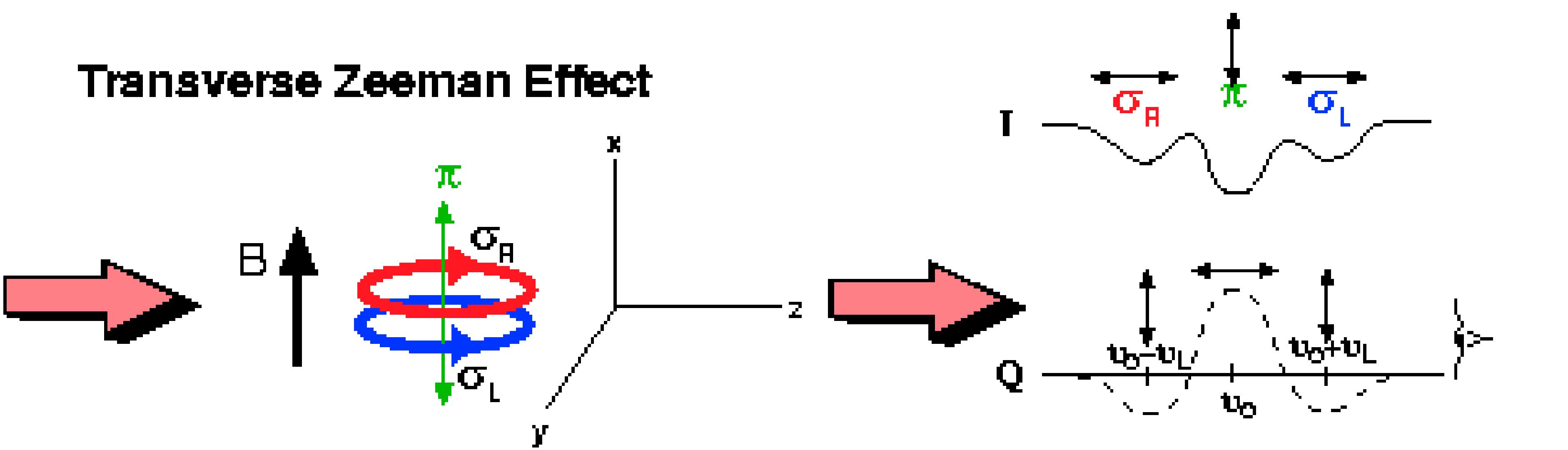

Zeeman effect: information content

- Line splitting
  - Stokes $I \Rightarrow B$
- Line broadening
  - Stokes I : no info on $\mathbf{B}$
- Polarization
  - Stokes $V \Rightarrow \langle B_{\mathrm{long}} \rangle$
  - Stokes $Q, U, V \Rightarrow \mathbf{B}$
- Atomic diagnostics (hot gas)
  - Zeeman effect (except some Ap stars & WDs)
- Molecular diagnostics (cool)
  - Zeeman & Paschen Back

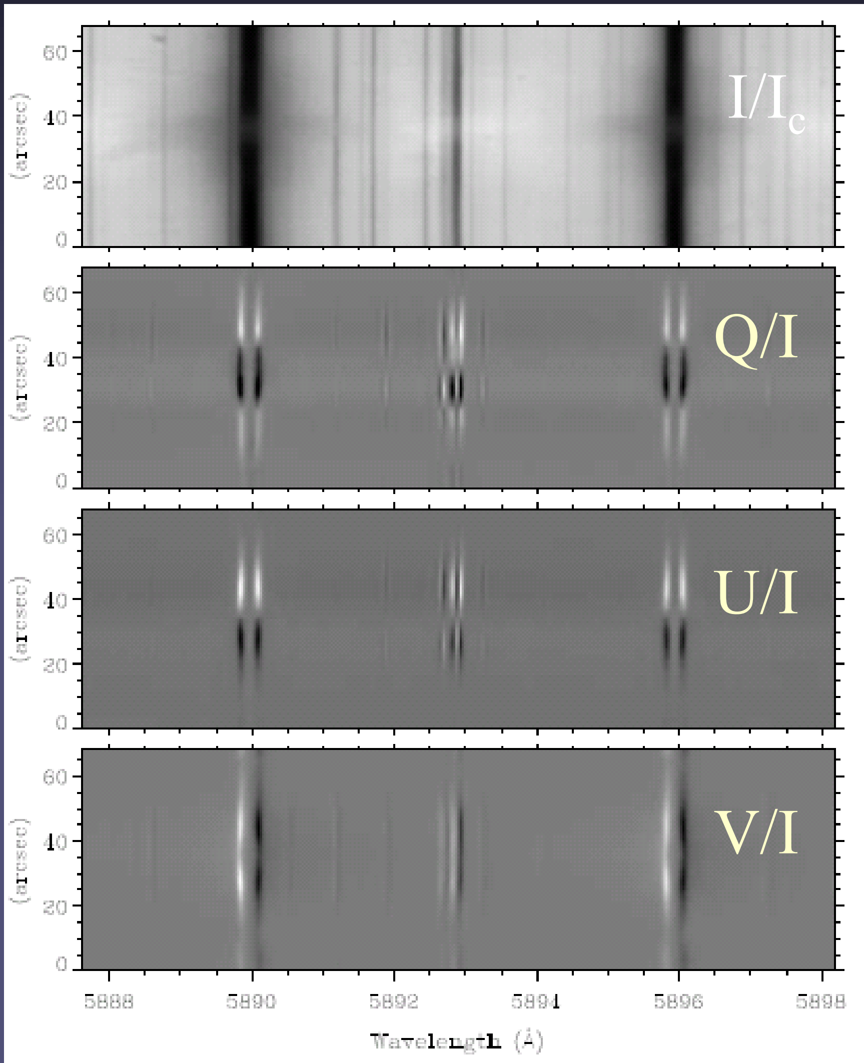

(ZIMPOL, J. Stenflo)

Effect of changing field strength

Formula for Zeeman splitting (for B in G, λ in Å):

$$\Delta\lambda_H = 4.67\ 10^{-13}\ g_{\mathrm{eff}}\, B\, \lambda^2 \quad [\text{Å}]$$

$$g_{\mathrm{eff}} = \frac{1}{2}(g_l + g_u) + \frac{1}{4}(g_l + g_u)(J_l(J_l+1) - J_u(J_u+1))$$

g_{eff} is the effective Landé factor of line

For large $g_{\mathrm{eff}} B\lambda^2$: $\Delta\lambda_H = \Delta\lambda$ betw. σ-component peaks

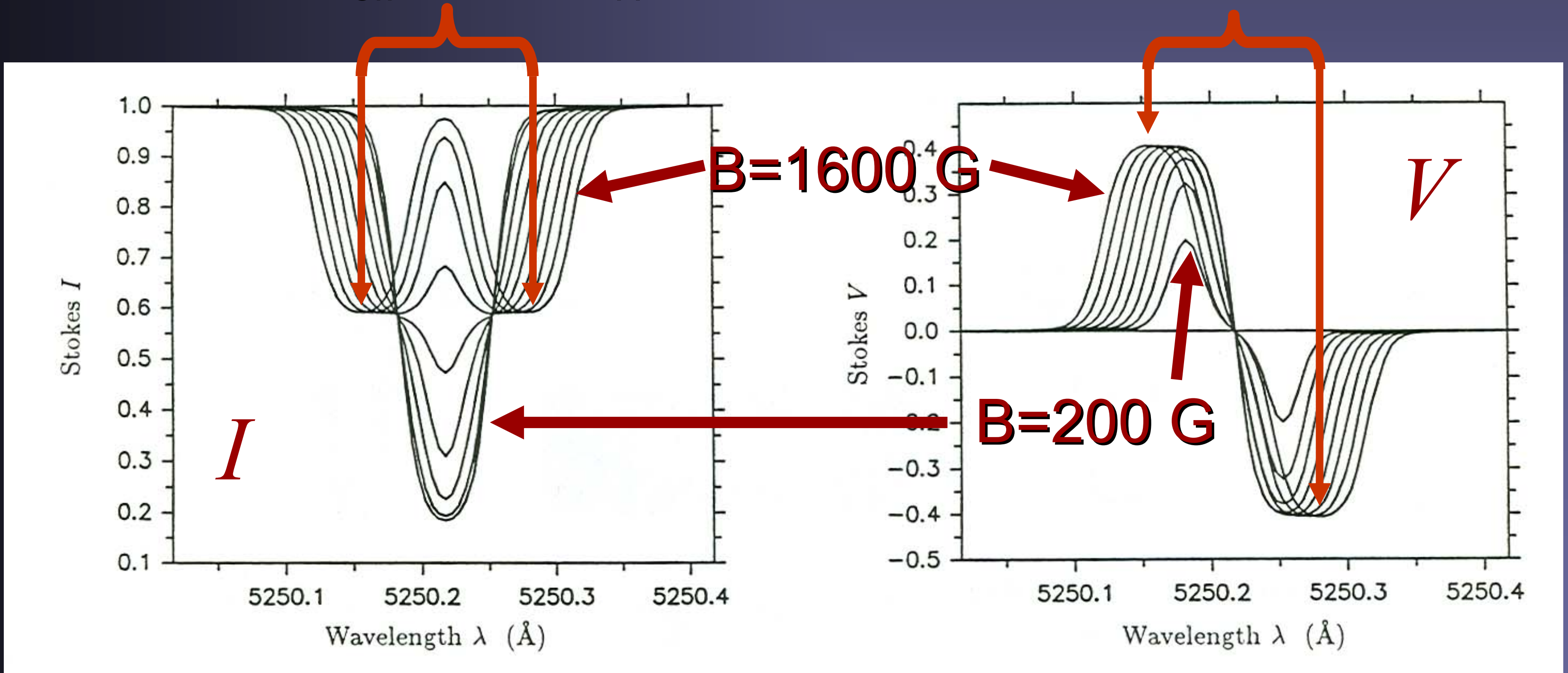

Zeeman splitting ~ λ^2

Fe I 1564.28nm

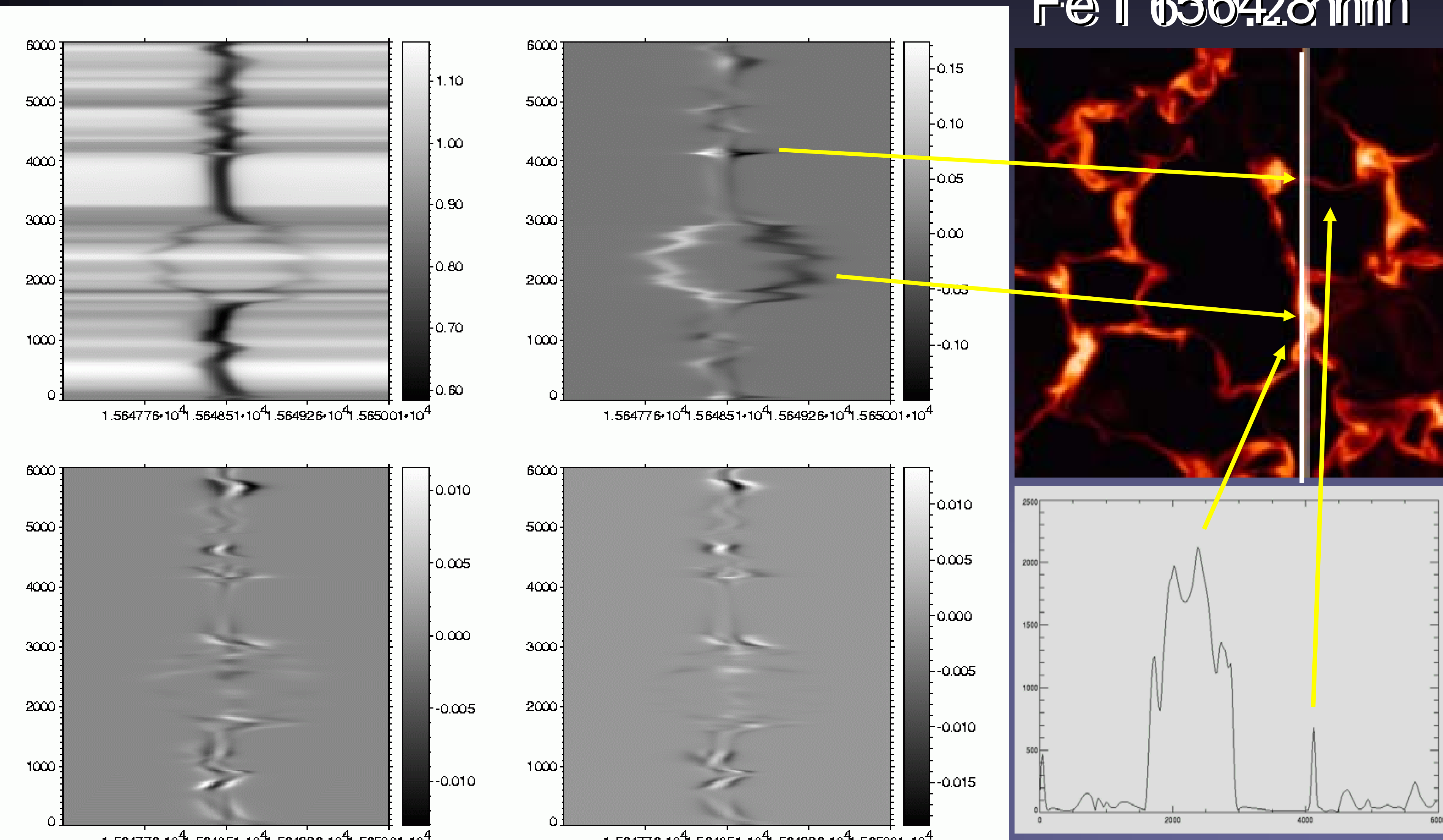

Dependence on B, γ, and φ

- $I \sim \kappa_\sigma(1+\cos^2\gamma)/4 + \kappa_\pi \sin^2\gamma/2$
- $Q \sim B^2 \sin^2\gamma \cos 2\varphi$
- $U \sim B^2 \sin^2\gamma \sin 2\varphi$
- $V \sim B \cos \gamma$

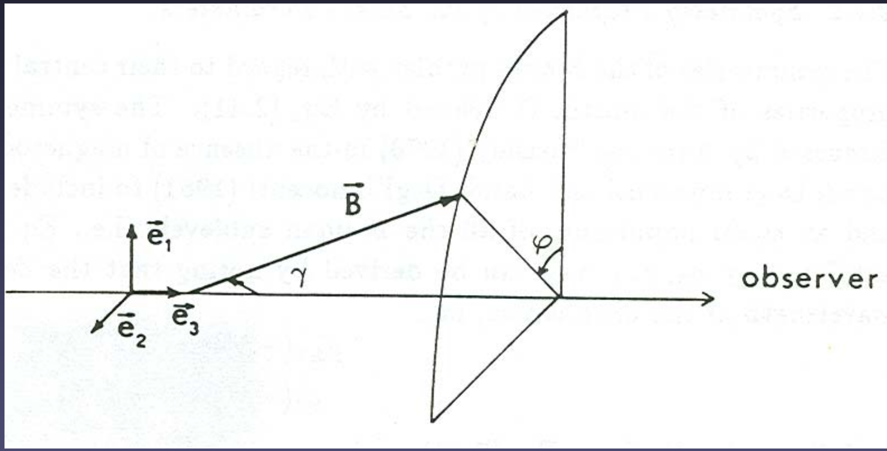

J.M. Borrero

- V: longitudinal component of B
- Q, U: transverse component of B
- Above formulae for Q,U,V refer to relatively weak fields (e.g. B and B^2 dependence of field)
- Zeeman splitting etc. is hidden in κ_σ and κ_π. For Q, U, V these dependences have not been given for simplicity.

Dependence on B, γ, and φ

- $I \sim \kappa_\sigma(1+\cos^2\gamma)/4 + \kappa_\pi \sin^2\gamma/2$
- $Q \sim B^2 \sin^2\gamma \cos 2\varphi$
- $U \sim B^2 \sin^2\gamma \sin 2\varphi$
- $V \sim B \cos\gamma$

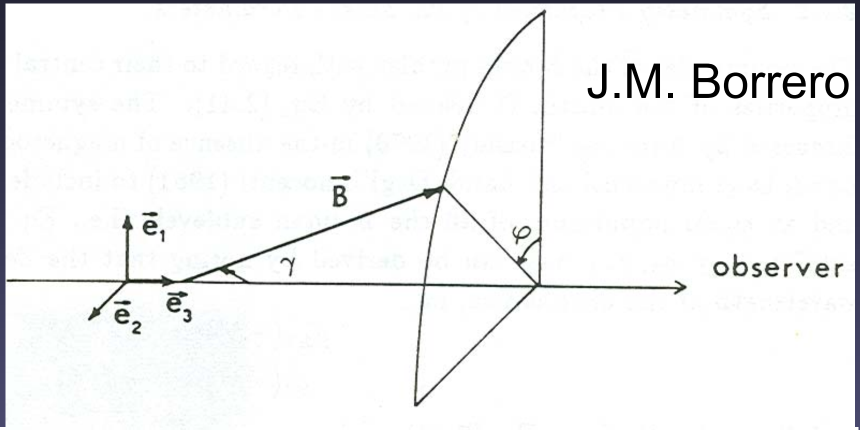

- Q, U: transverse component of B
- V: longitudinal component of B
- Formulae for Q,U,V refer to weak fields
- κ_σ and κ_π (splitting etc.) not given for Q,U,V for simplicity

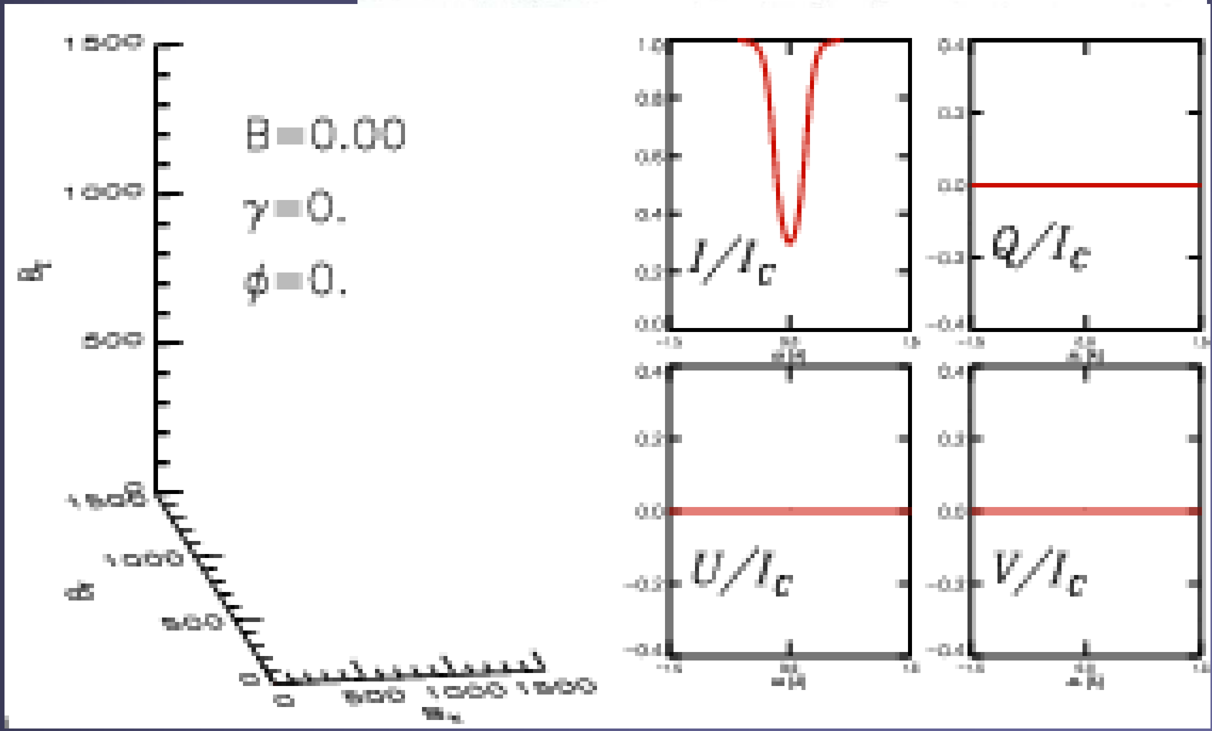

Magnetograms

- Magnetograph: Instrument to make maps of (net circular) polarization in wing of Zeeman sensitive line
- Useful when star can be resolved, e.g. Sun
- Image: Example of magnetogram obtained by MDI
- Conversion of polarization into magnetic field requires a careful calibration.

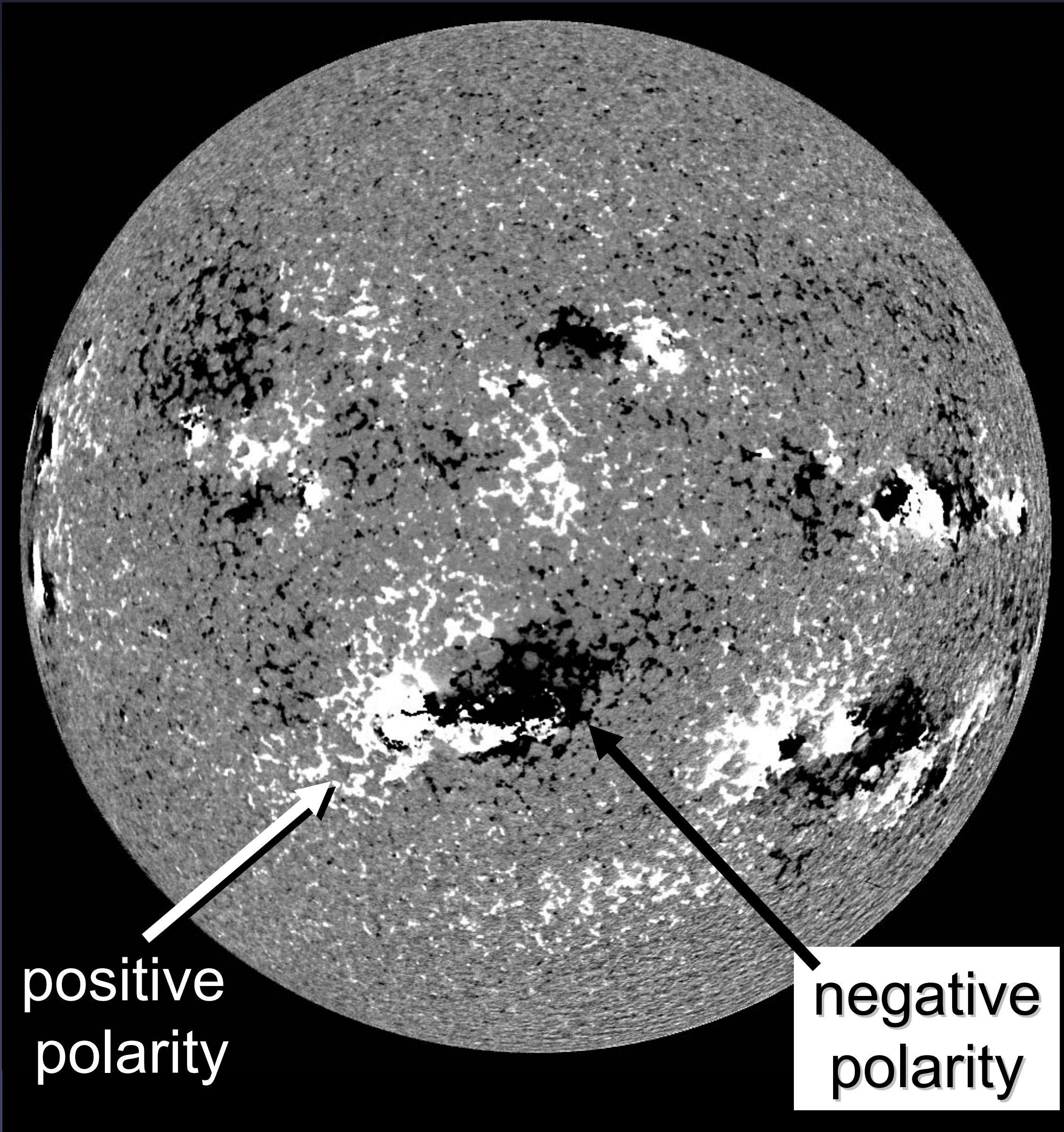

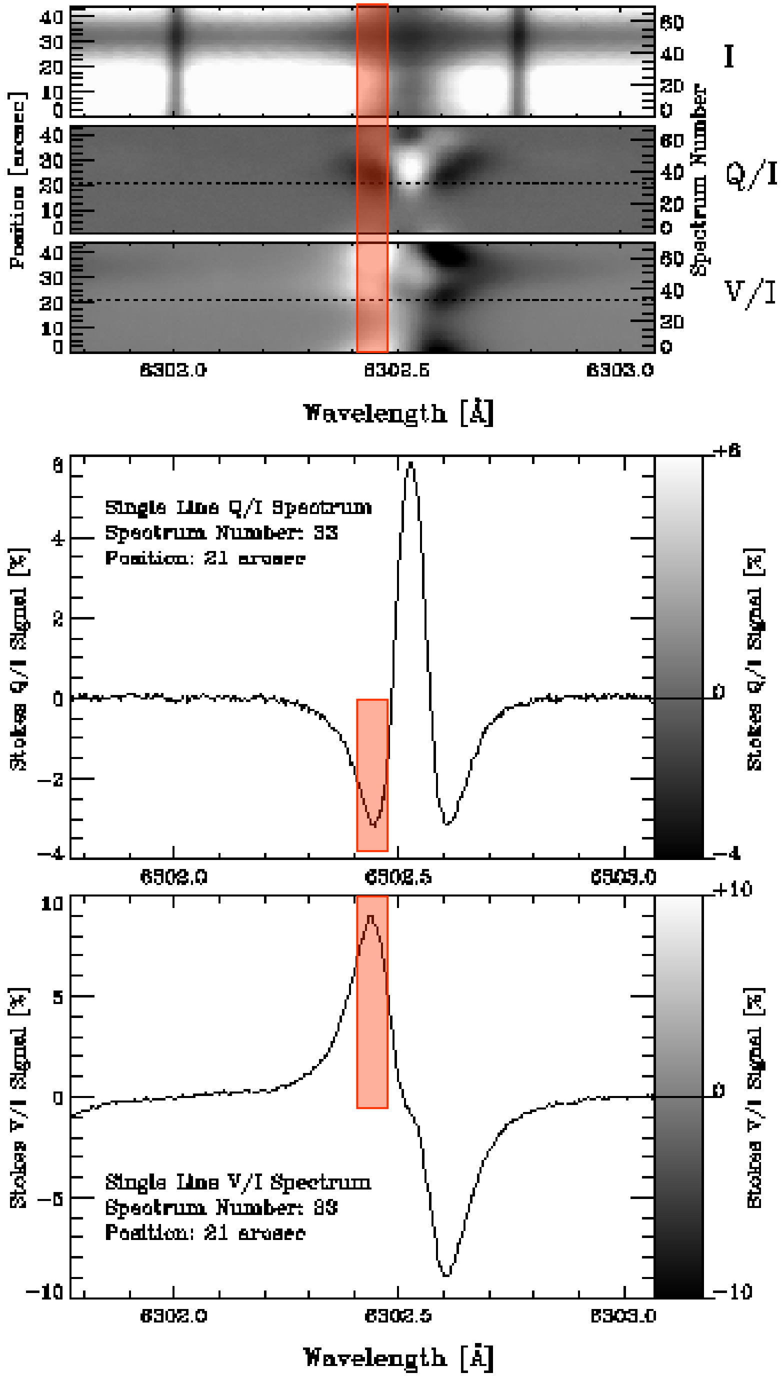

What does a magnetogram show?

- Plotted at left:
  - Top: Stokes I, Q and V along a spectrograph slit
  - Middle: Sample Stokes Q profile
  - Bottom: Sample Stokes V profile
  - Red bars: example of a spectral range used to make a magnetogram. Often only Stokes V is used (simplest to measure), gives longitudinal component of B.

Synoptic charts

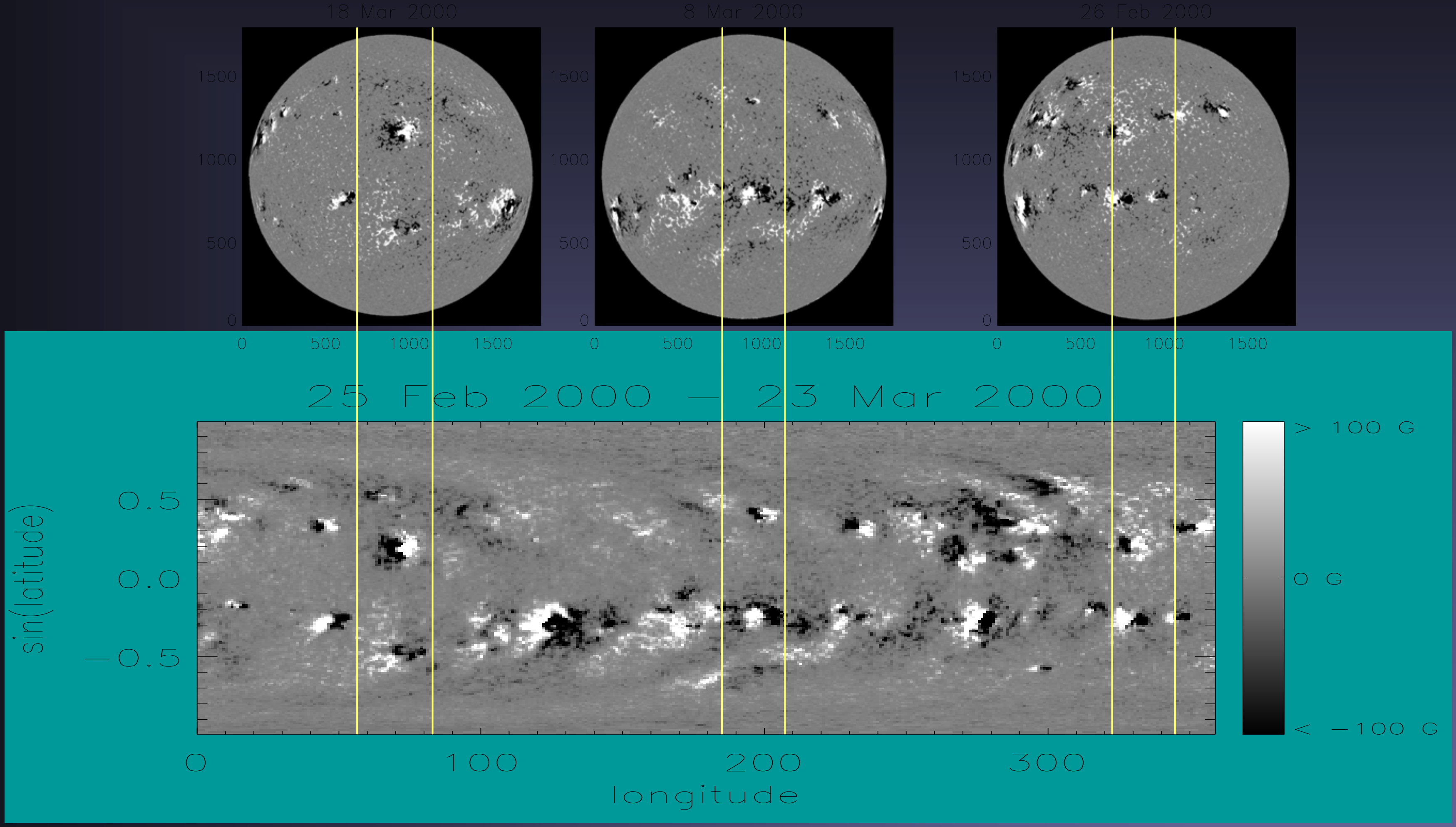

Synoptic maps approximate the radial magnetic flux observed near the central meridian over a period of 27.27 days (= 1 Carrington rotation)

Dependence on B, γ, and φ

- $I \sim \kappa_\sigma(1+\cos^2\gamma)/4 + \kappa_\pi \sin^2\gamma/2$
- $Q \sim B^2 \sin^2\gamma \cos 2\varphi$
- $U \sim B^2 \sin^2\gamma \sin 2\varphi$
- $V \sim B \cos\gamma$

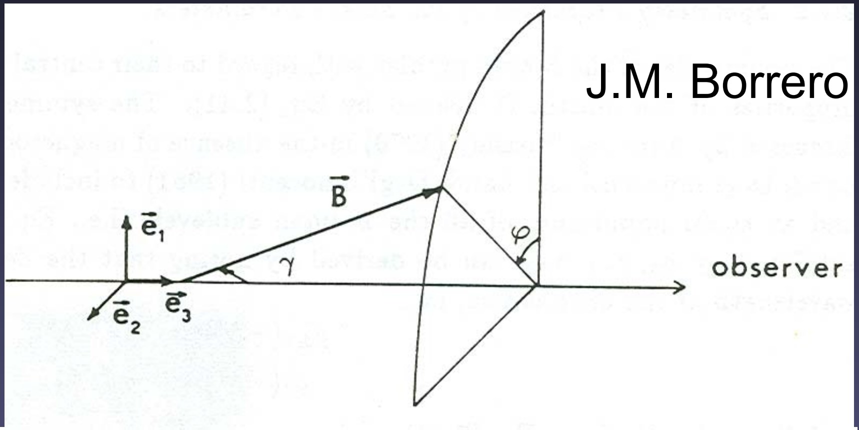

- Q, U: transverse component of B
- V: longitudinal component of B
- Formulae for Q, U, V refer to weak fields
- κ_σ and κ_π (splitting etc.) not given for Q, U, V for simplicity

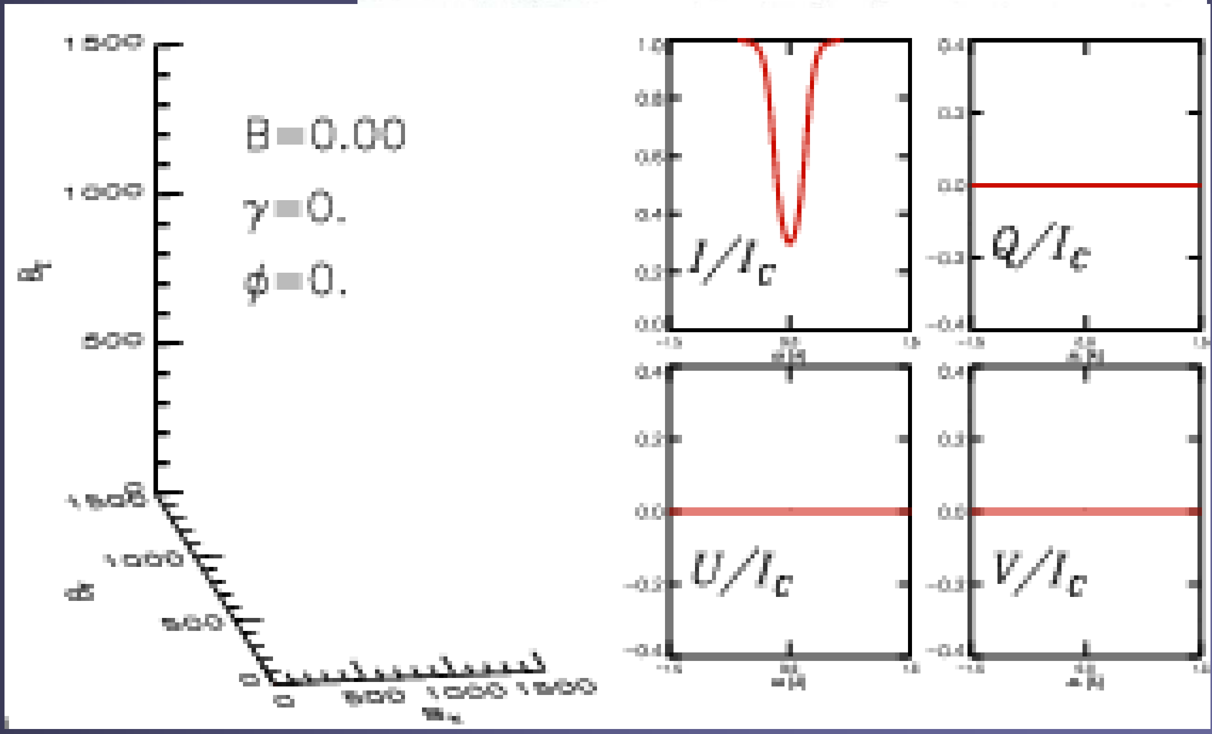

Measured Magnetic Field at Sun's Surface

Month long sequence of magnetograms (approx. one solar rotation)

MDI/SOHO
May 1998

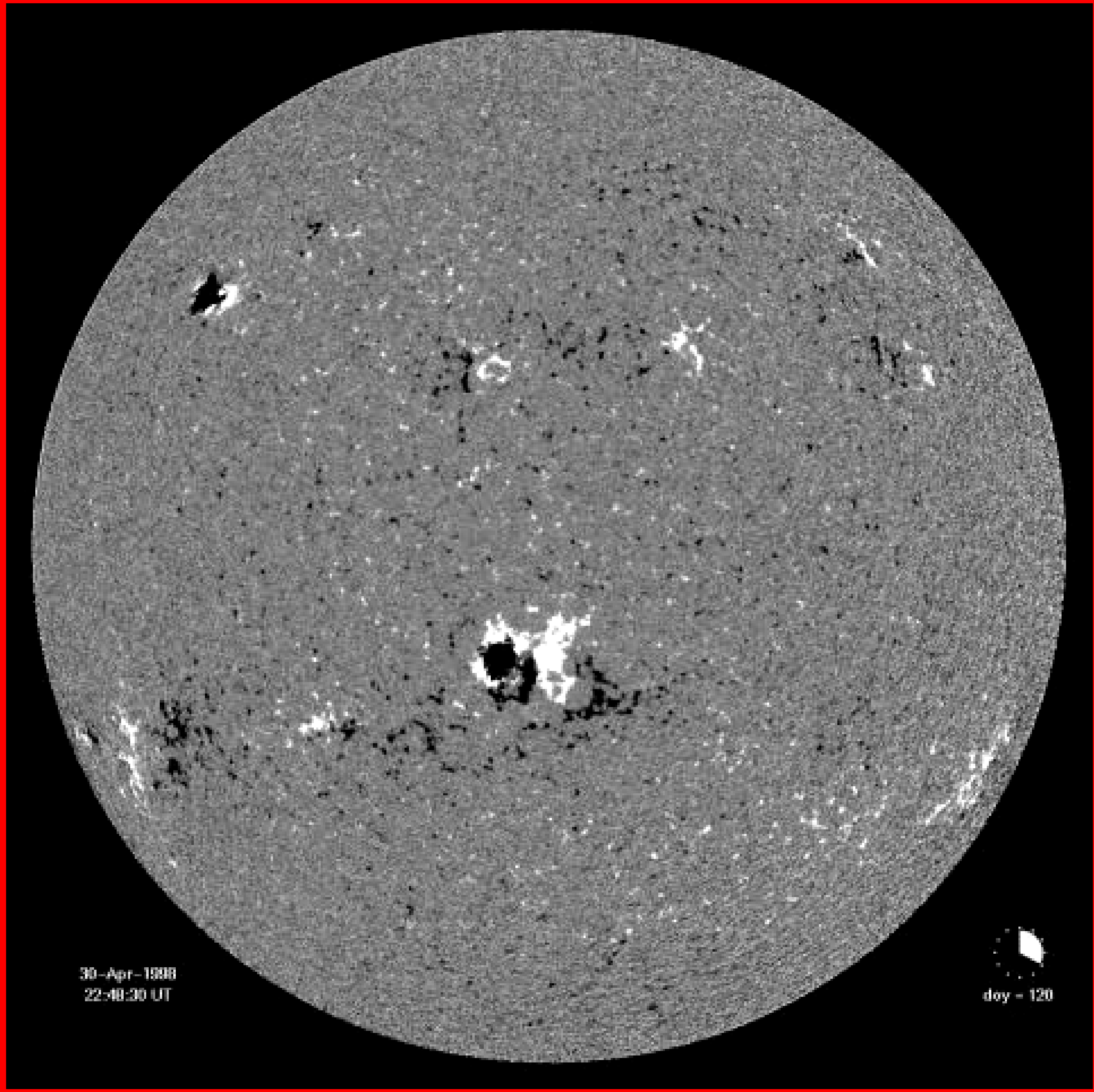

Cancellation of magnetic polarity

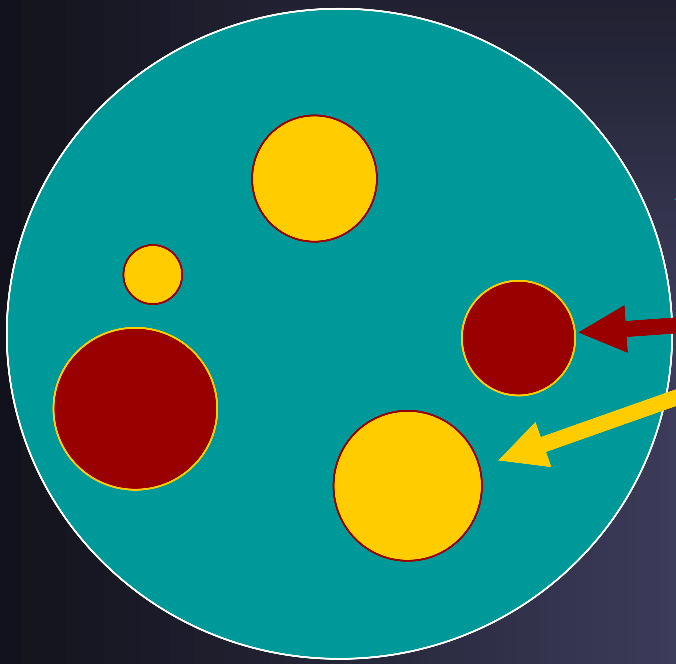

Spatial resolution element

Unresolved magnetic features with field strength B and filling factor

$$f = \sum_i A_i / A_{\mathrm{tot}}$$

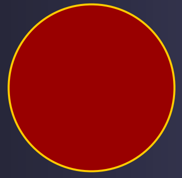

= positive polarity magnetic field

= negative polarity magnetic field

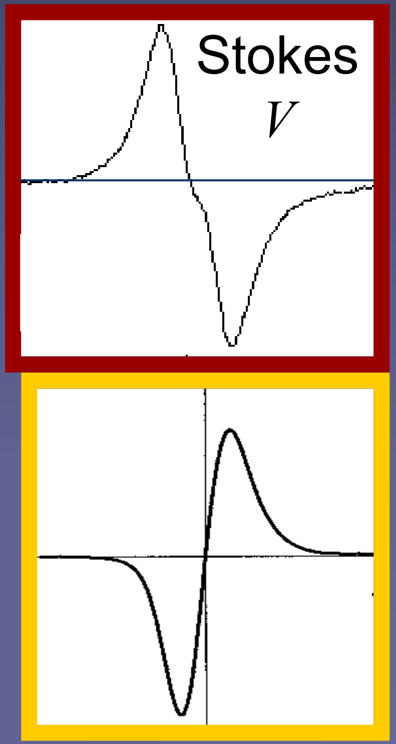

Stokes *V* signal cancellation

Stokes V signal only samples the net magnetic flux.
Extreme case:

negative polarity magnetic flux = positive polarity magnetic flux

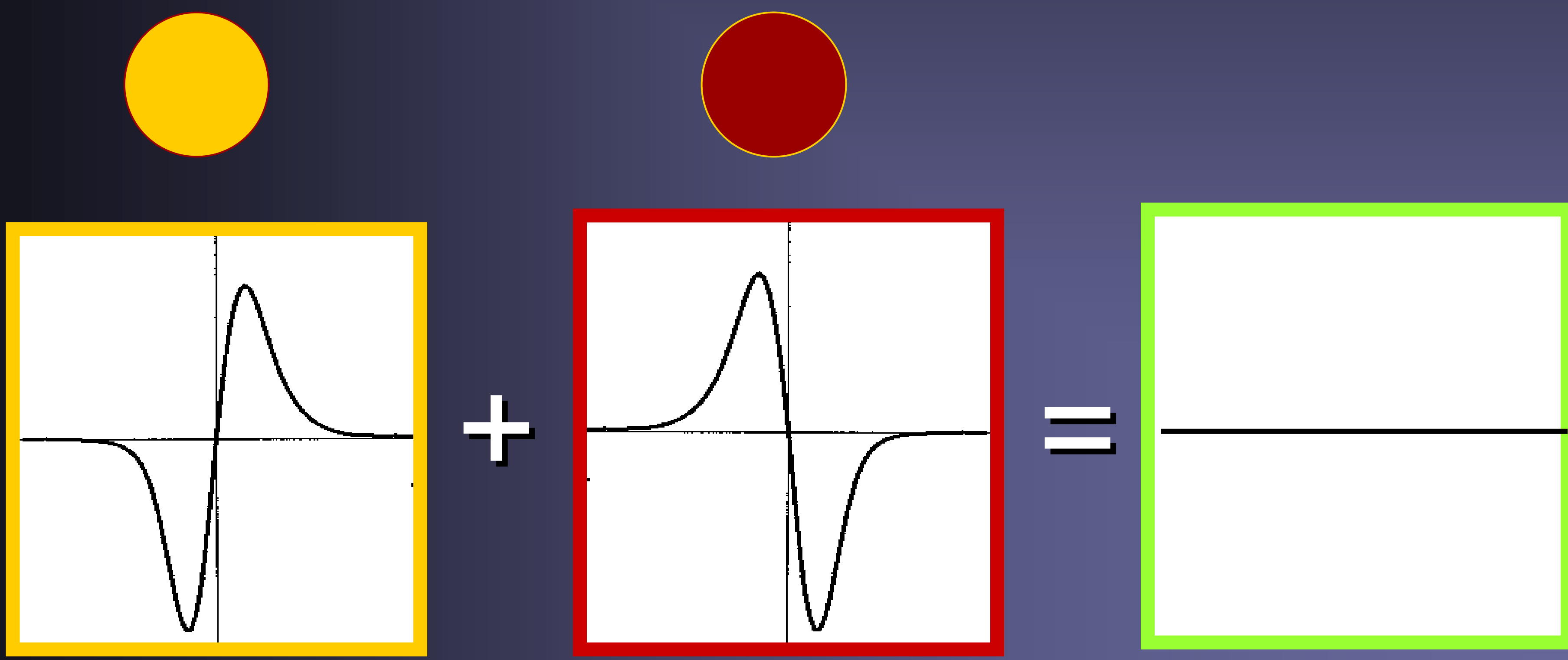

Scattering polarisation at Sun's limb

- If collisions are rare, light is scattered
- Illumination of atoms is anisotropic due to:
  - Limb darkening ($dT/dz < 0$, where T = temp.)
  - atom high in atmosph.
- Scattering + anisotropy ➔ linear polarisation parallel to limb

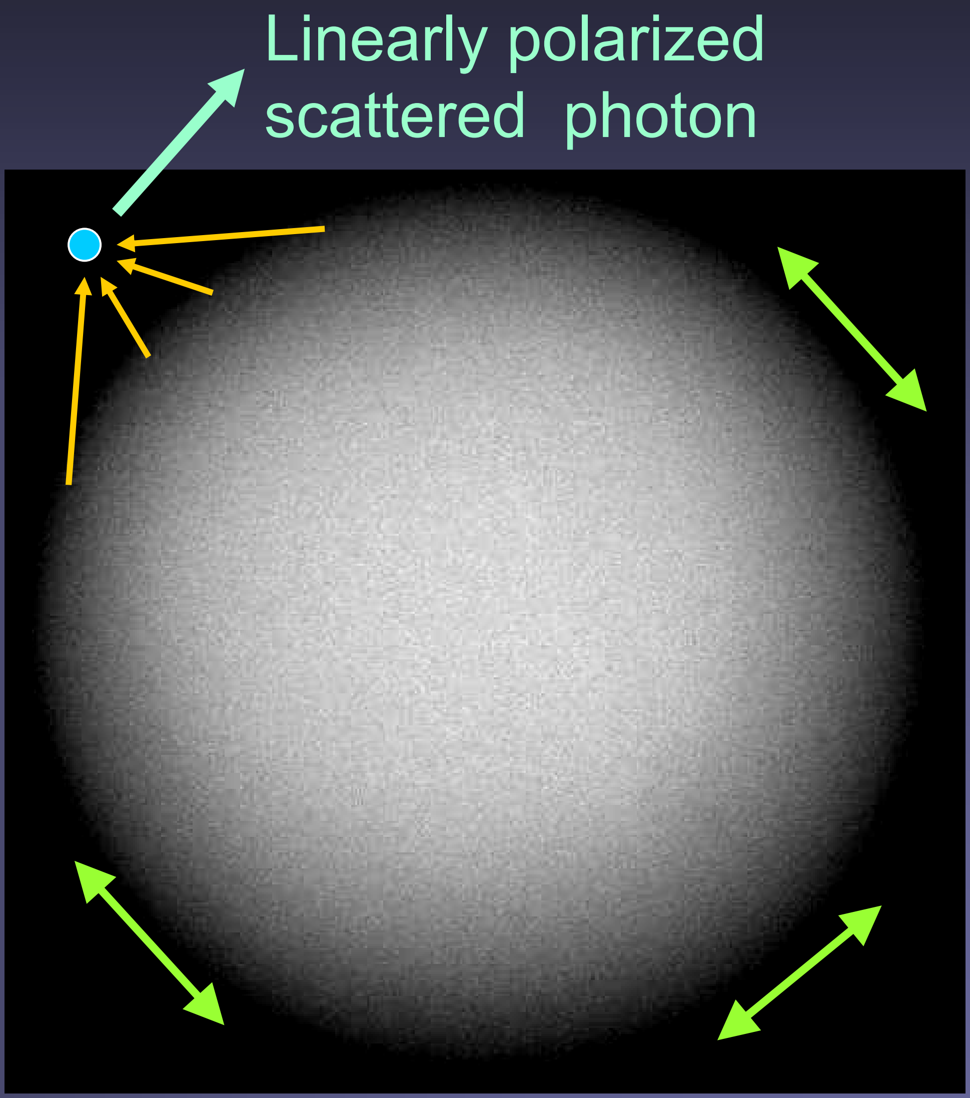

- Hanle effect: Modification of scattering polarisation by magnetic field. 2 effects:
- Depolarisation
  - depends on field orientation
  - depends on B (it is complete if $\Delta\lambda_H$ >> natural line width, i.e. for $B > 0.1\text{-}100$ G)
  - also present for unresolved mixed polarity fields
- Rotation of polarisation plane
  - depends on B, γ, χ
  - only if field is spatially resolved

Hanle effect

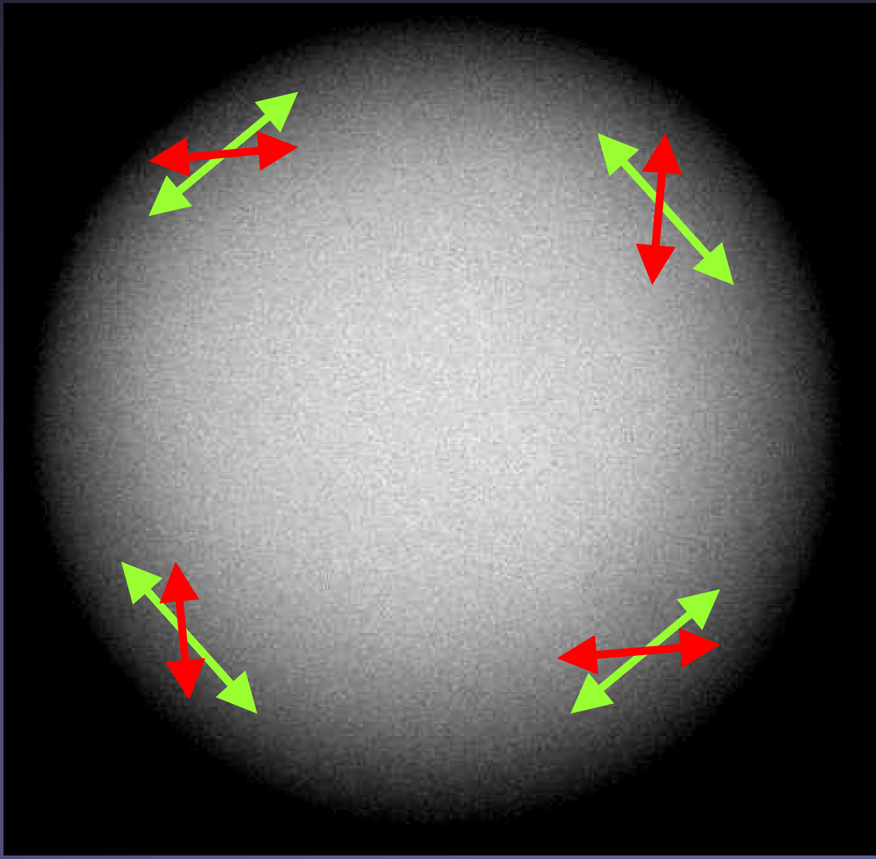

Signature of Hanle effect for spatially resolved field

Hanle diagnostics: simple examples

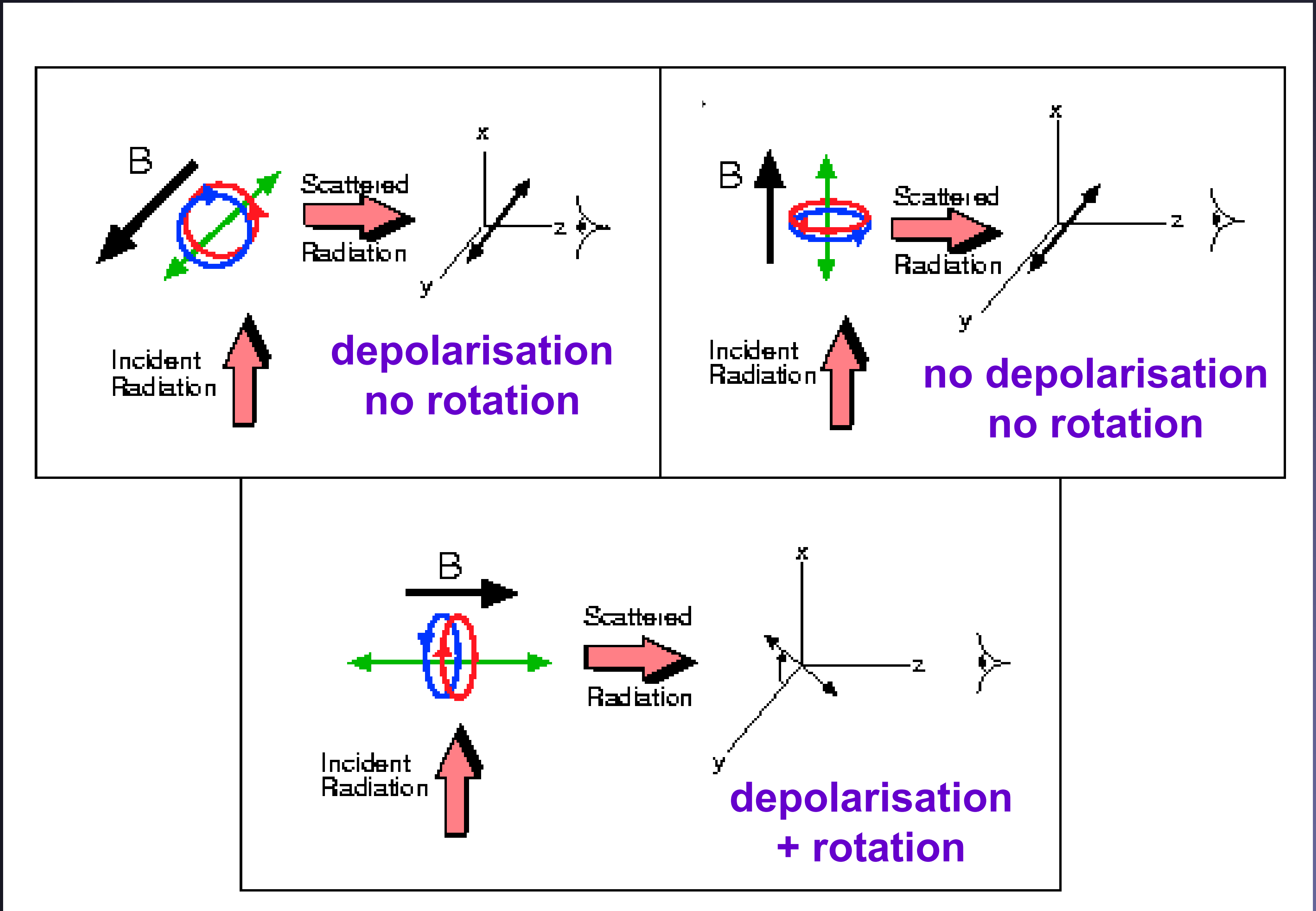

Example of Hanle rotation & depolarisation

- More complex to describe Hanle than Zeeman effect
- Hanle parameters:
  - Depolarization factor p/p_{max} where p is polarization degree for B≠0, p_{max} is p for B=0
  - Angle of rotation β, with $\tan 2\beta = U/Q$ (β=0 for B=0)
- Atmospheric parameters
  - Field strength parameter Ω, with $\Omega = 2 g_{\mathrm{u}} \omega_{\mathrm{L}} / \gamma_{\mathrm{N}} \sim B$, where γ_{N} is natural damping constant, ω_{L} is Larmor frequency, g_{u} is Landé factor of upper level,

$$\gamma_N = \frac{\mu_0 e^2 \omega^2}{6\pi\, m_e c} \qquad \omega_L = \frac{e}{2m_e} B$$

  - Field azimuth χ, with χ=0 for B || LOS

Hanle effect example (contd.)

- Hanle depolarisation in general changes between $0.2B_0$ and $5B_0$

$$B_0 = \frac{2m\gamma_N}{eg_u}$$

- Expression for B_0 is equivalent to saying that for $B=B_0$ we have $\omega_L = \gamma_N$

Stenflo 1994

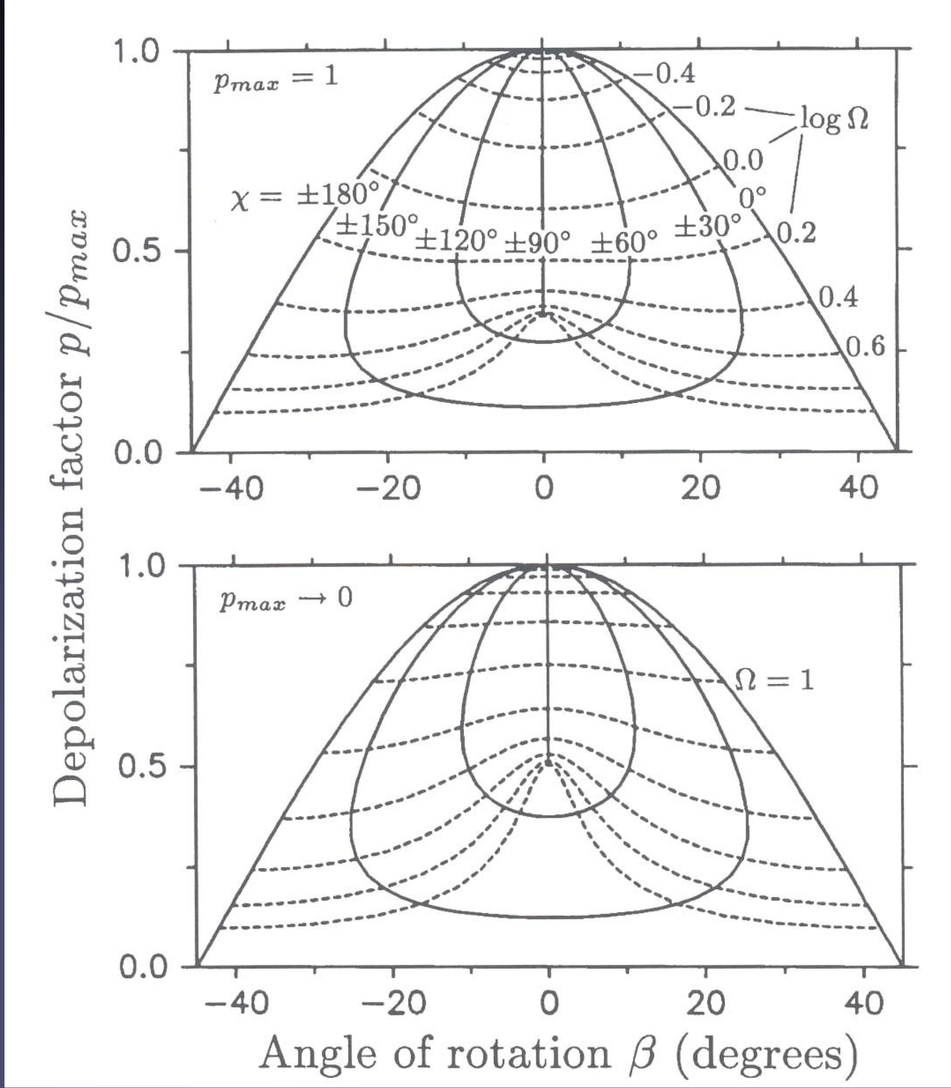

Illustration for horizontal field seen exactly at limb, scattering radiation coming exactly from below

The Sun's large-scale magnetic structure

Magnetic flux per region

Active regions

$$\Phi_{\text{act reg}} \approx 5 \cdot 10^{20} \ldots 5 \cdot 10^{22}\ \text{Mx}$$

Ephemeral regions

$$\Phi_{\text{eph reg}} \approx 10^{18} - 5 \cdot 10^{20}\ \text{Mx}$$

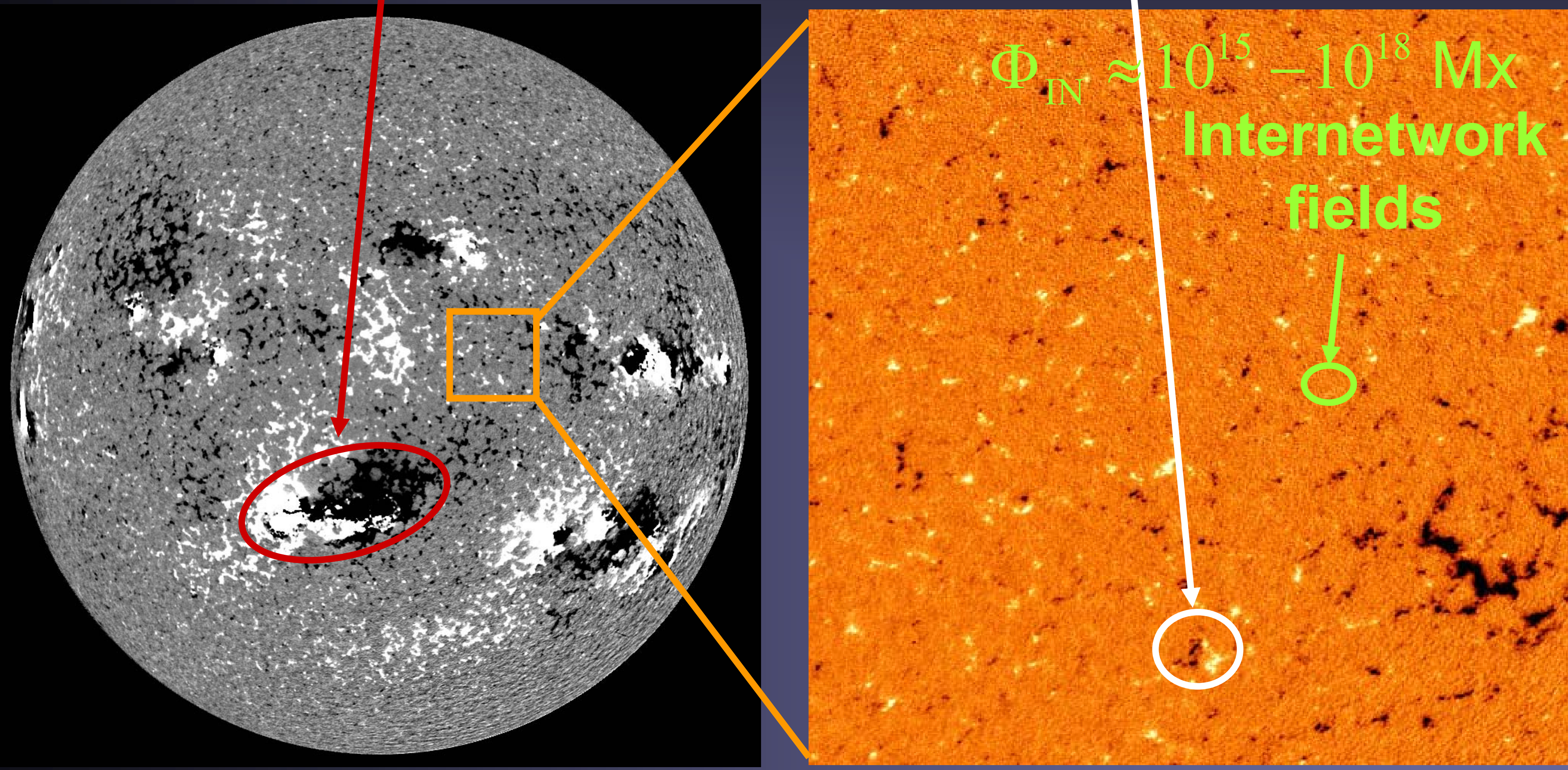

SOHO/MDI magnetograms

Magnetic flux emerging over solar cycle

Active regions

$\dot{\Phi} \approx 3 \cdot 10^{23} \ldots 3 \cdot 10^{24}$ Mx/yr

Ephemeral regions

$\dot{\Phi} \approx 2 \ldots 4 \cdot 10^{26}$ Mx/yr

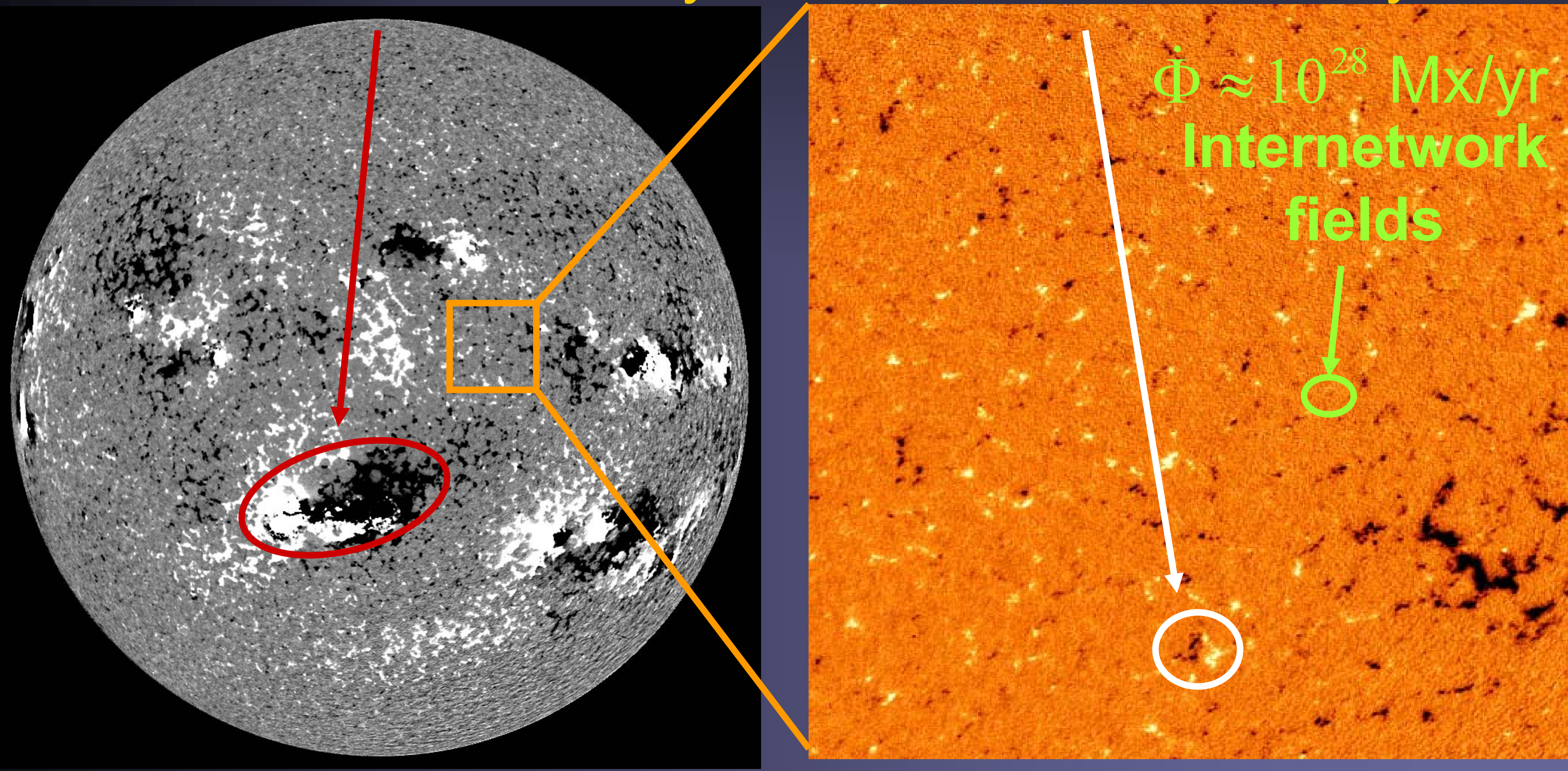

SOHO/MDI magnetograms

What are active regions composed of?

Magnetic structure of active regions is determined by

- sunspots
- pores
- plage or facular magnetic elements

- Spots: $\Phi = 10^{20}$-10^{22}
- Pores: $\Phi = 3 \cdot 10^{18}$-$3 \cdot 10^{20}$
- MEs: $\Phi = 10^{17}$-$3 \cdot 10^{18}$

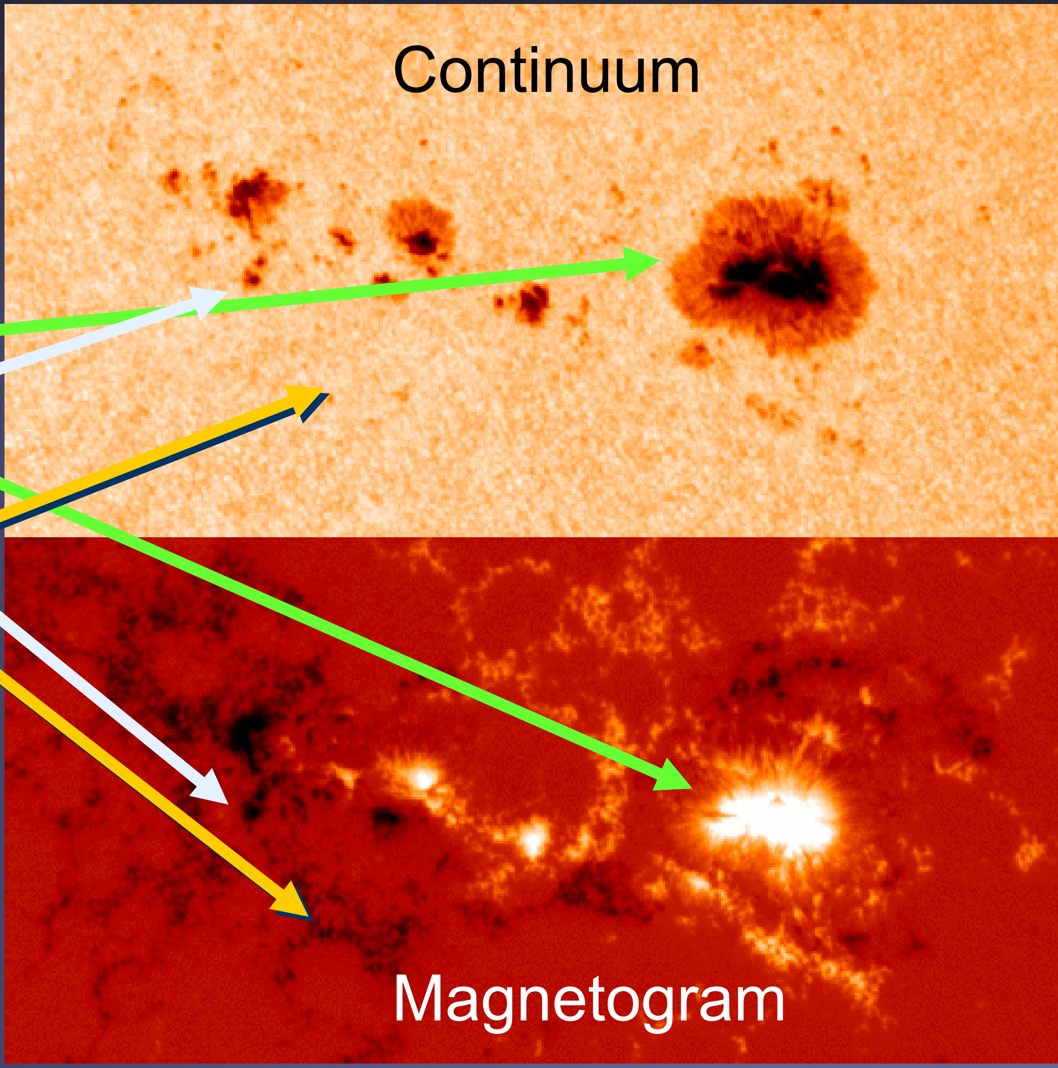

Emergence and evolution of active region seen in white light (sunspots)

Tilt angle of sunspot groups

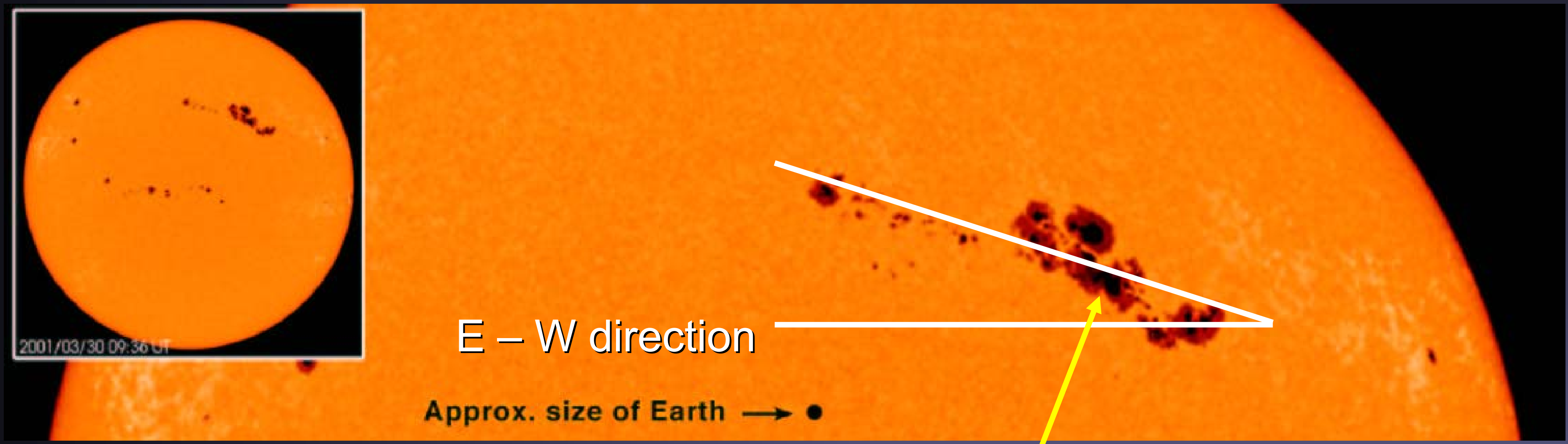

Following spots closer to pole

Tilt angle $\gamma \propto \sin(\lambda)$
("Joy´s law")

Here λ = latitude

Magnetic field in the convection zone

- Magnetic field in AR & ER is produced by dynamo located near bottom of convection zone (in overshoot layer)

➔ toroidal flux tubes in pressure balance with surroundings:

$$\frac{B_i^2}{8\pi} + P_i = P_e + \frac{B_e^2}{8\pi}$$

- If $B_\mathrm{i} > B_e$ and $T_\mathrm{i} = T_\mathrm{e}$, then $\rho_\mathrm{i} < \rho_e$ ➔ intense B-fields are evacuated and buoyant relative to surroundings (Parker instability).
- Buoyancy dominates over curvature for $B \geq 10^5$ G (Ferriz Mas & Schüssler 1992)
- Flux tubes form loops that move towards and eventually break through the solar surface

Emergence at surface

- Active region lies at intersection of flux tube with solar surface
- Each polarity corresponds to a footpoint of loop
- Loop rises on into corona

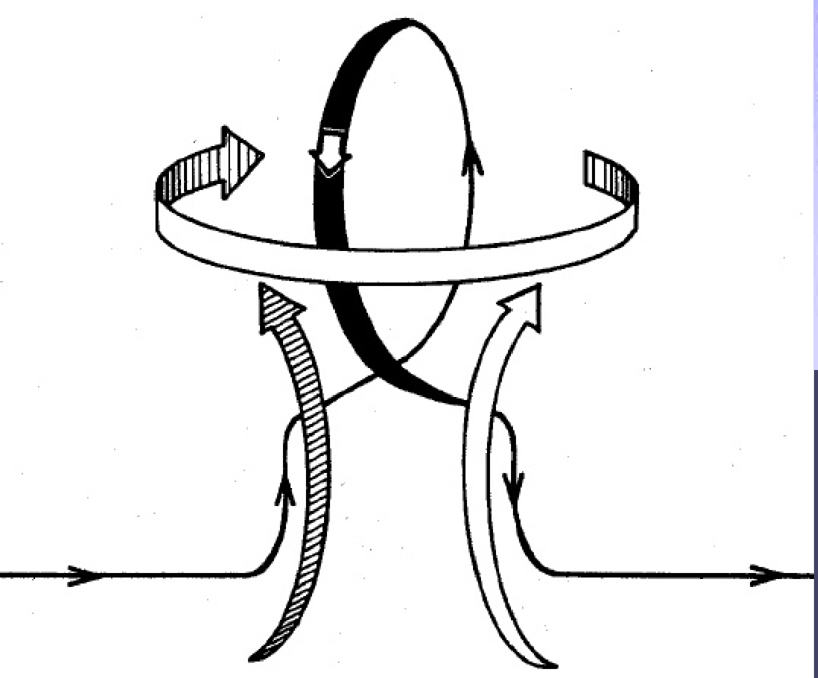

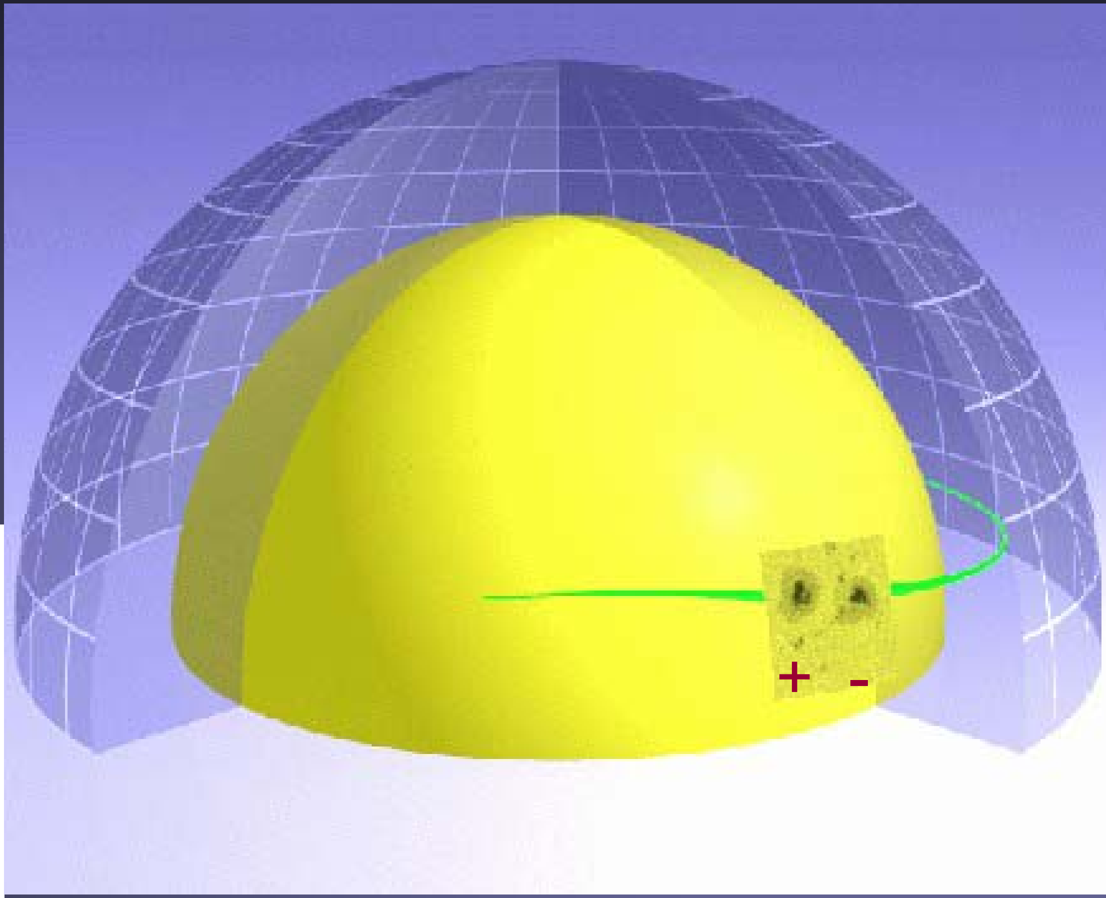

Coriolis force causes rising tube to writhe & get a poloidal comp.

Results of flux tube rise computations

- To get correct emergence latitudes & tilt angles $B \geq 10^5$ G at base of convection zone (Choudhury & Gilman, Fan, etc.)
- Lower B lead to emergence latitudes >30° and too strong tilt angles, or the FTs never reach the surface ($P_{\mathrm{i}} > P_{\mathrm{e}}$)
- Computations in 3-D show: flux tubes must be twisted above a critical amount in order to survive up to the surface without being shredded

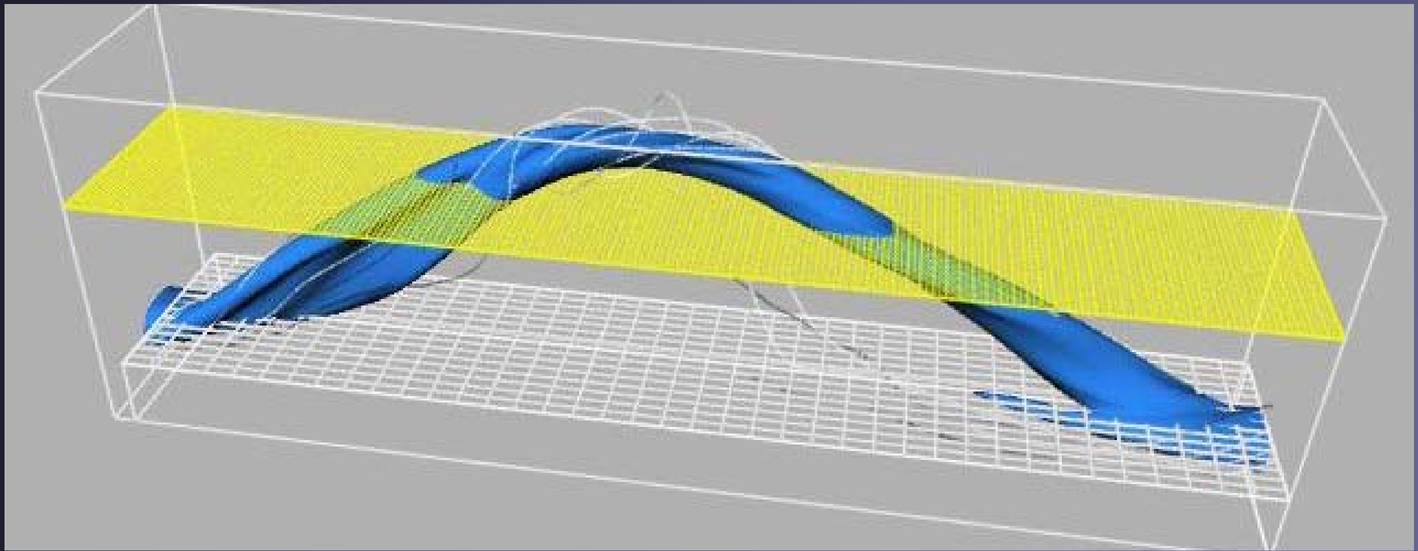

One kind of field, or different kinds? Is magnetic morphology self-similar?

Self-similarity of features of different sizes: they have a fractal dimension d, which connects Perimeter P and Area A of a feature (d is obtained statistically)

$$P \propto A^{d/2} \qquad d \approx 1.6$$

(Roudier & Muller 1987, Ribes et al. 1996, Meunier 2004, Criscuoli et al. 2007, etc.)

The Solar Activity Cycle

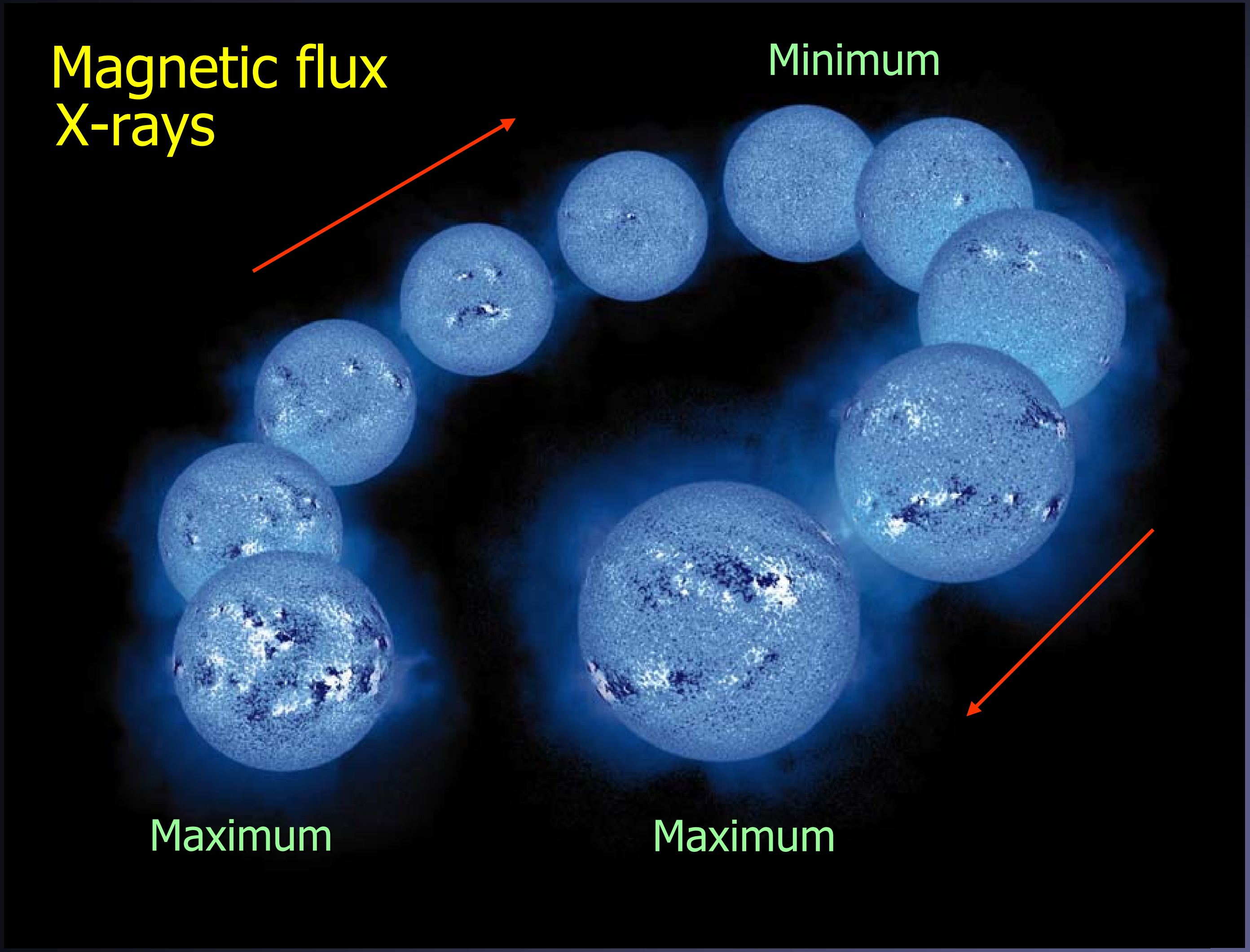

The short-wave radiation varies strongly through the activity cycle: from a factor 2 in the UV (<100nm) up to a factor 100 in X-rays.

The magnetic flux at the solar surface also varies quasi-periodically over the 11-year solar cycle.

Solar corona during eclipses

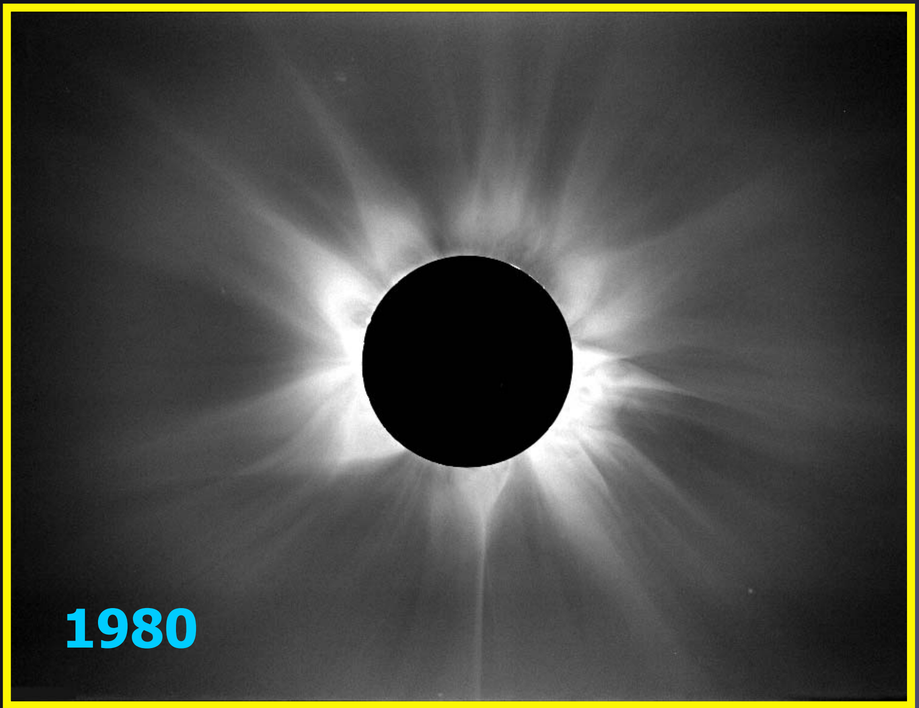

Activity maximum

Activity minimum

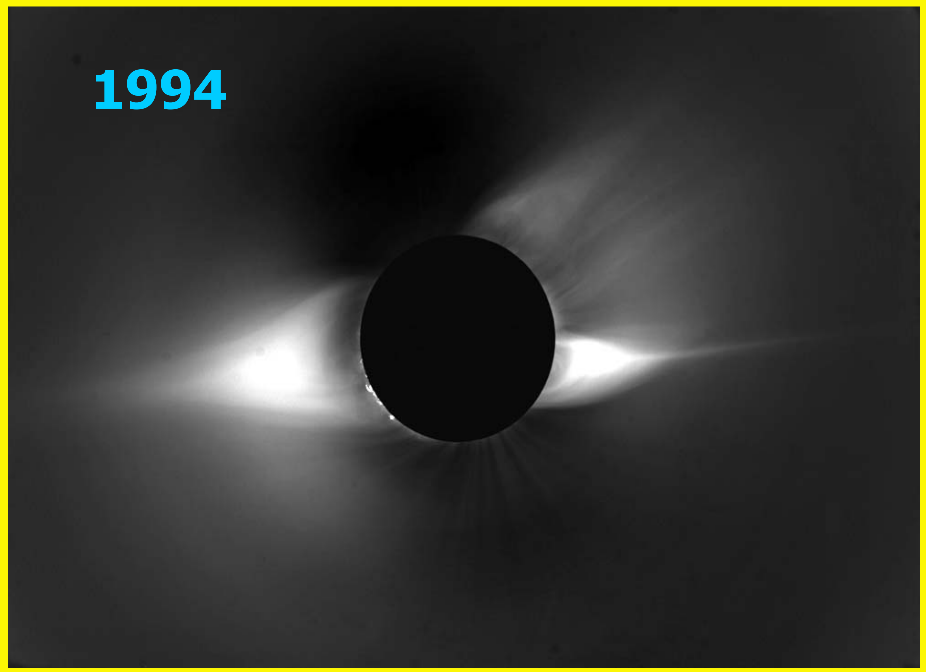

The butterfly diagram

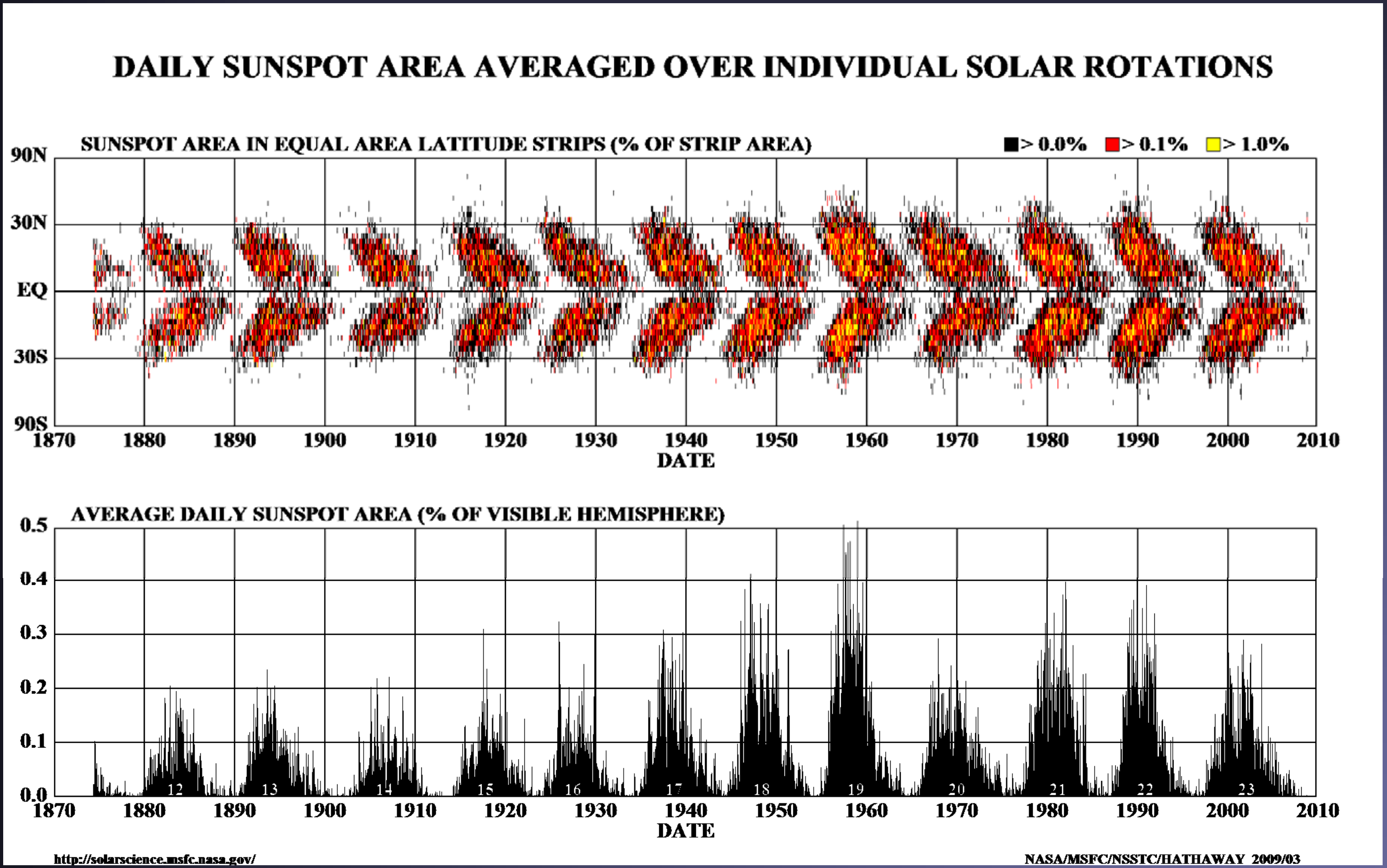

Magnetic butterfly diagram:
Azimuthal averages of unsigned flux

- Unsigned flux displays very similar butterfly diagram to the sunspots (no major surprise)
- There are signs of additional features:
  - flux moving periodically to the poles from active bands
  - some concentration of field at the poles

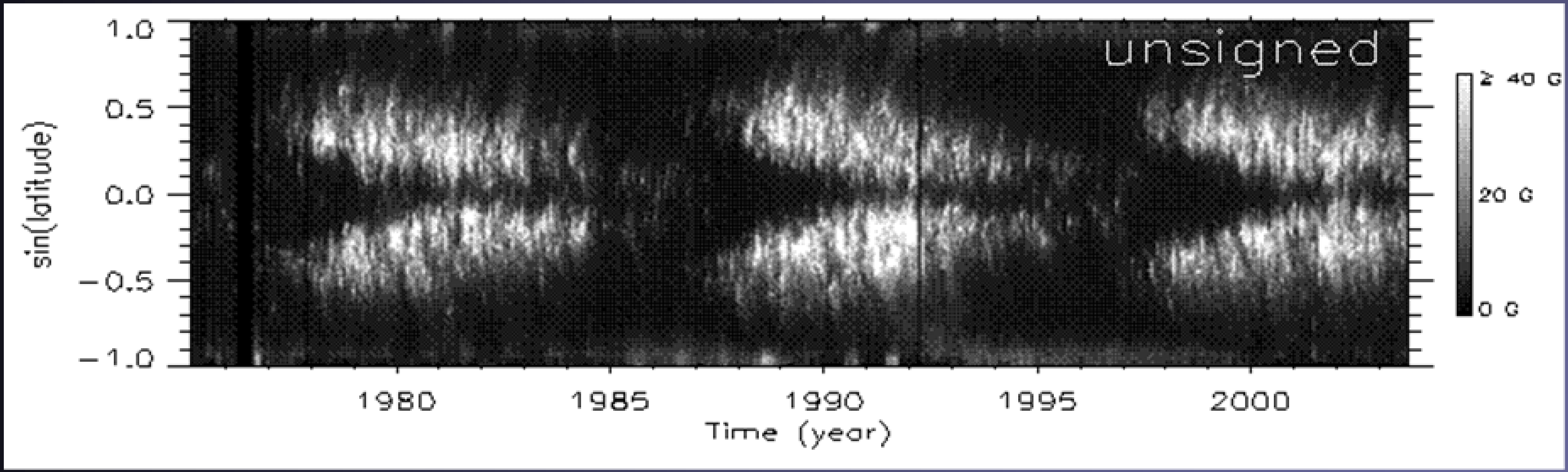

Butterfly diagram of magnetic flux

Azimuthal average of net magnetic flux
Active regions now weaker, since bipolar
Polar fields stronger, since unipolar

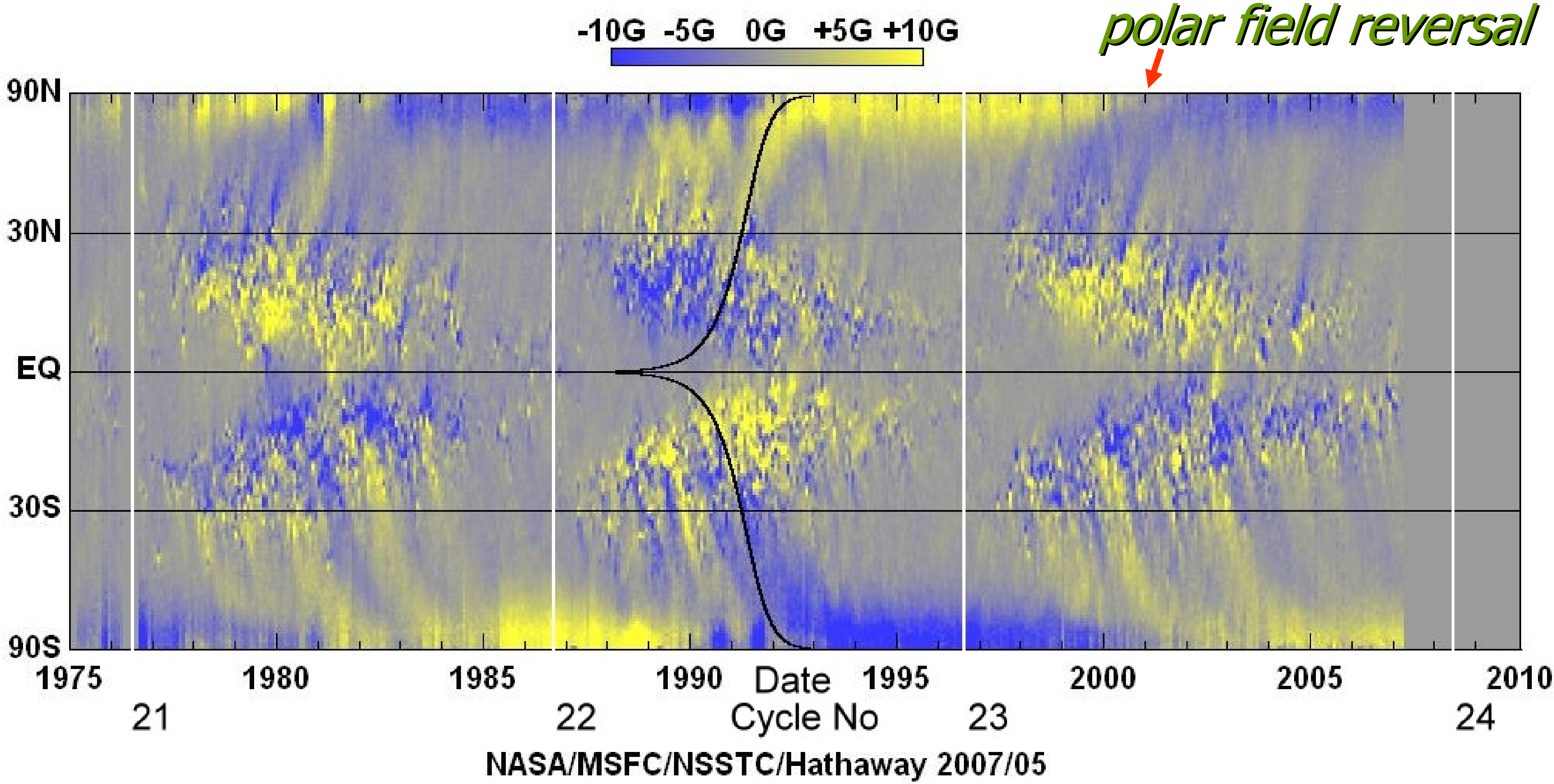

Magnetic cycle: Hale's polarity law

Polarity is re-established after 22 years, length of magnetic cycle

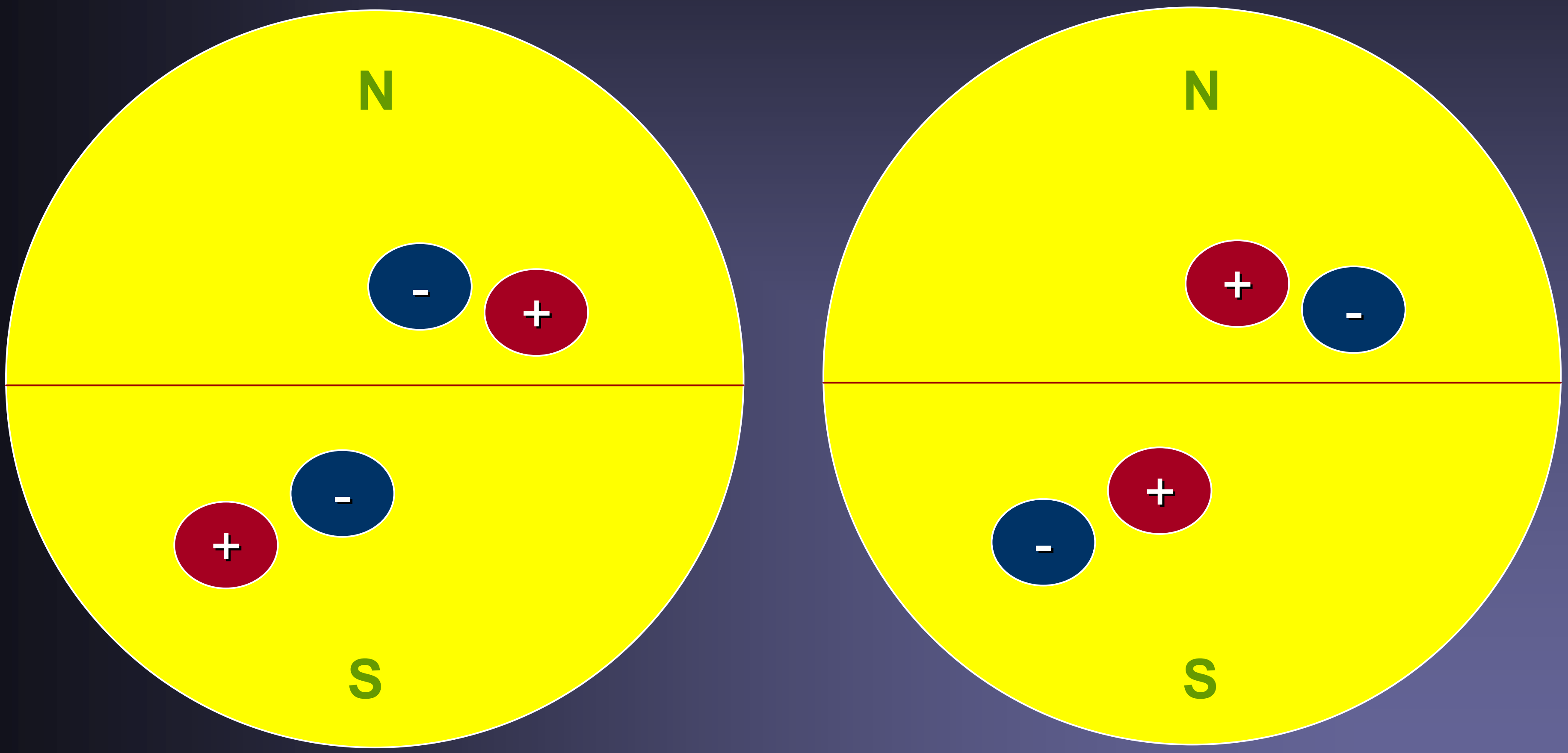

cycle n

cycle n+1

Telescopically measured number of sunspots since 1610

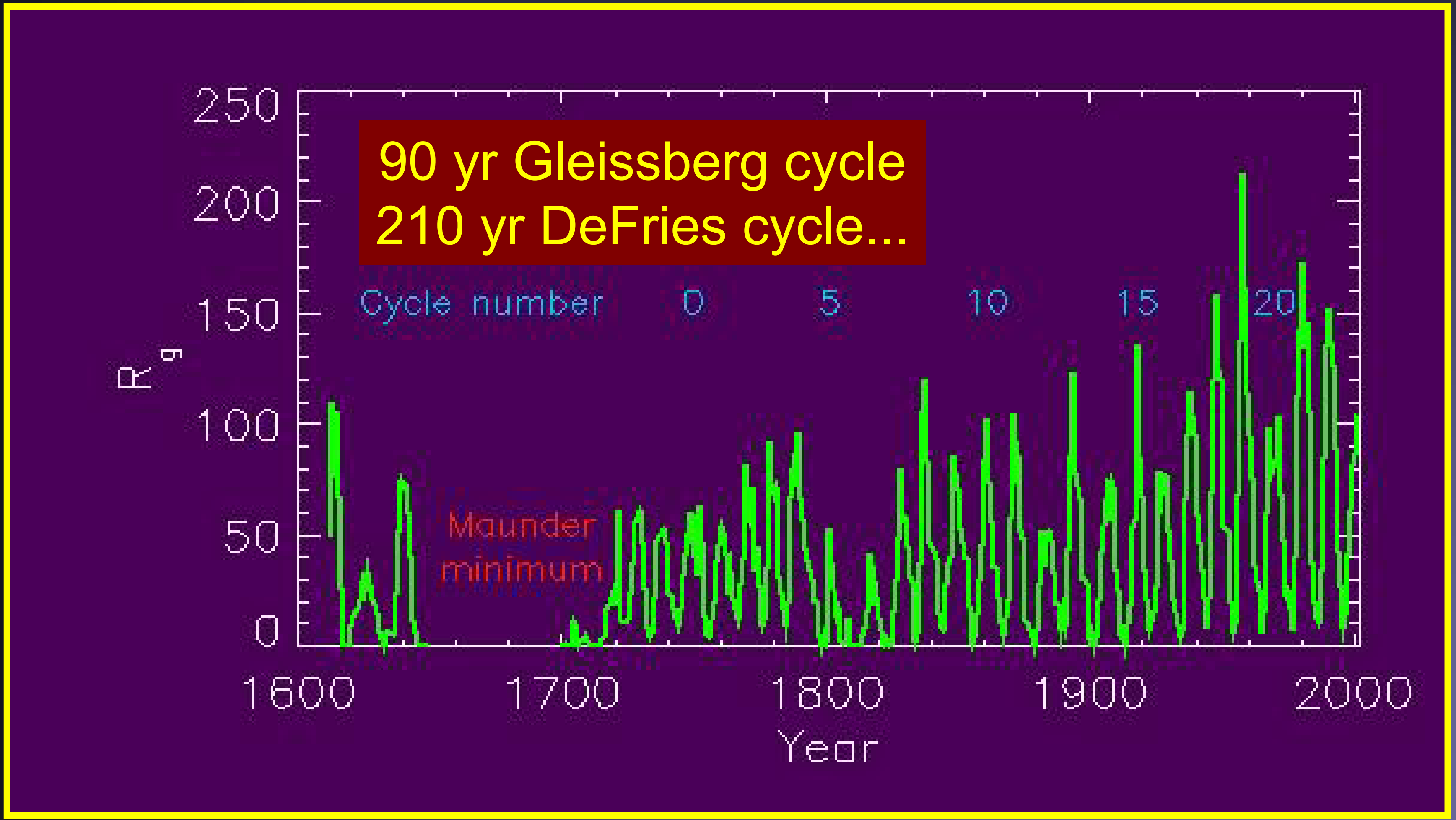

Telescopically measured number of sunspots since 1610

Is the Maunder minimum a unique event, or are grand minima common? What about the current period of high activity (grand maximum)?

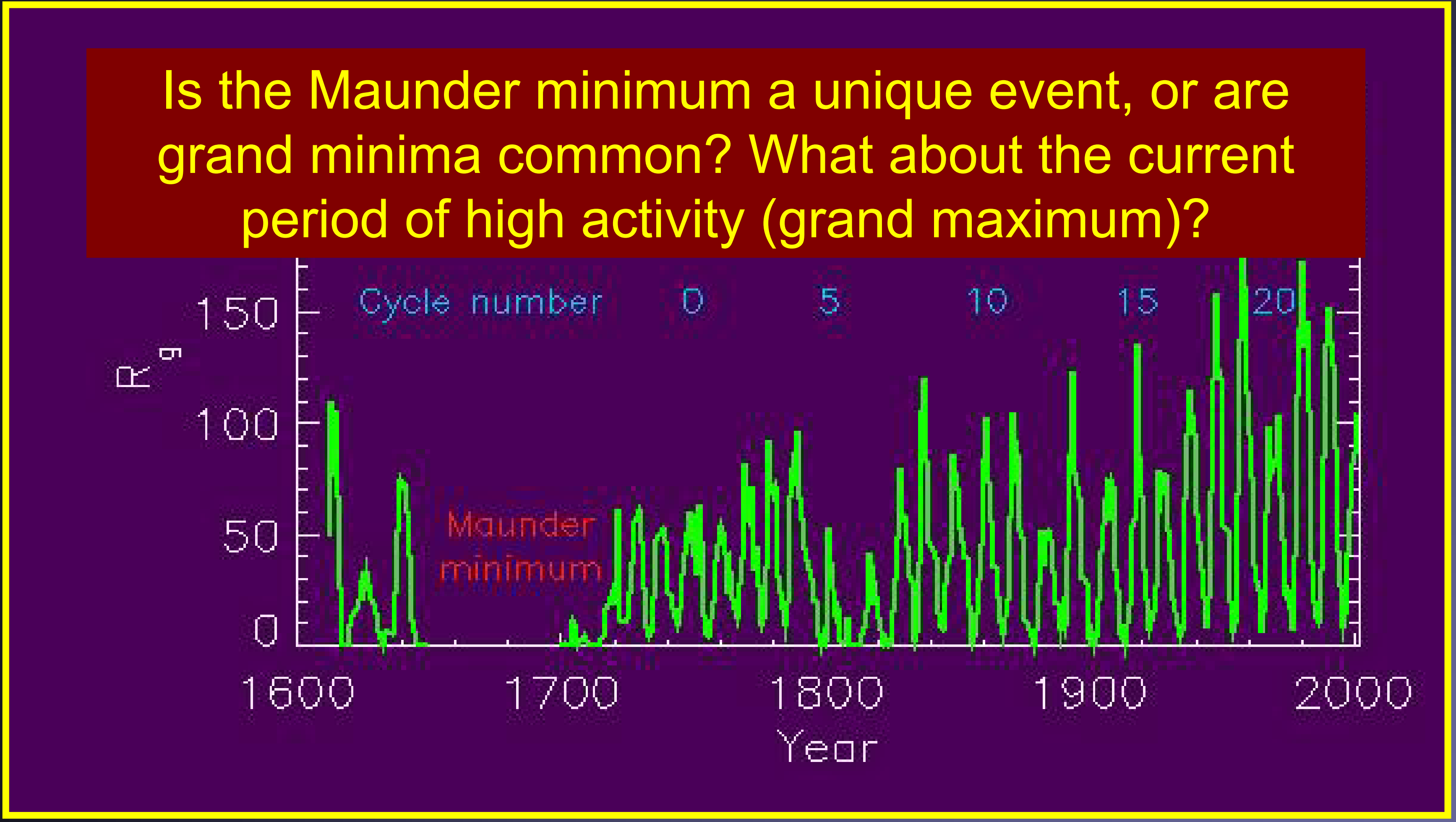

Open and closed magnetic flux

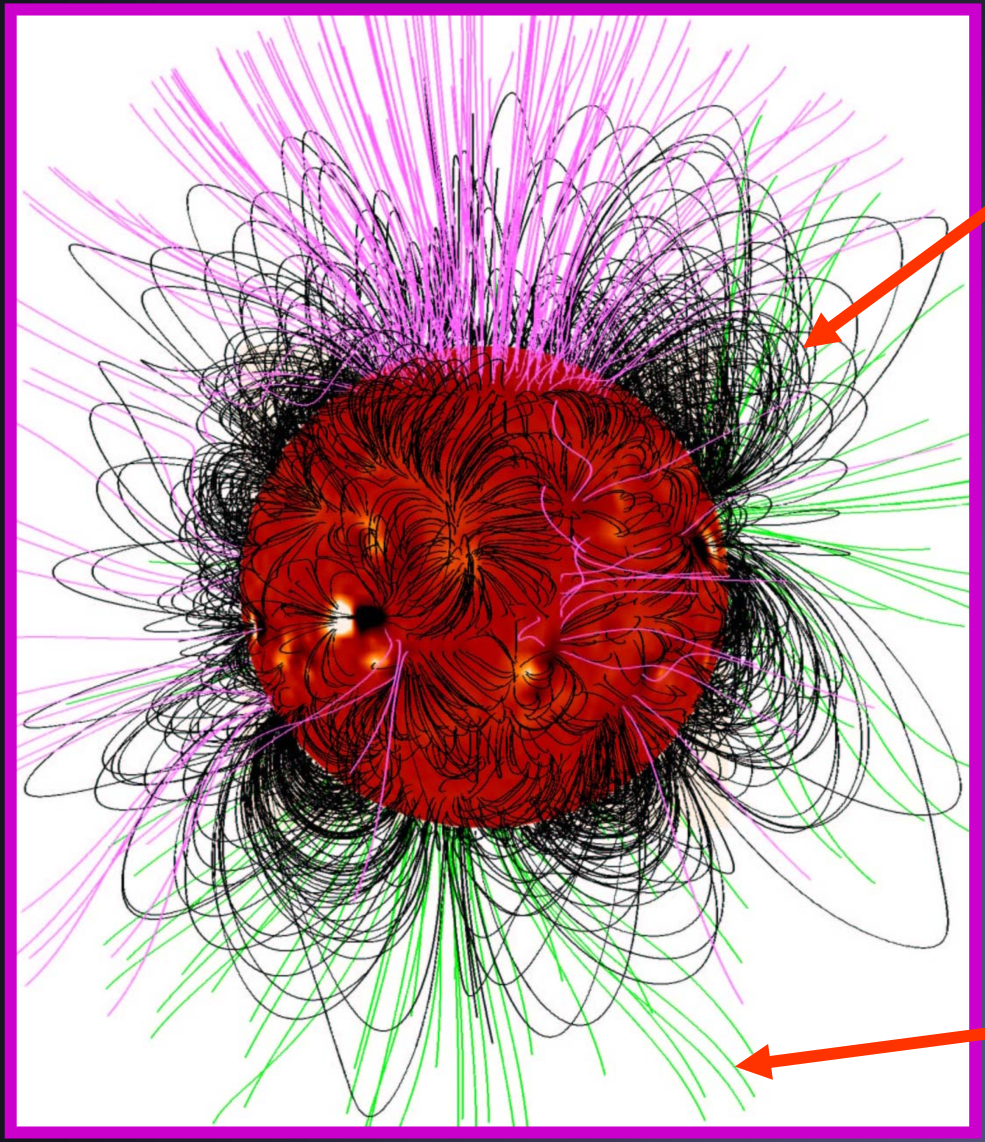

Closed flux: slow solar wind

Most of the solar flux returns to the solar surface within a few $R_\odot$ (closed flux)

A small part of the total flux through the solar surface connects as open flux to interplanetary space

Open flux: fast solar wind

Evidence for Secular Change: Interplanetary Magnetic Field

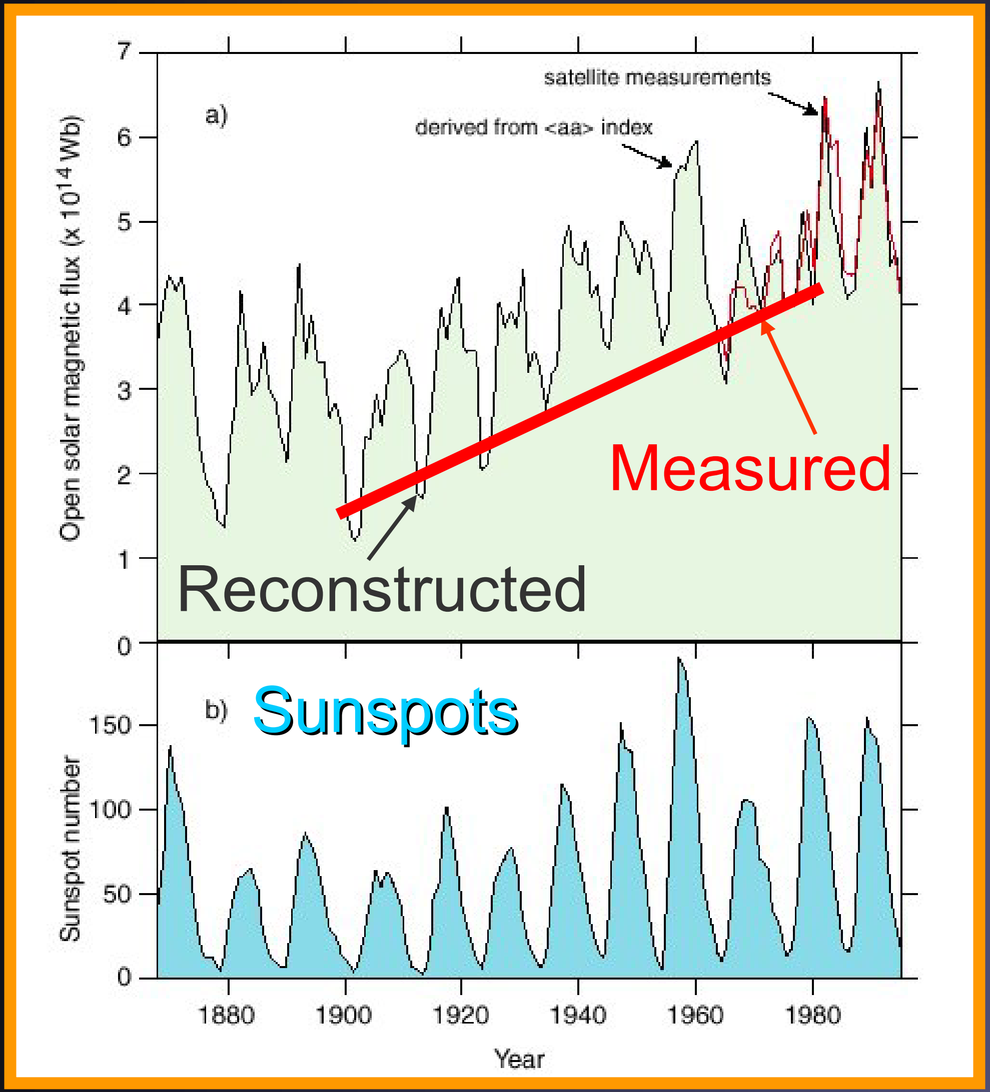

- Reconstructed from geomagnetic aa index
- Interplanetary B-field (≈ Sun's open flux; Ulysses) doubled during the last century

➔ What produced this doubling?

Lockwood et al. 1999, Rouillard et al. 2007

Secular Change of the Sun's Magnetic Flux: a Mechanism

- Underlying concept: overlapping solar cycles (Wilson et al. 1991: extended solar cycle). Overlap can be produced by
  - emergence of flux of new cycle (e.g. in ephemeral regions) before end of previous cycle (K. Harvey 1992)
  - long lifetime (decay time) of open (and closed) flux

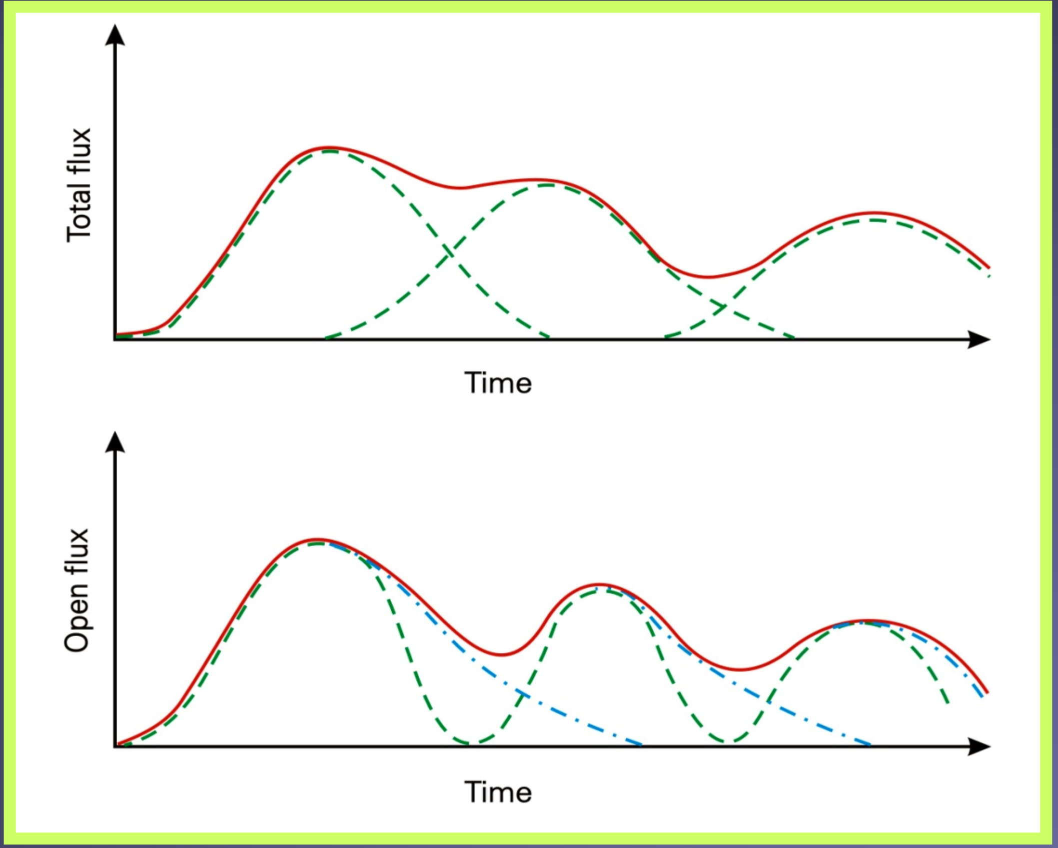

Solanki et al. 2000, 2002

Ephemeral Regions: Extended Cycle

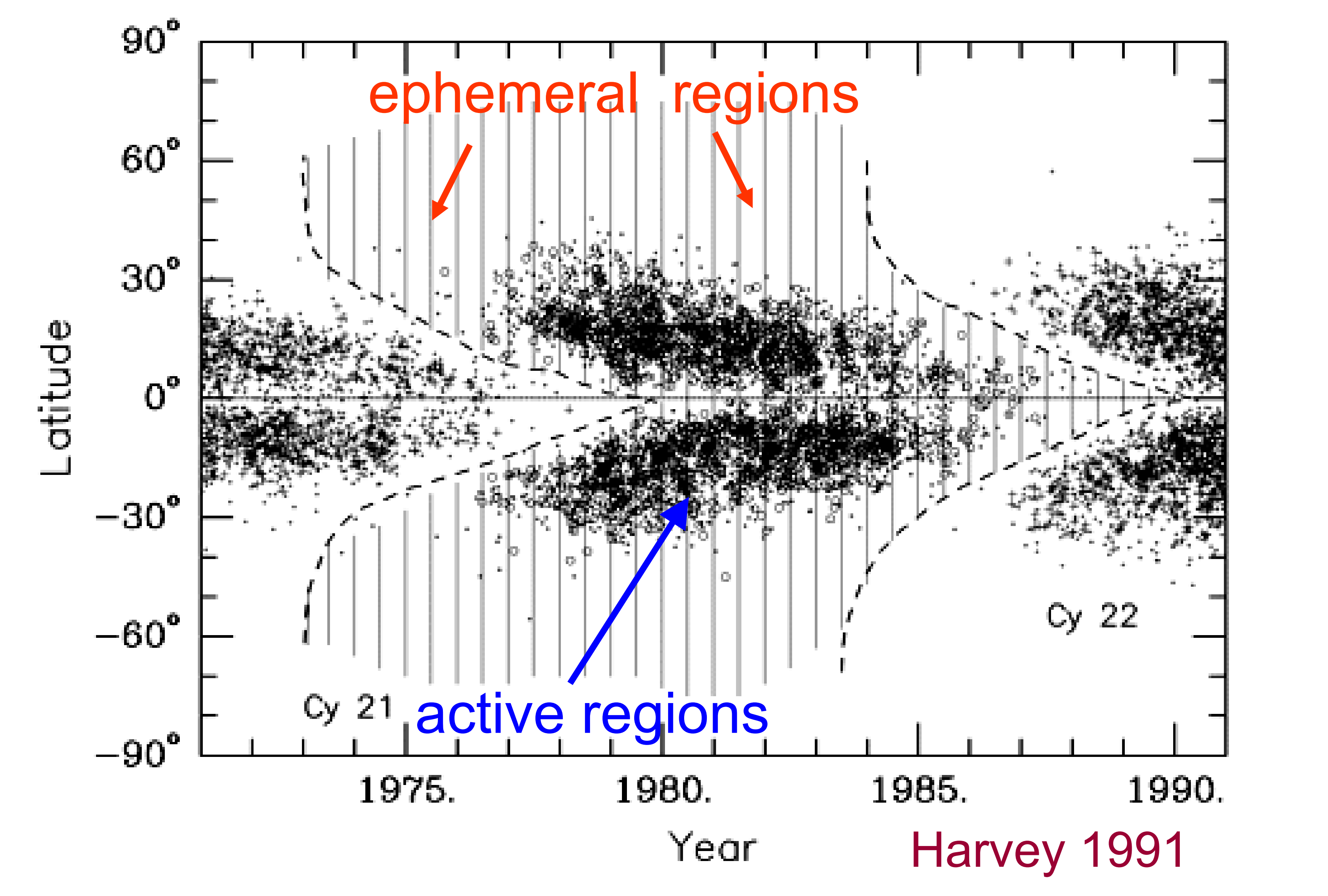

Reconstruction of Open Flux back to 1700

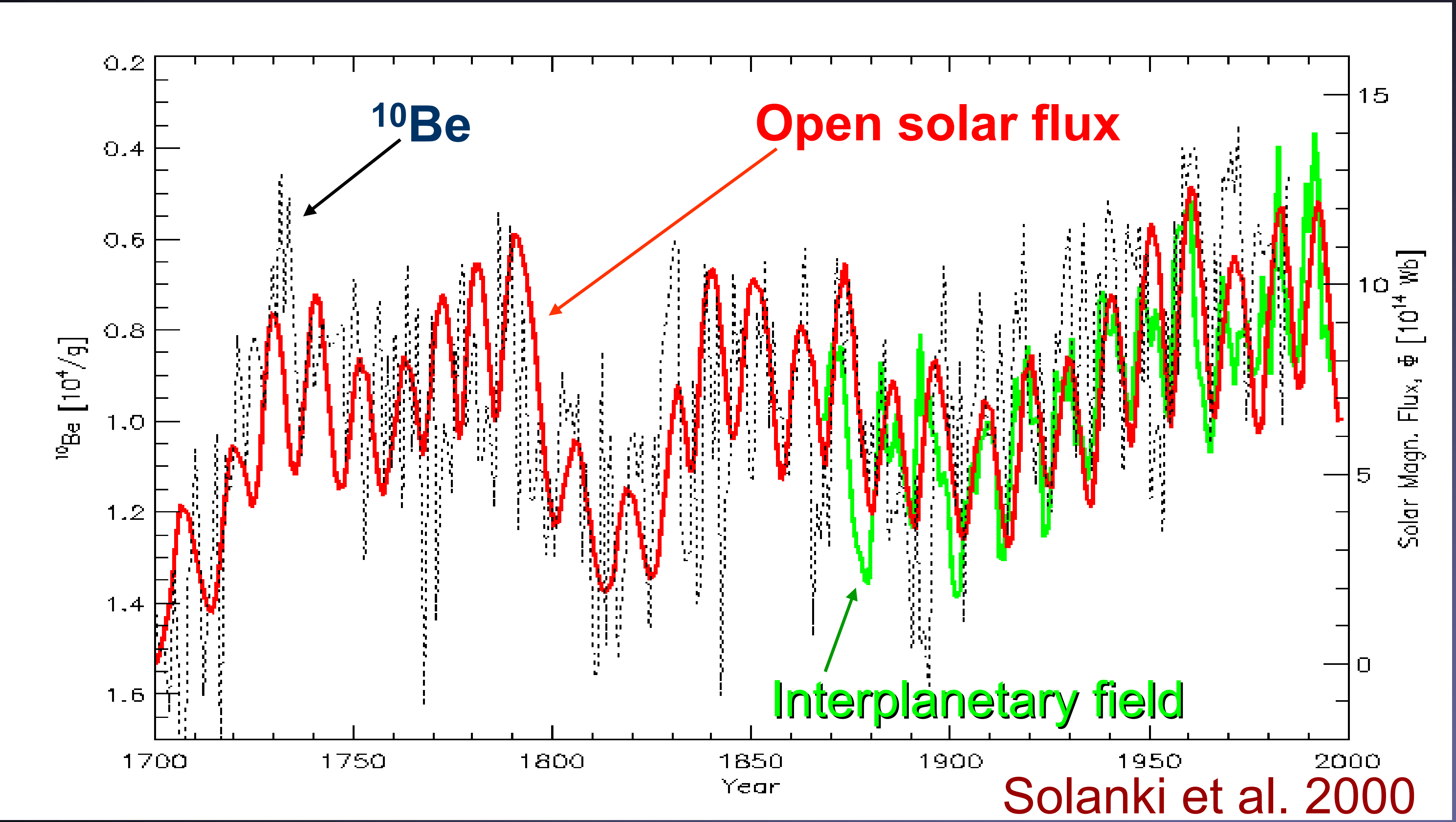

Model also predicts very similar trend for solar total magnetic flux → solar irradiance should also show secular trend

Cosmic Rays, the Sun & Tree Rings

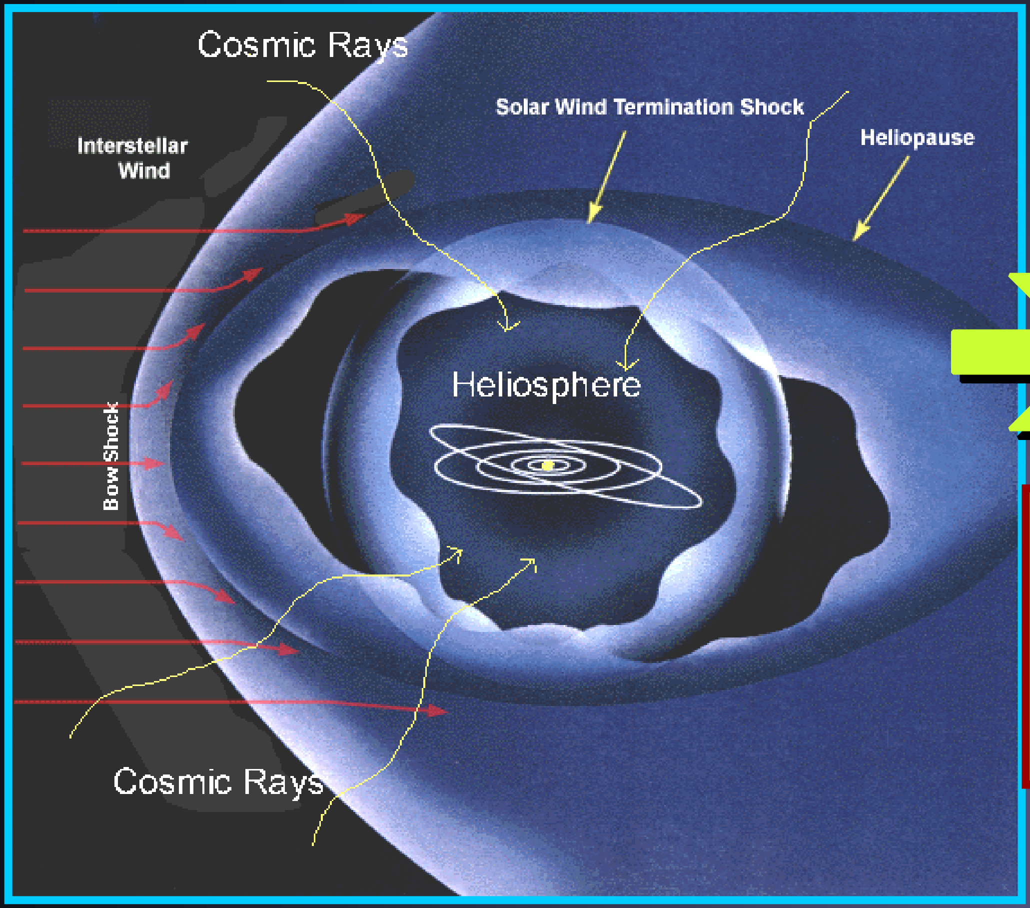

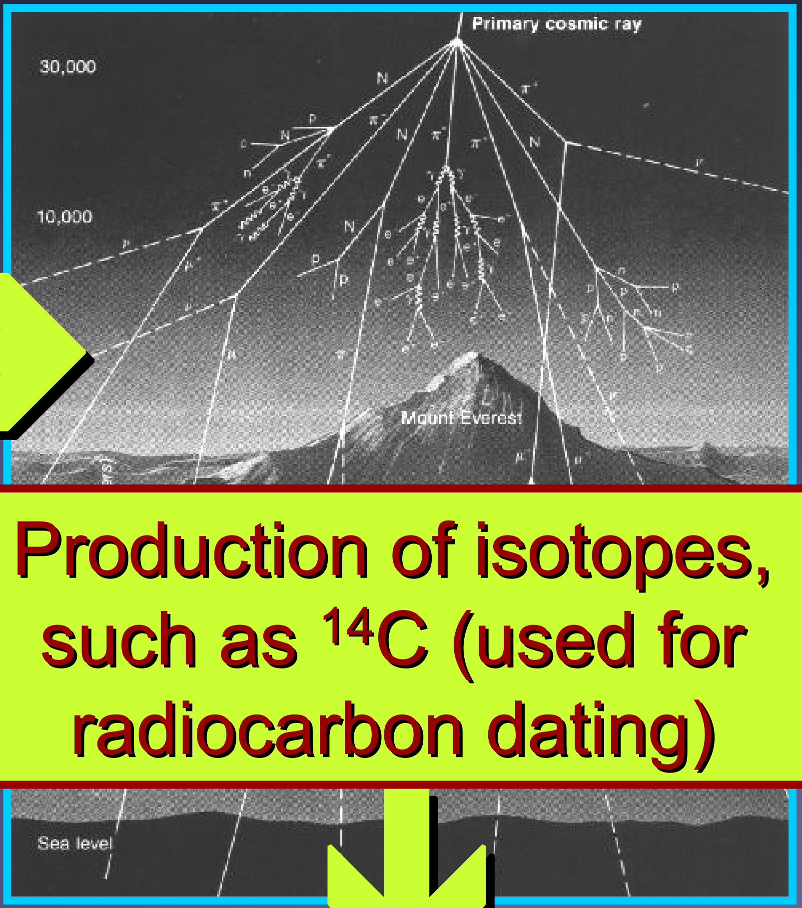

Production of isotopes, such as ^{14}C (used for radiocarbon dating)

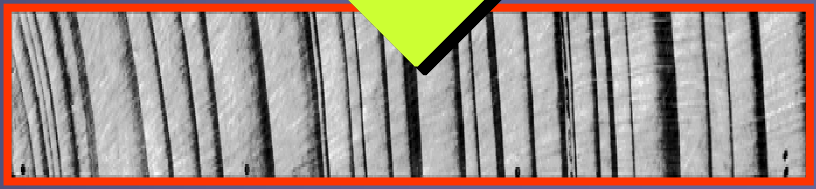

Flux of cosmic rays is changed by solar activity

Beyond the telescopic record

From cosmogentic ^{14}C (or ^{10}Be)

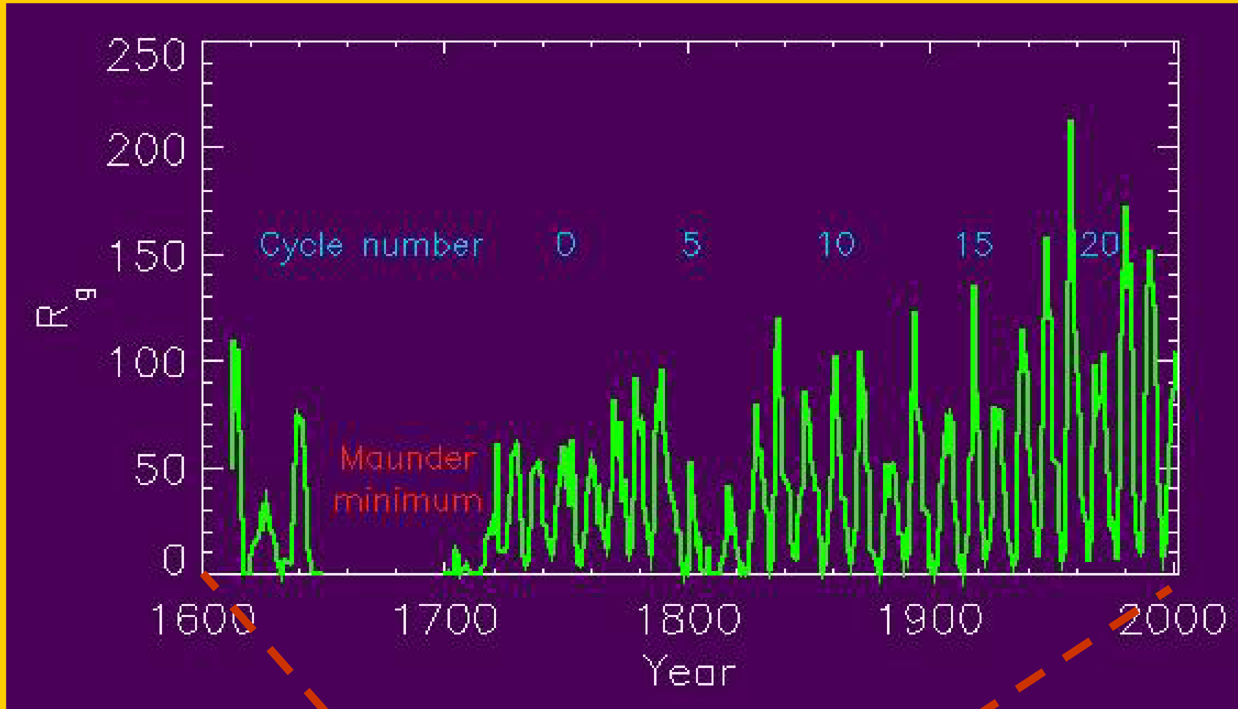

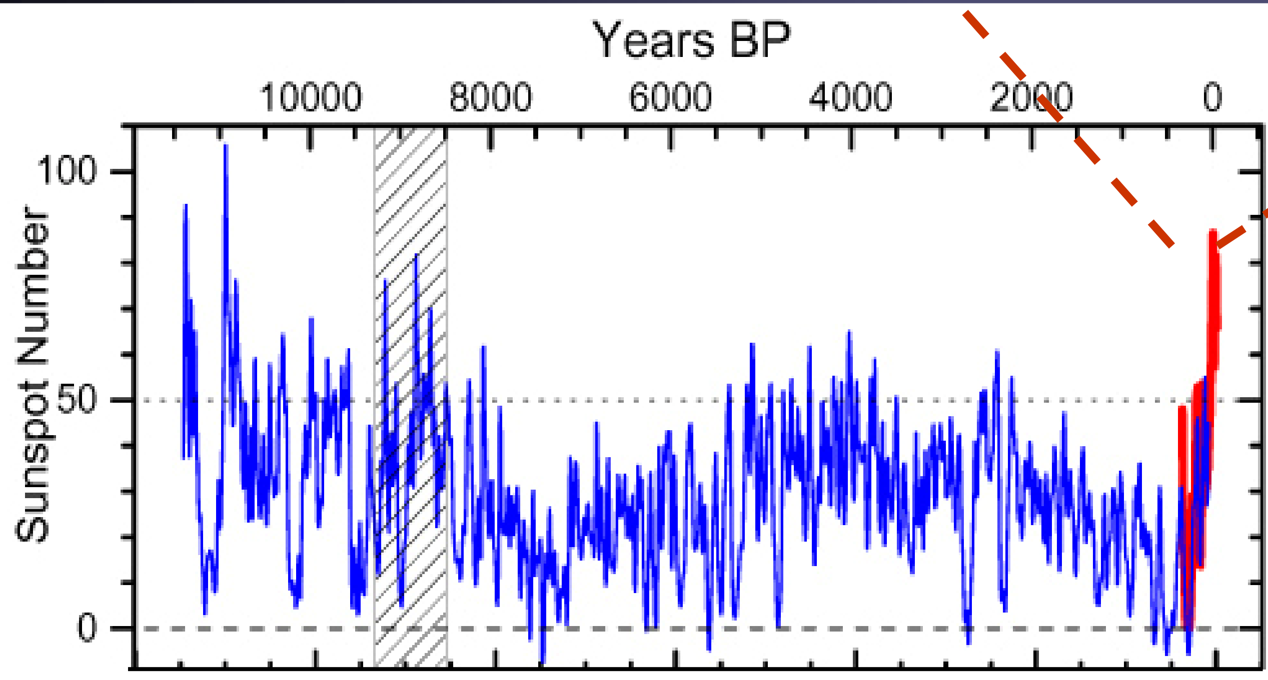

Solanki et al. 2004; Usoskin et al. 2006; 2007; Vonmoos et al. 2007; Abreu et al. 2008

Beyond the telescopic record

From cosmogentic ^{14}C (or ^{10}Be)

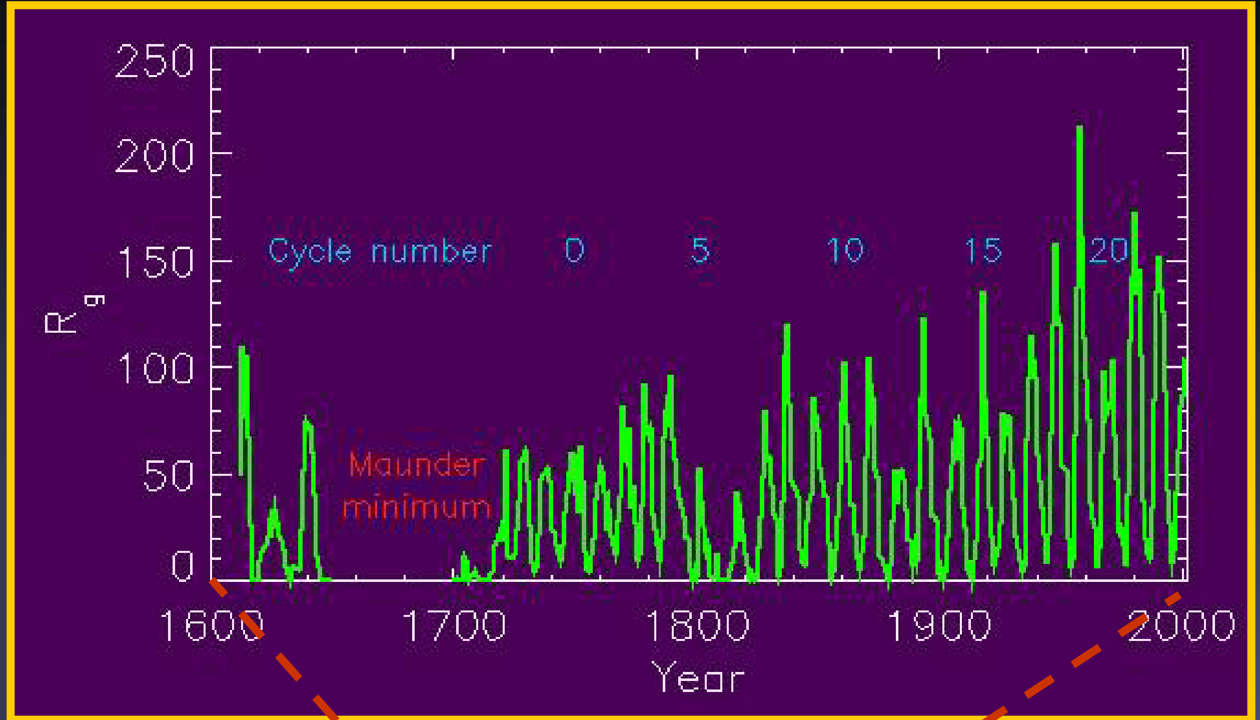

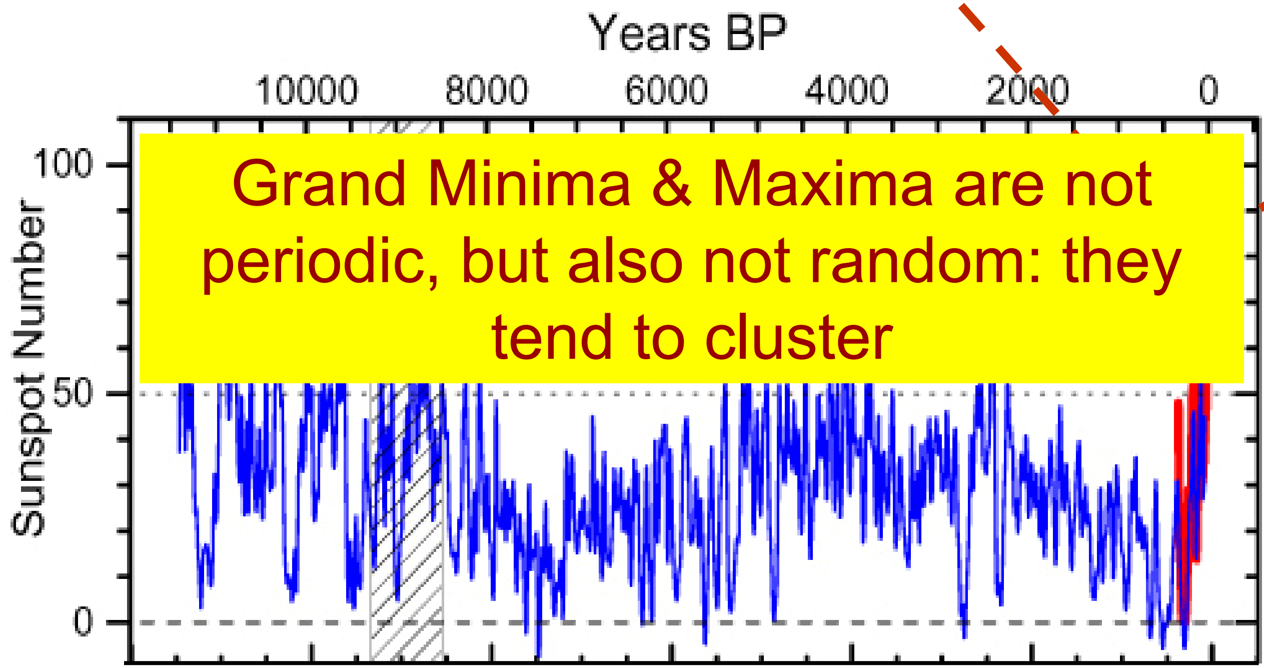

Solanki et al. 2004; Usoskin et al. 2006; 2007; Vonmoos et al. 2007; Abreu et al. 2008

Are we living in special solar times?

- Last 50-60 years have seen strongest activity cycles during the last 400 years. Sun has spent only a few % of the last 10000 years at such high activity levels
- Since 2006 we are in a particularly long and weak minimum, weakest in 80 years
  - exceptionally few sunspots
  - open flux is very low
  - irradiance is very low
  - solar wind is exceptionally weak
- What does the future hold for solar activity? Are we about to leave the Grand Maximum of activity?

How will the next cycle be?

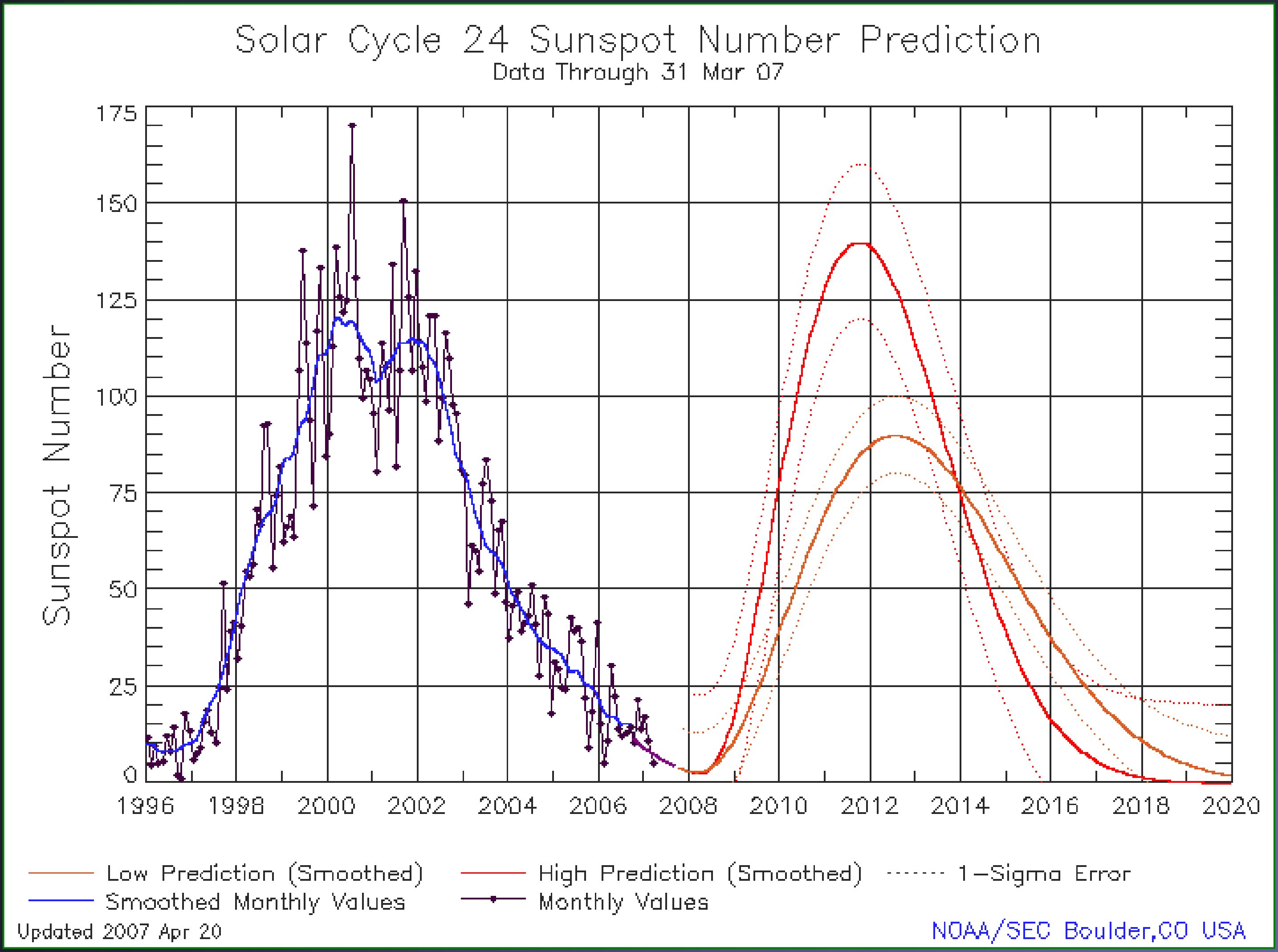

Predicted next cycle: how does it compare with reality?

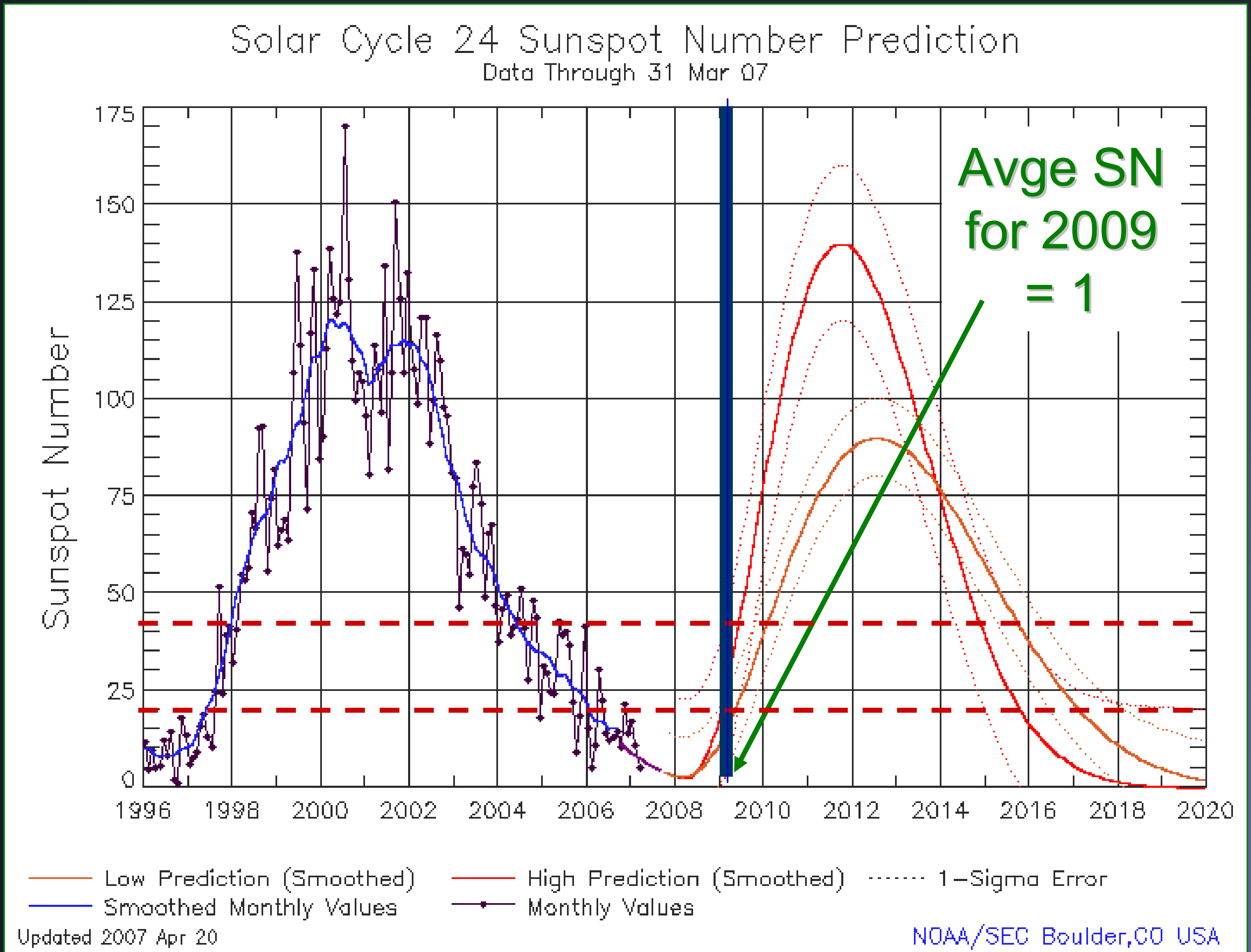

Sunspot magnetic fields

What are Sunspots?

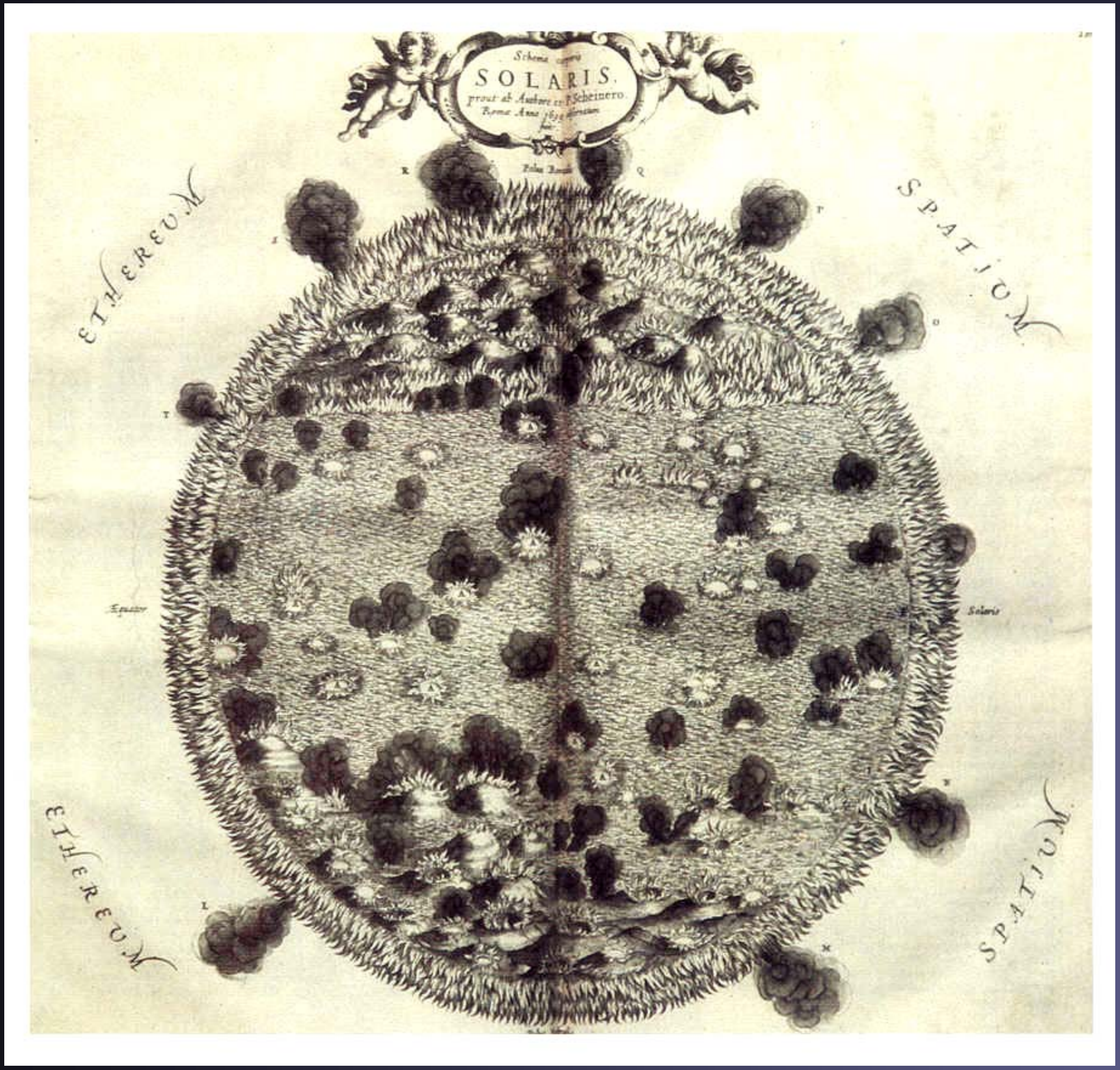

Slag on lava?

Clouds of smoke?

Holes in the Sun ?

Cyclones?

Sunspot structure & dynamics

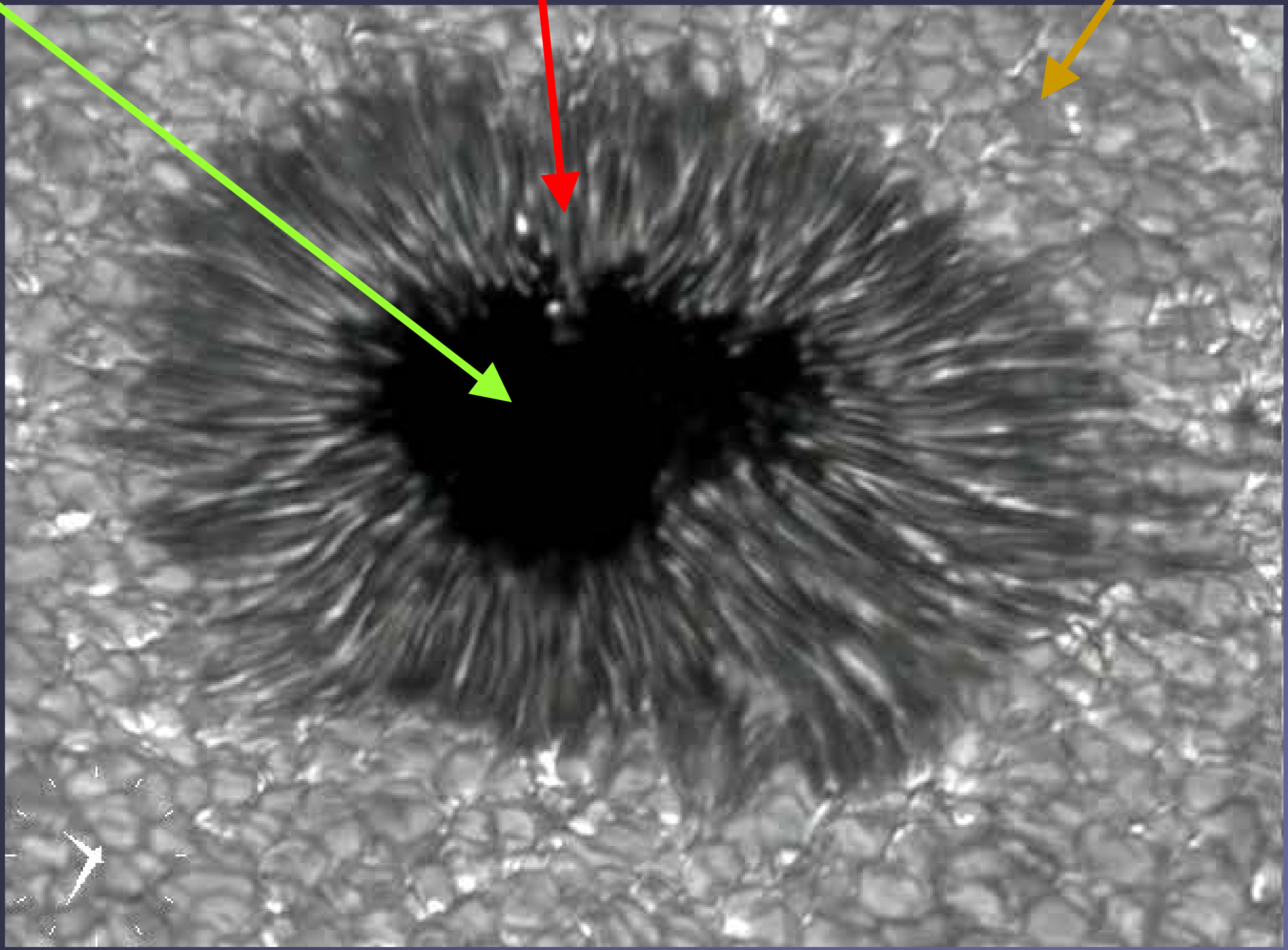

$T_{\mathrm{eff}} \approx 4500$ K

$T_{\mathrm{eff}} \approx 5500$ K

$T_{\mathrm{eff}} \approx 5800$ K

Evershed effect

- Observation: Penumbra seen at $\mu<1$ shows
  - on limb side: Doppler red shift
  - on disc side: Doppler blue shift
- Interpretation: horizontal OUTflow of material from inner penumbra to outer
- Low resolution: 1-2 km/s, high resolution: supersonic

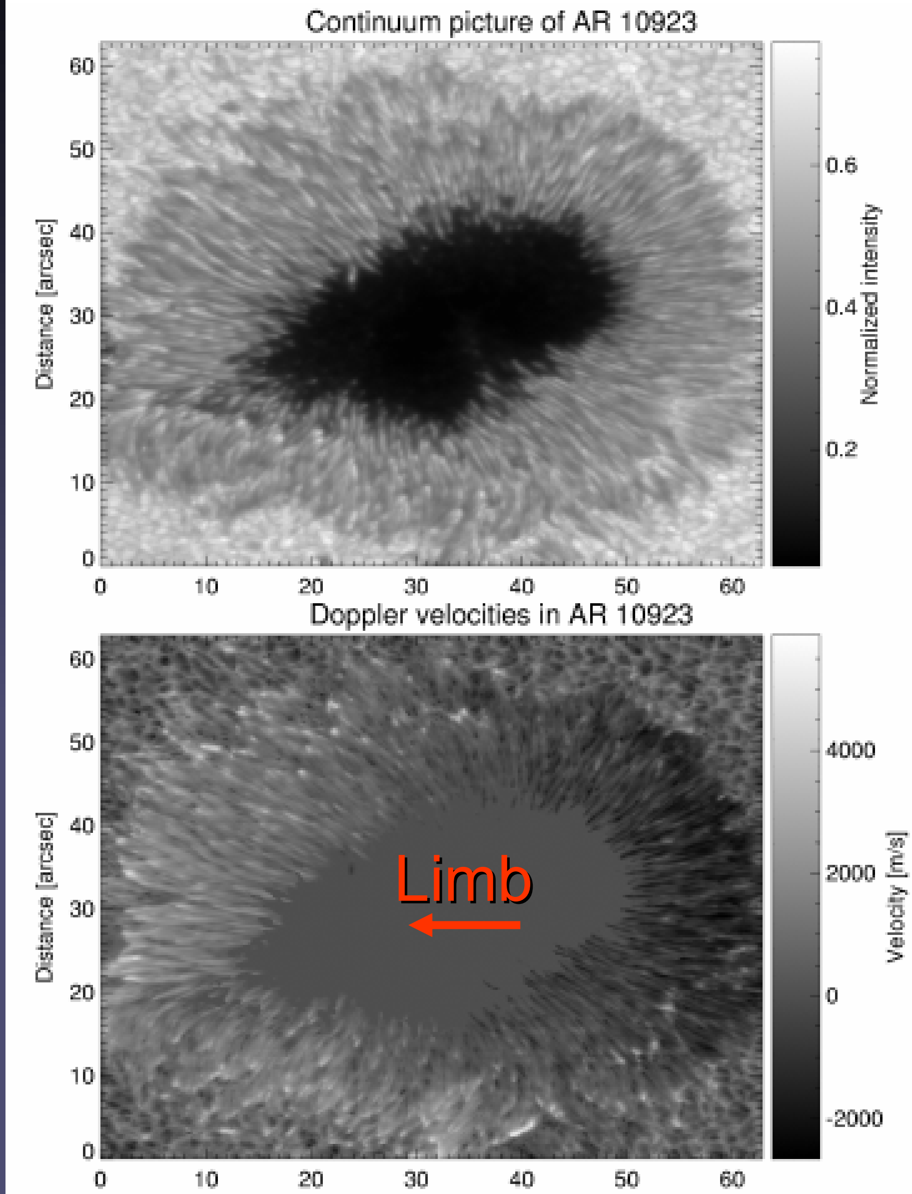

bright: redshift, dark: blueshift

Regimes of solar magnetoconvection

Magnetic activity in cool stars is driven by the interaction of the magnetic field with convection, i.e. magnetoconvection

Sunspots allow us to probe magneto-convection for stronger fields, on larger scales than other magnetic features

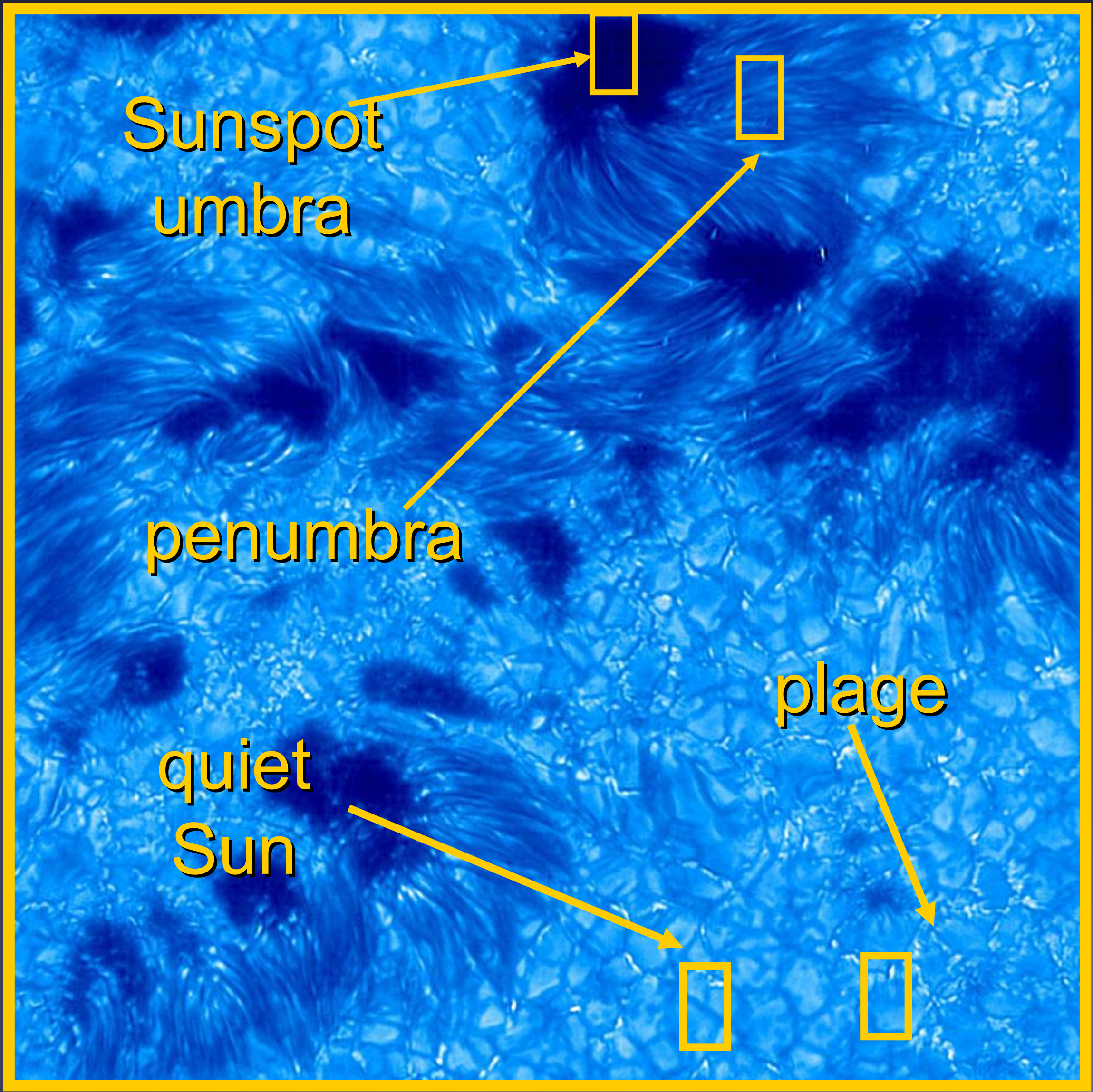

Sunspots, some properties

- Field strength: Peak values 2000-4000 G
- Brightness: umbra: 20% of quiet Sun, penumbra: 75%
- Sizes: Log-normal size distribution. Overlap with pores (log-normal = Gaussian on a logarithmic scale)
- Lifetimes: τ between hours & months: Gnevyshev-Waldmeier rule: $A_{max} \sim \tau$, where A_{max} = max spot area.

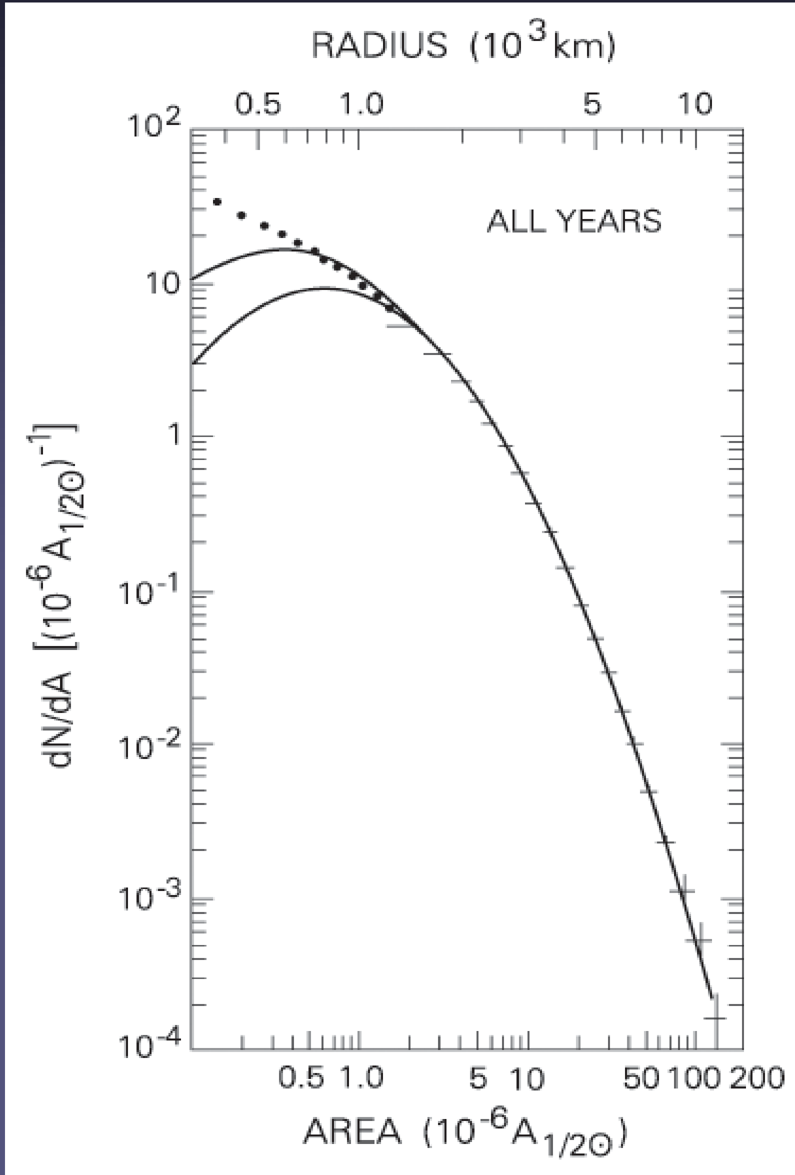

Magnetic structure of sunspots

- B drops steadily from 2000 – 4000 G in umbra towards boundary, $B(R_{\mathrm{spot}}) \approx 1000$ G
- At centre, field is vertical. It becomes almost horizontal near R_{spot}
- Regular spots have a field structure similar to a buried dipole

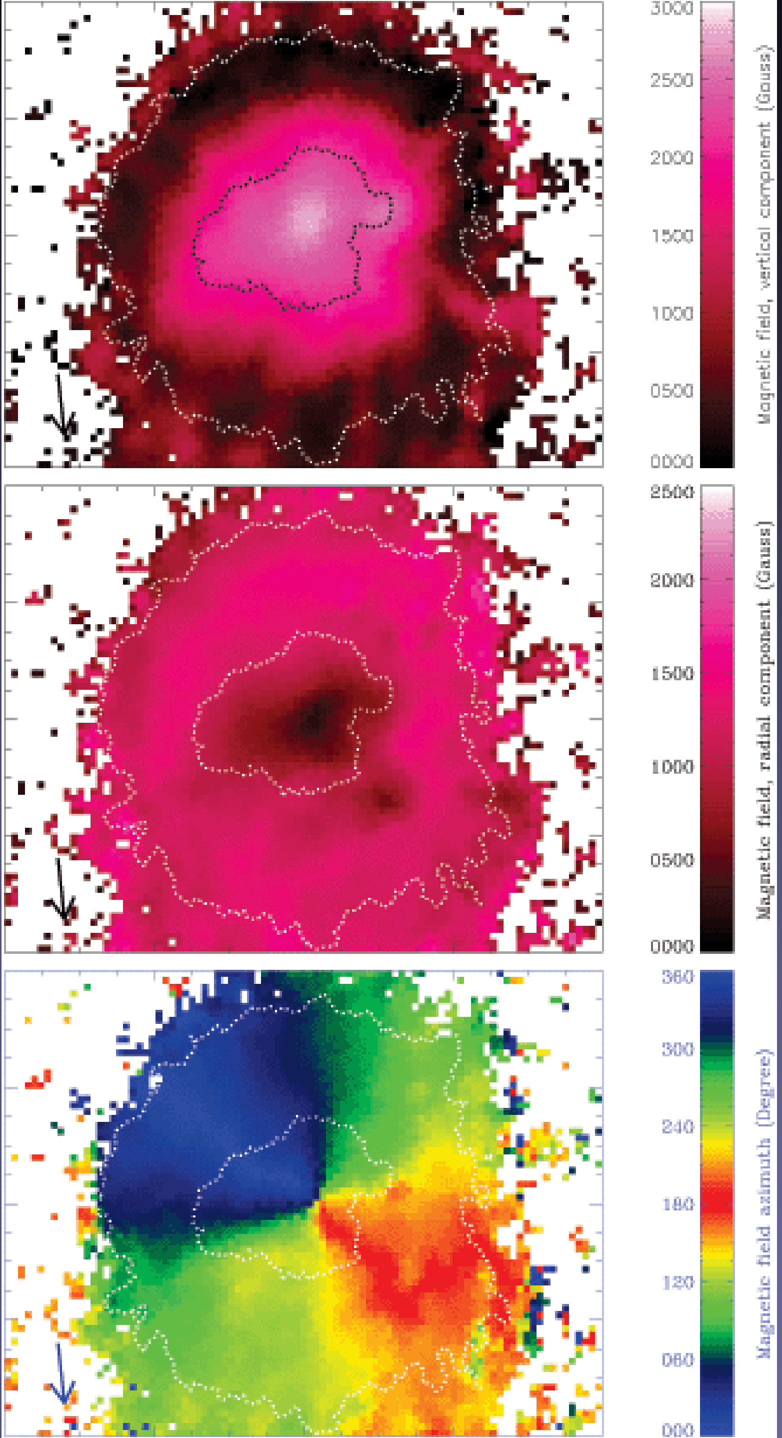

Magnetic flux tubes

- Sunspots are intersections of the solar surface with large magnetic flux tubes
- In CZ and in photosphere most magnetic energy is in concentrated magnetic flux tubes (bounded by topologically simple surface=current sheet)
- Pressure balance: $\frac{B_1^2}{8\pi} + P_1 = P_2 + \frac{B_2^2}{8\pi}$
- Thick flux tubes such as spots, $R > H_P$, where H_P is the pressure scale height, display strong variation across their cross-section. Pressure balance valid only across boundary.

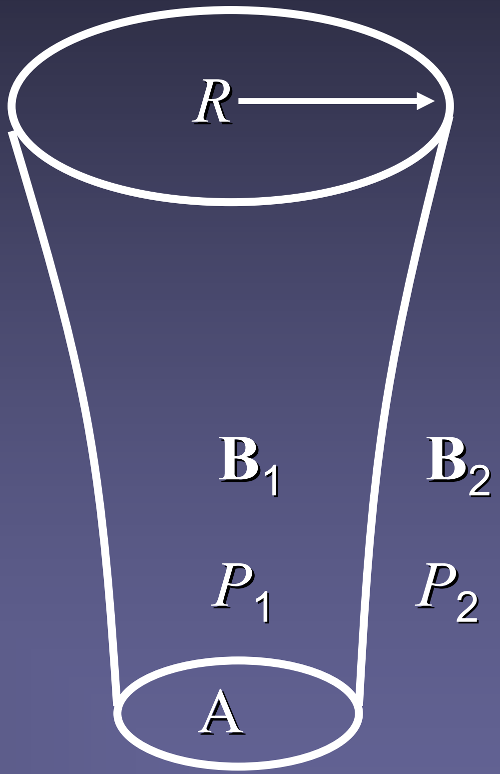

Rump of a flux tube

The Wilson effect

- Near the solar limb the umbra and centre-side penumbra disappear

➔ We see 400-800 km deeper into sunspots than in photosphere

- Correct interpretation by Wilson (18th century).

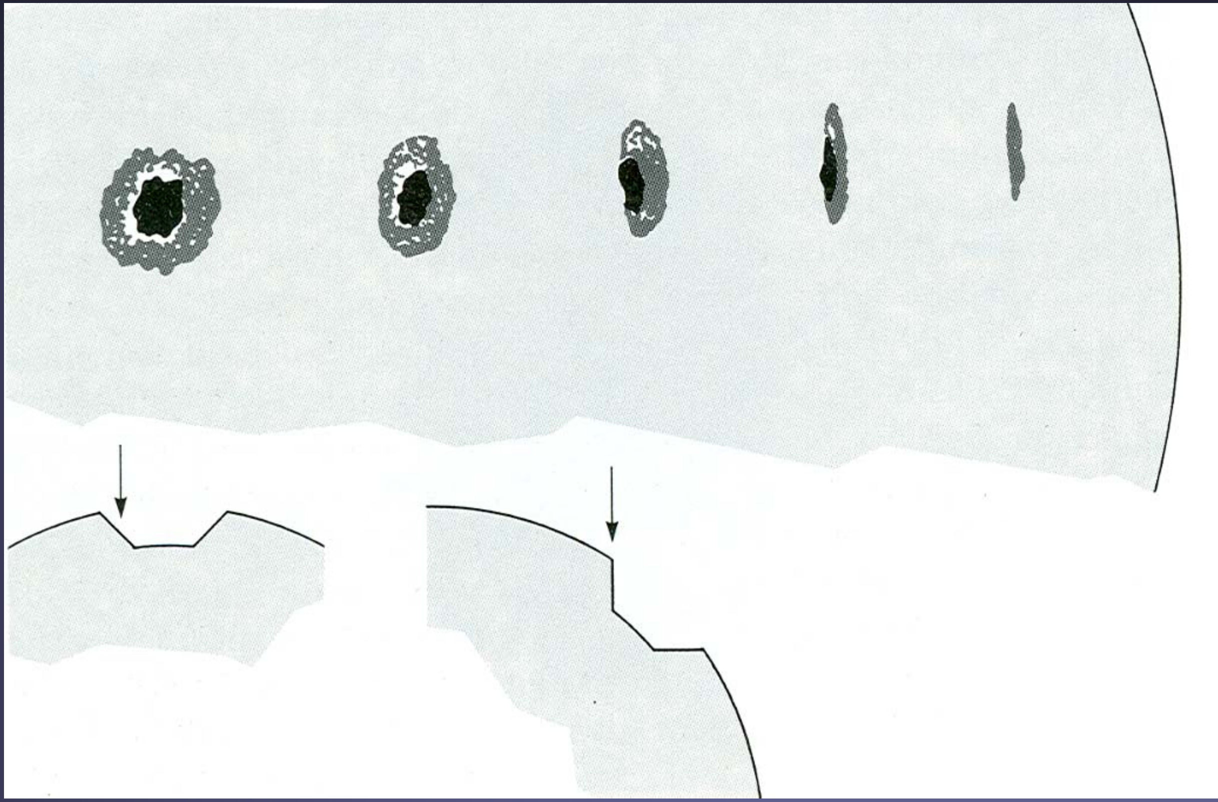

Other interpretation by e.g. W. Herschell: photosphere is a layer of hot clouds through which we see deeper, cool layers: the true, populated surface of the Sun.

Why do we see deeper inside sunspots, or what causes the Wilson effect?

- Darkness: Opacity in the solar photosphere is due to the H^- ion, which depends strongly on temperature. In sunspots temperature is lower ➔ opacity is lower ➔ we see deeper. Responsible for ≈½ of observed effect
- Magnetic field: Magnetic field produces a pressure ~$B^2/8\pi$. Due to pressure balance with surroundings:

$$\frac{B_{\text{spot}}^2}{8\pi} + P_{\text{spot}} = P_{\text{surr}} \rightarrow P_{\text{spot}} << P_{\text{surr}} \rightarrow \rho_{\text{spot}} << \rho_{\text{surr}}$$

Opacity in spot is decreased. Responsible for ½ of observed effect

Why are sunspots dark?

- Basically the strong magnetic field, not allowing motions across the field lines, quenches convection inside the spot.
- Since convection is the main source of energy transport just below the surface, less energy reaches the surface through the spot → dark

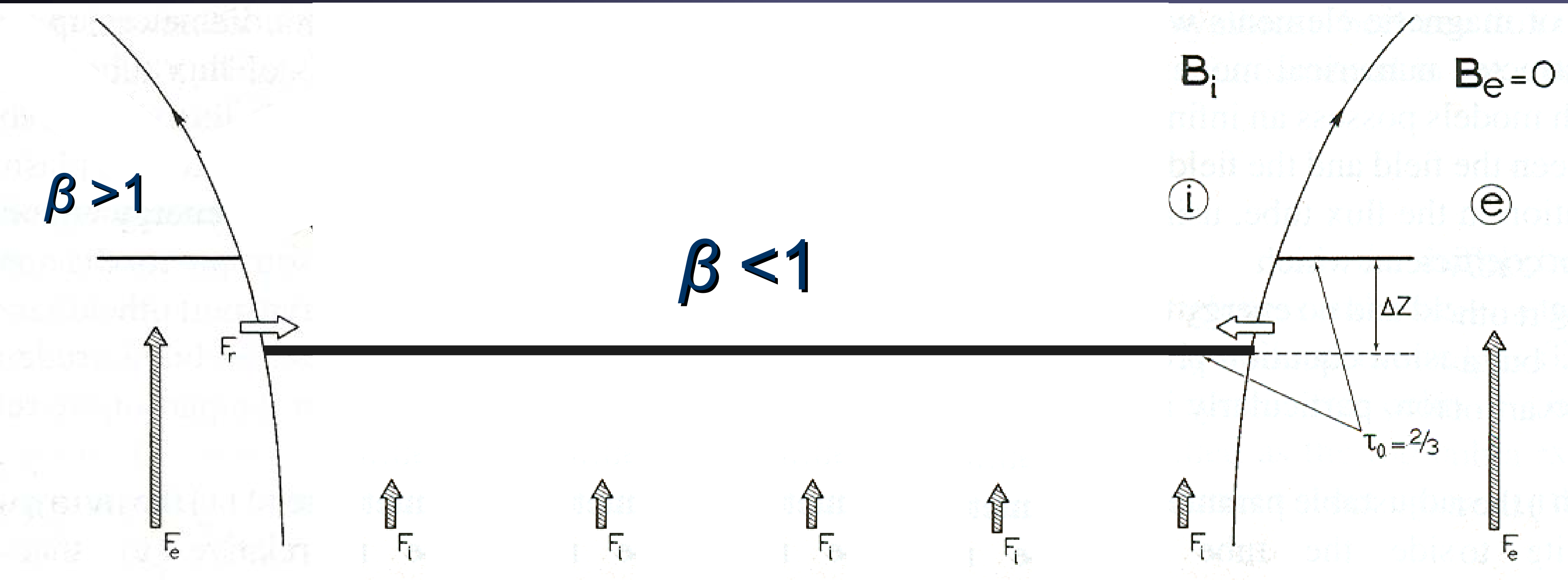

Why are sunspots dark? II

- Where does the energy blocked by sunspots go? Spruit (1982)

→ Short diffusive timescale of CZ: blocked heat is redistributed in CZ within 1 month – 1 year (at most only very weak bright rings around sunspots)

Large heat capacity of CZ: the additional heat does not lead to a measurable increase in temperature

- Long time scale for thermal relaxation of the CZ (Kelvin-Helmholtz timescale): 10^5 years → excess energy is released almost imperceptibly (KH timescale: how long can Sun shine using only its gravitational energy)

Solar irradiance during passage of a sunspot group

- The Sun as a whole darkens when spots move across its disc
- I.e. the blocked heat does not reappear somewhere else on a timescale of days to weeks

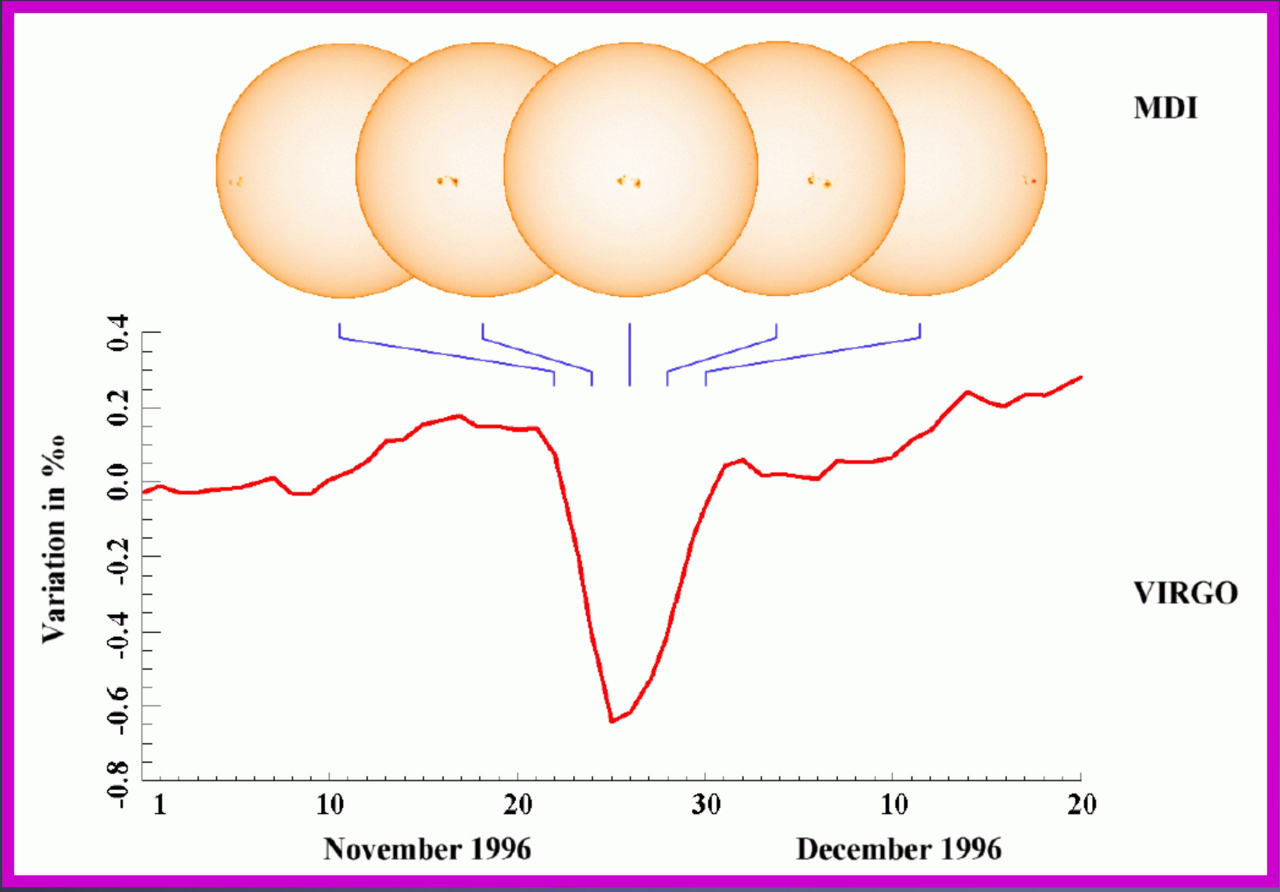

Why are sunspots so bright?

- Sunspot umbra:
  - 20% of photospheric radiative flux
  - 2000-4000 G mainly vertical field

- Sunspot penumbra:
  - 75% of photospheric radiative flux
  - 1000-2000 G complex, more horizontal field

- For both: normal convection completely quenched (Gough & Tayler 1966). Radiation carries <10% of energy from solar interior.

➔ Some form of magnetoconvection must be acting at small scales that transports the missing energy flux

Current view of fine-structure of penumbra

Penumbra is bigger hurdle than umbra (75% of energy flux) and much more controversial

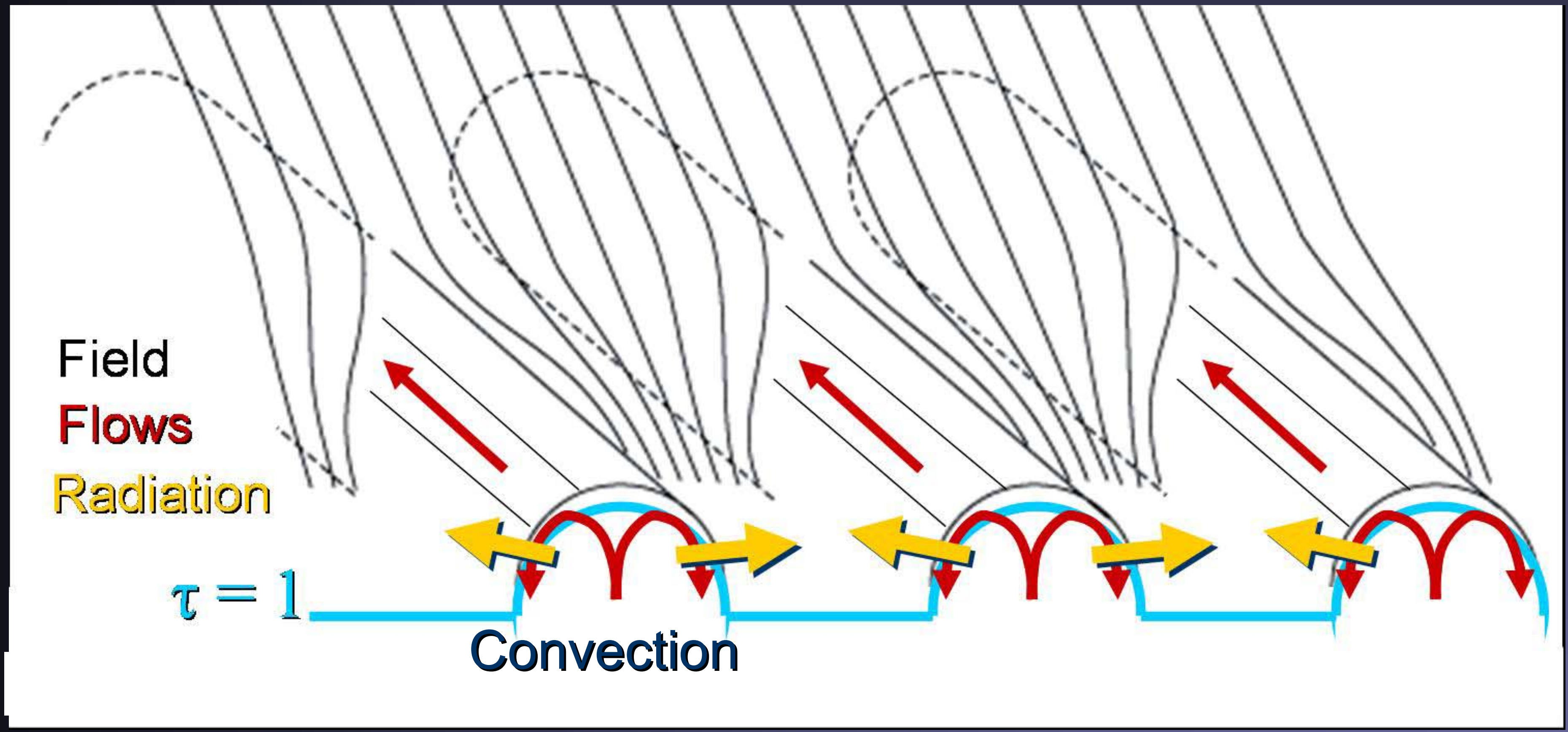

Zakharov et al. 2008, Rempel et al. 2008

MHD simulation of a sunspot

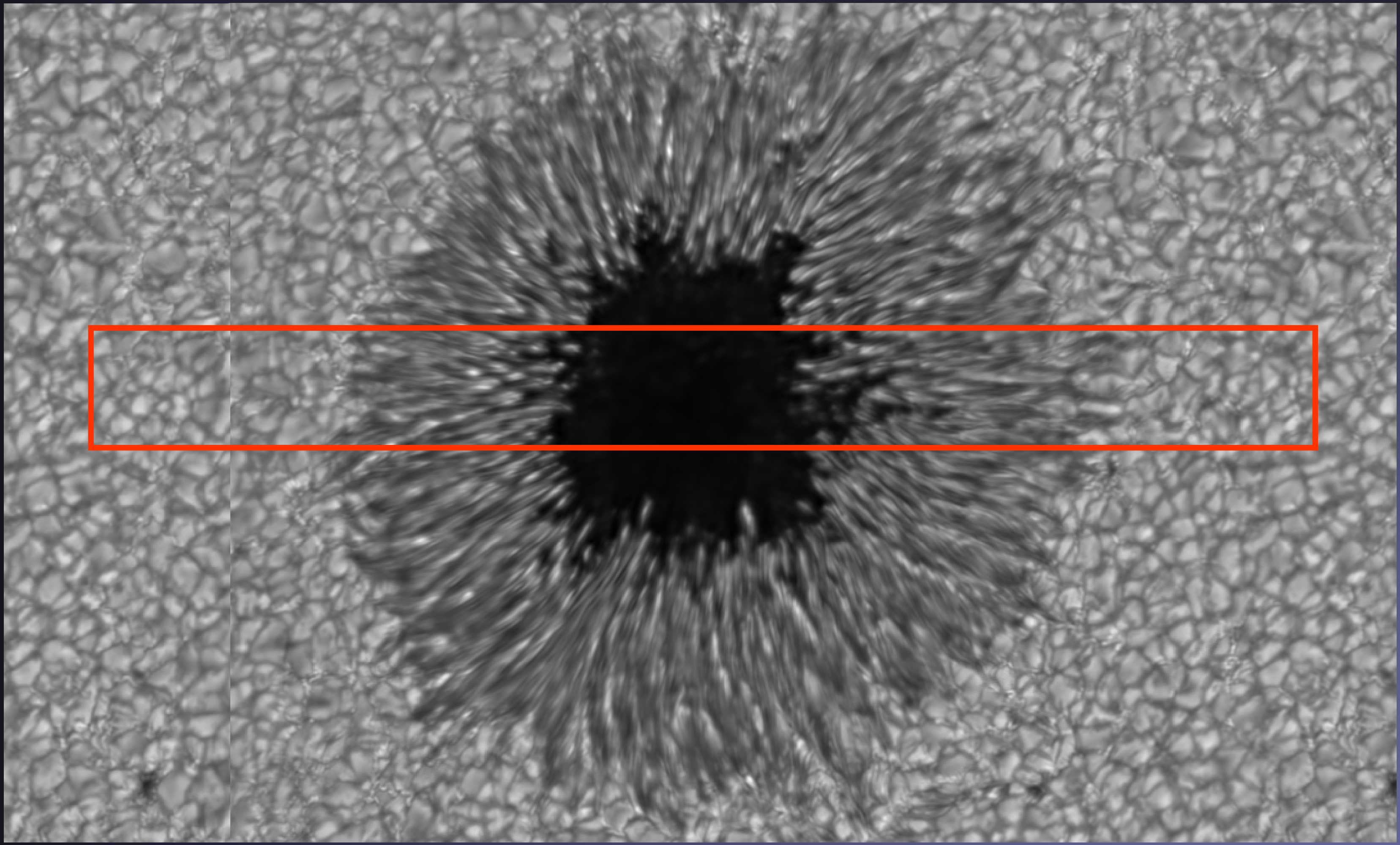

Red box represents the simulation box overlain on image of an observed spot

Detailed structure of a penumbral filament

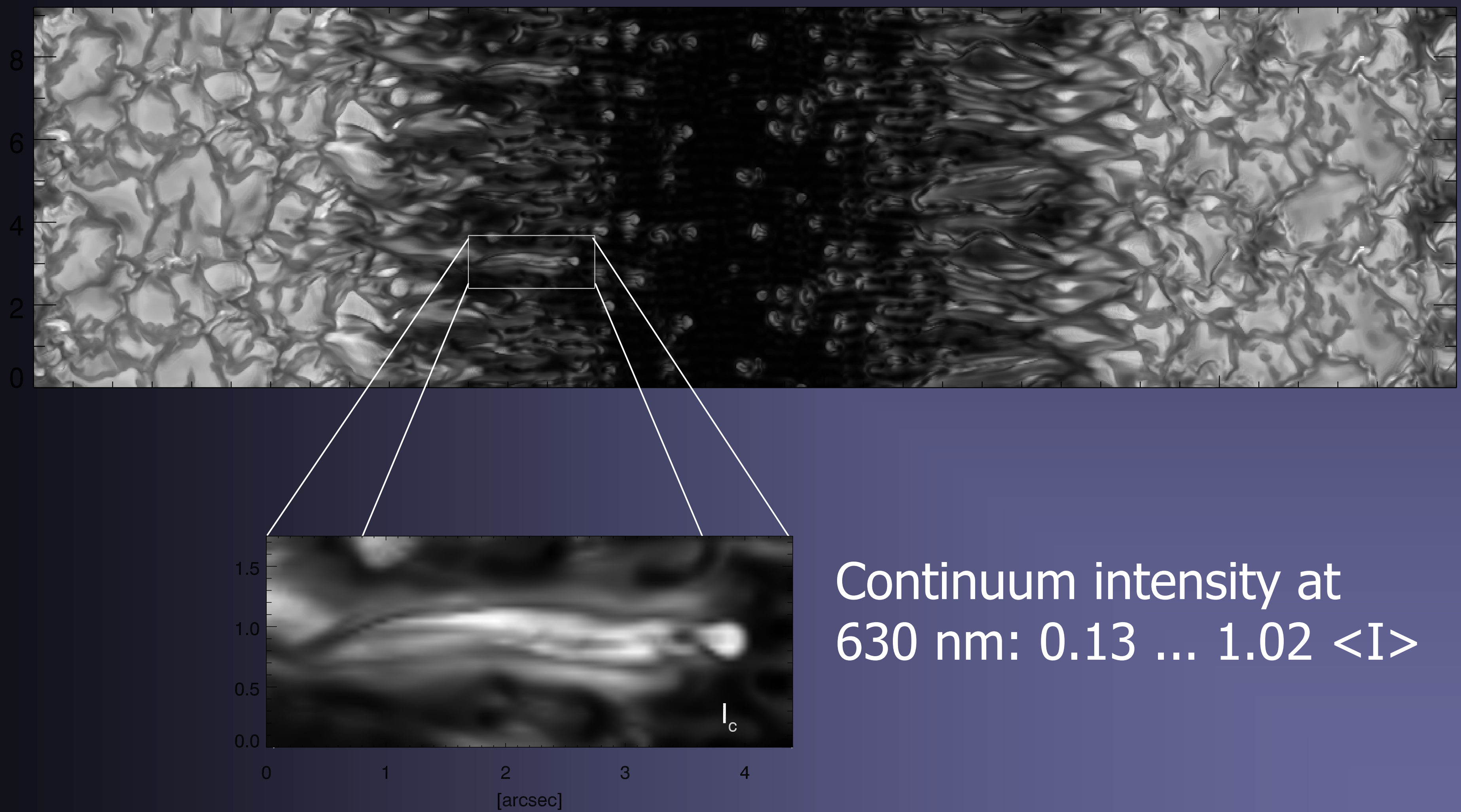

Continuum intensity at 630 nm: 0.13 ... 1.02 <I>

Cuts perpendicular to the filament

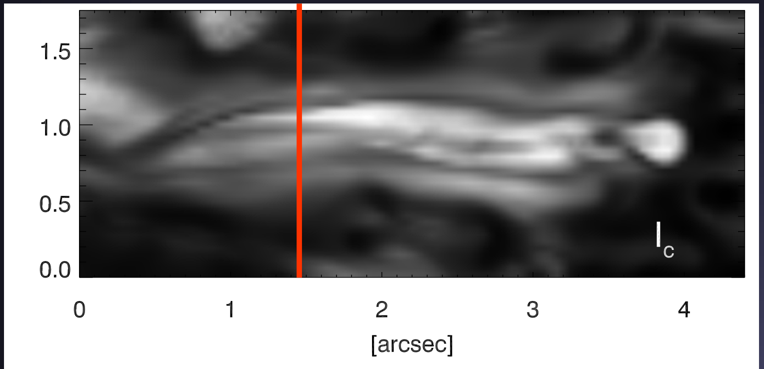

The filament is formed by a hot, sheet-like convective upflow that turns over and flows down at the sides of the filament

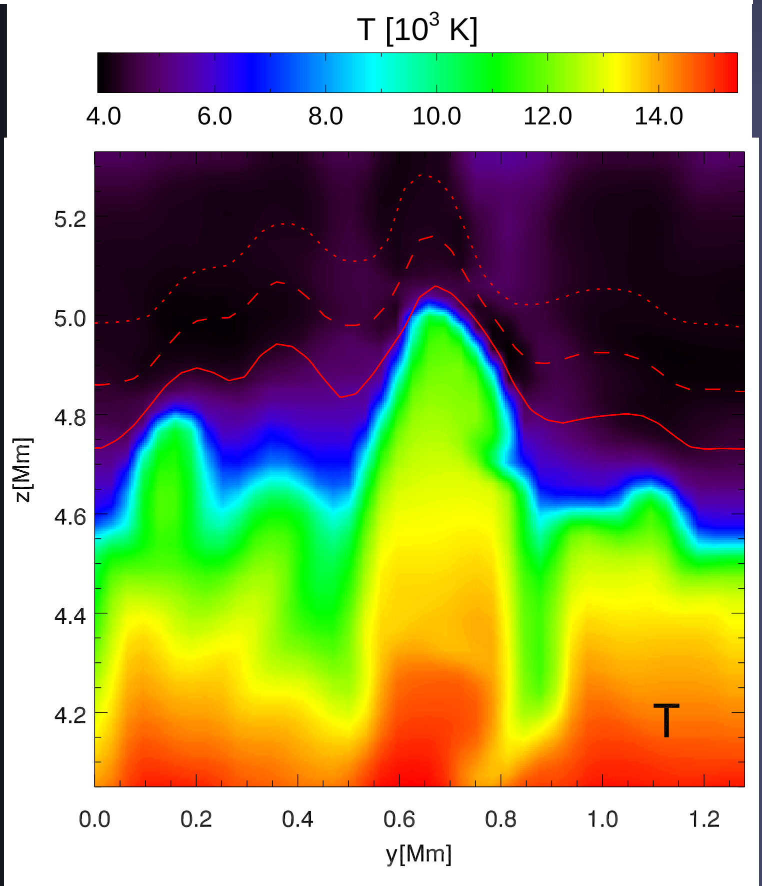

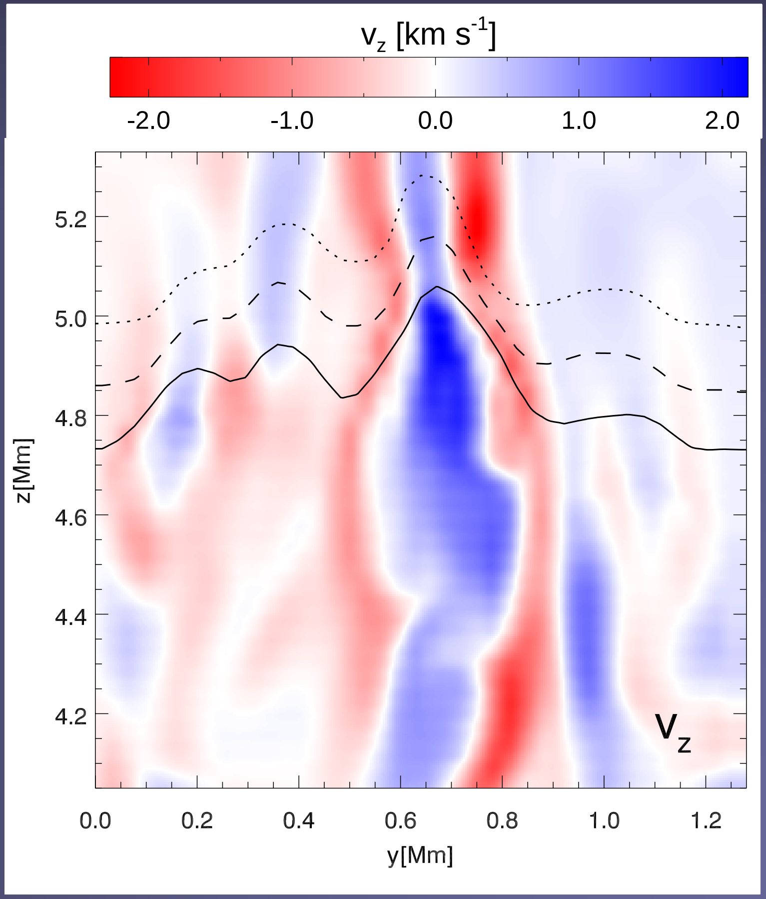

Cuts perpendicular to the filament

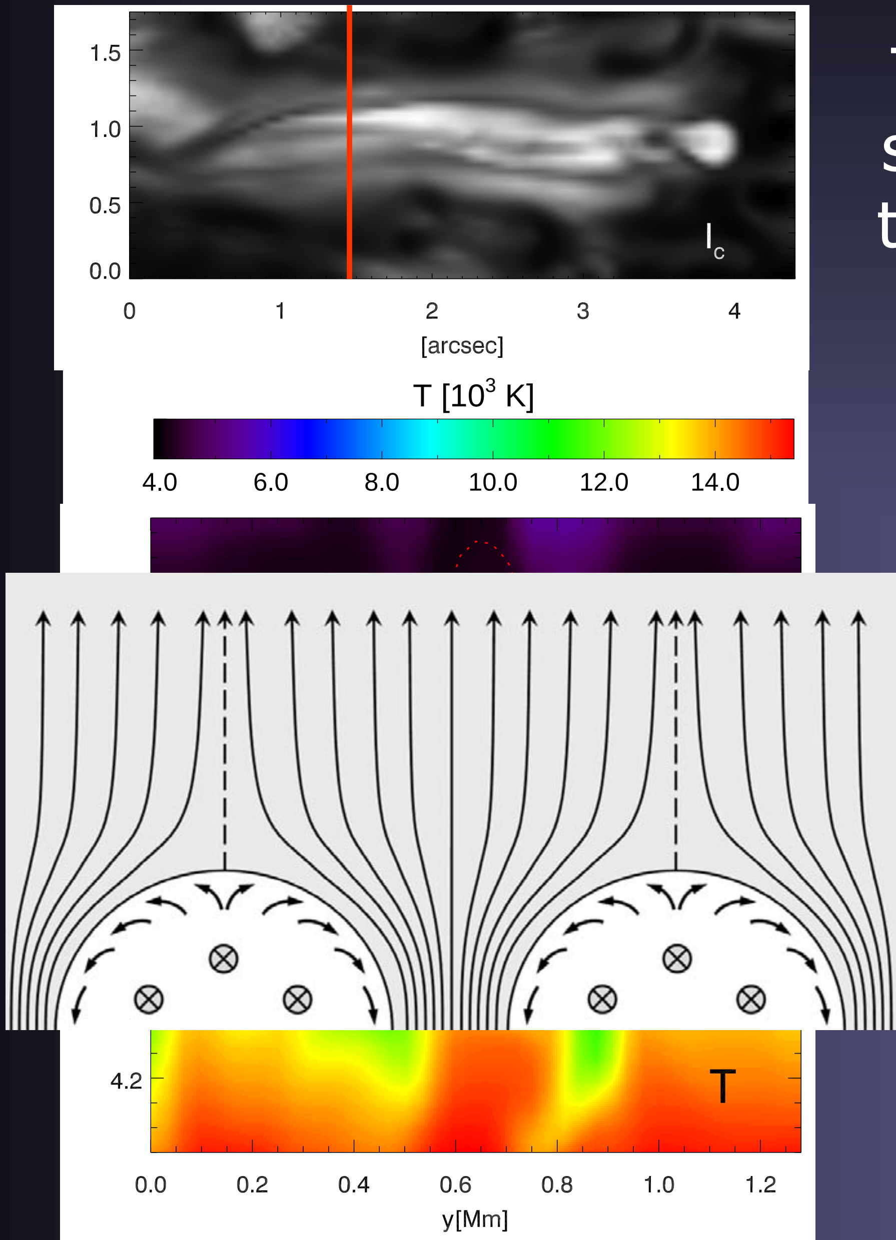

The filament is formed by a hot, sheet-like convective upflow that turns over and flows down at the sides of the filament

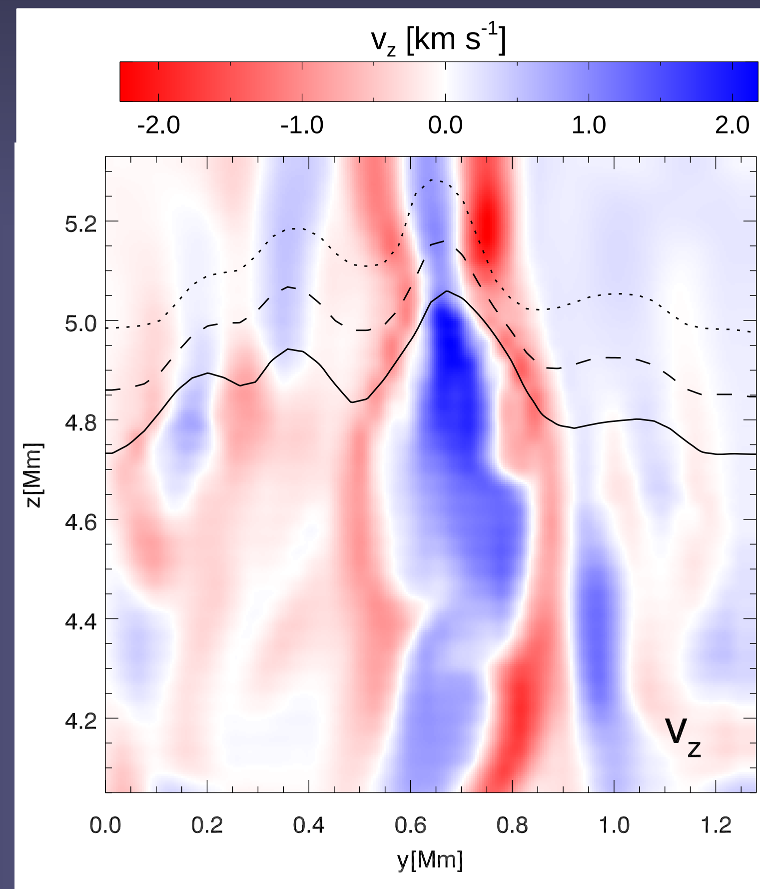

Non-spot magnetic fields

Non-spot fields

- Sunspots cover in general <0.2% of solar surface
- What about the remaining 99.8%?
- What are plage or facular regions & network composed of?

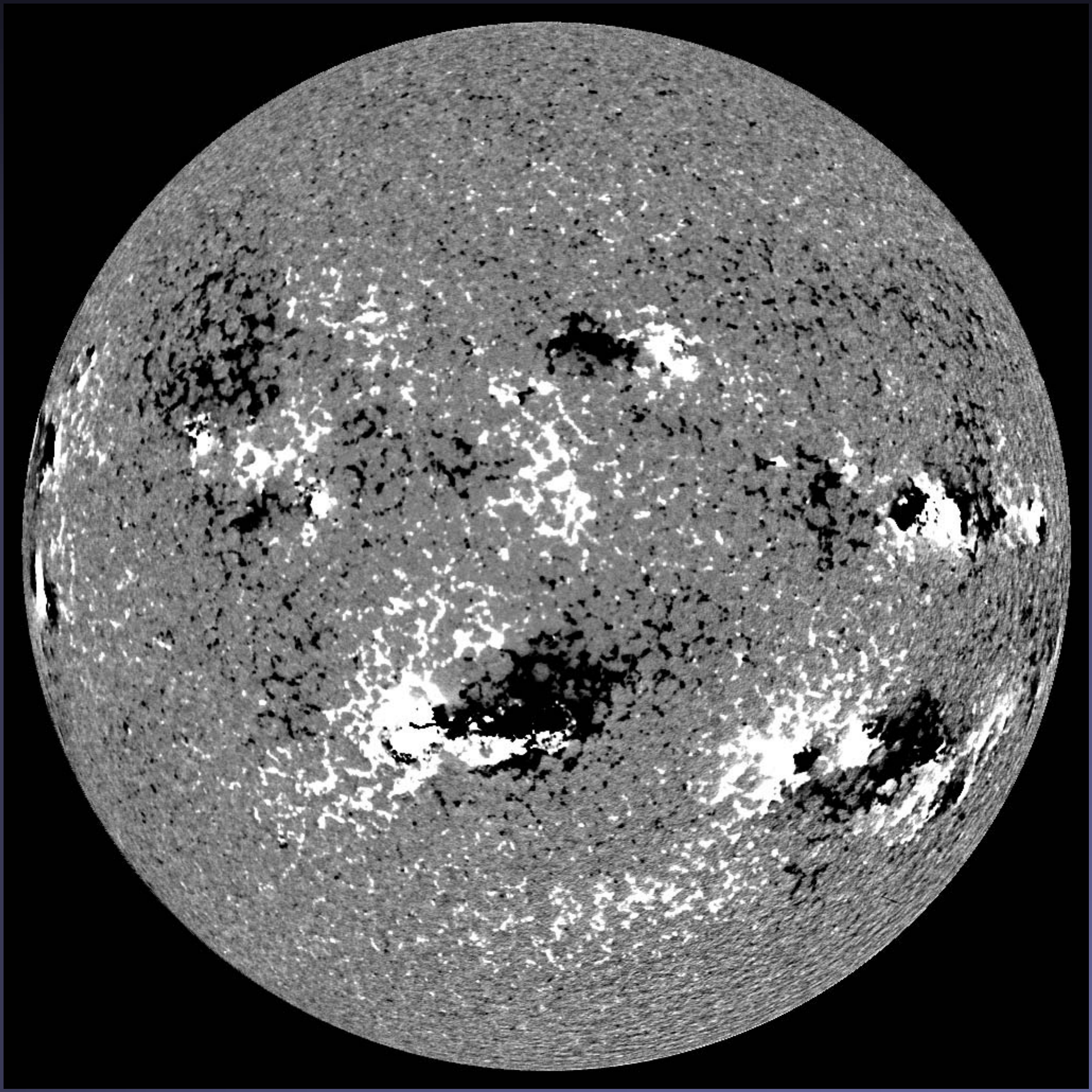

Facular fields

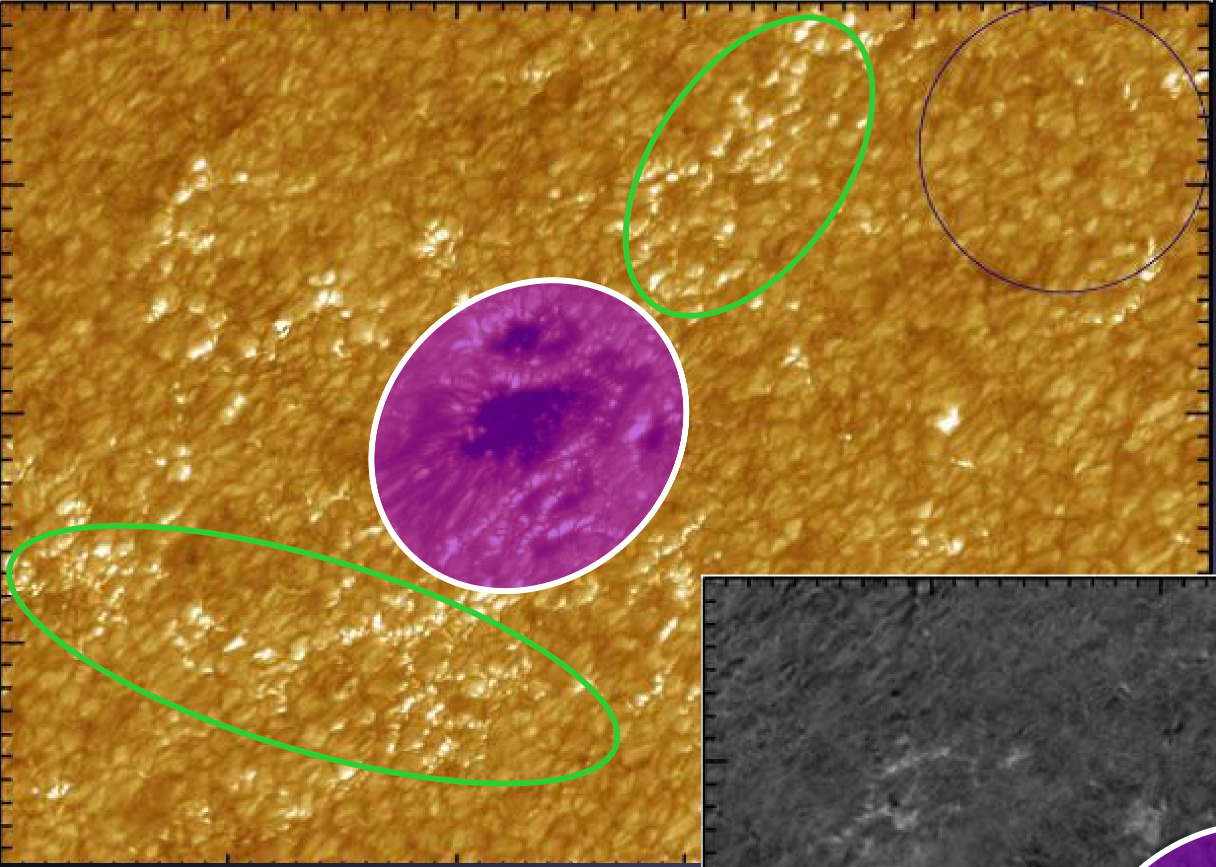

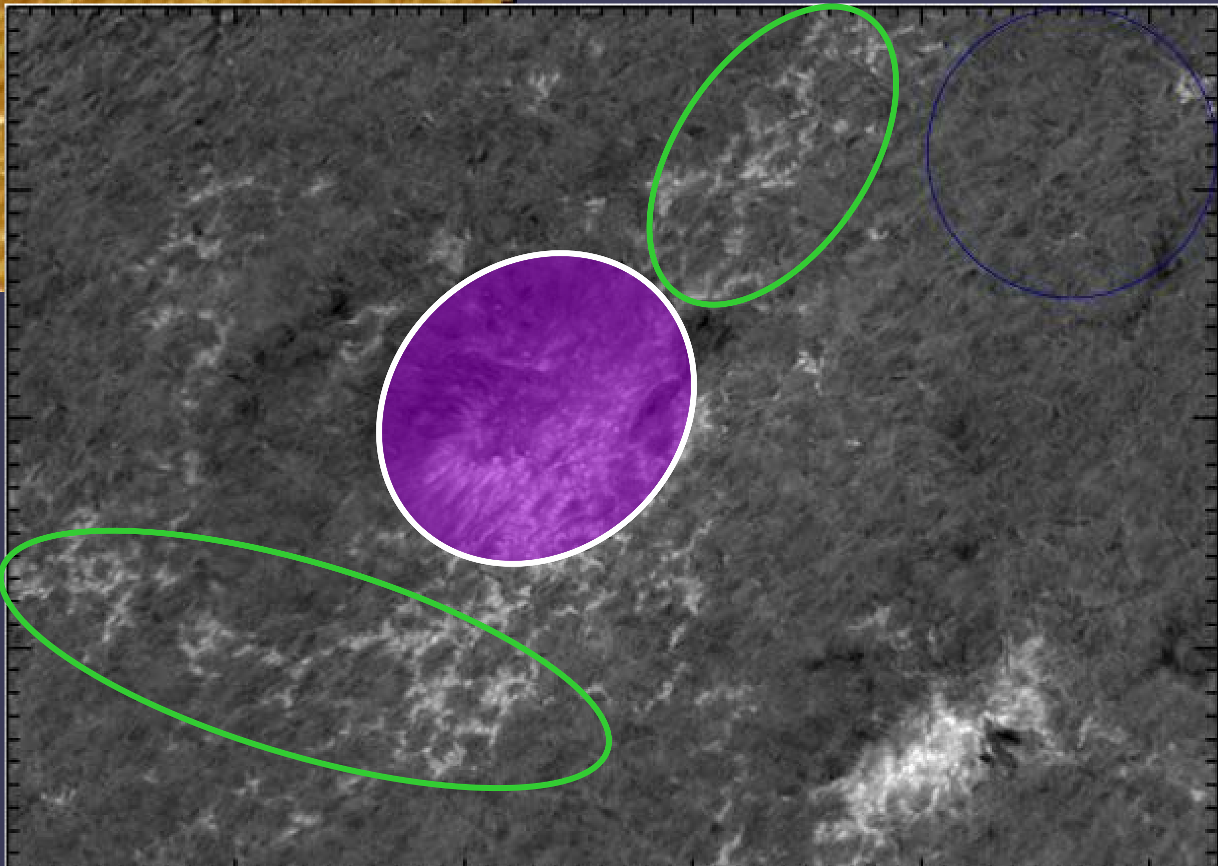

Facular fields are composed of magnetic elements, small (<300 km diameter) flux tubes.

Magnetic flux tubes

- Magnetic elements are intersections of solar surface & small magnetic flux tubes
- Thin flux tubes, $R<H_P$, where H_P is the pressure scale height, display no variation across their cross-section
- Pressure balance: $\dfrac{B_1^2}{8\pi} + P_1 = P_2 + \dfrac{B_2^2}{8\pi}$
- In hydrostatic equilibrium with $T = \text{const}$, $P_1 \sim \exp(-z/H_p)$ ➔ $B_1 \sim \exp(-z/2H_p)$
- Magnetic flux is conserved ➔ $\iint B(x,y,z)\,dxdy = \text{const}$

➔ For thin tube: $BR^2 = \text{const}$ ➔ $R \sim \exp(+z/2H_p)$

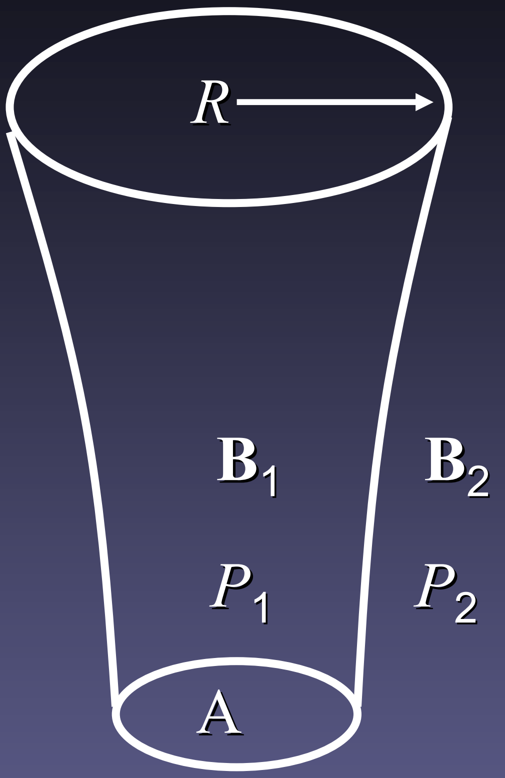

Rump of a flux tube

Temperature contrast vs. size

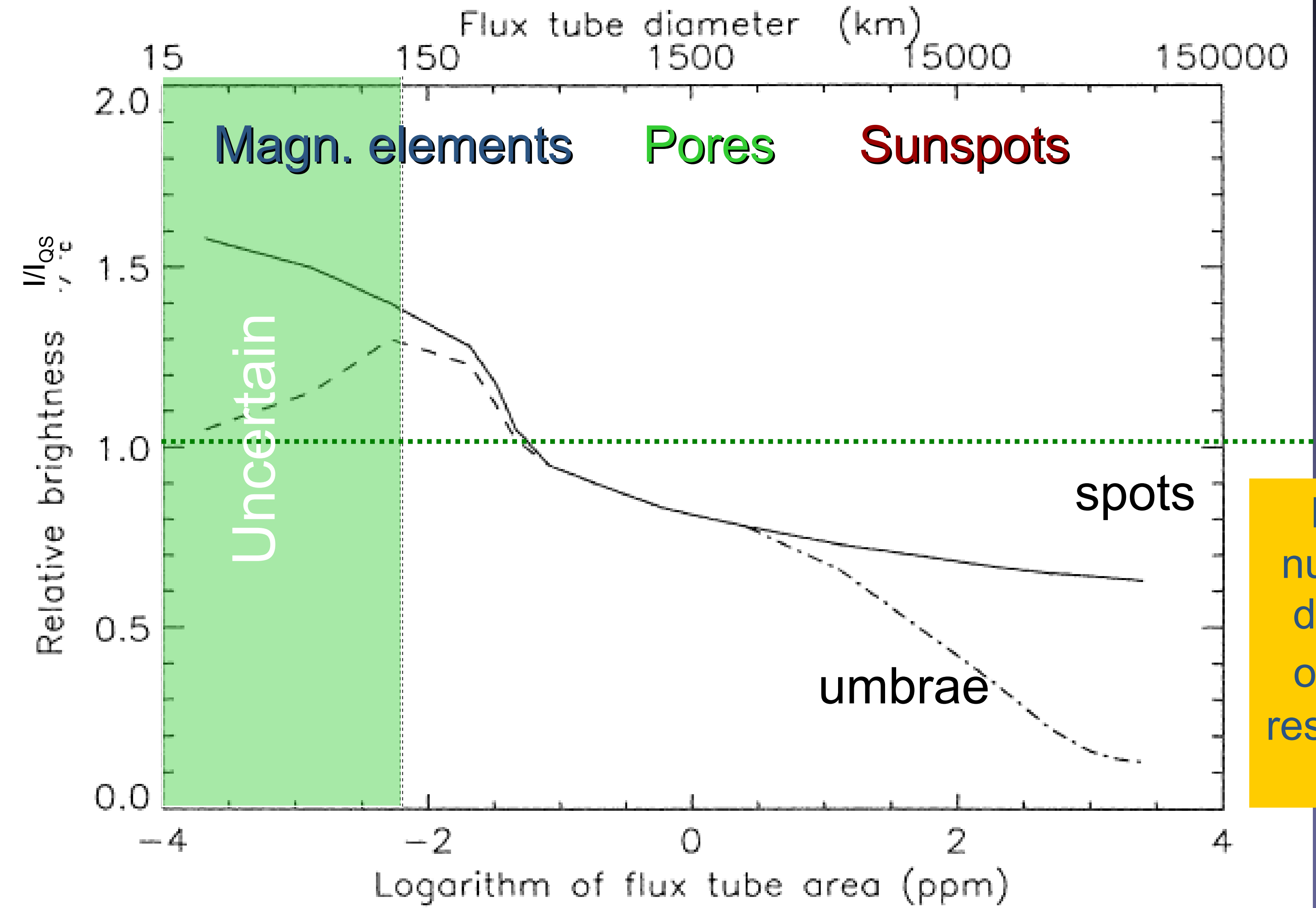

Exact numbers depend on λ, μ, resolution, etc.

Surprisingly constant field strength

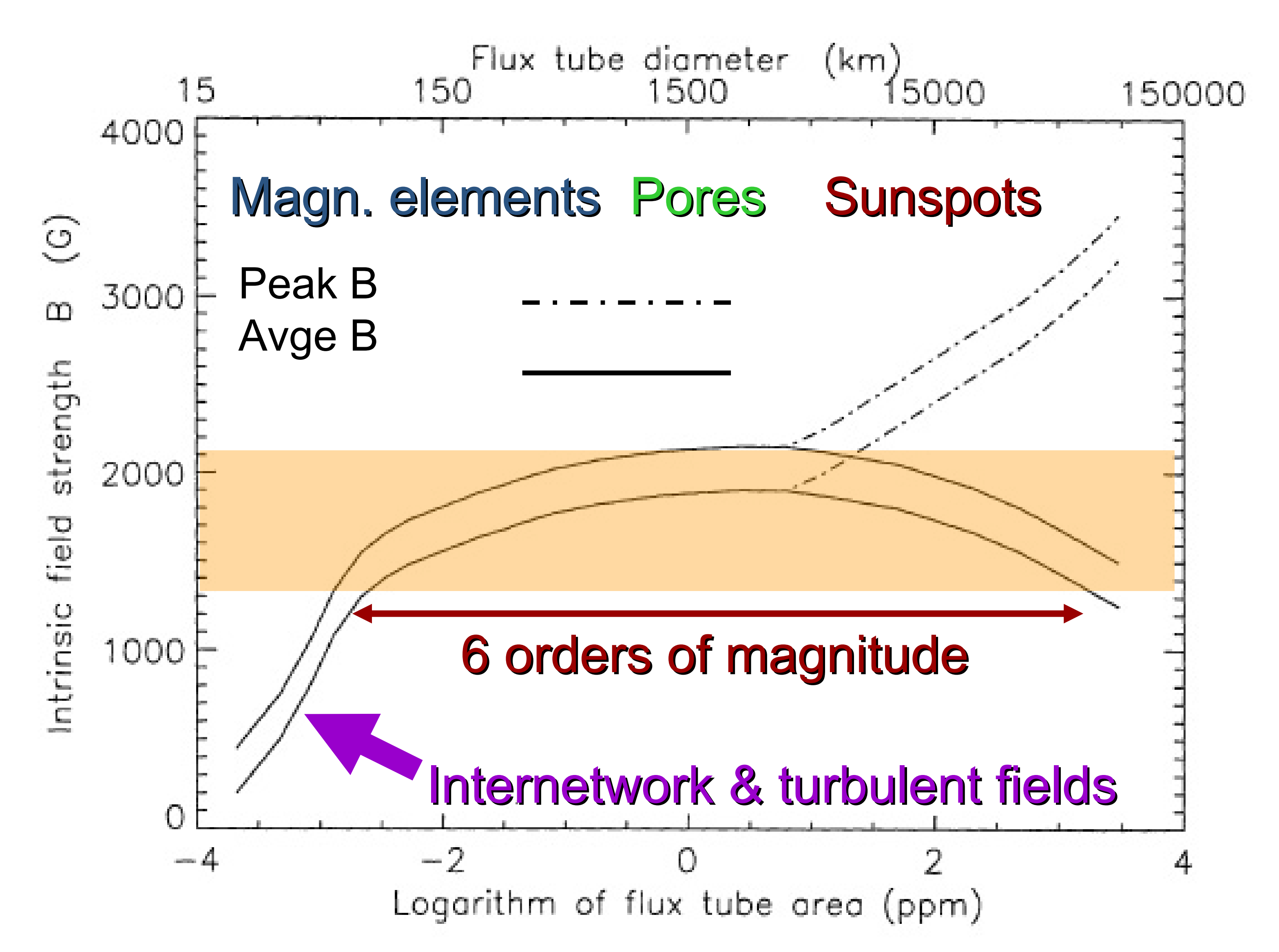

Convective intensification

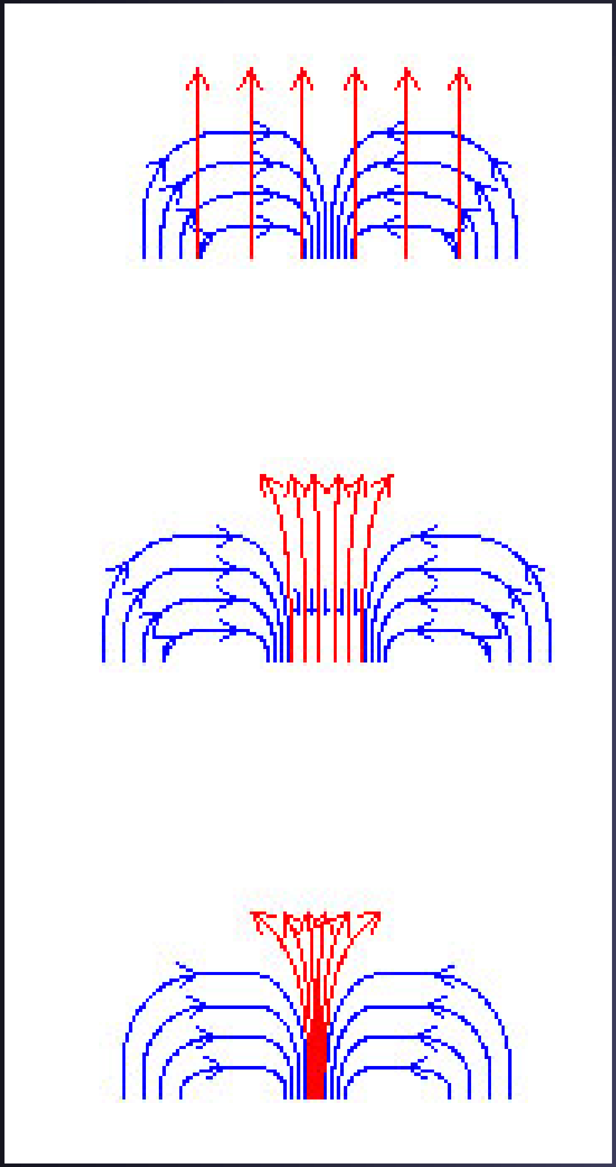

- Flux advection by horizontal flow (flux expulsion)
- Suppression of convection, cooling and downflow
- Evacuation, field intensification

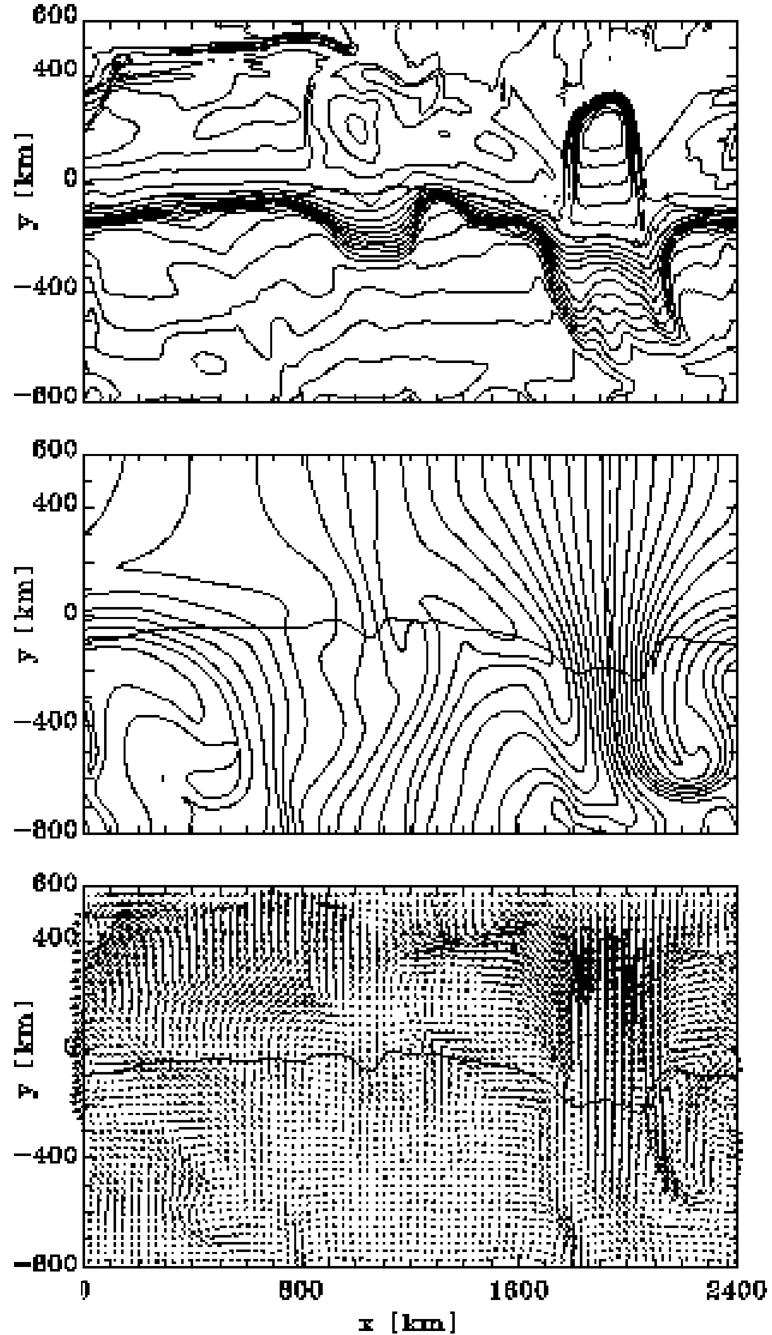

Convective intensification

- 2D, compressible
- radiation, ionization
- 2400 x 1400 km^2
- 240 x 140 points (10 km hor. resol.)
- <B> = 100, 200, 400 G
- collapse + rebound

(Grossmann-Doerth, Schüssler & Steiner, 1998)

t = 100s

Magnetic elements: brightness

- Convection quenched by magnetic field (red arrows) ➔ heat blocked
- Inflow of radiation into evacuated flux tube through hot walls (yellow arrows). Excess heat flux

➔Enhanced emission. Inflow wins since FTs are narrow: diameter ~ Wilson depress.

- Excess energy comes partly from deep CZ (over Kelvin-Helmholtz timescale

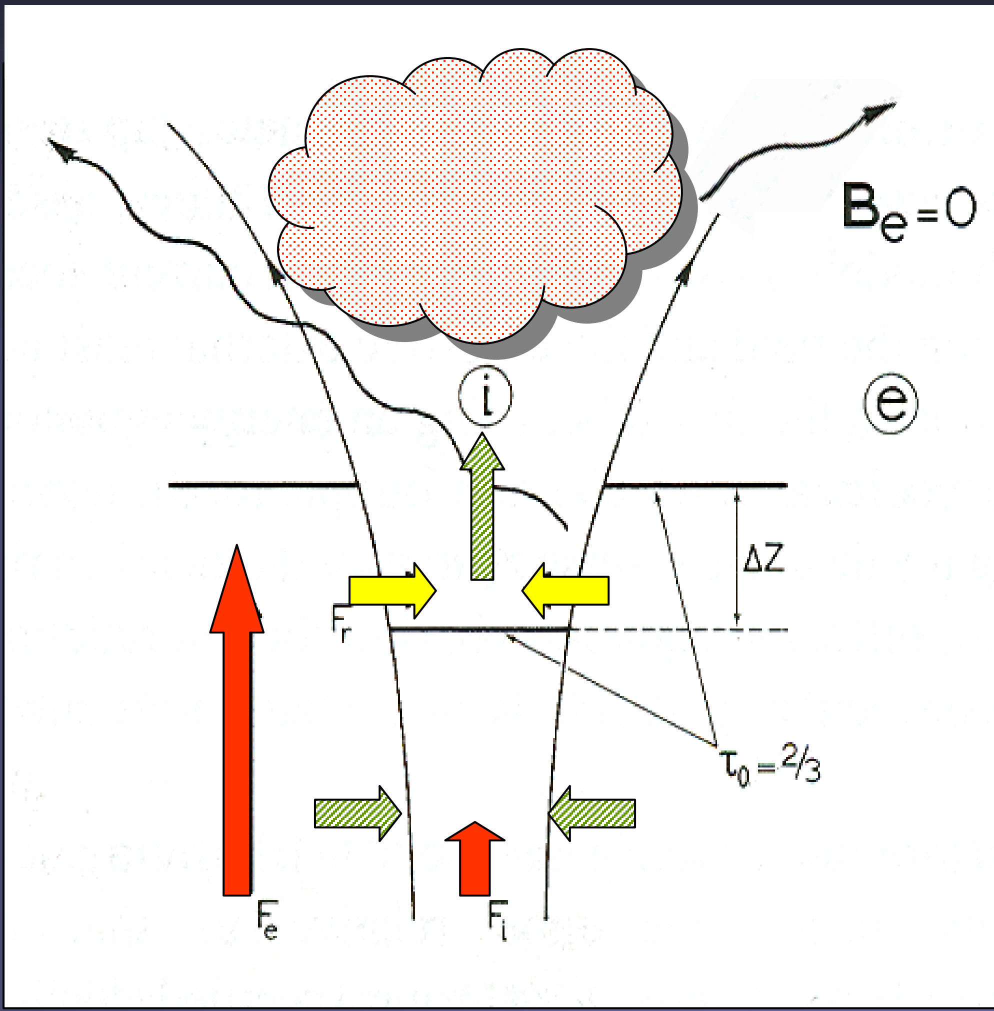

Faculae lead to brightening of the whole Sun

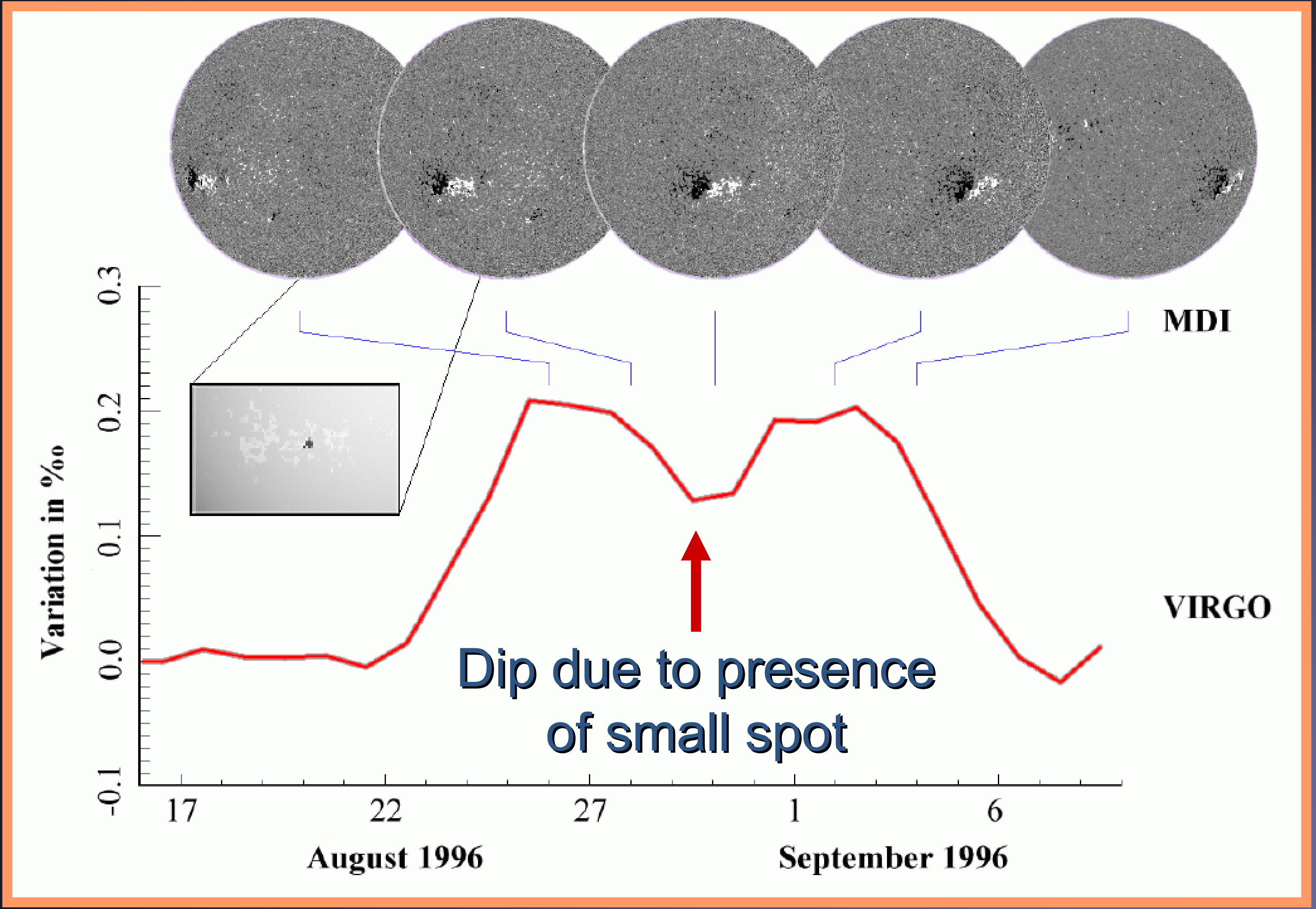

Why are faculae best seen near limb?

The Sun in White Light, with limb darkening removed

MDI on SOHO

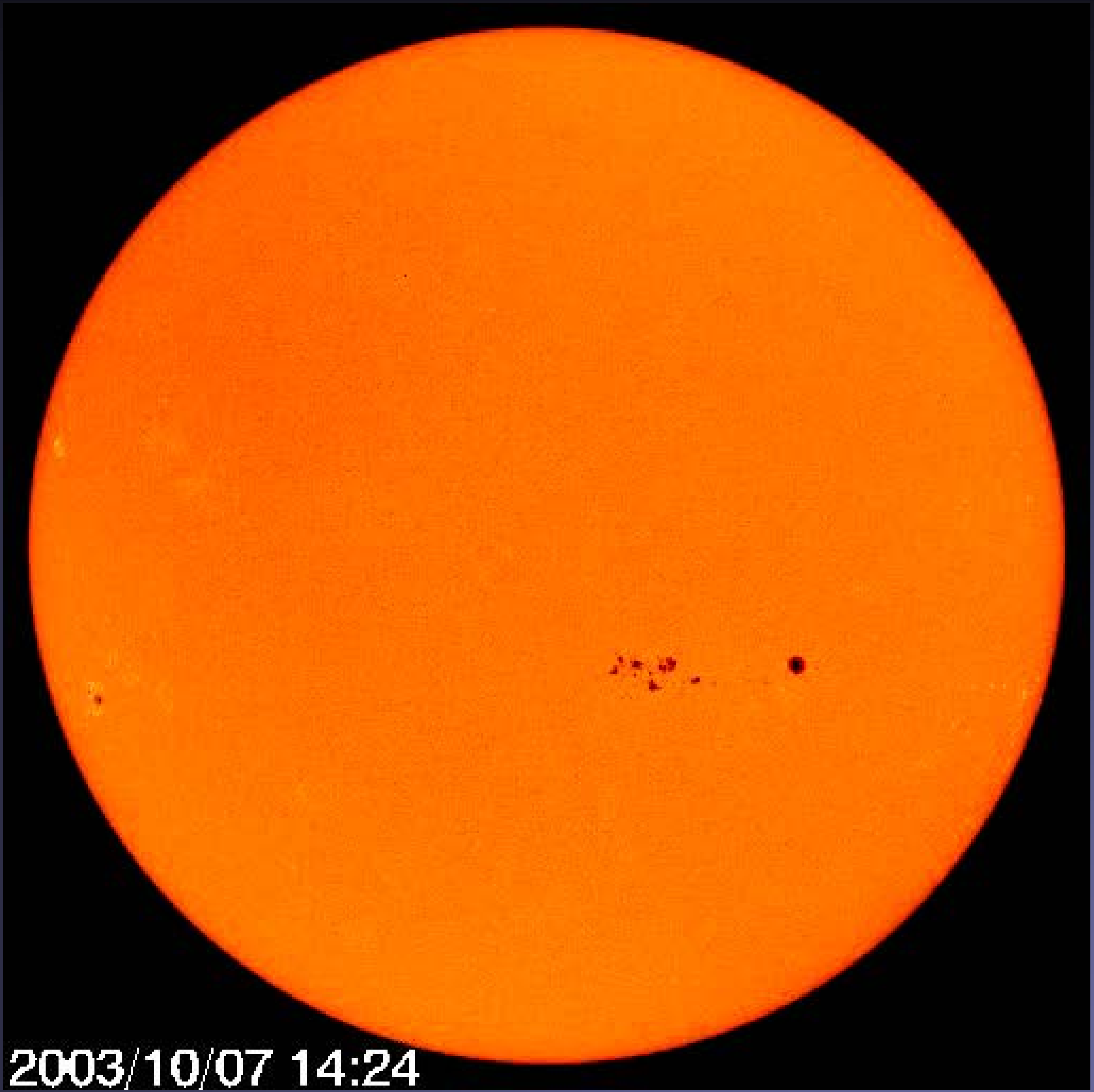

Flux-tube brightening near limb

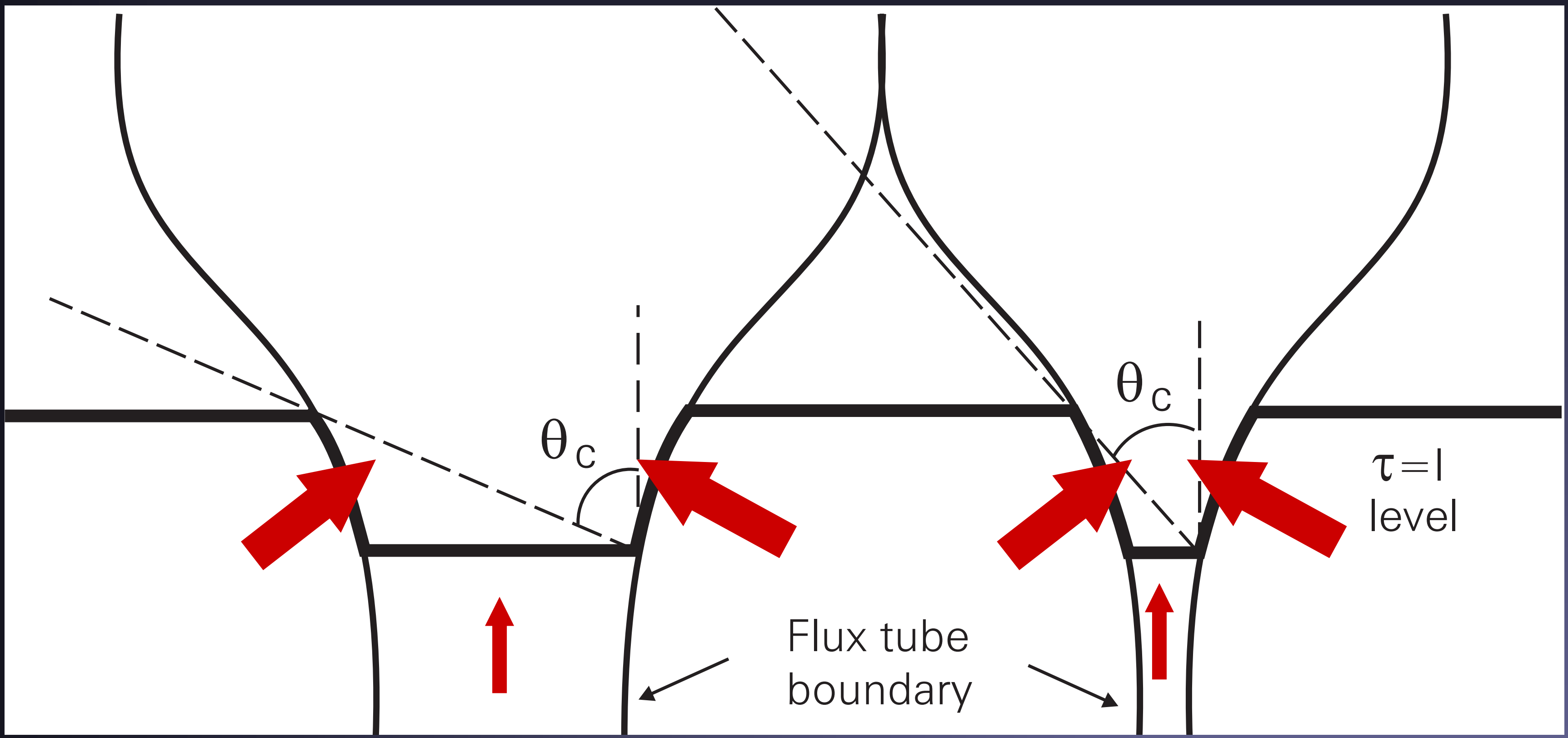

- The flux tubes expand with height (pressure balance
- Most energy radiates into them through walls, which are hot.
- They appear brightest when hot walls are well seen, i.e. near limb (closer to limb for larger tubes)

Facular brightening

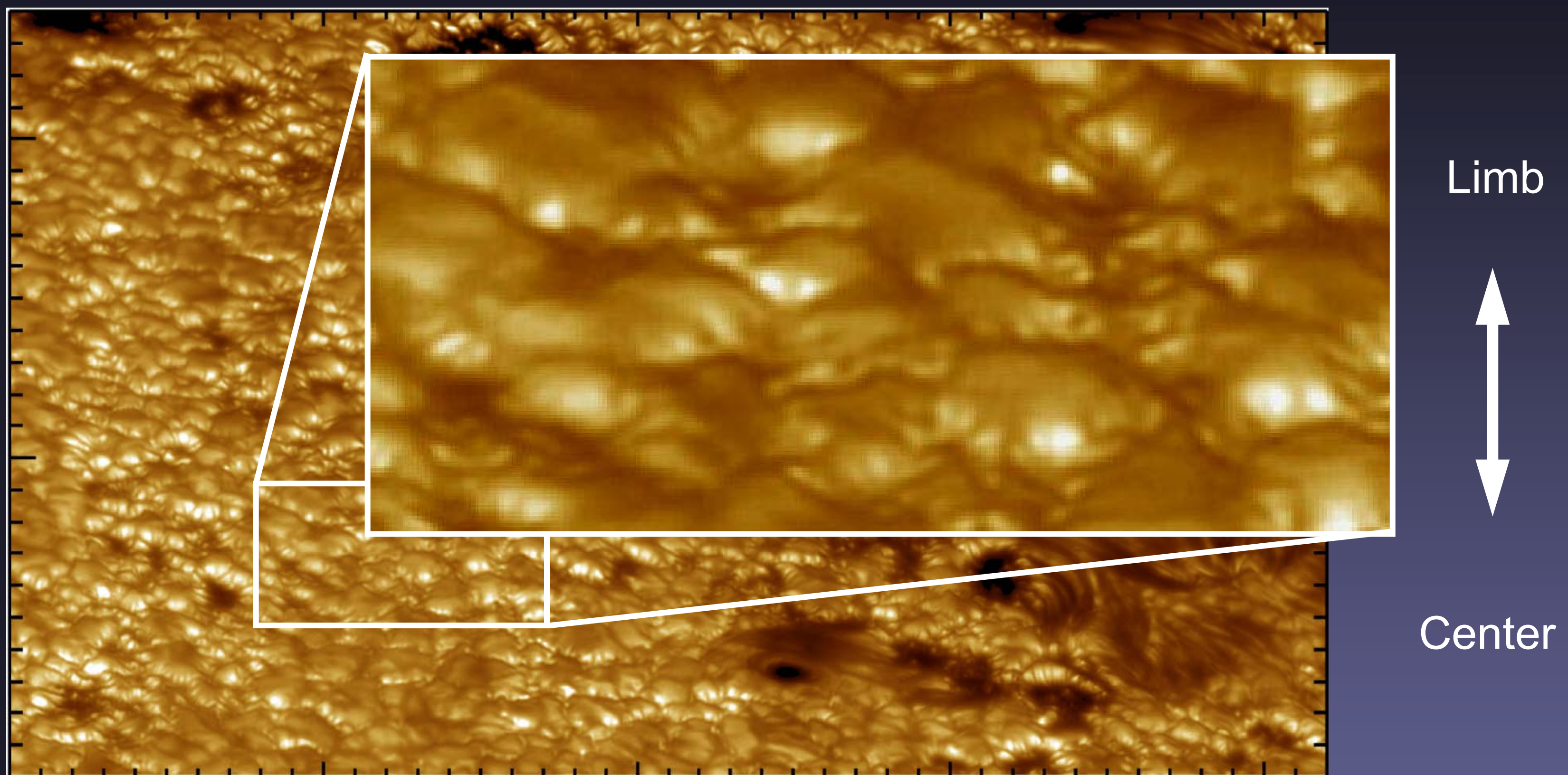

(continuum image: SST, La Palma θ=60° λ=488nm)

Recent observations reveal:
(Lites et al. 2004)

- 3D appearance of faculae
- extension up to 0.5”
- narrow dark lanes centerward of faculae

B_z
(Z=0)
>500G
>1000G
>1500G

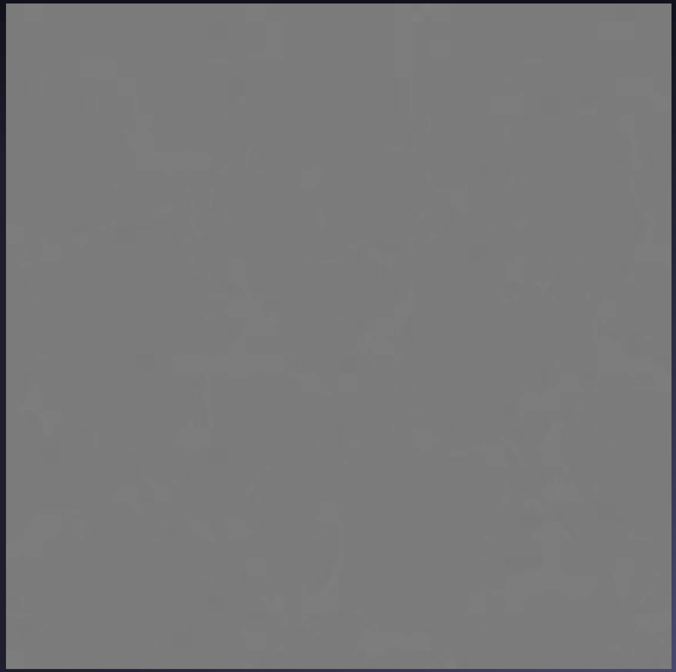

6 Mm

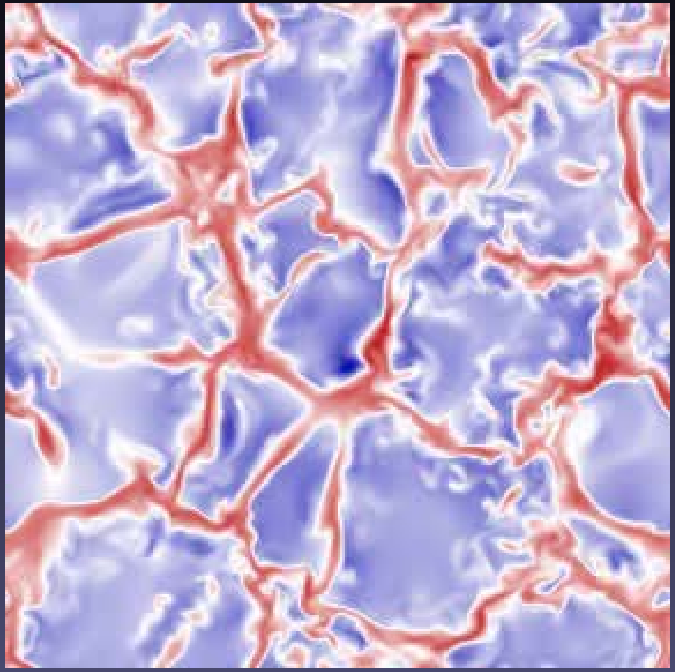

v_z
(Z=0)

3-D compressible radiation-MHD simulations

Plage: $B_Z(t=0) = 200$ G

Grid Size: 288 x 288 x 100

Vertical extent: 1.4 Mm

Horizontal extent: 6 Mm

Vögler et al. 2005

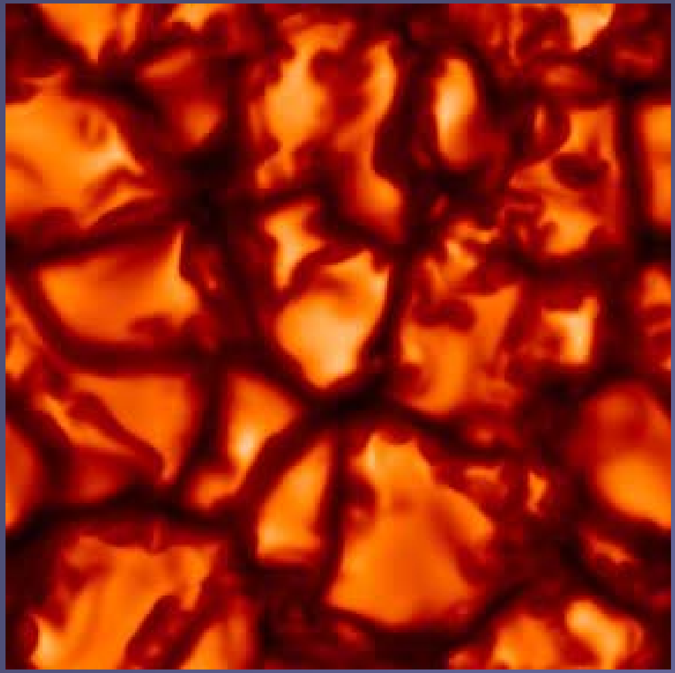

I_c
(Z=0)

Vertical cut through sheet-like structure

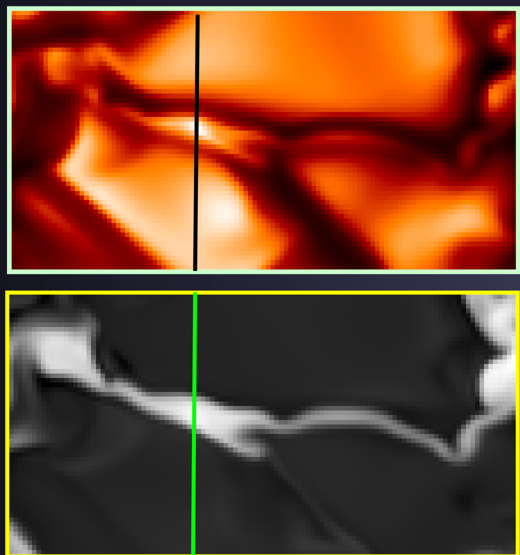

I

B_z

- partial evacuation leads to a depression of the τ=1 level
- lateral heating from hot walls (Spruit 1976)

→Brightness enhancement of small structures

Radiation flux vectors &

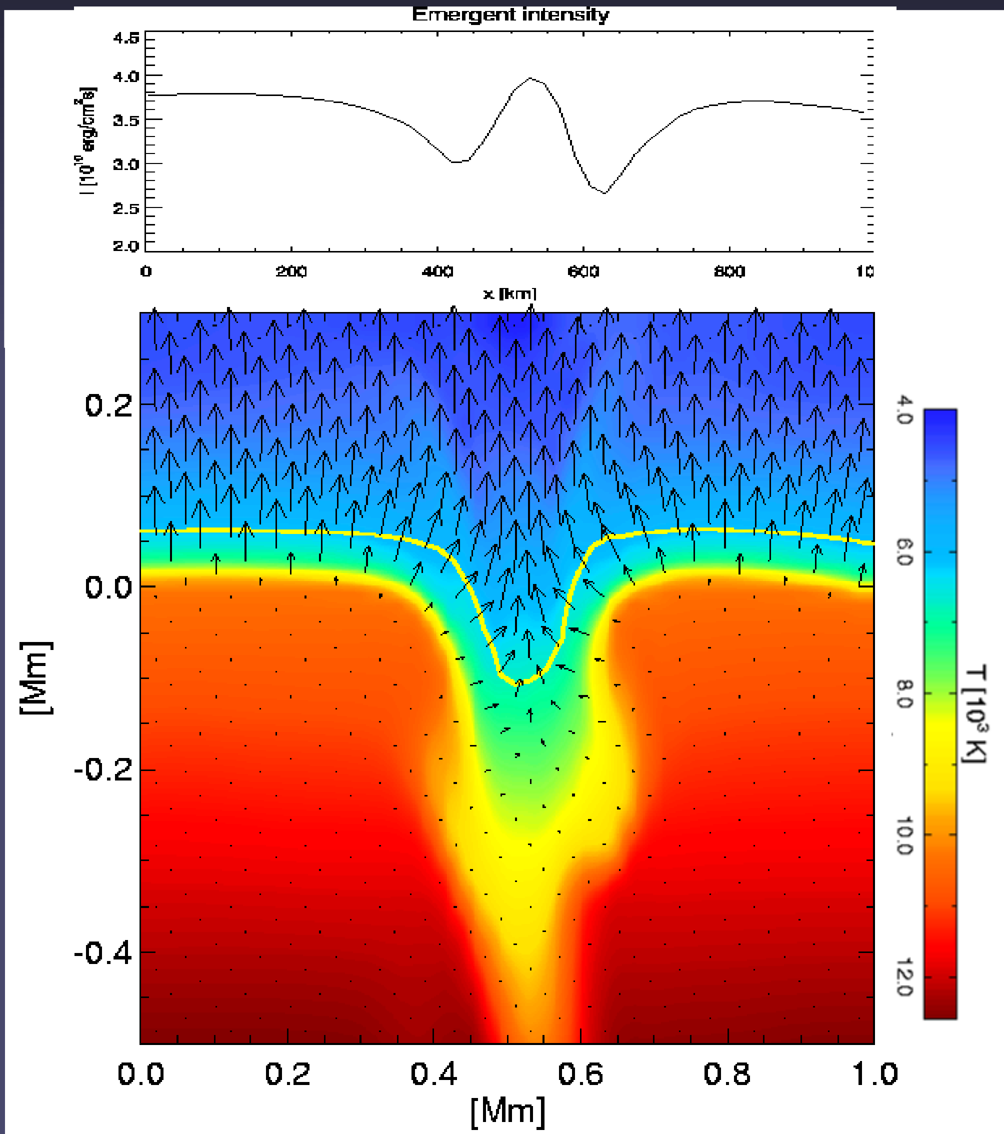

From quiet Sun to strong plage

Probability density function of field strength around τ=1

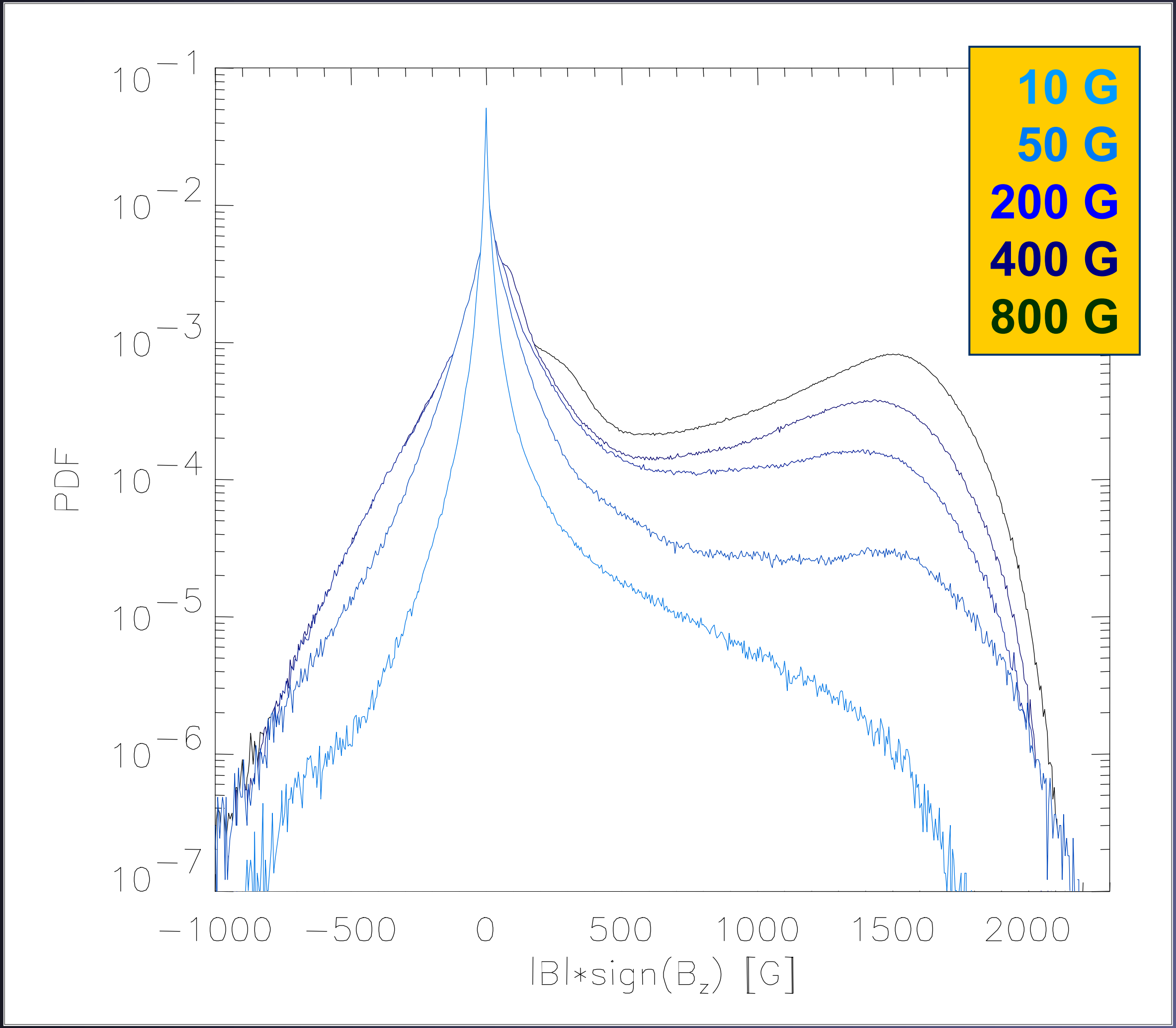

- Weak fields: exponential or lognormal
- Strong fields: Gaussian
- Efficiency of convective field intensification decreases for small B_0

Facular brightening

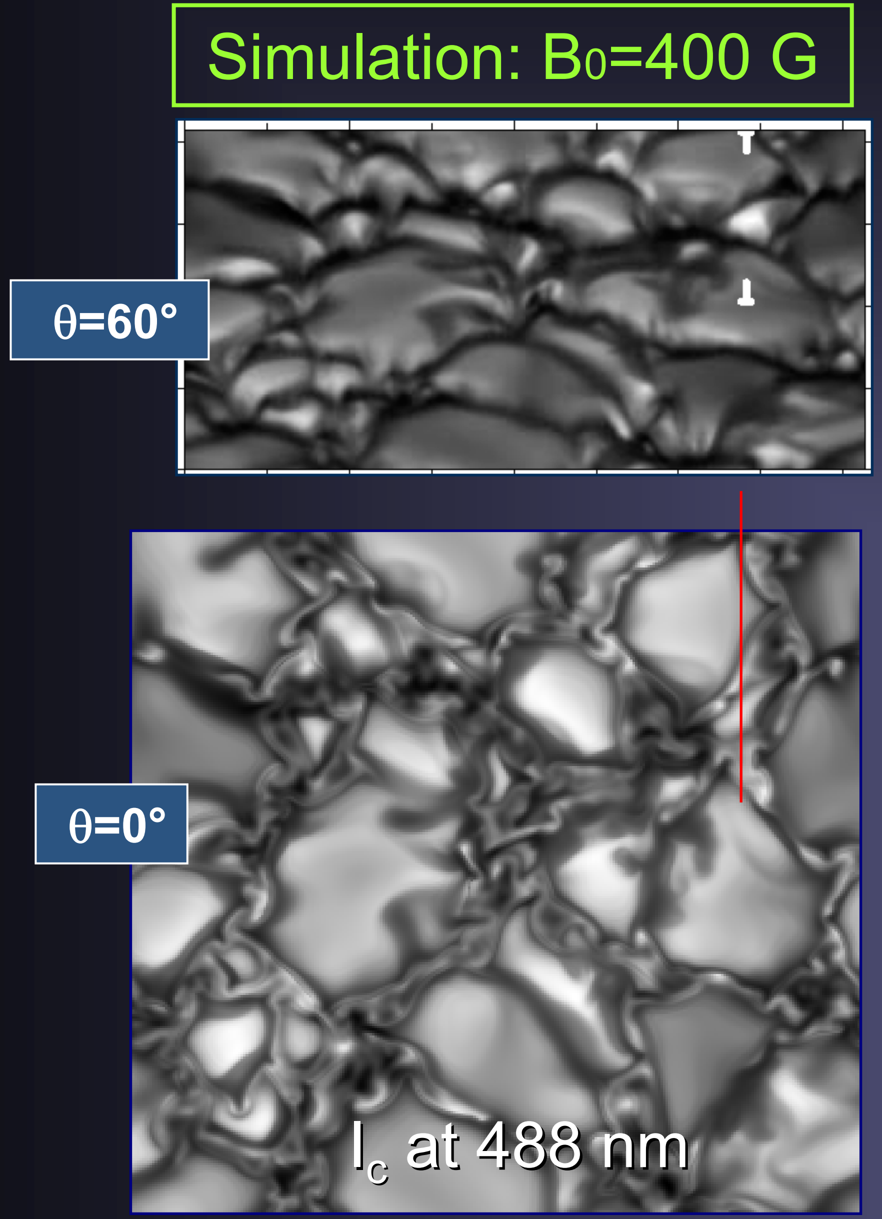

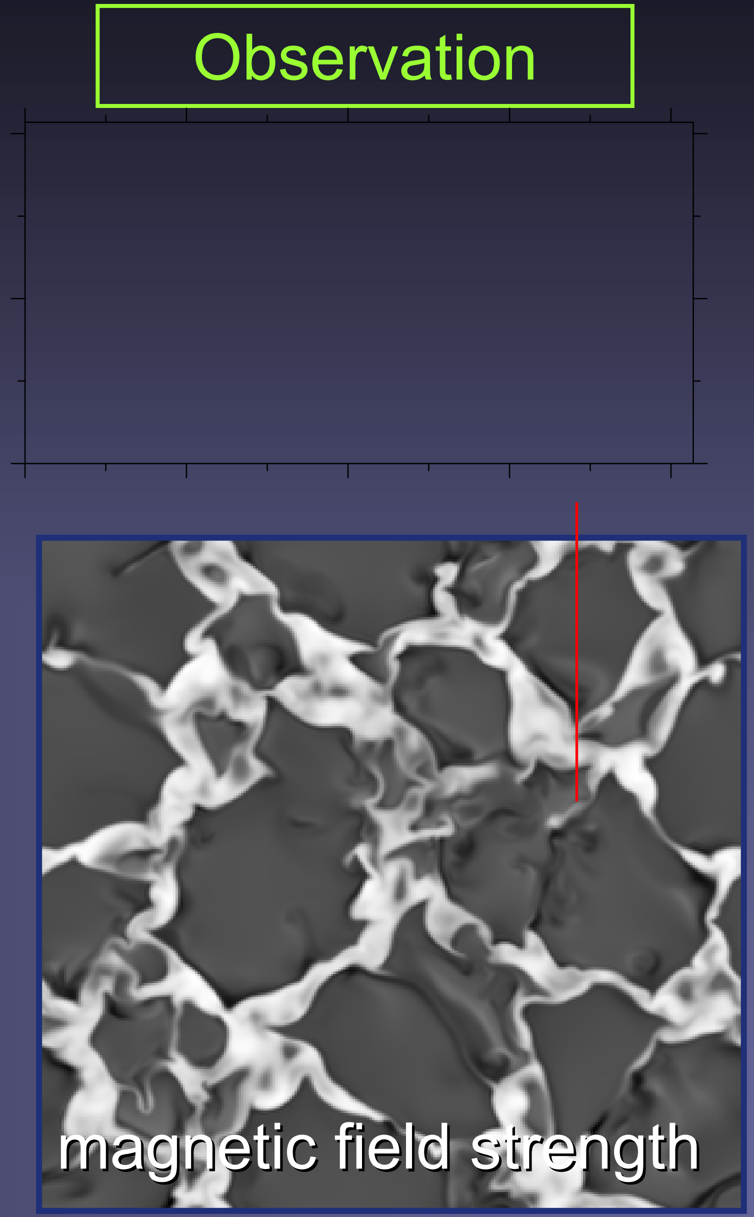

(Keller et al. 2004)

Supergranules and magnetic field

- Magnetogram: black and white (oppos. polarities)
- Horizontal velocity: arrows
- Divergence: blue arrows > 0; red arrows: < 0
- Supergranule boundaries: yellow
- Magnetic field at edges of supergranules, as in simulations for granules

→ B swept out by flow of supergranules

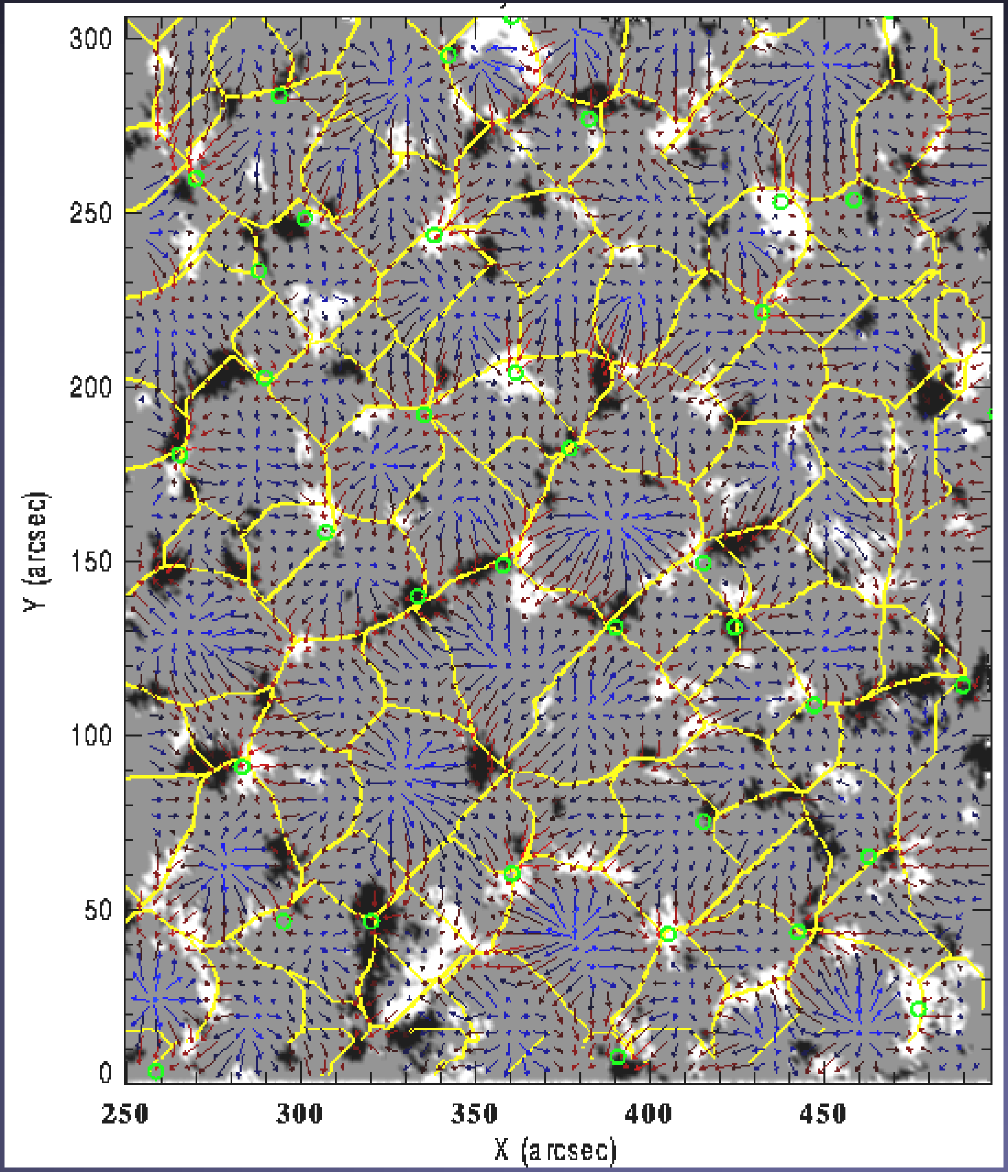

What is between the flux tubes?

- **Internetwork:** Zeeman effect → mainly horizontal hG fields, forming small, low-lying loops. Fed by emergence of small (10^{17} Mx) dipoles in granules
- **Turbulent field:** Hanle effect → "Zeeman invisible" field mixed on small scales. Same as internetwork field, or separate? Trujillo Bueno et al. (2004) propose that turbulent field dominates magnetic energy density in photosphere

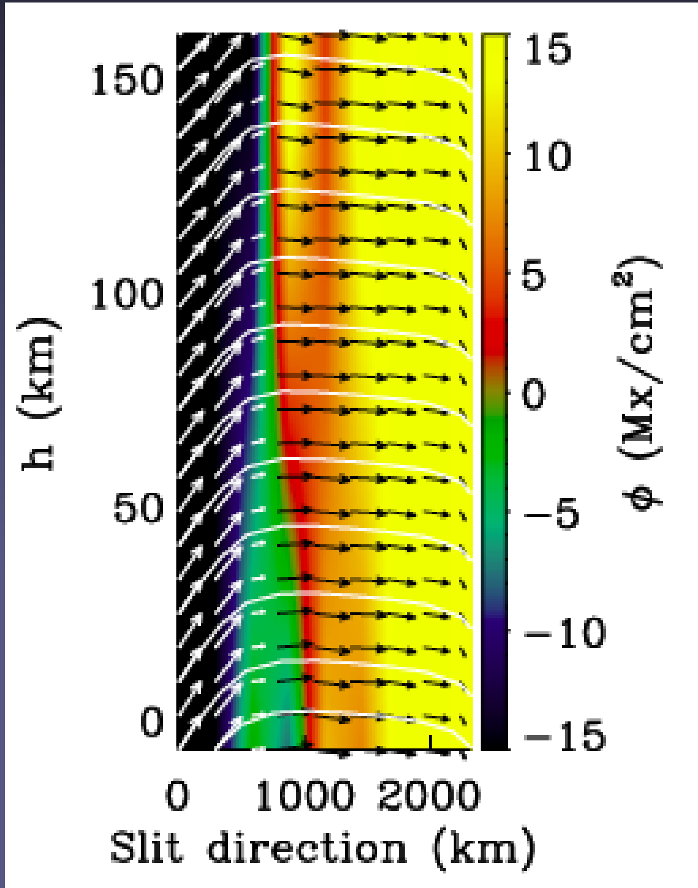

Martinez et al. 2007

Which dynamo feeds QS flux?

- Active and ephemeral regions: main dynamo (orientation of bipolar regions & solar cycle variation of their number and location)
- IN & turbulent fields: not yet decided
  - local turbulent dynamo (Cattaneo 1999; Vögler & Schüssler 2007; 2008)
  - main dynamo, with fluctuations due to flux recycling (e.g. Ploner et al. 2002; de Wijn et al. 2005)

Surface dynamo

Vögler and Schüssler 2007

$B_{vertical}$ Continuum intensity

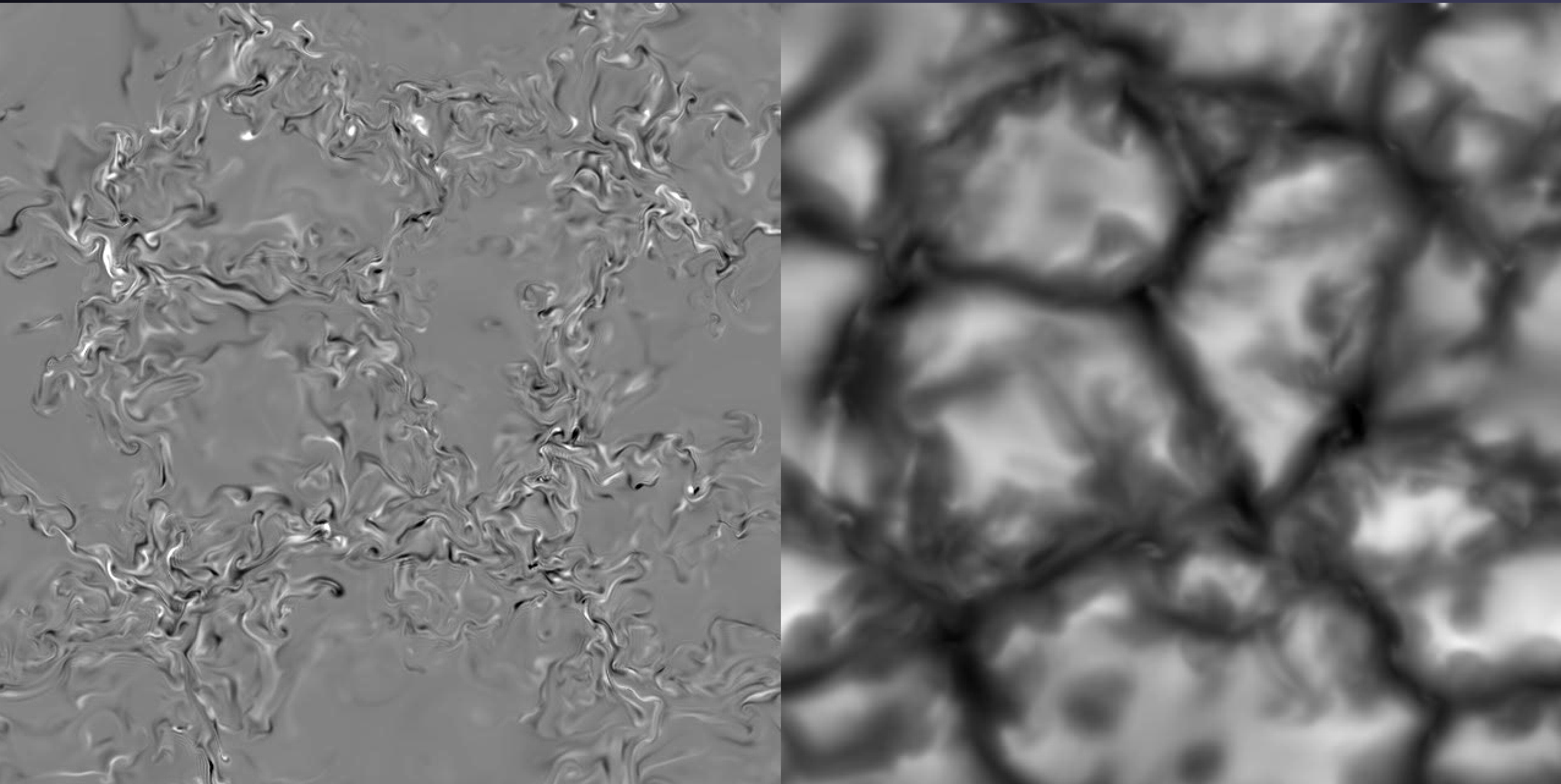

Manifestations of the magnetic field in the Sun's atmosphere

1-D stratification of the solar atmosphere

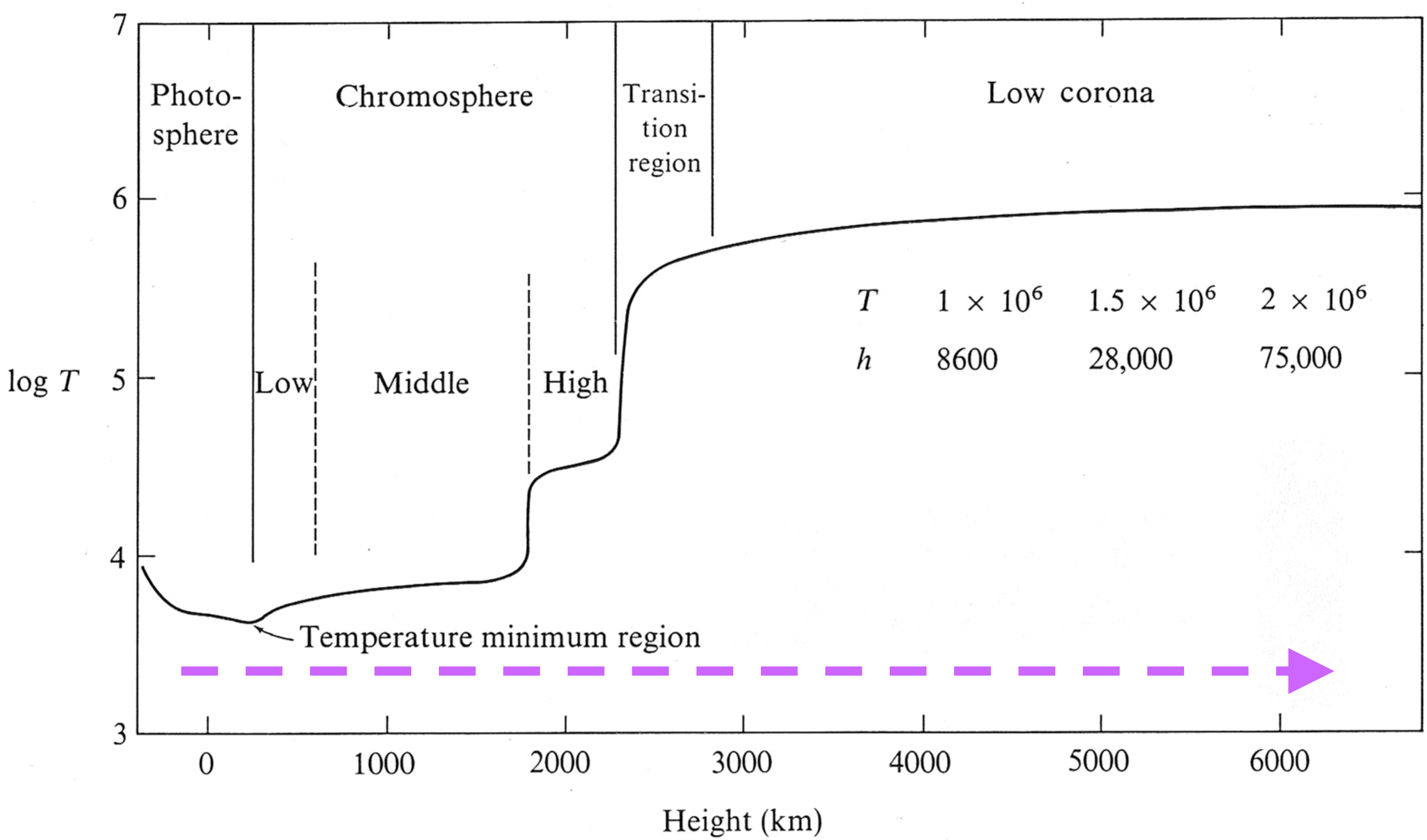

Sun’s magnetic field correlates with brightness in most atmospheric layers

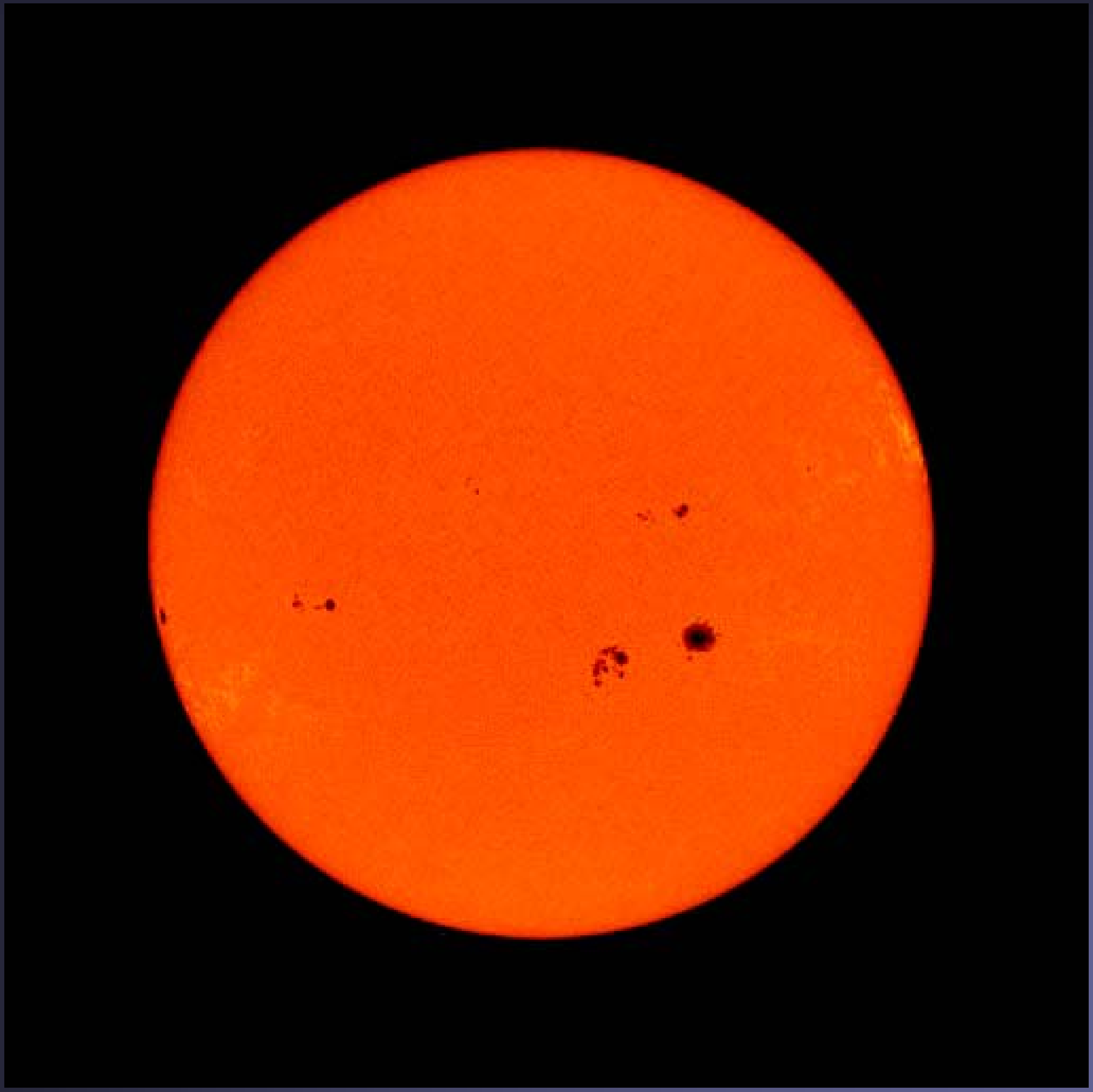

Photospheric influence of field: variations of total irradiance

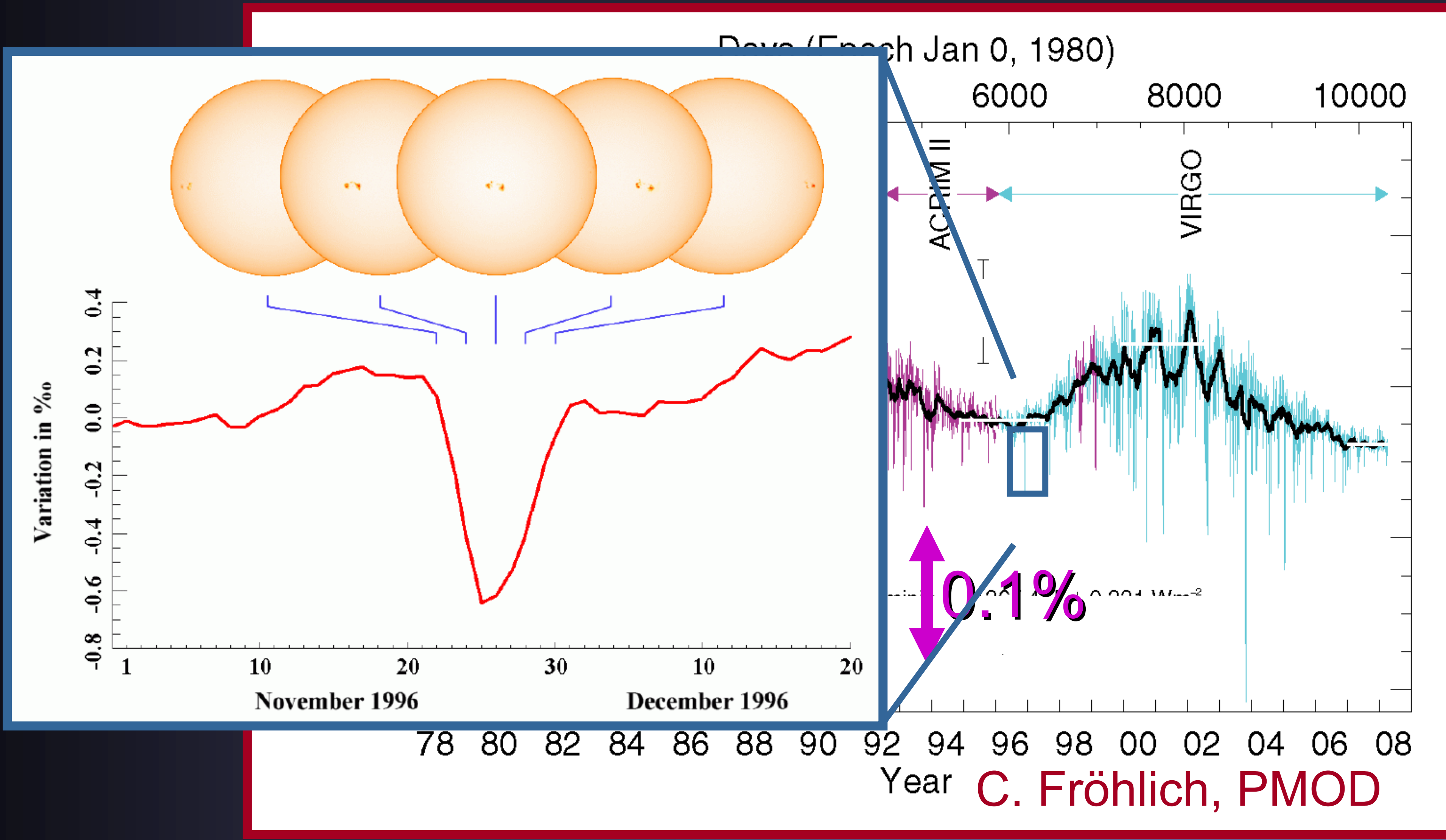

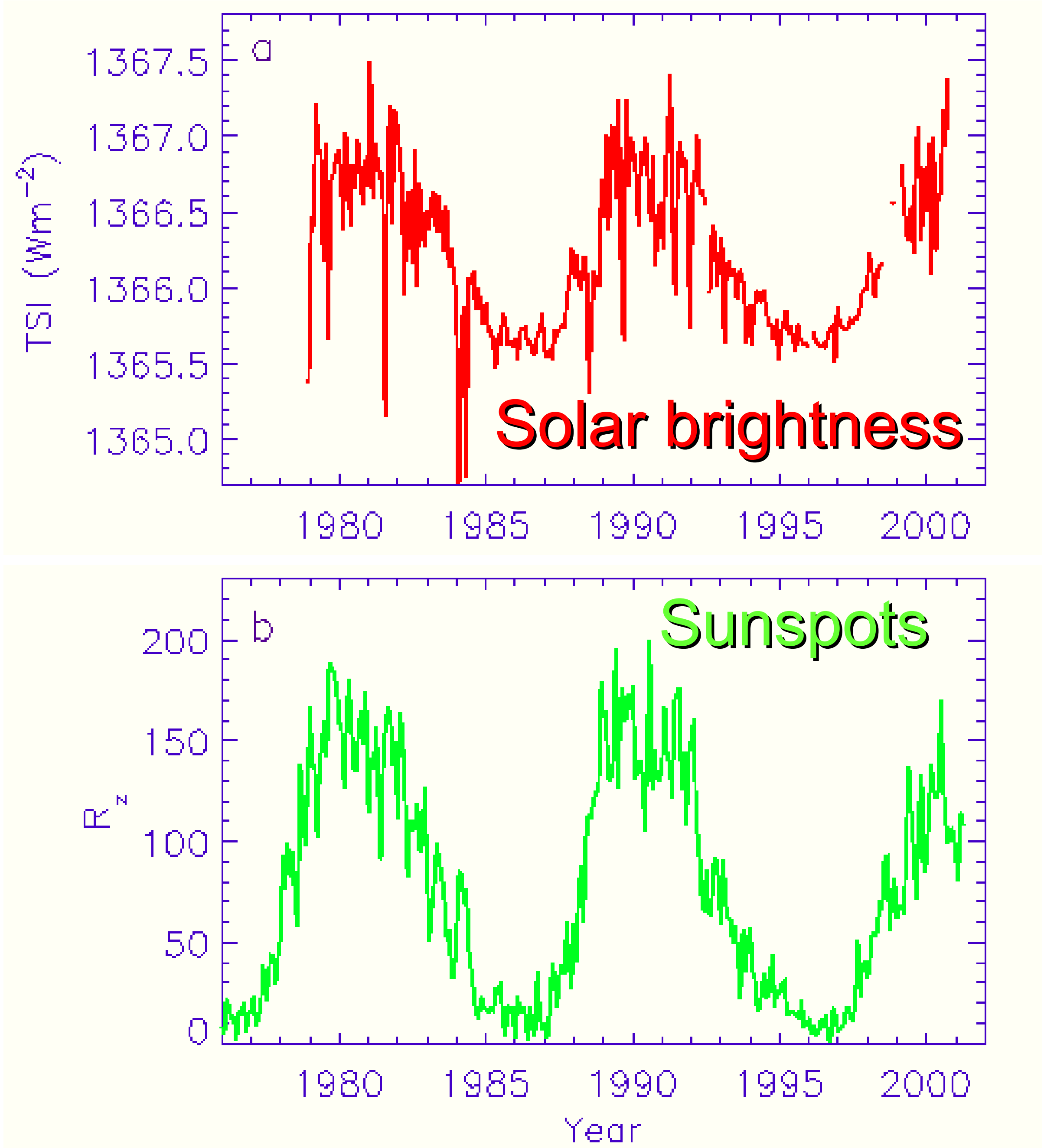

Solar brightness
a
TSI (Wm^-2)
1367.5
1367.0
1366.5
1366.0
1365.5
1365.0
1980
1985
1990
1995
2000
Sunspots
b
R_z
200
150
100
50
0
1980
1985
1990
1995
2000
Year

Faculae

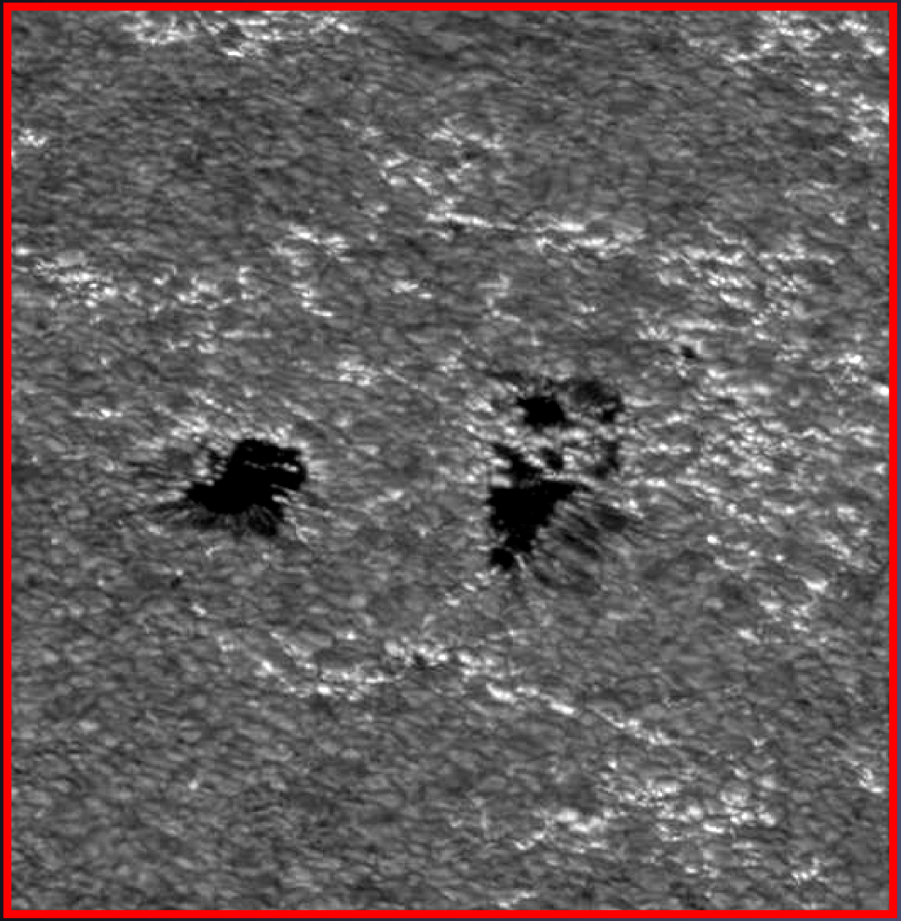

Area covered by faculae increases faster from Min. to Max. of solar activity than the area covered by sunspots

Magnetic Field & Brightness Changes

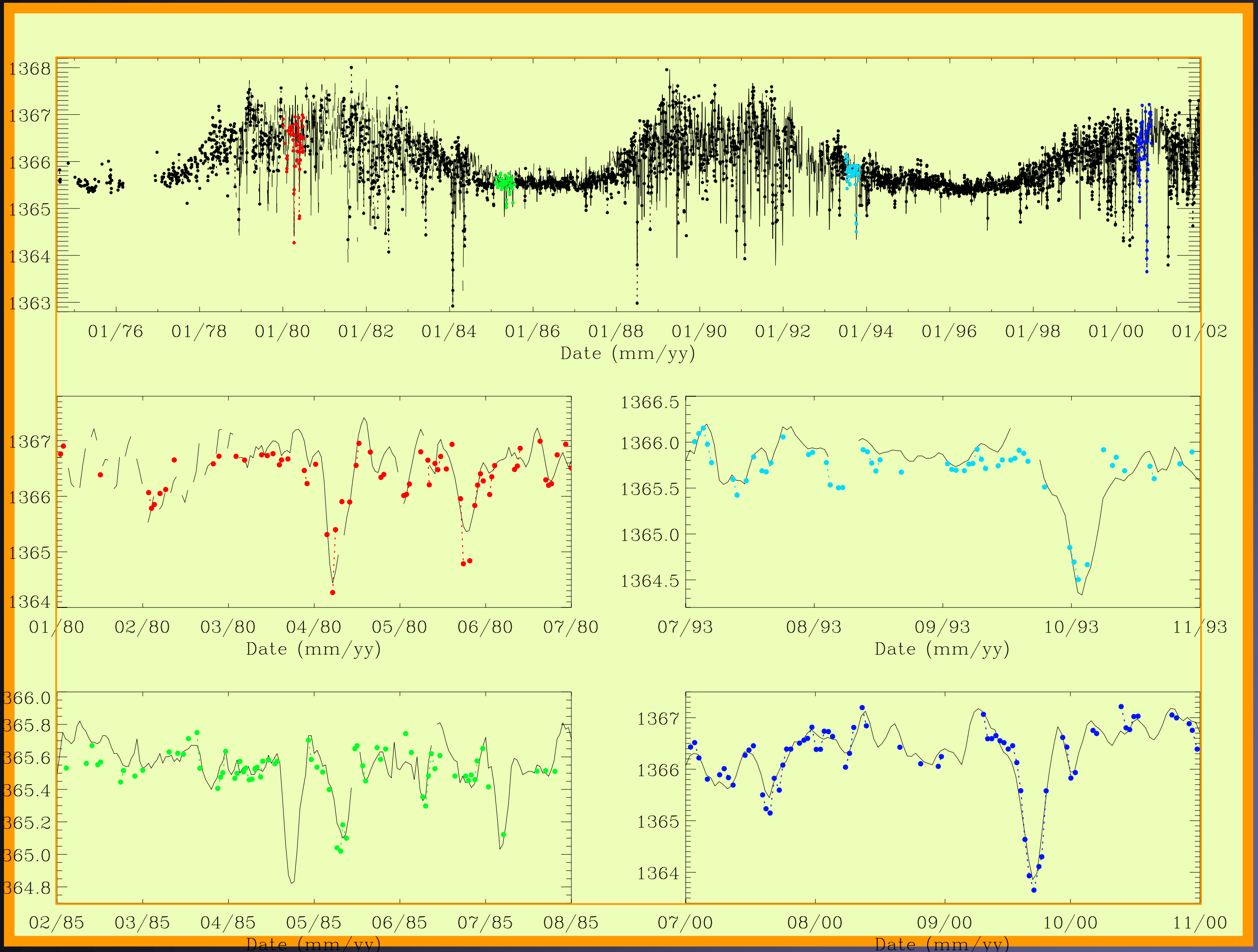

Wenzler et al. 2006

Model: based on assumption that brightness changes are caused by magnetic field at solar surface

Obs.: by various Instruments

Magnetic Field & Brightness Changes

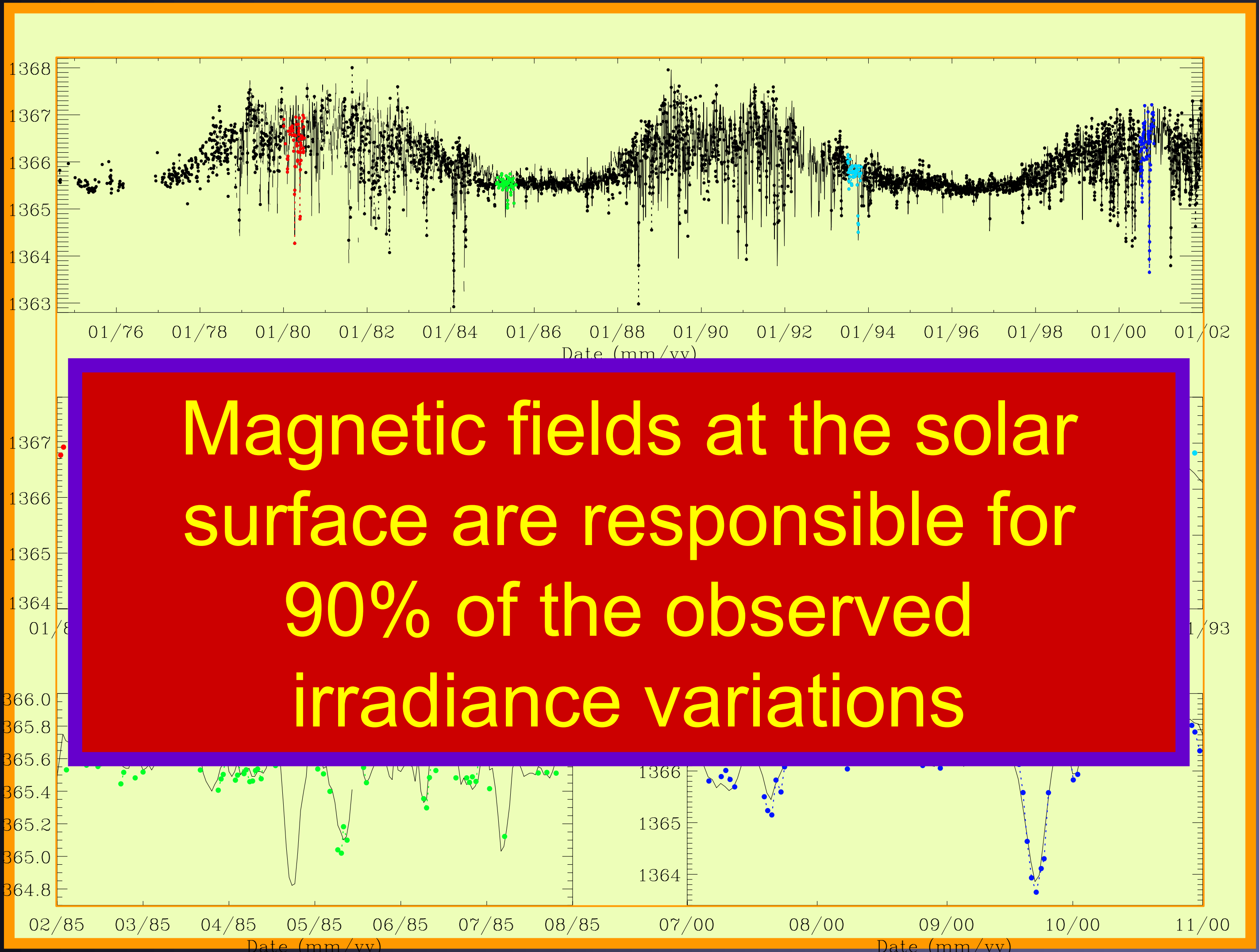

Model: based on assumption that brightness changes are caused by magnetic field at solar surface

Obs.: by various Instruments

Wenzler et al. 2006

Chromospheric structure and magnetic field

Spots plages

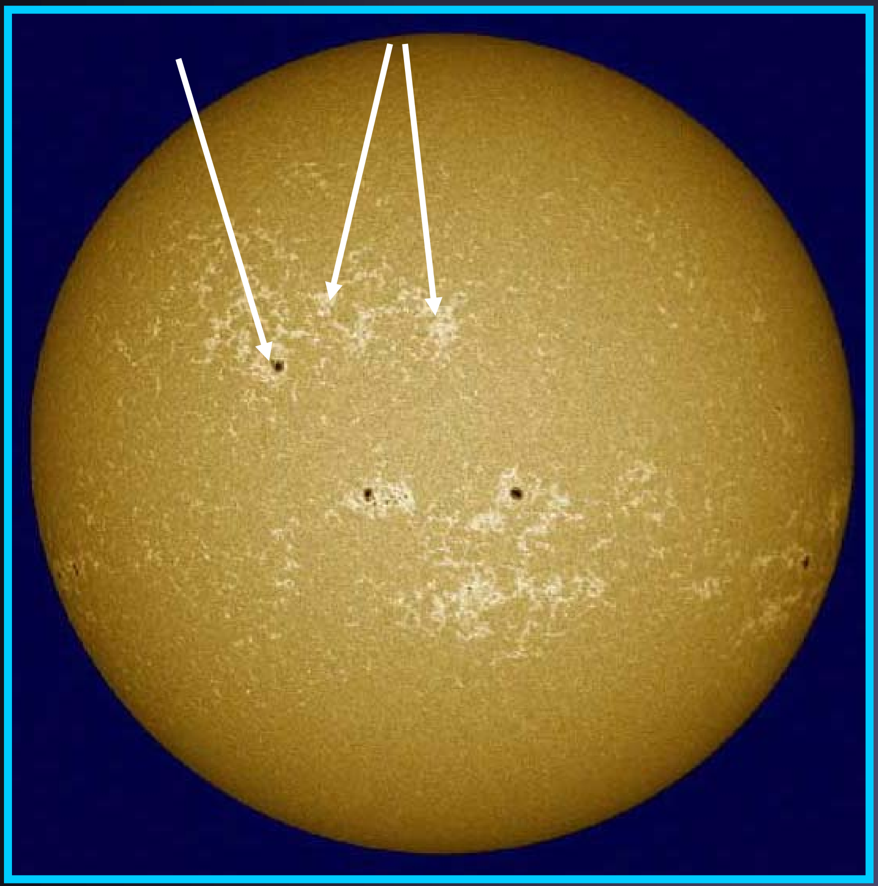

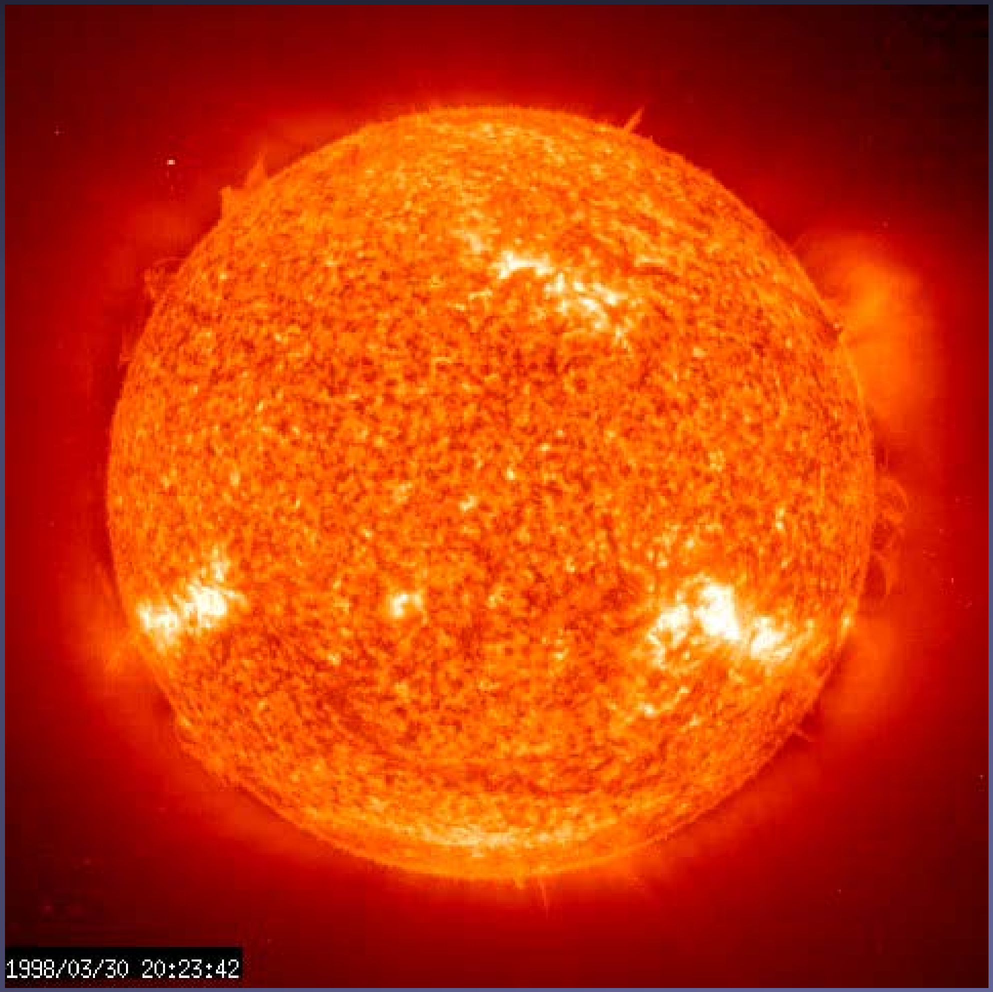

7000 K gas Ca II K

5 10^4 K gas (EIT He 304 Å)

Ca II K as a magnetic field proxy

- Ca II H and K lines, the strongest lines in the visible solar spectrum, become brighter with non-spot magnetic flux.
- $I_{core}/I_{wing} \sim <B>^{0.6}$
- Magnetic regions (except sunspots) appear bright in Ca II H+K ➔ Ca plage and network regions

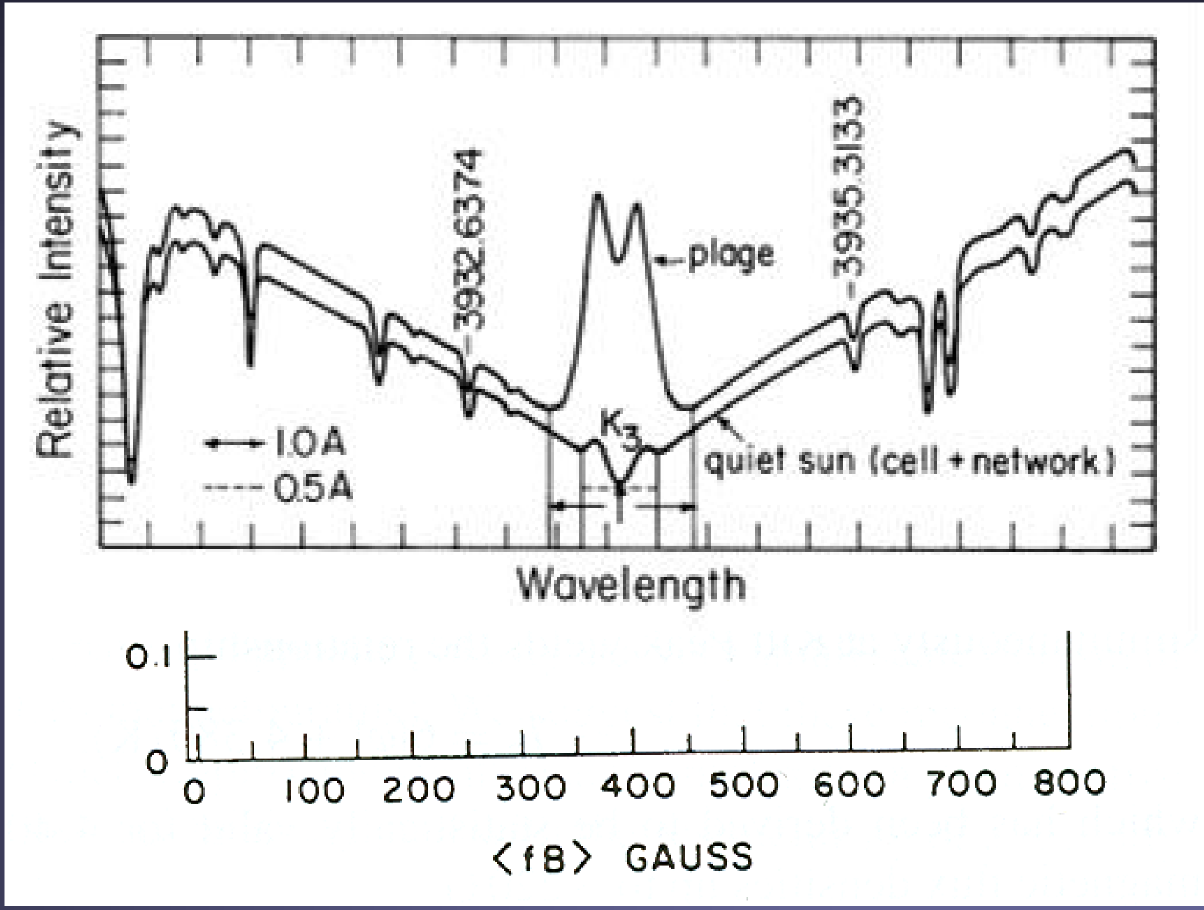

Schrijver et al. 1989, Rezaei et al. 2007

Important for tracing stellar activity

Why are magnetic elements bright in the chromosphere?

- **Photosphere:** energy enters flux tube through shaking by convection. Transported up by waves, or is stored as excess energy in field (tension forces)
- **Chromosphere:** release of excess energy channelled by field to higher layers (MHD wave dissipation)

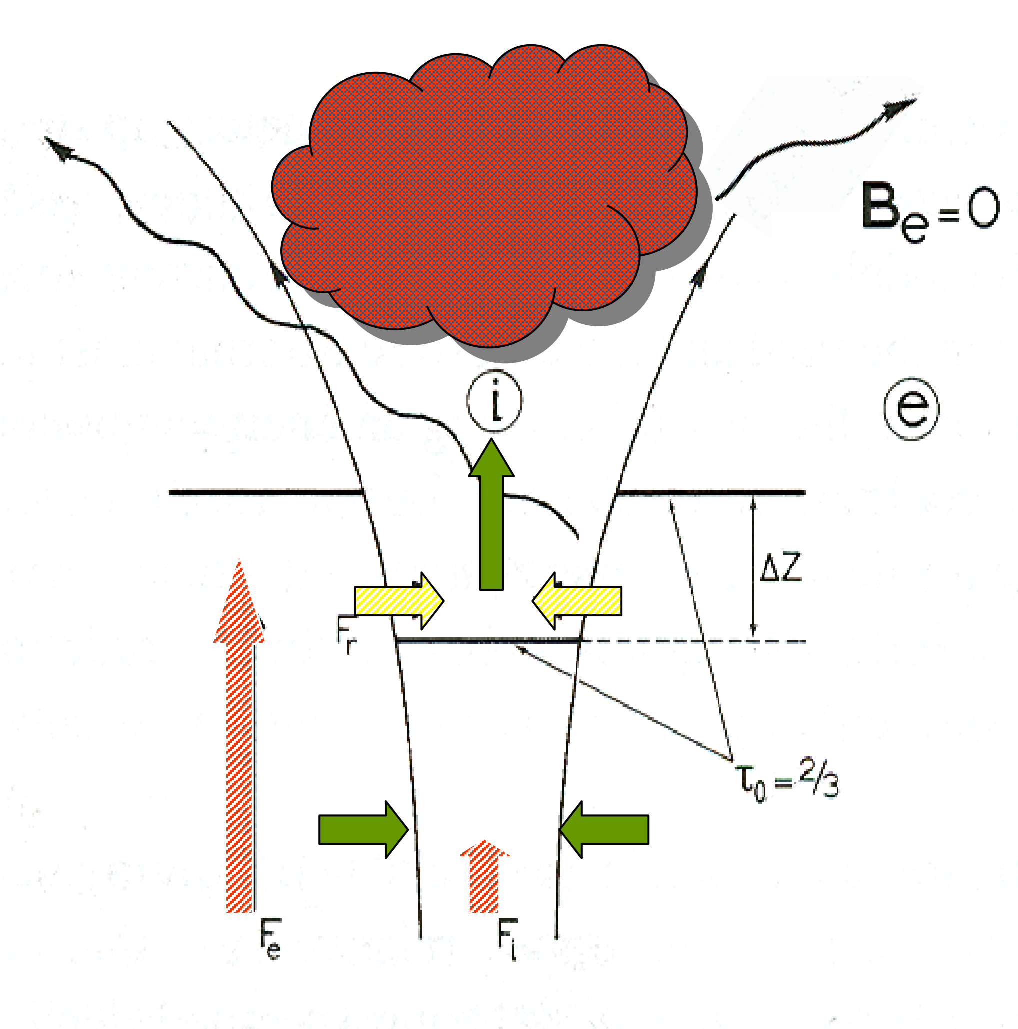

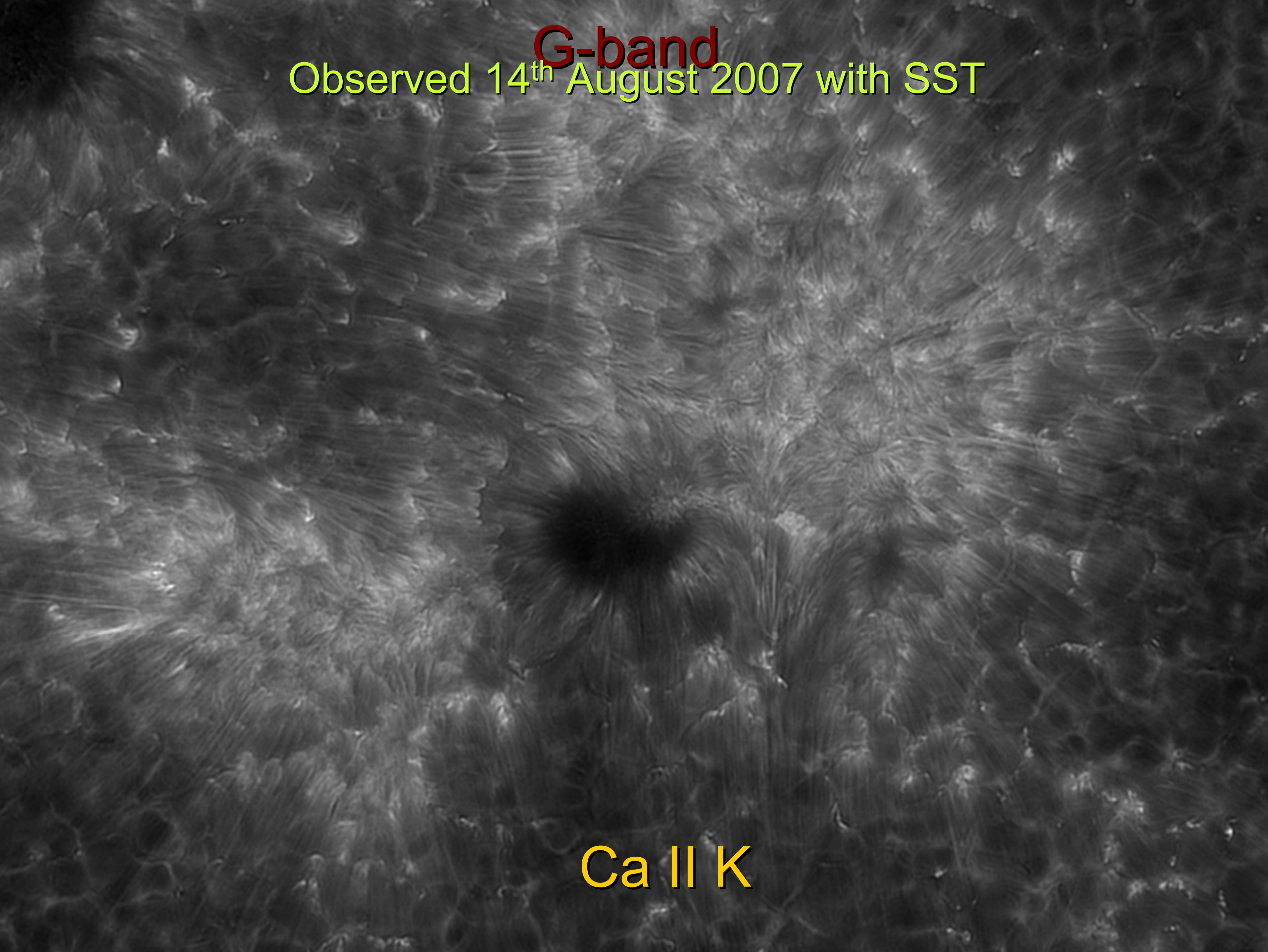
G-band
Observed 14th August 2007 with SST
Ca II K

Magnetic canopies

- Observational evidence exists for the presence of horizontal fields in chromosphere
- Can be produced with FT model if interior of FT is hotter than surroundings
- Pressure scale height $H_P \sim T$
- $T_i > T_e \rightarrow H_{P,i} > H_{P,e} \rightarrow$ above a critical height Z_c: $P_i > P_e$

$\rightarrow$ above Z_c field is not confined & expands horizontally

$\rightarrow$ above Z_c field fills all corona

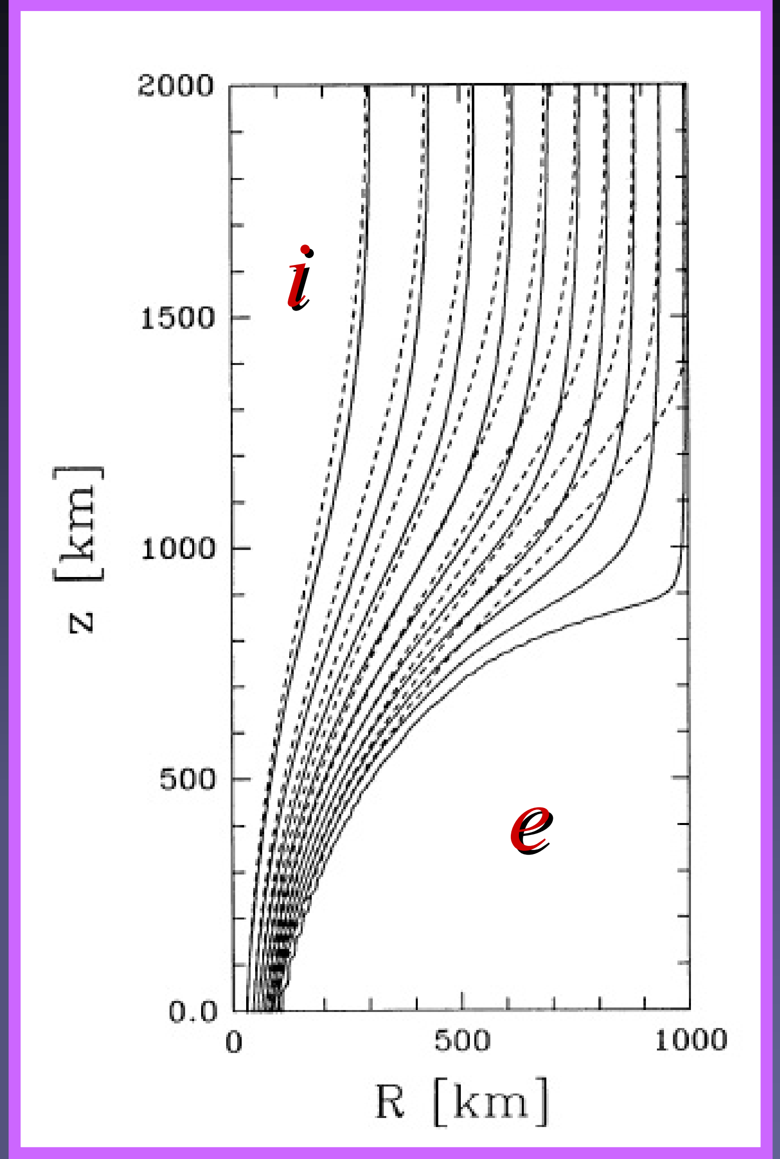

$T_i = T_e$ ....

$T_i > T_e$ ————————

Chromospheric structure

- Spicules
- Prominences and filaments

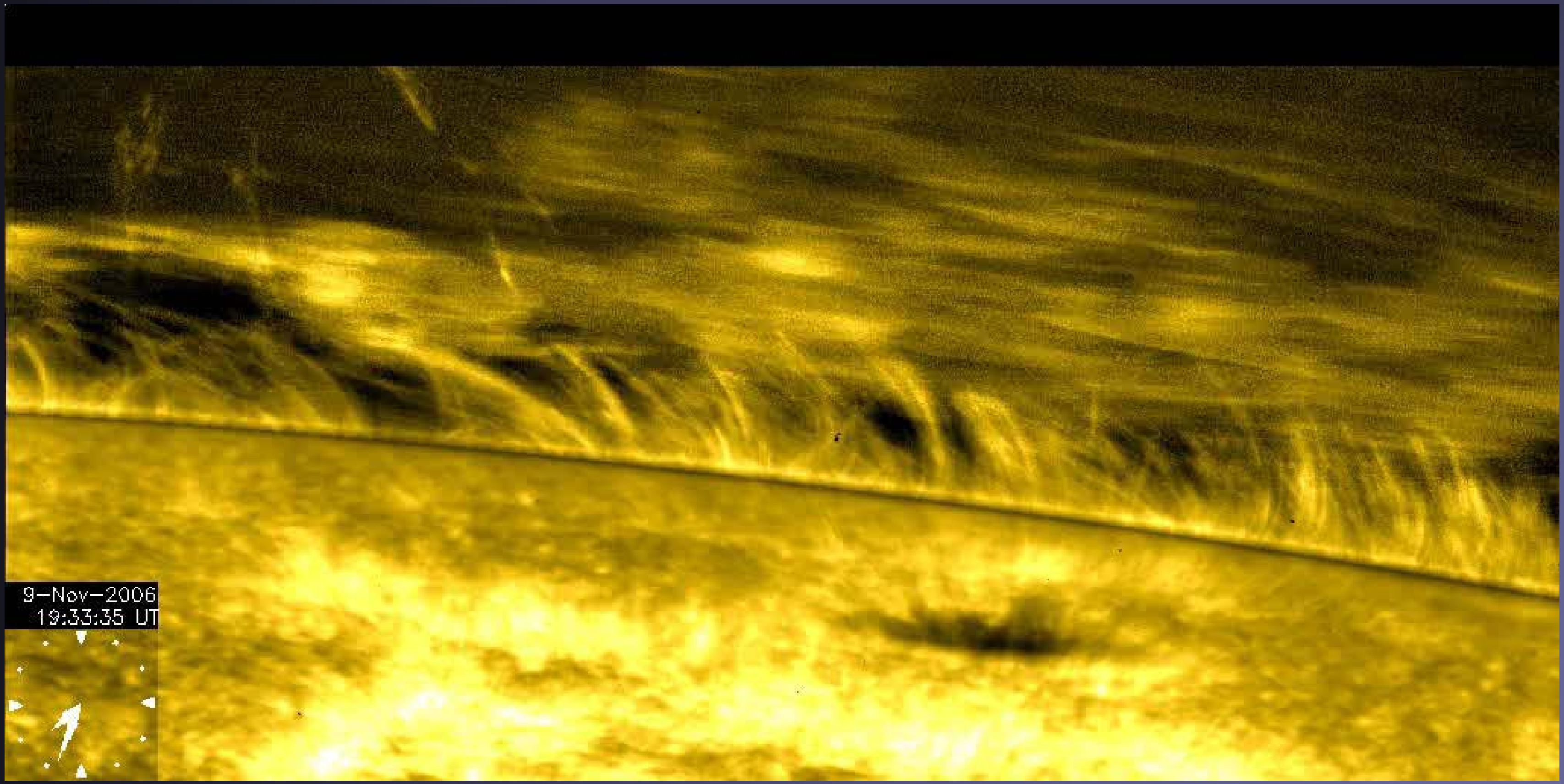

Cartoon of quiet Sun atmosphere

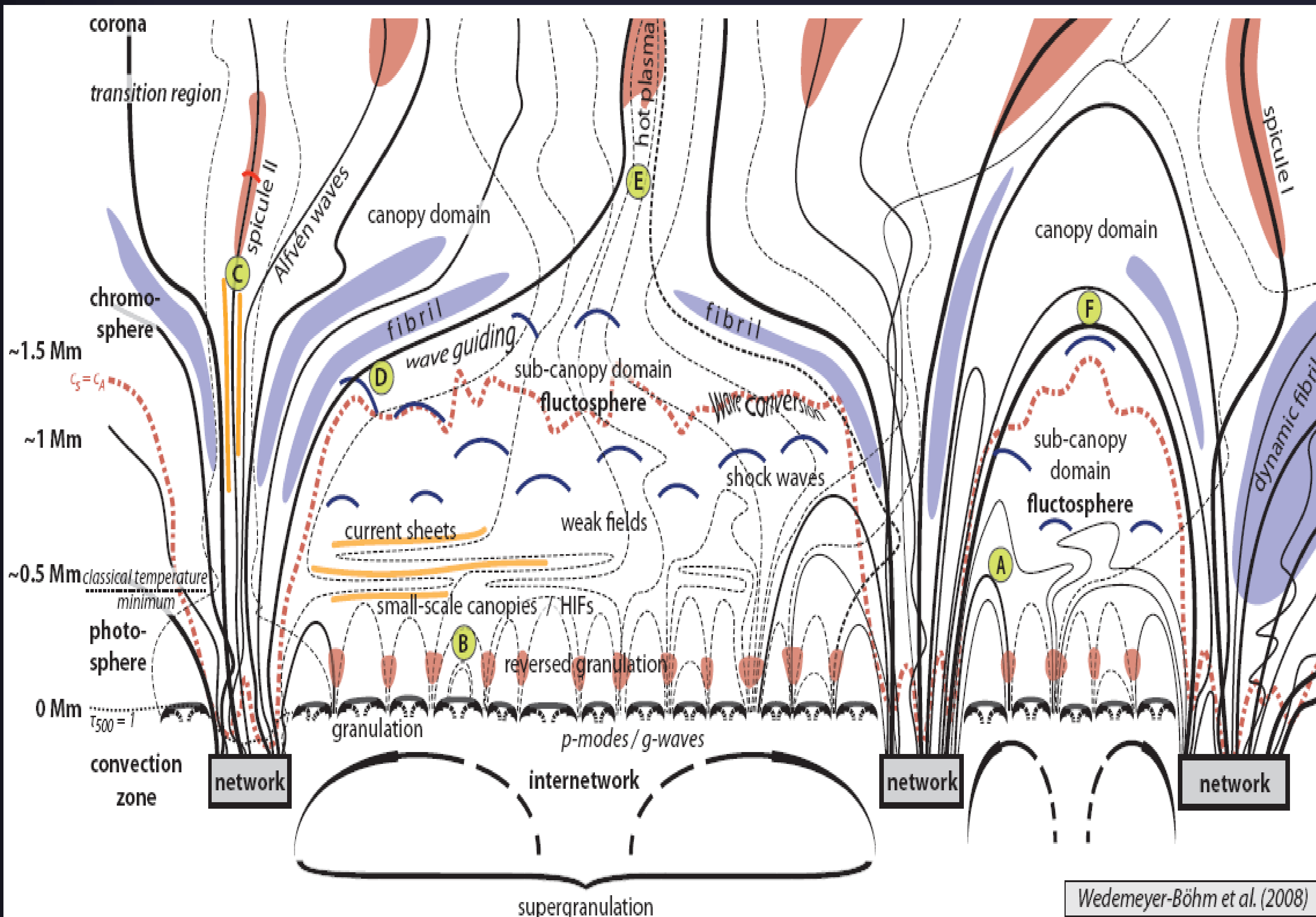

Prominence material supported by magnetic field

- Density of prominence material is ~2 orders of magnitude higher than of surrounding corona
- Prominence gas has to be supported against gravity
- Magnetic field curved upward can provide this support, since ionized gas can only flow along field lines

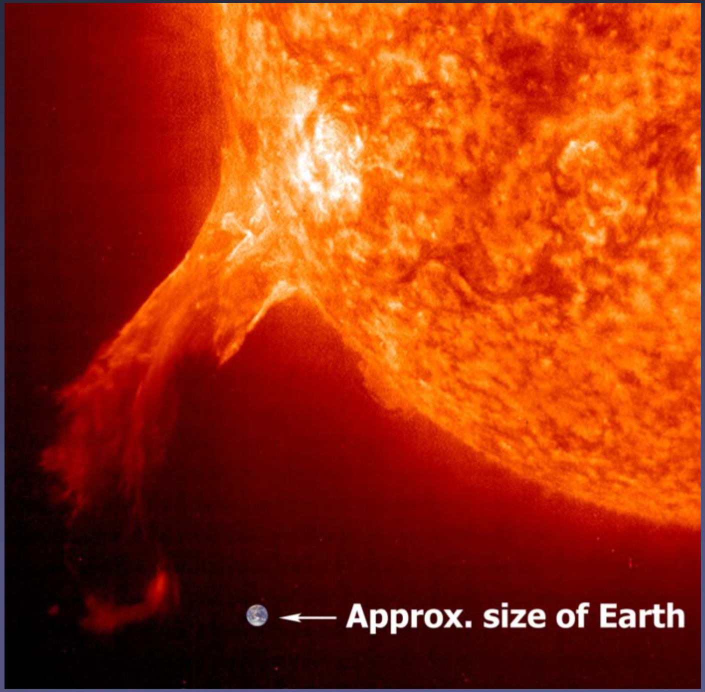

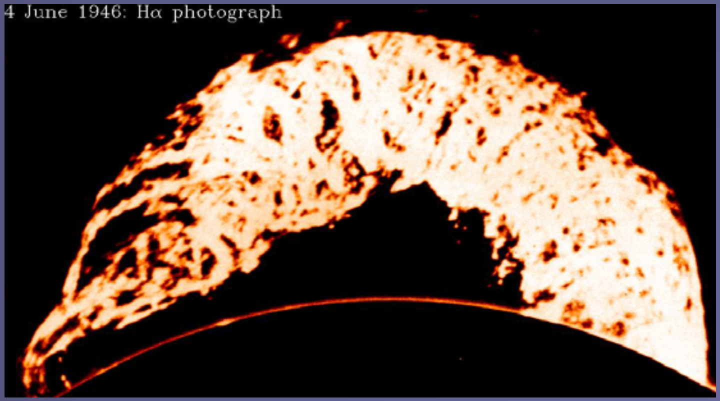

Prominence models

Kippenhahn-Schlüter (below), Kuperus-Raadu (below right) and flux tube (right; 3-D Kuperus-R.)

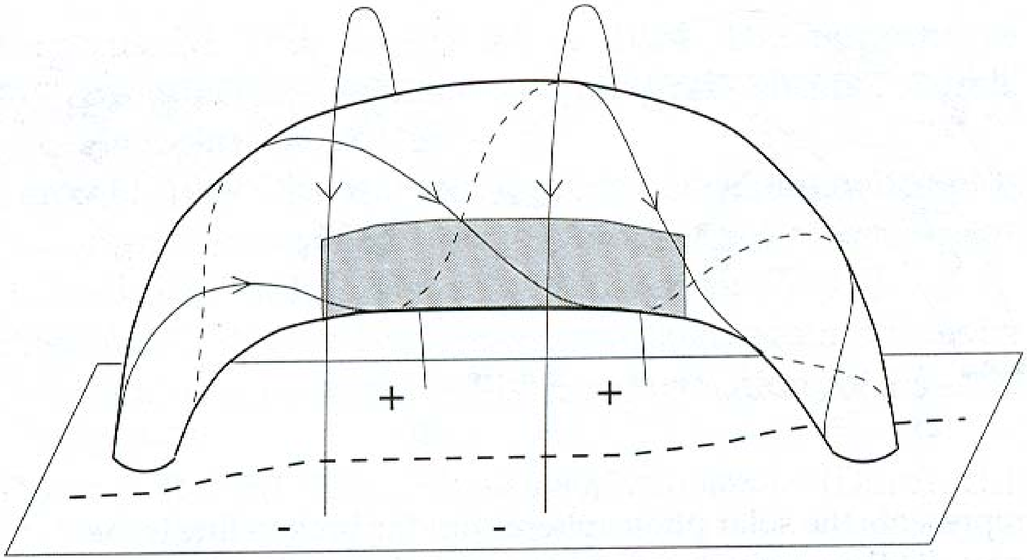

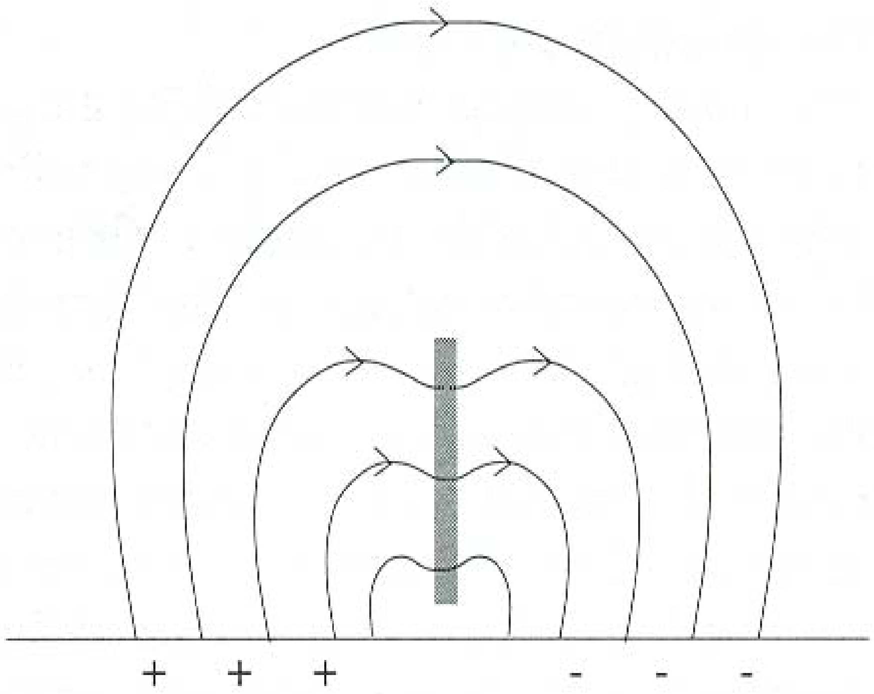

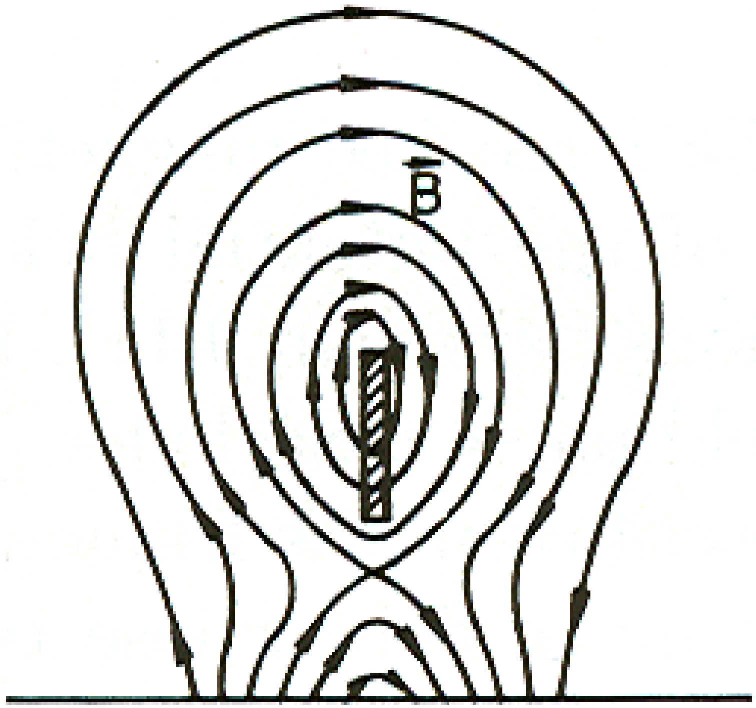

The Hot and Dynamic Corona

Corona during an Eclipse

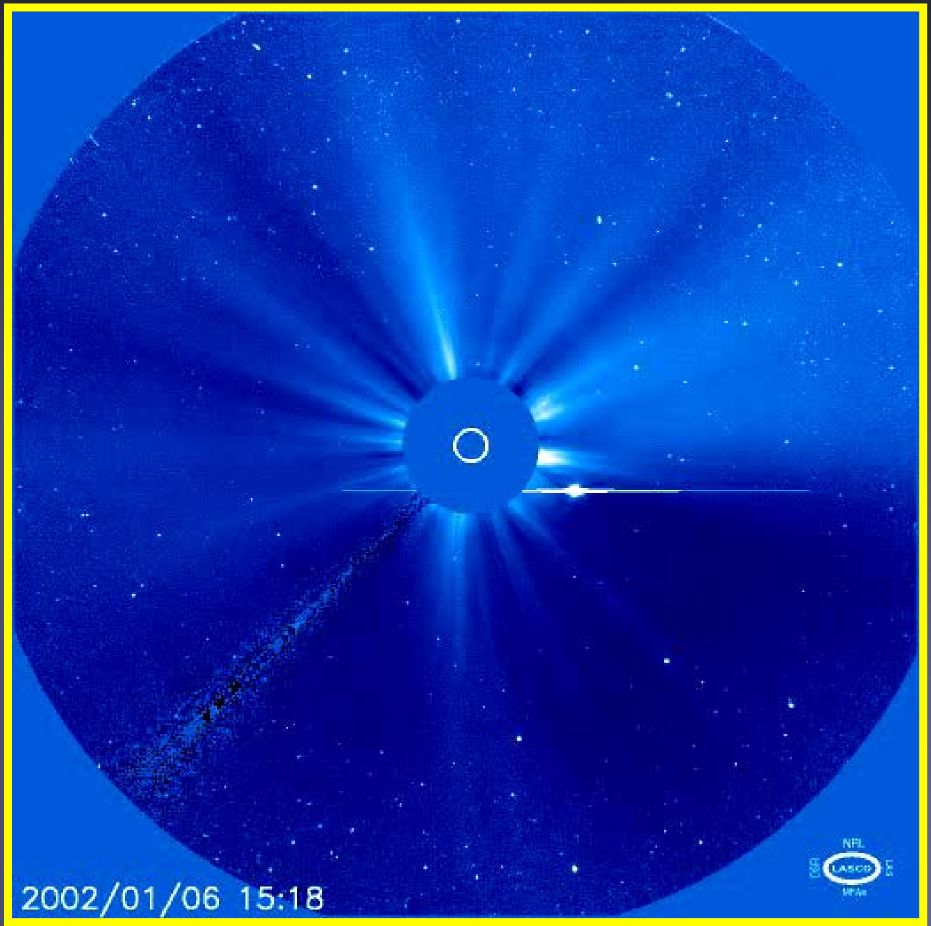

Coronagraphic observations
(LASCO C3 / SOHO, MPS)

The Hot and Dynamic Corona

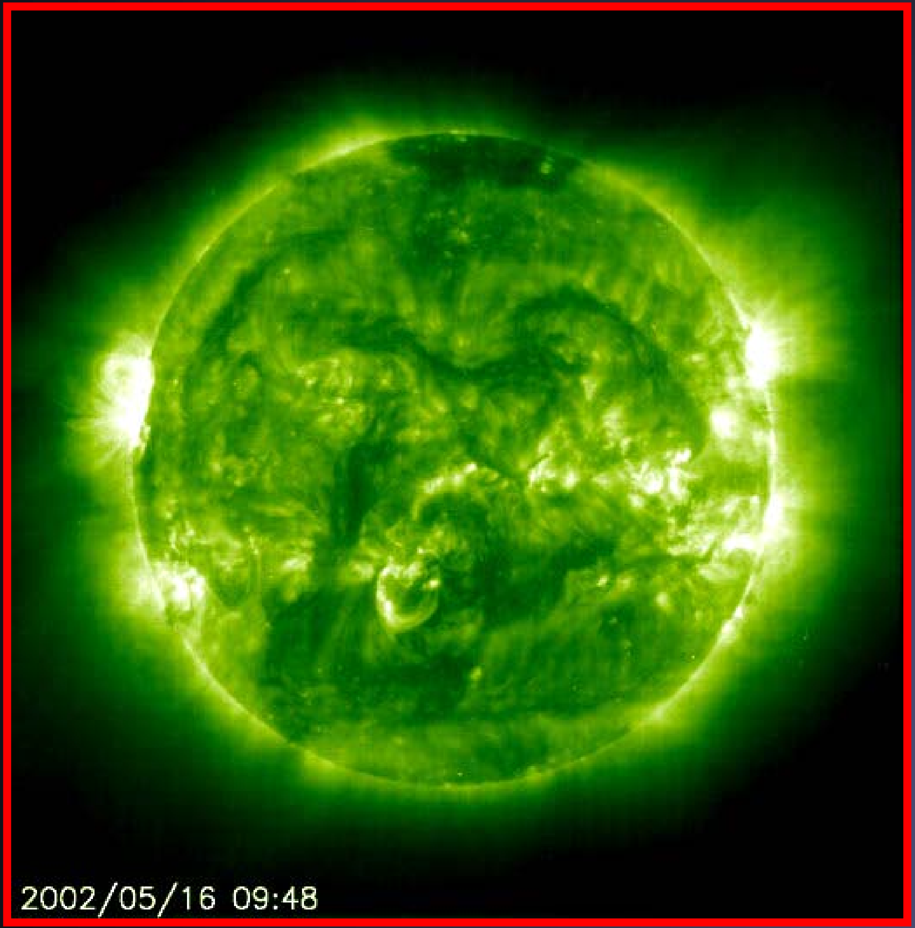

EUV Corona: Plasma at >1 Mio K (EIT 195 Å)

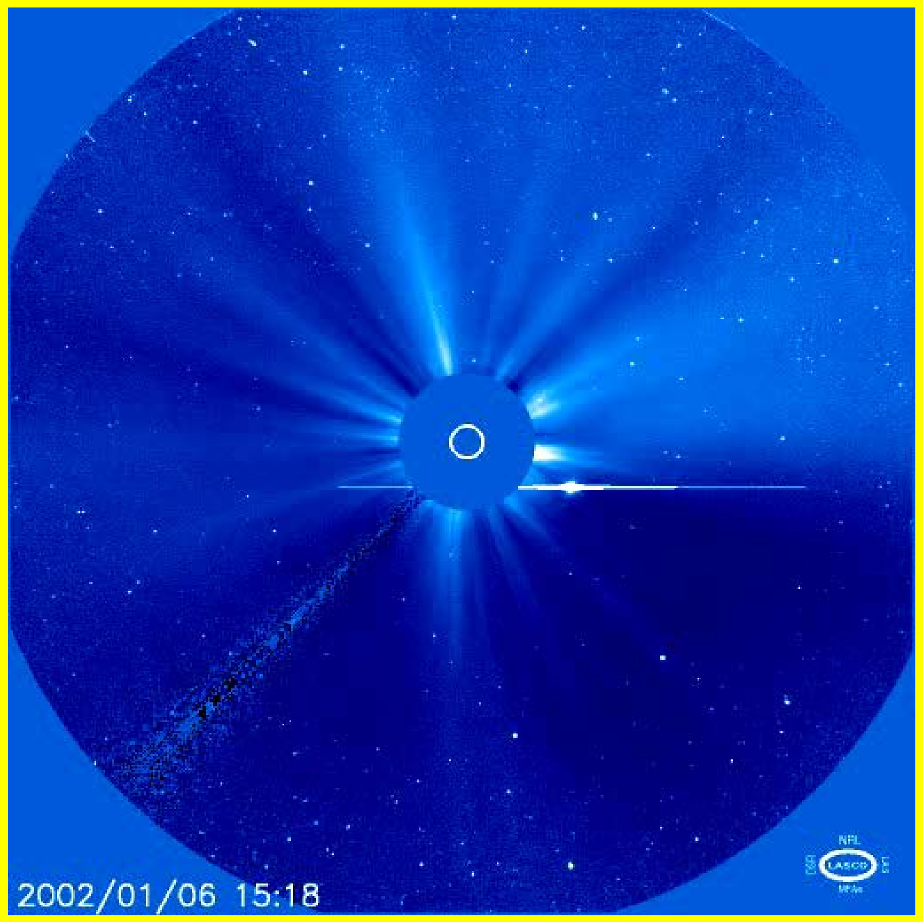

Coronagraphic observations (LASCO C3 / SOHO, MPS)

Coronal structures

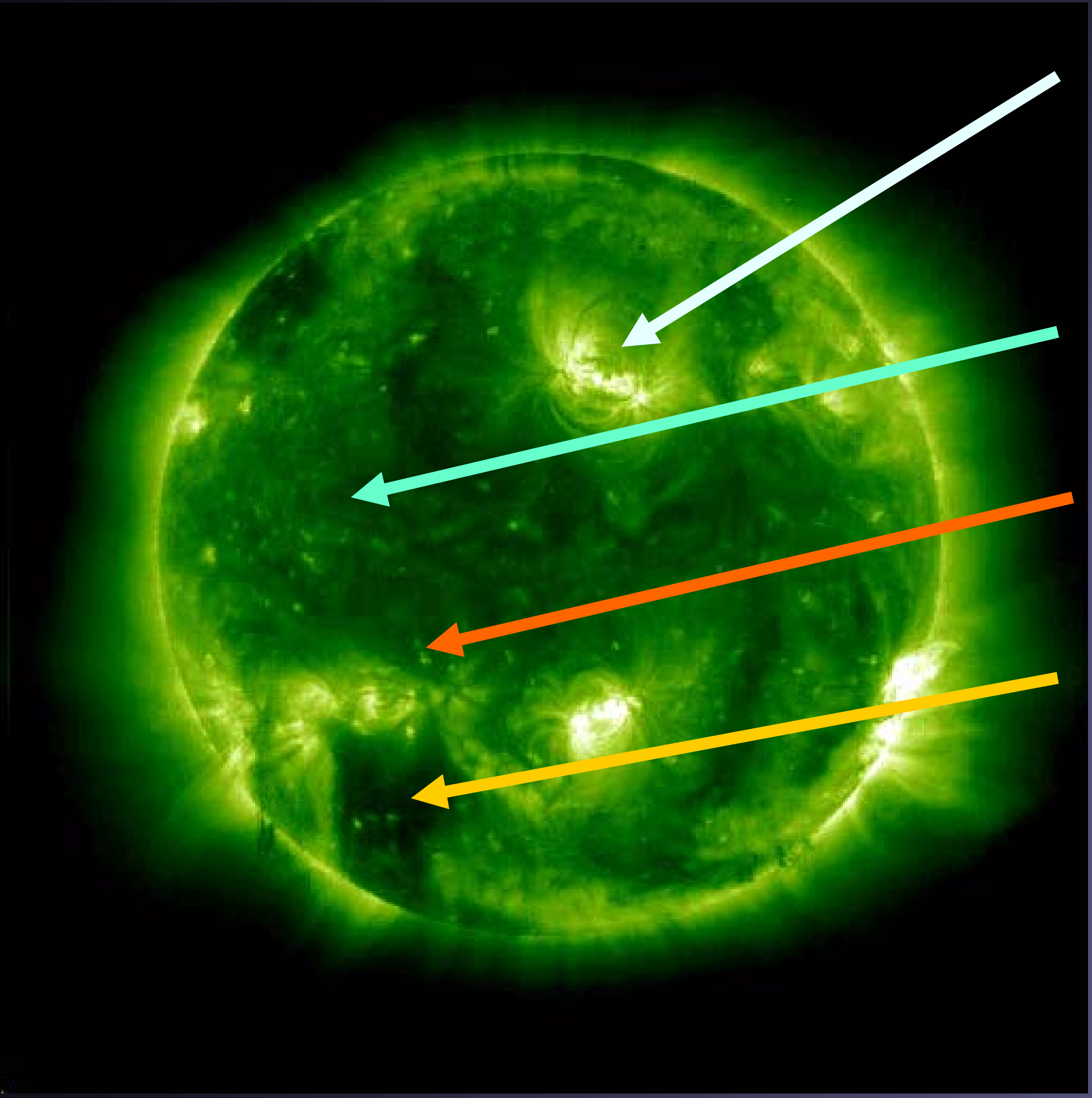

- Active region (loops)
- Quiet Sun
- X-ray bright point
- Coronal hole
- Arcades

Fe XII 195 Å
(1.500.000 K)
17 May - 8 June 1998

Coronal structure: active region loops

TRACE, 1999

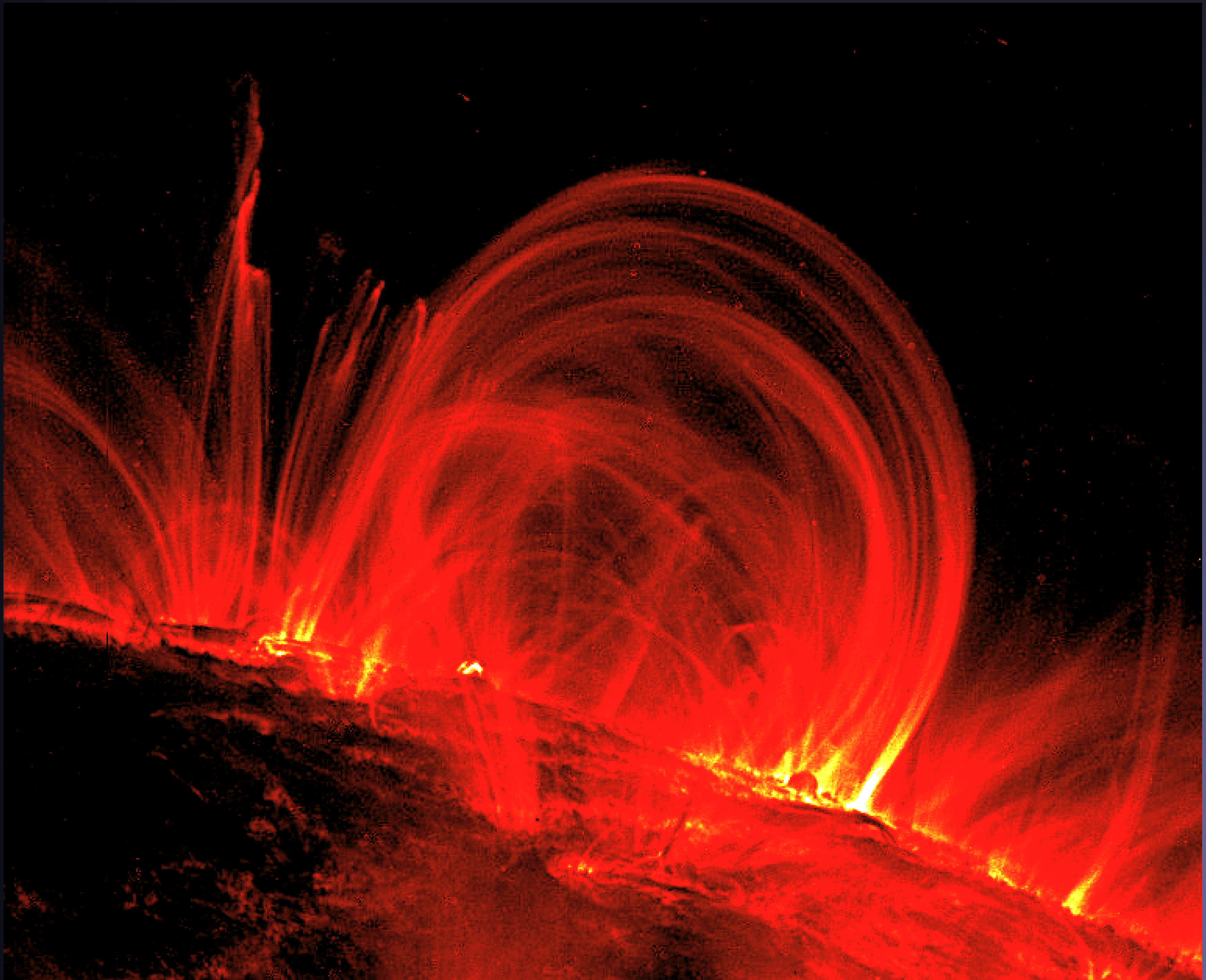

Coronal temperature & density

- Different temperatures & densities co-exist in the corona
- Range of temps: <1 MK (Coronal hole) to 10 MK (act. region)
- e^- densities (inner corona):
  - Loop: 10^{10} particles cm^{-2}
  - Coronal hole: 10^7 particles cm^{-2}

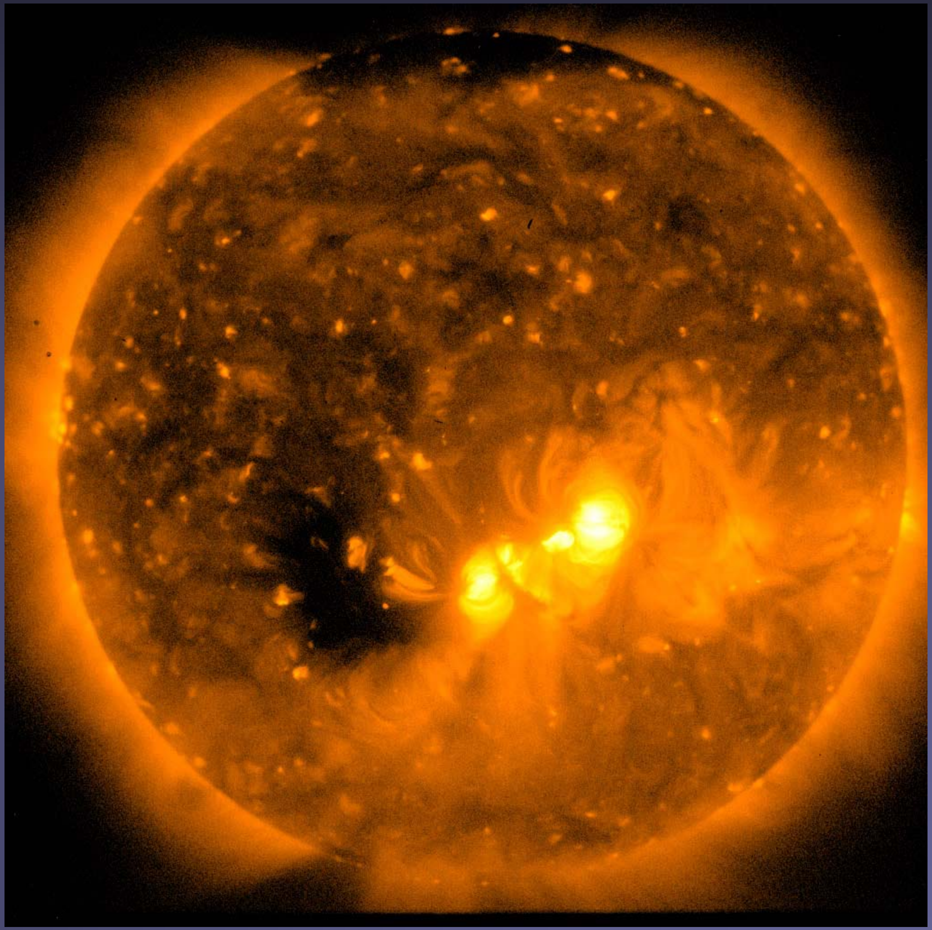

Hinode XRT: 2-5MK gas

Flux Tubes, Canopies, Loops and Funnels

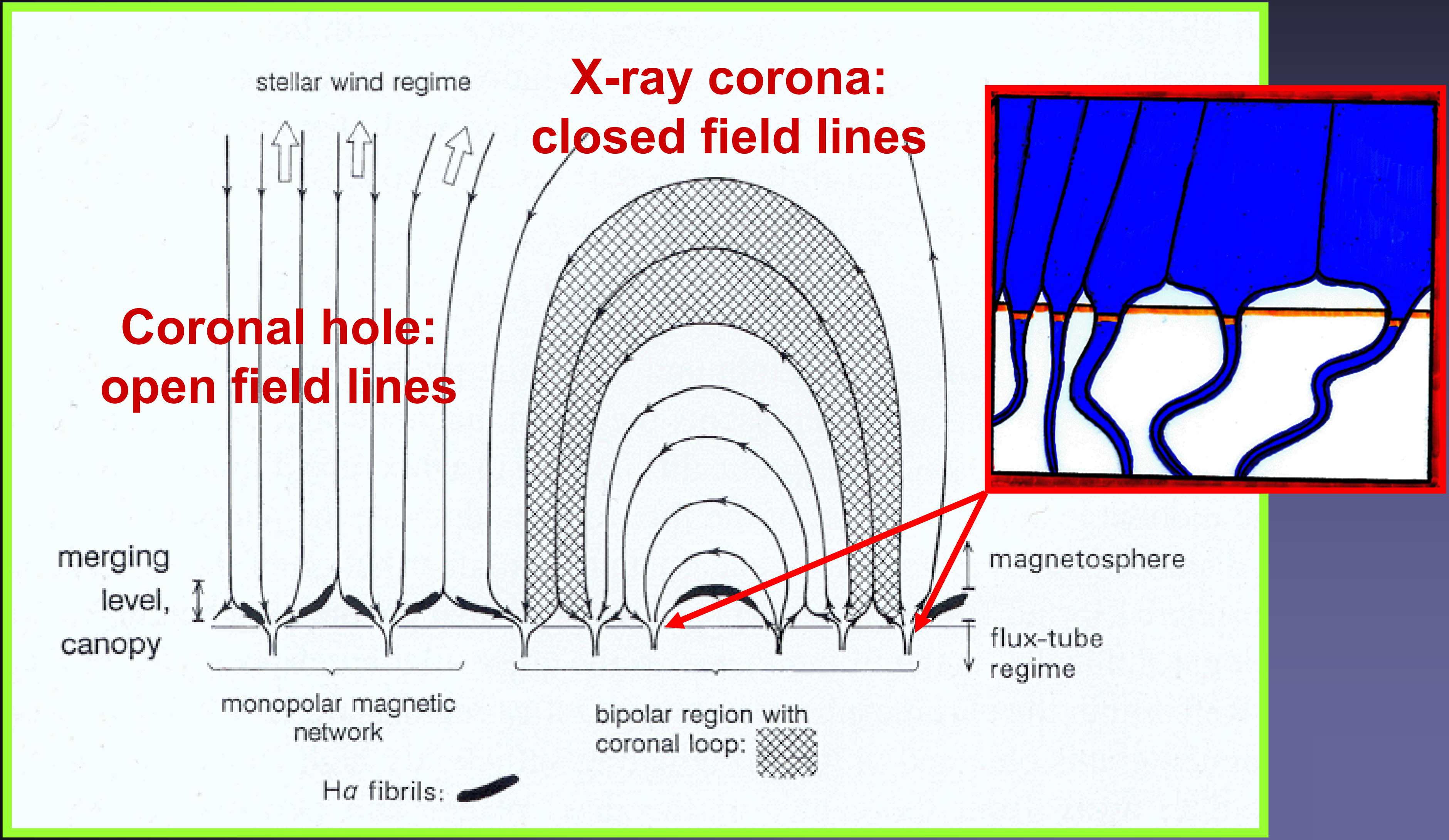

Energy budget: Open & closed coronal field

magnetically closed

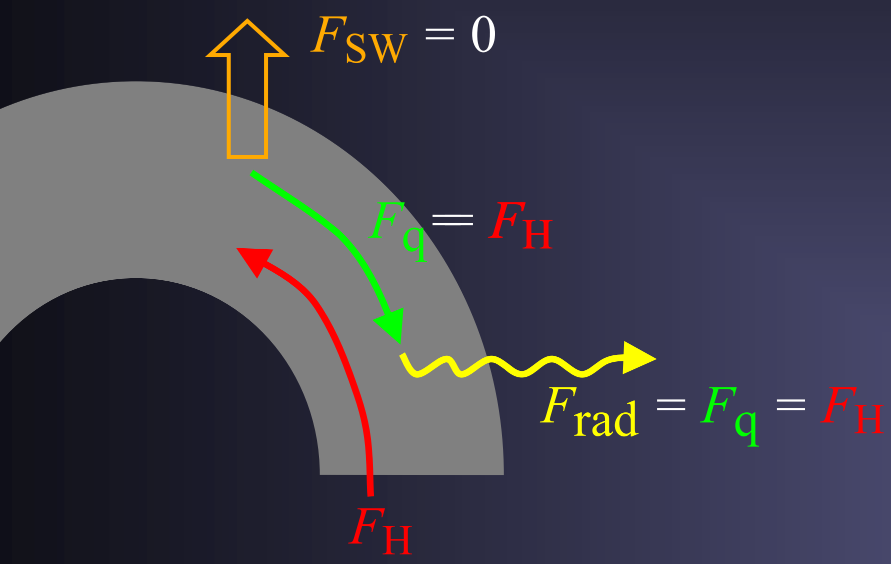

radiation ≈ 100 % of energy input

magnetically open

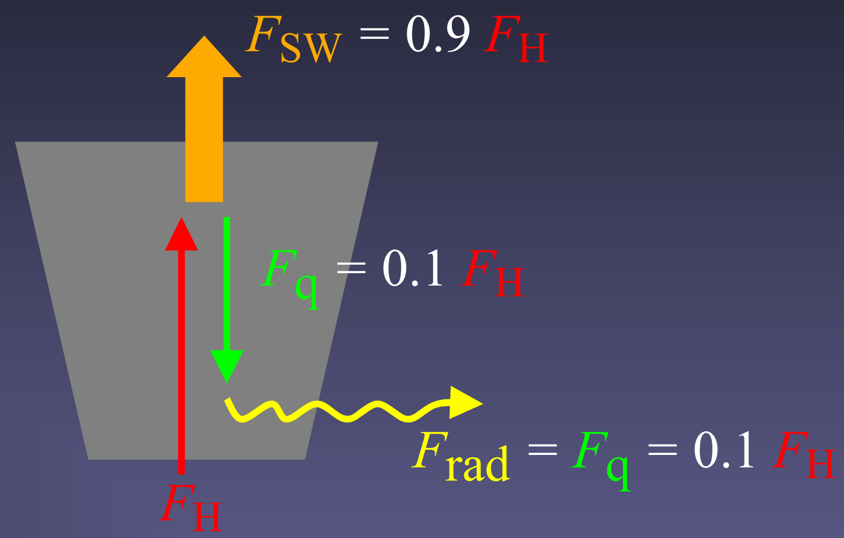

radiation ≈ 10 % of energy input

F_H = Energy flux heating the gas; F_q = Conductive energy flux; F_{SW} = Solar wind flux

Assume the same energy input into open and closed regions:

almost ALL emission we see on the disk outside coronal holes originates from magnetically closed structures (loops) !

kindly provided by Hardi Peter

Sources of solar wind: fast wind

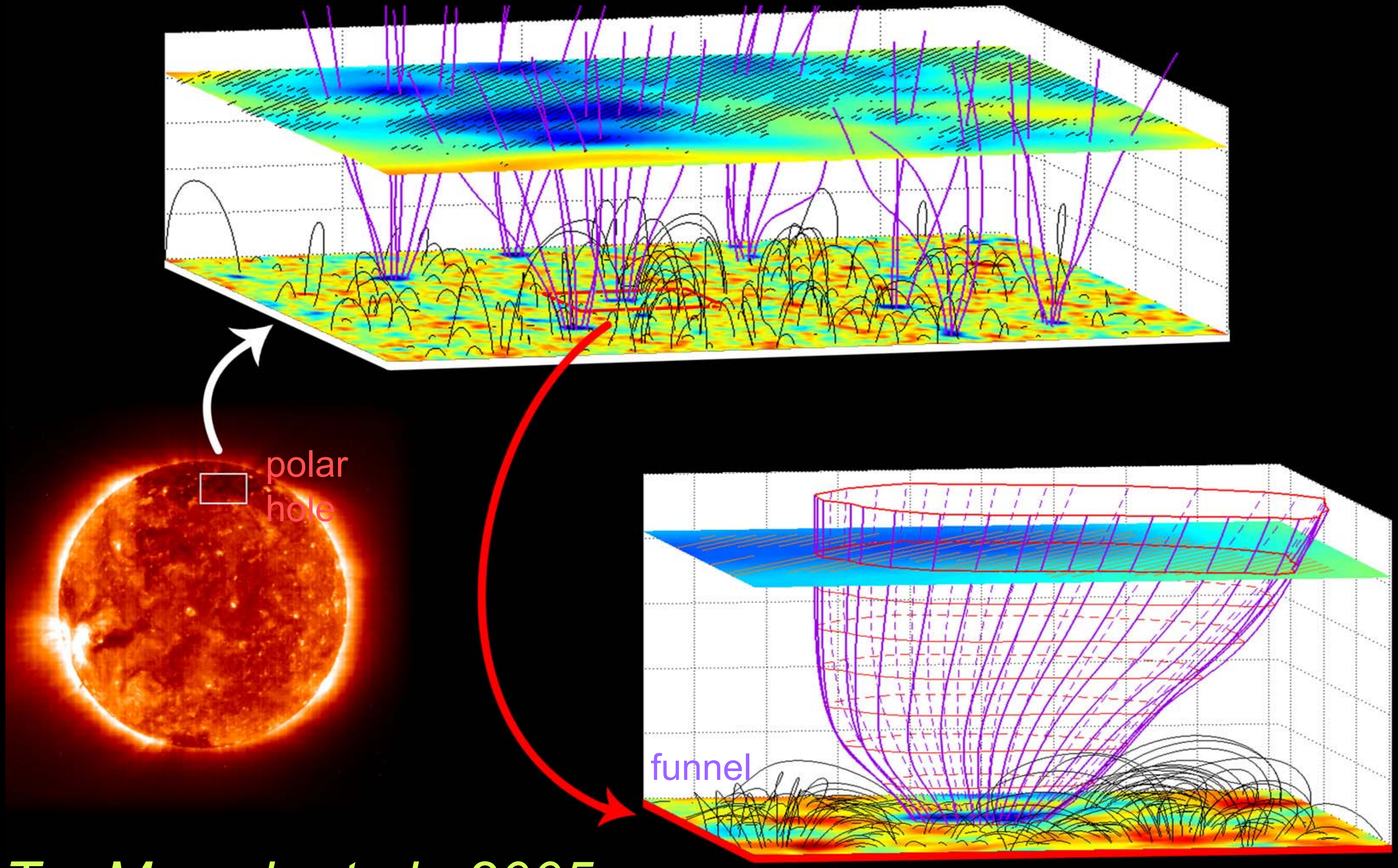

Tu, Marsch et al., 2005

TRACE 171Å observations of flare and post flare arcade near limb

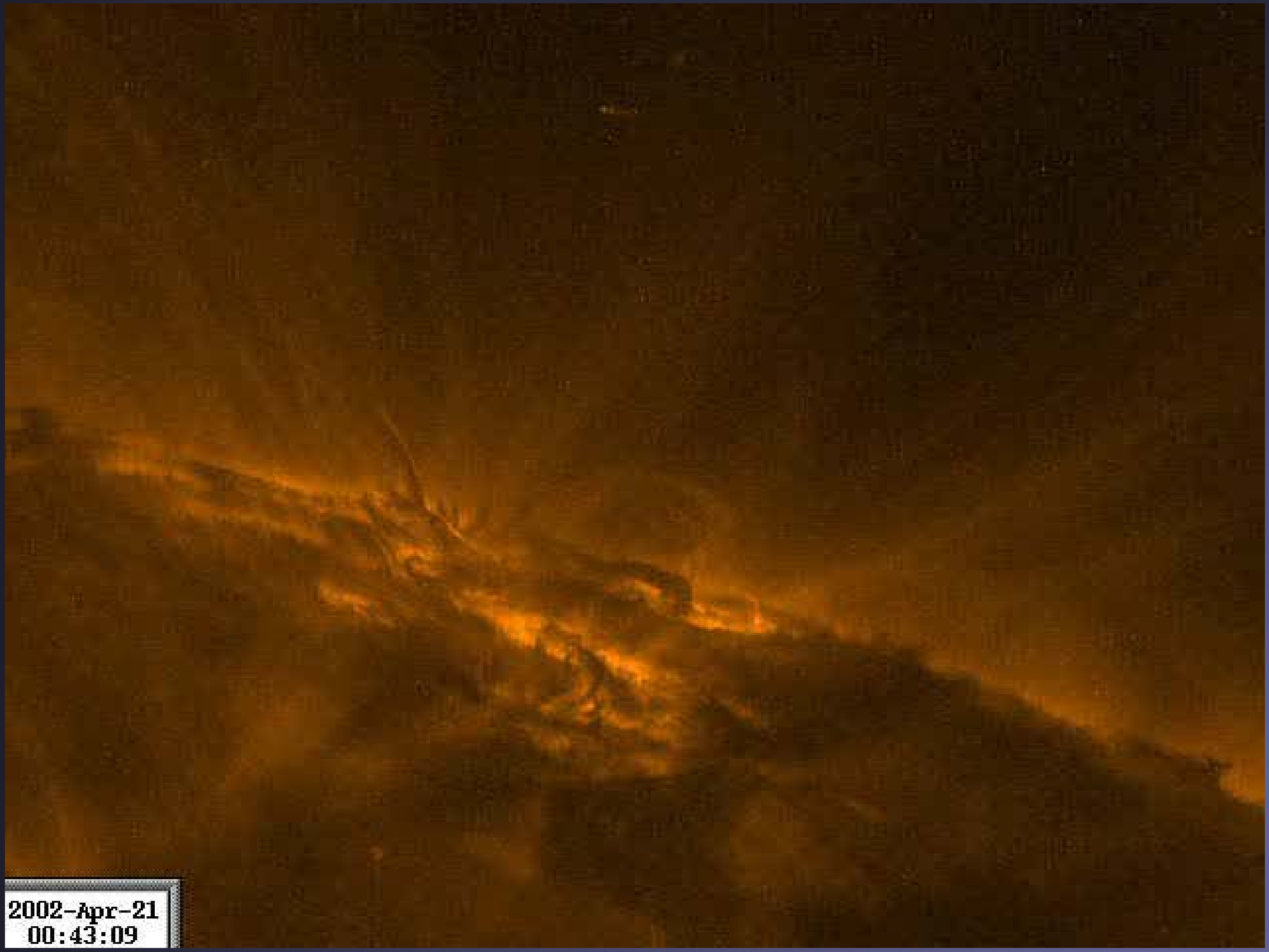

Coronal mass ejection (CME)

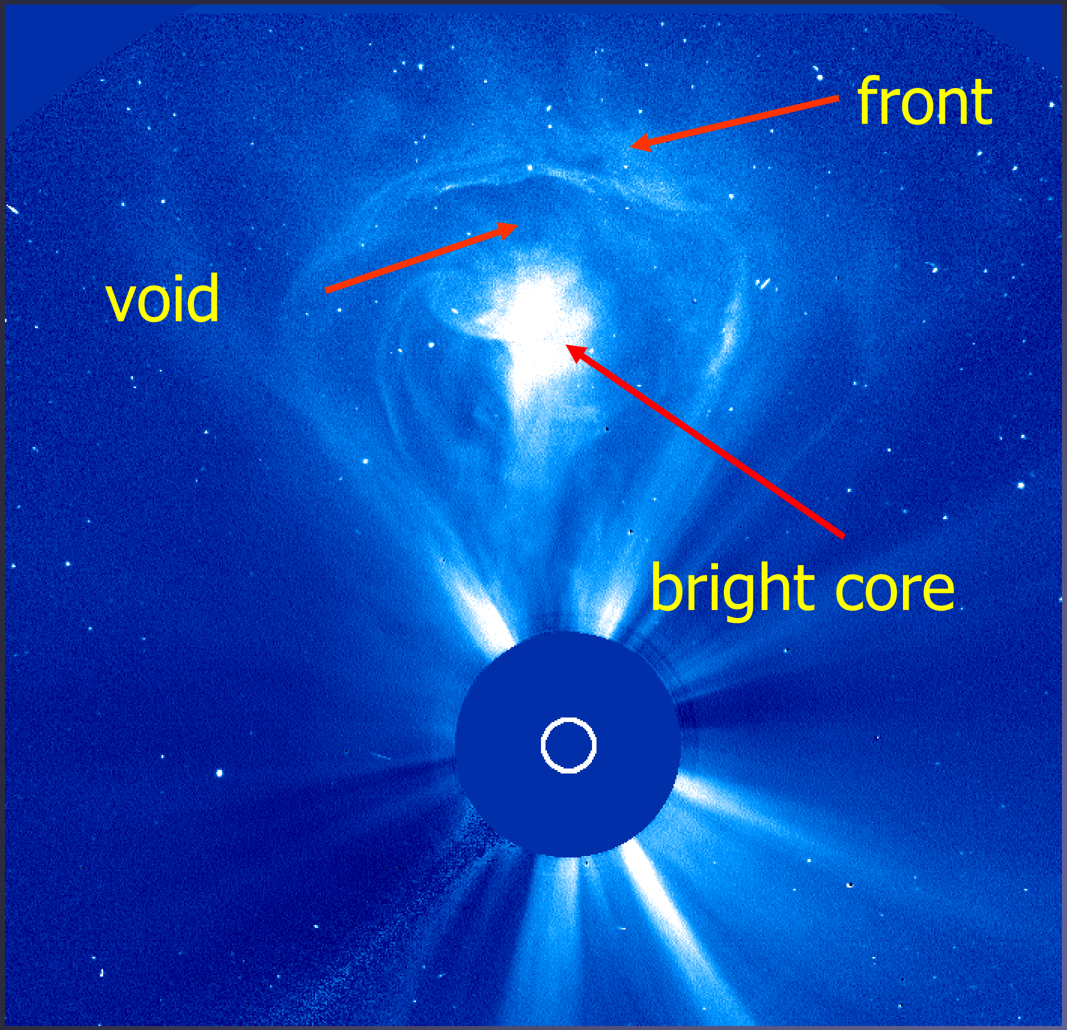

Plasma β vs. height in solar atmosphere

Plasma β: ratio of thermal to magnetic energy density:

$$\beta = \frac{8\pi P}{B^2}$$

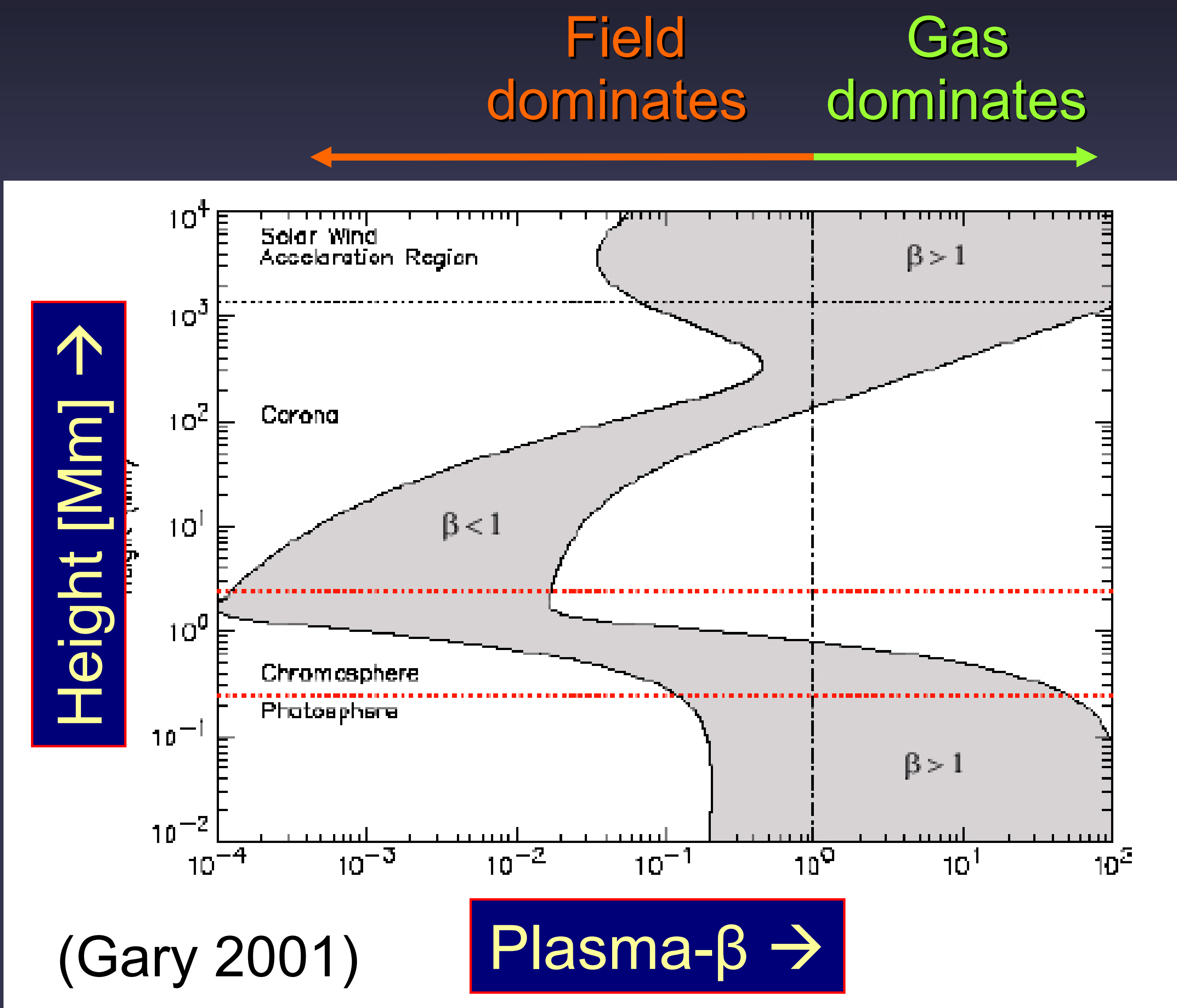

(Gary 2001)

Energy input into corona

Random footpoint motions of a loop will lead to a braiding of the field (first proposed by Parker 1983)

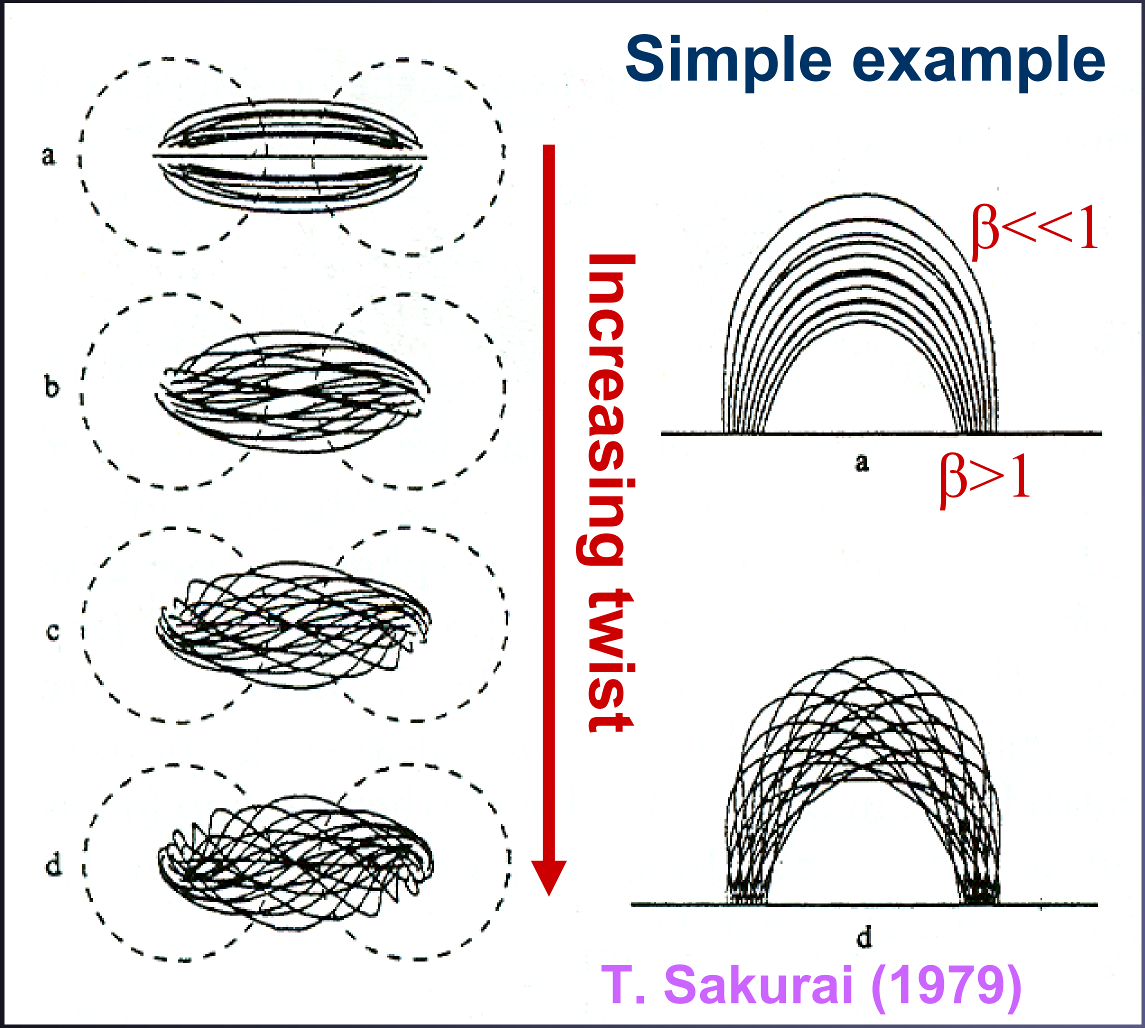

Starting from loop-like potential field, i.e. lowest energy configuration, energy in field can be increased by moving the loop footpoints

Source of footpoint motion: magneto-convection

Structure and dynamics at small spatial scales

Radiation-MHD Simulations of small-scale magnetic fields

Intensity Vögler et al. Magnetic field

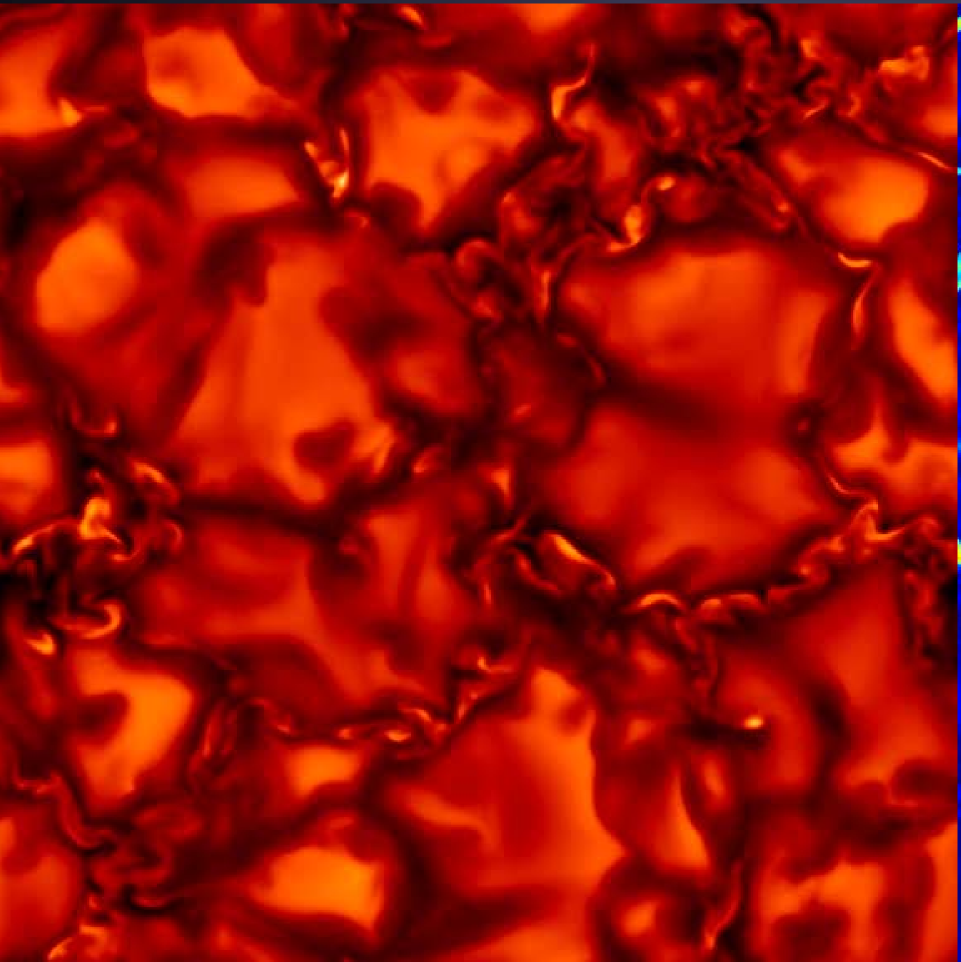

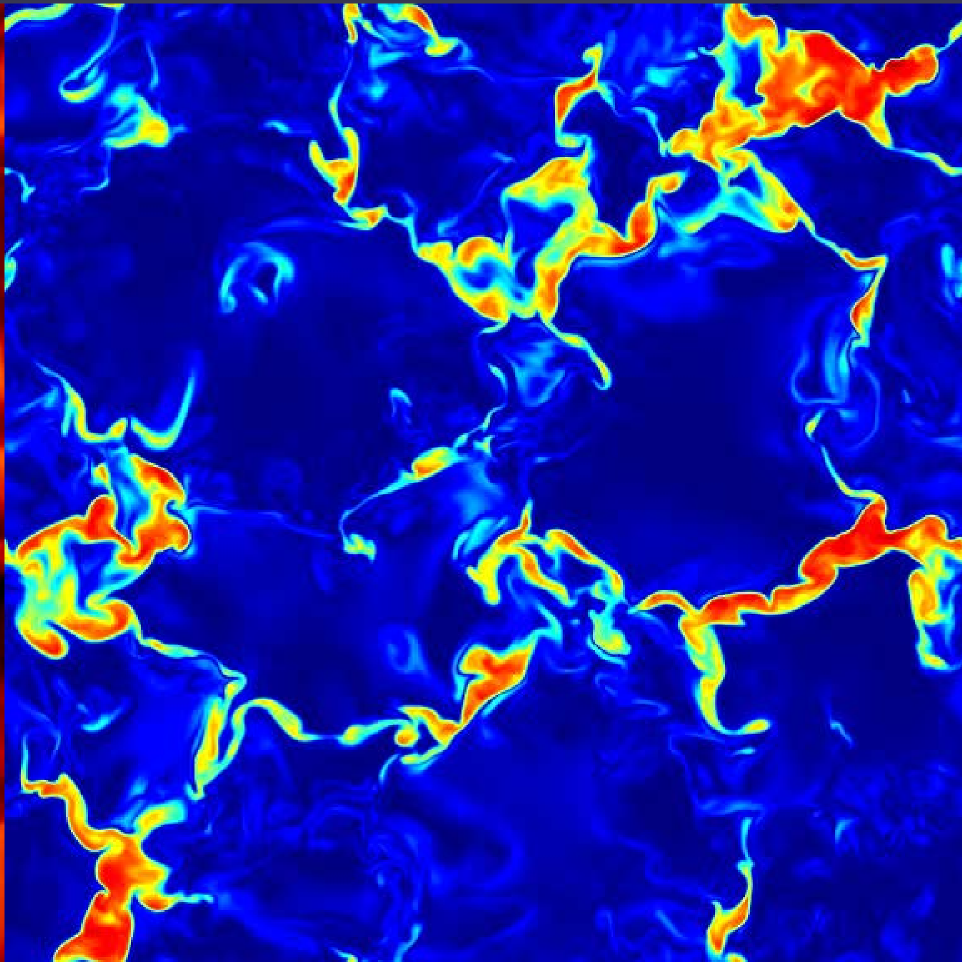

Magnetic coupling & coronal heating

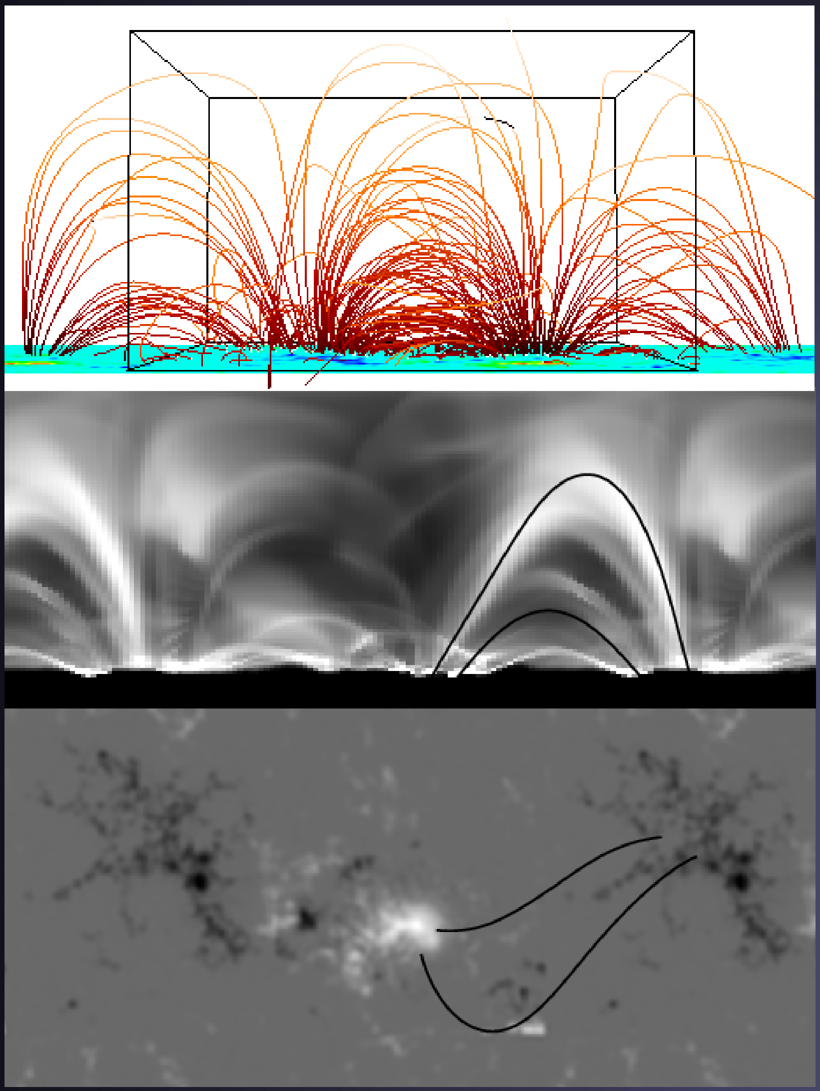

Gudiksen & Nordlund (2002)

Coronal loops maintained at MK temperatures by current dissipation

↑

Braiding of coronal magnetic field lines

↑

Emergence of new flux and interaction with convection: Magnetic footpoint motions

Magnetic reconnection (2-D)

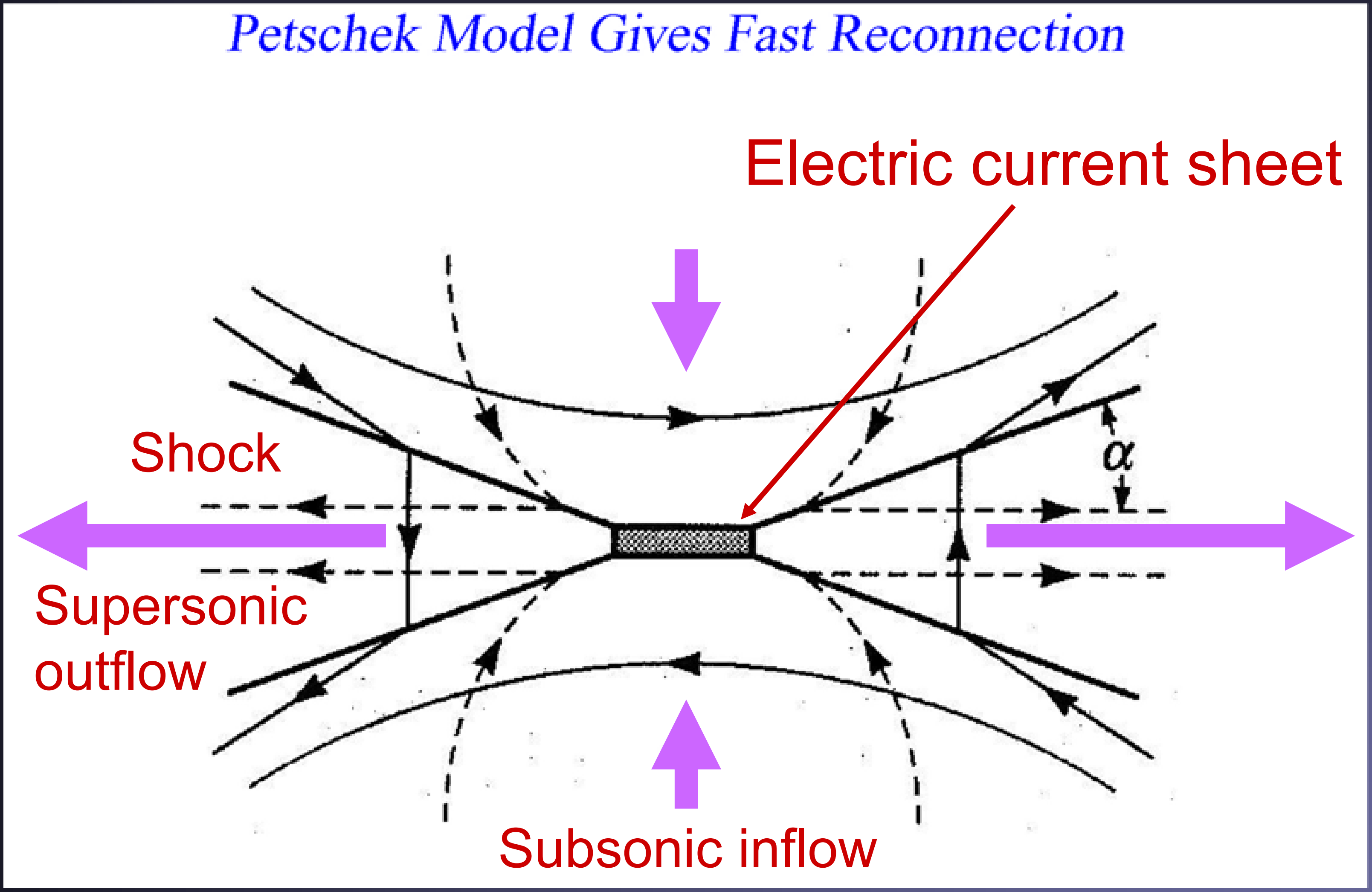

Electric Current Sheet at Coronal Base

He I 10830 Å reveals electric current sheet (tangential discontinuity of magnetic vector) at coronal base

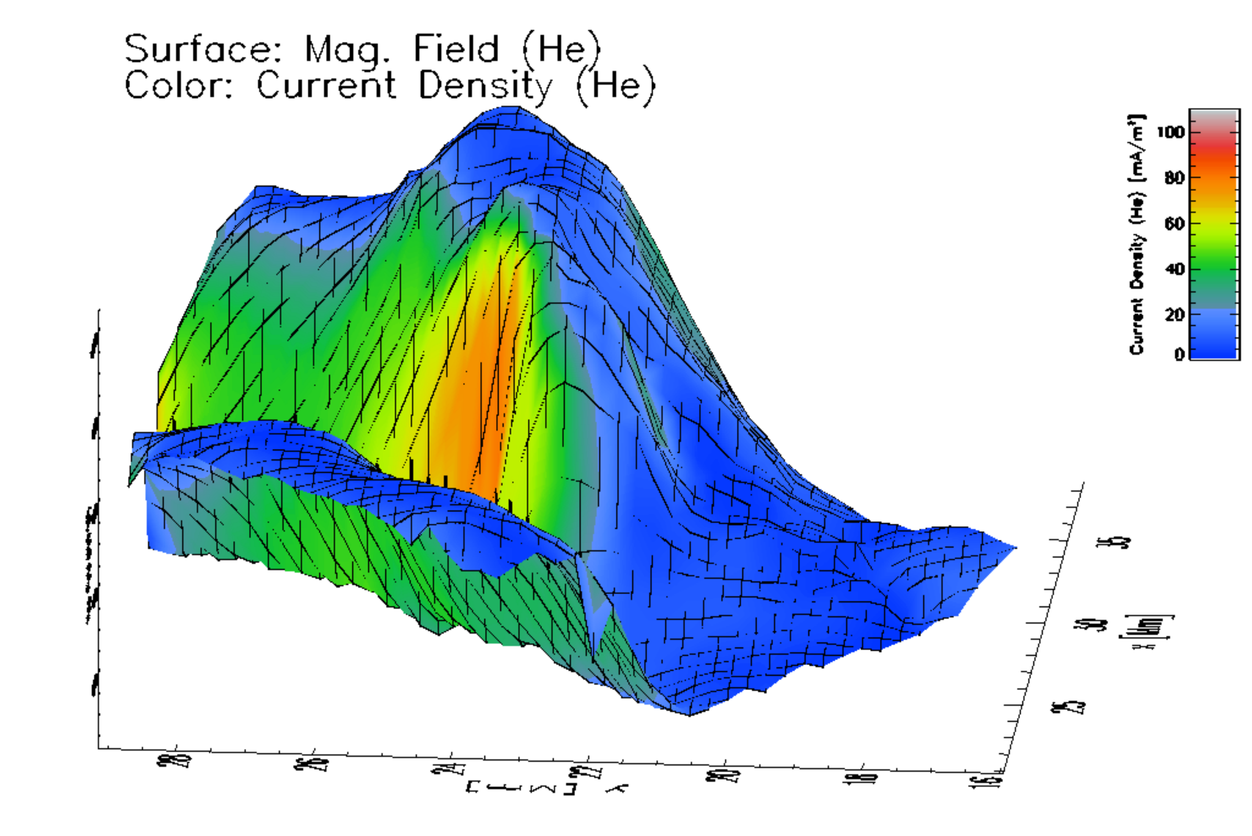

Solanki et al. 2003, Animation: A. Lagg

Observed in emerging flux region

Surface: magnetic field strength (note the valley)

Colour: current density

Explosive events: evidence for reconnection

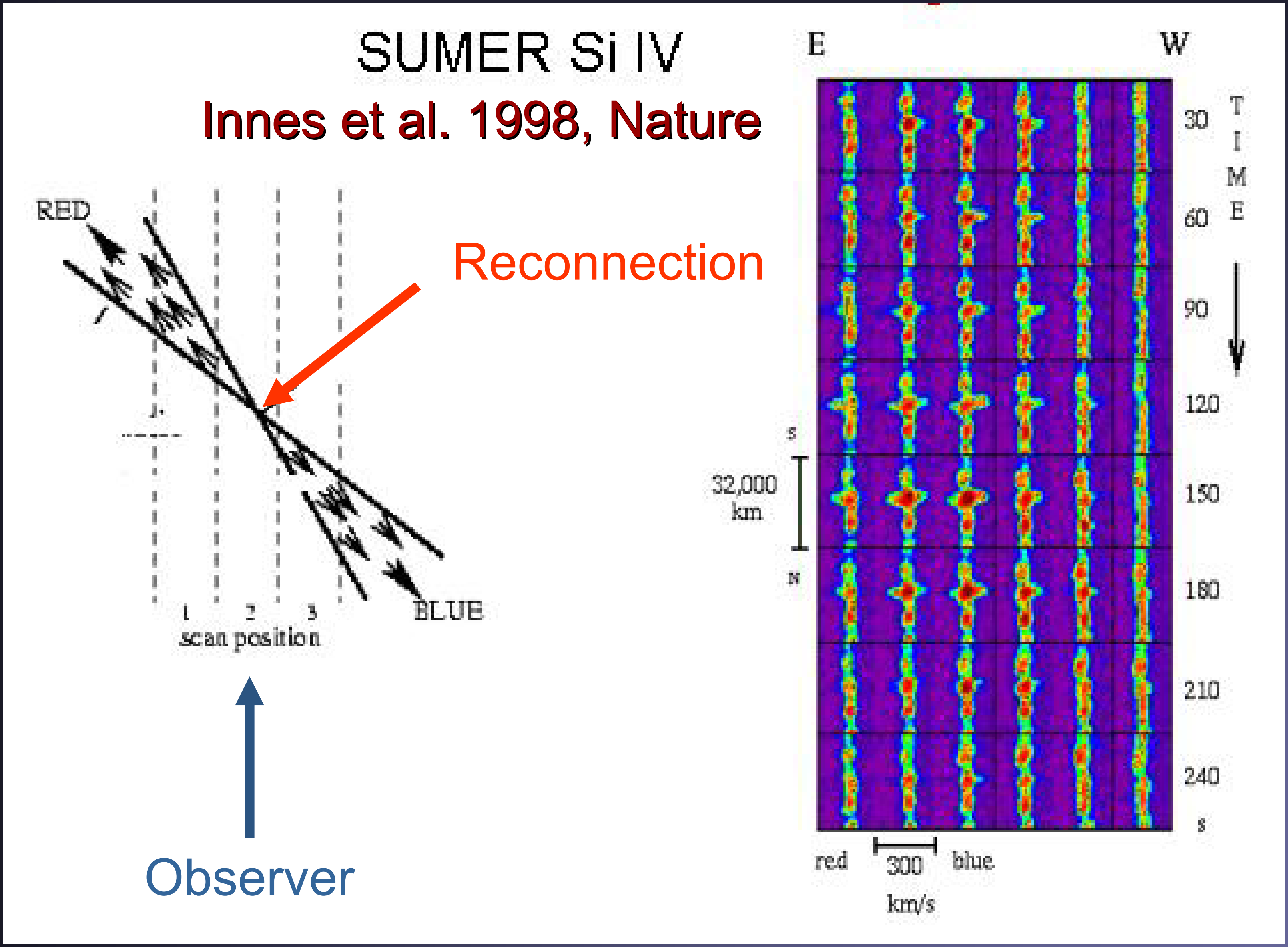

Magnetic fields in the upper solar atmosphere

Methods of determining the magnetic field above the solar photosphere

- Zeeman effect in chromospheric or coronal spectral lines (visible and IR)
- Hanle effect in chromospheric or coronal spectral lines (VUV, NUV, visible, IR)
- Gyroresonance emission at radio wavelengths
- Free-free emission at radio wavelengths
- Faraday rotation at radio wavelengths
- Coronal loop oscillations (EUV)
- In situ measurements in the heliosphere
- Extrapolation from photospheric magnetograms using potential or force-free fields

Problems with coronal field measurements

- In spite of this richness of techniques we know far less about the field in the corona than in the photosphere, where we can only employ 2 techniques
- Reasons:
  - Field in corona is much weaker than in photosphere: typically a few 10 G vs. 1000 G
  - S/N is much lower in corona than in photosphere (factor of $>10^3$)
  - corona is optically thin (for most techniques):
    - field can cancel even along line of sight!
    - we do not know where we are sampling the field

Zeeman effect: B near base of corona

- Measurement of Zeeman effect (full Stokes vector) in He I 10830 Å
- Gives full magnetic vector at base of corona, in prominences & cool (freshly emerged) loops
- Advantages:
  - Optically thin: formation details not required
  - Allows high spatial resolution

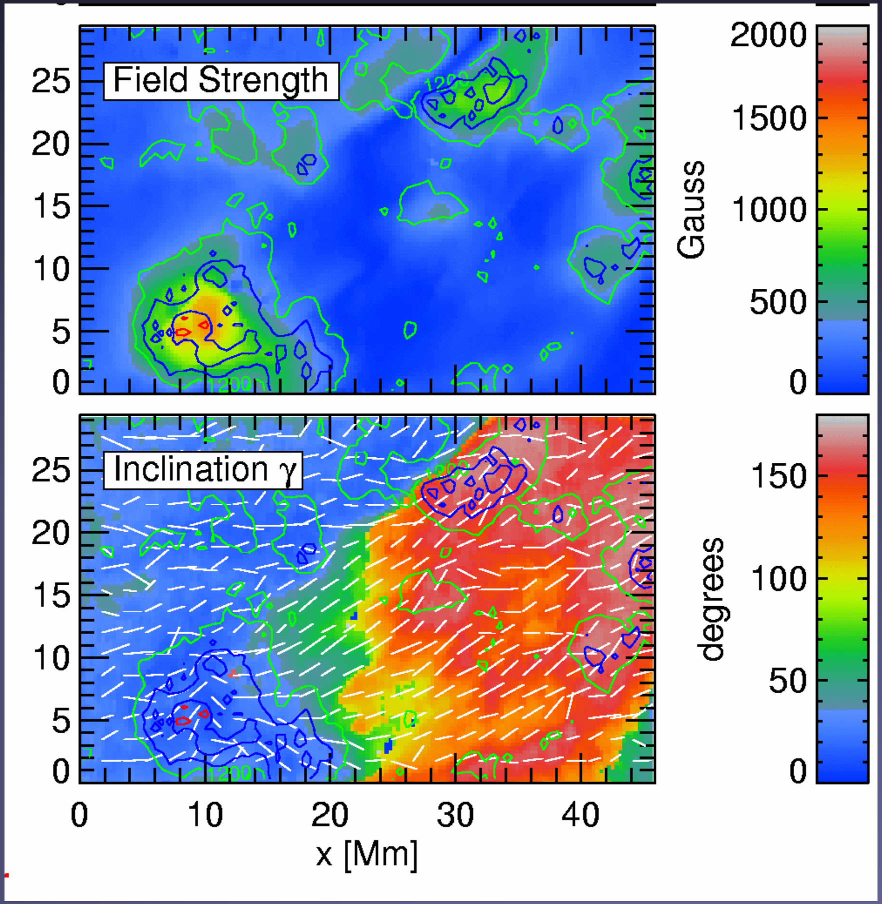

Solanki et al. 2003, Lagg et al. 2004

Disadvantage: formation height?

Structure of Cool Magnetic Loops

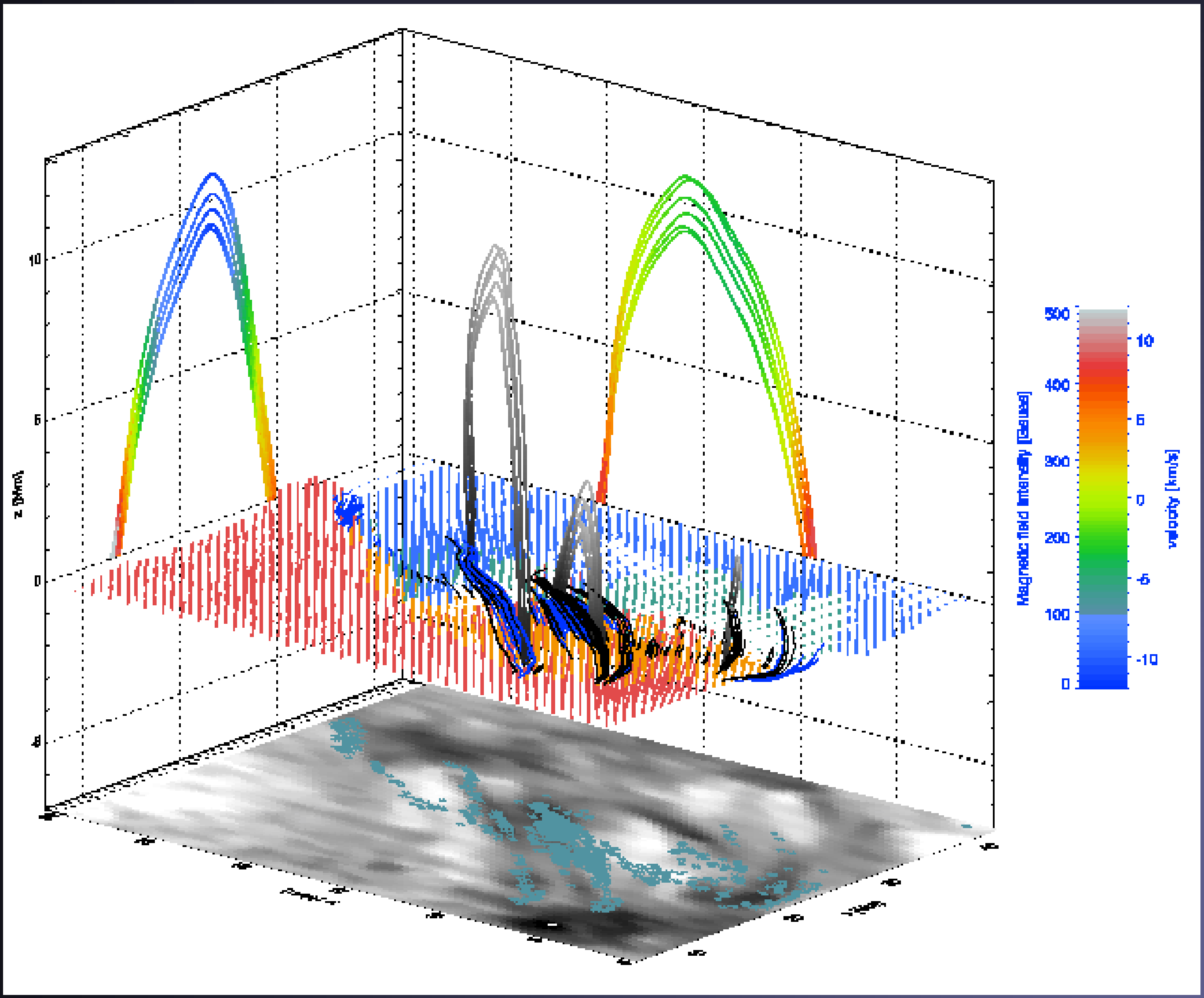

Magnetic loops deduced from measurements of He I 10830 Å Stokes profiles in an emerging flux region.

Left projection: Field strength

Right projection: Vertical velocity

Solanki et al. 2003 (A. Lagg)

Testing Magnetic Extrapolations

- Force-free field with $\alpha(x,y,z)$ reproduces loops reconstructed from observations better than force-free field with α=const. and far better than a potential field extrapolation

➔ Loops harbour strong currents while still emerging

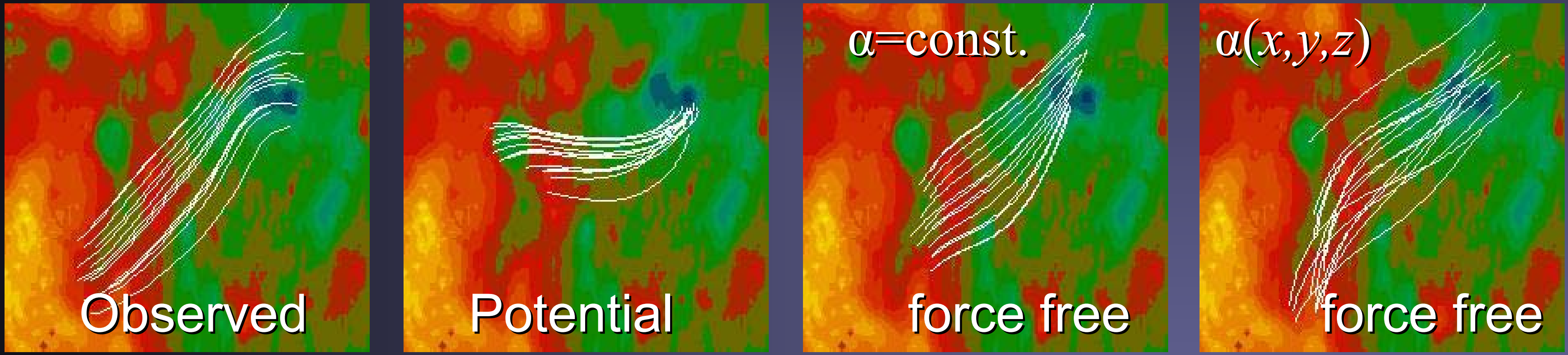

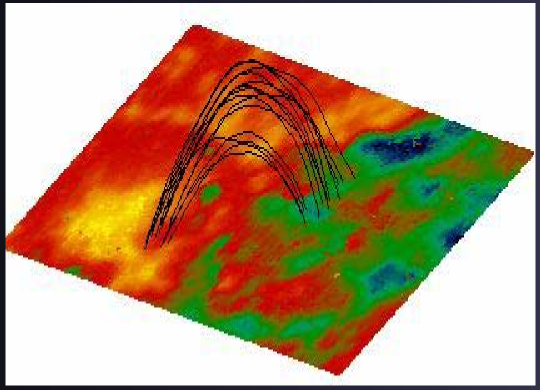

$$\nabla \times \mathbf{B} = 0$$

$$\nabla \times \mathbf{B} = \alpha \mathbf{B}$$

Wiegelmann et al. 2005

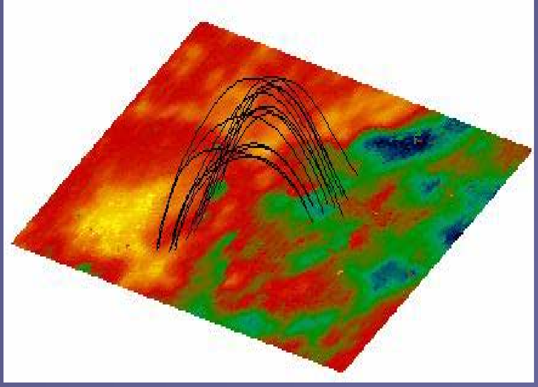

STEREO: Solar-TErrestrial RElations Observatory

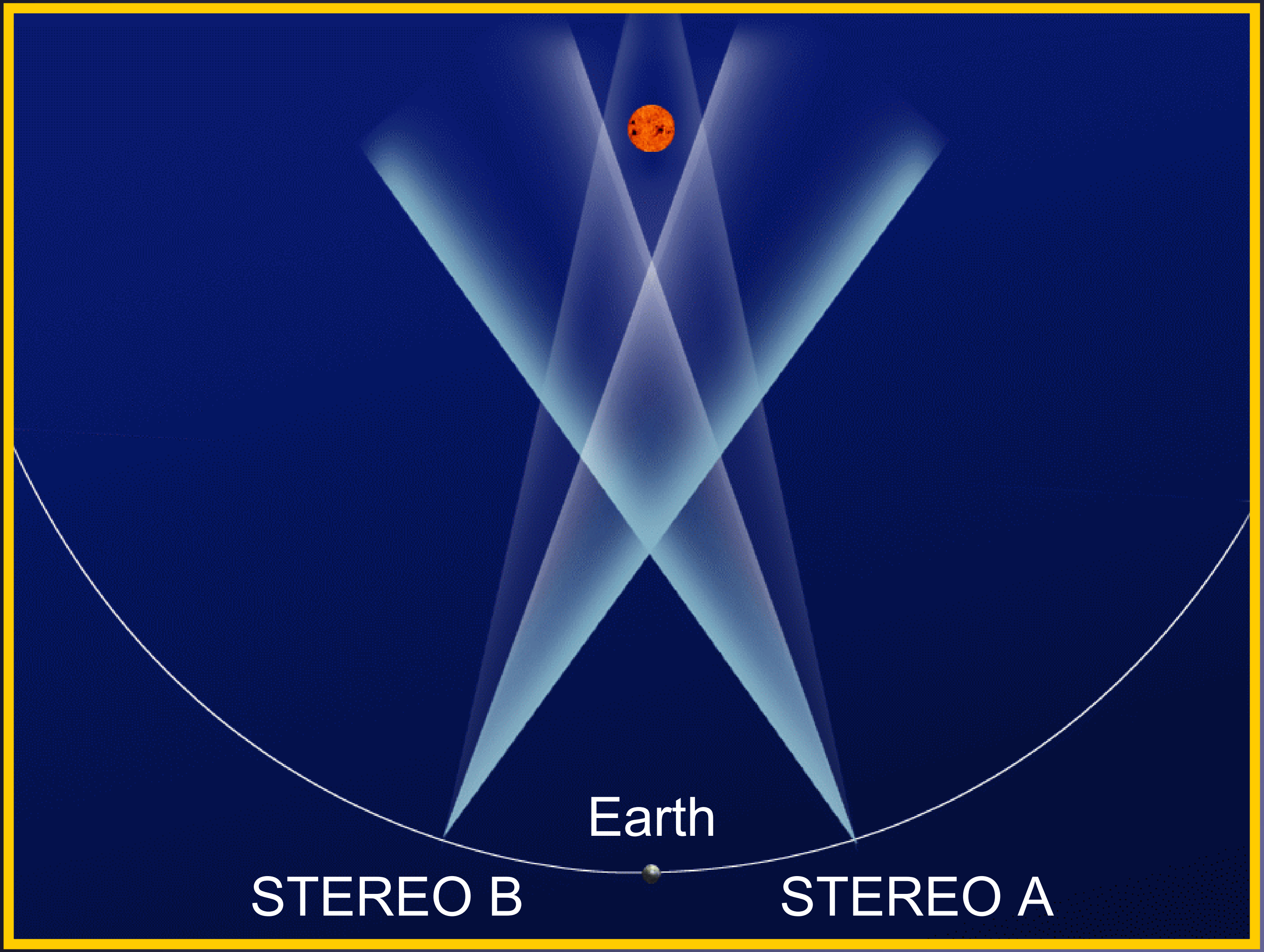

Coronal loops in 3-D

Yellow lines: First stereoscopic reconstruction of coronal loops observed by the two STEREO spacecraft looking at the Sun from different directions.

Red lines: magnetic field extrapolations starting from magnetogram on solar surface

Feng et al. 2007

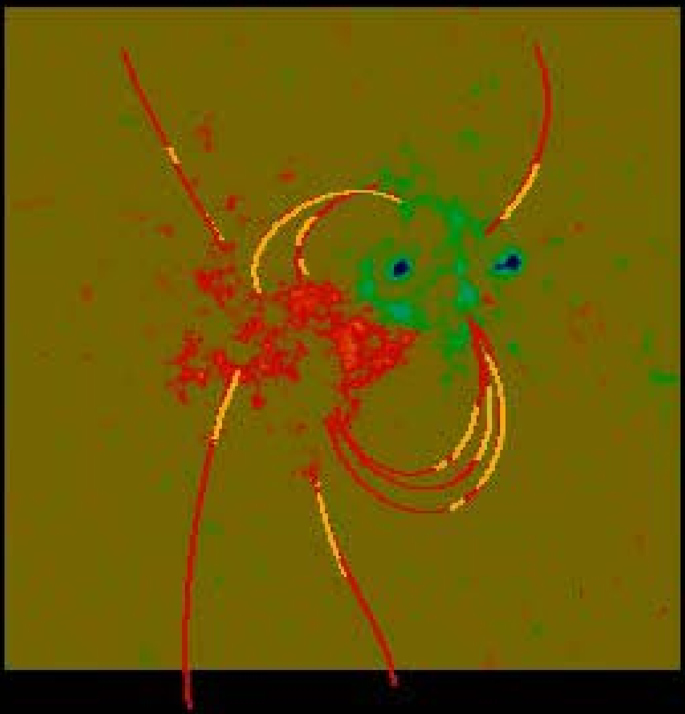

Coronal Zeeman & Hanle effect

- Coronagraphic obs. of Fe XIII 1074.4 & 1079.8 Å lines give B_z and azimuthal direction
- Integration through corona: limited spatial information
- Instrument: Coronal Multi-channel Polarimeter (CoMP): full Stokes

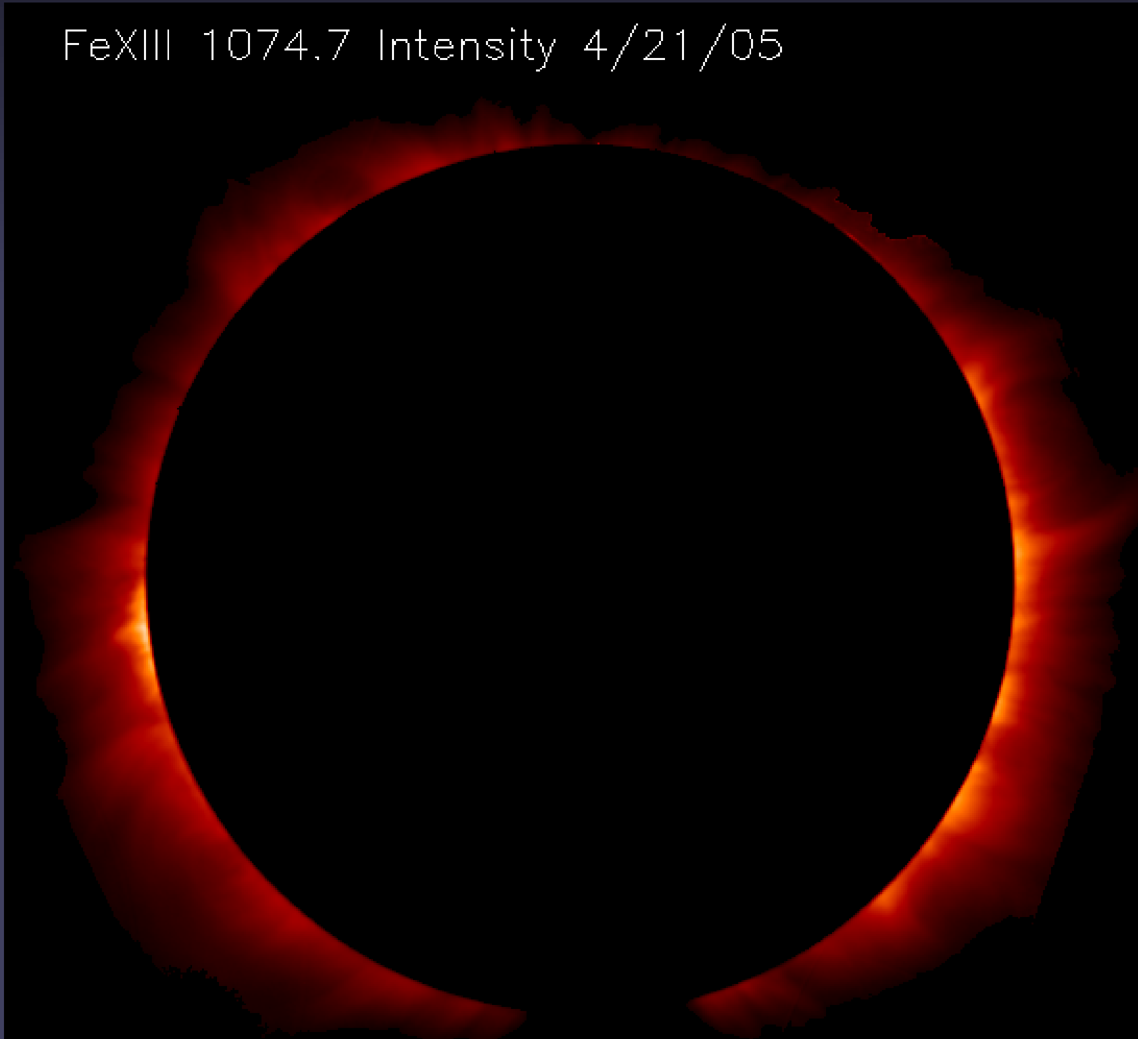

S. Tomczyk, 2004

Coronal Zeeman & Hanle effect

- Coronagraphic obs. of Fe XIII 1074.4 & 1079.8 Å lines give B_z and azimuthal direction
- Integration through corona: limited spatial information
- Instrument: Coronal Multi-channel Polarimeter (CoMP): full Stokes

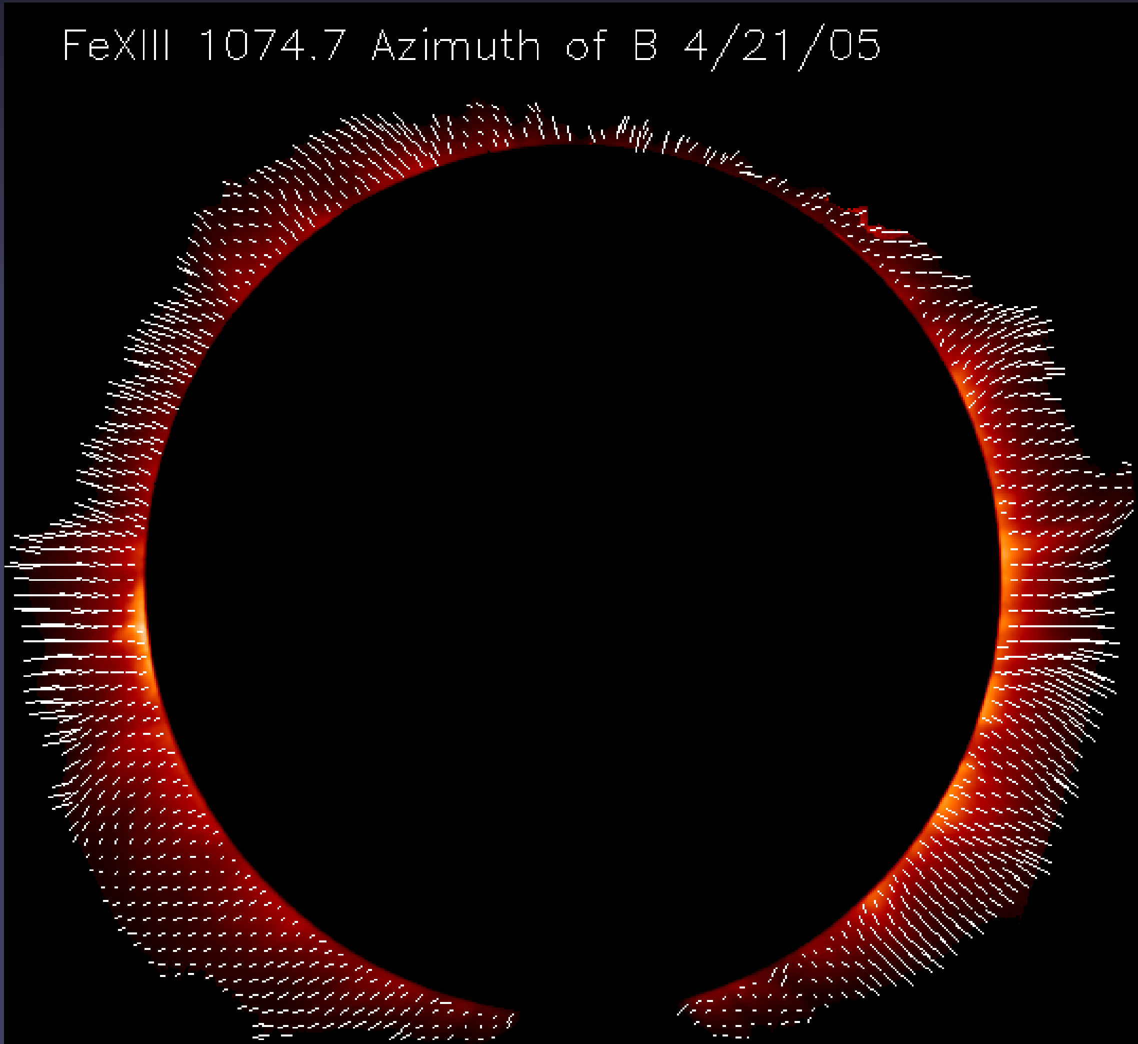

S. Tomczyk, 2004

Coronal Zeeman & Hanle effect

- Coronagraphic obs. of Fe XIII 1074.4 & 1079.8 Å lines give B_z and azimuthal direction
- Integration through corona: limited spatial information
- Instrument: Coronal Multi-channel Polarimeter (CoMP): full Stokes

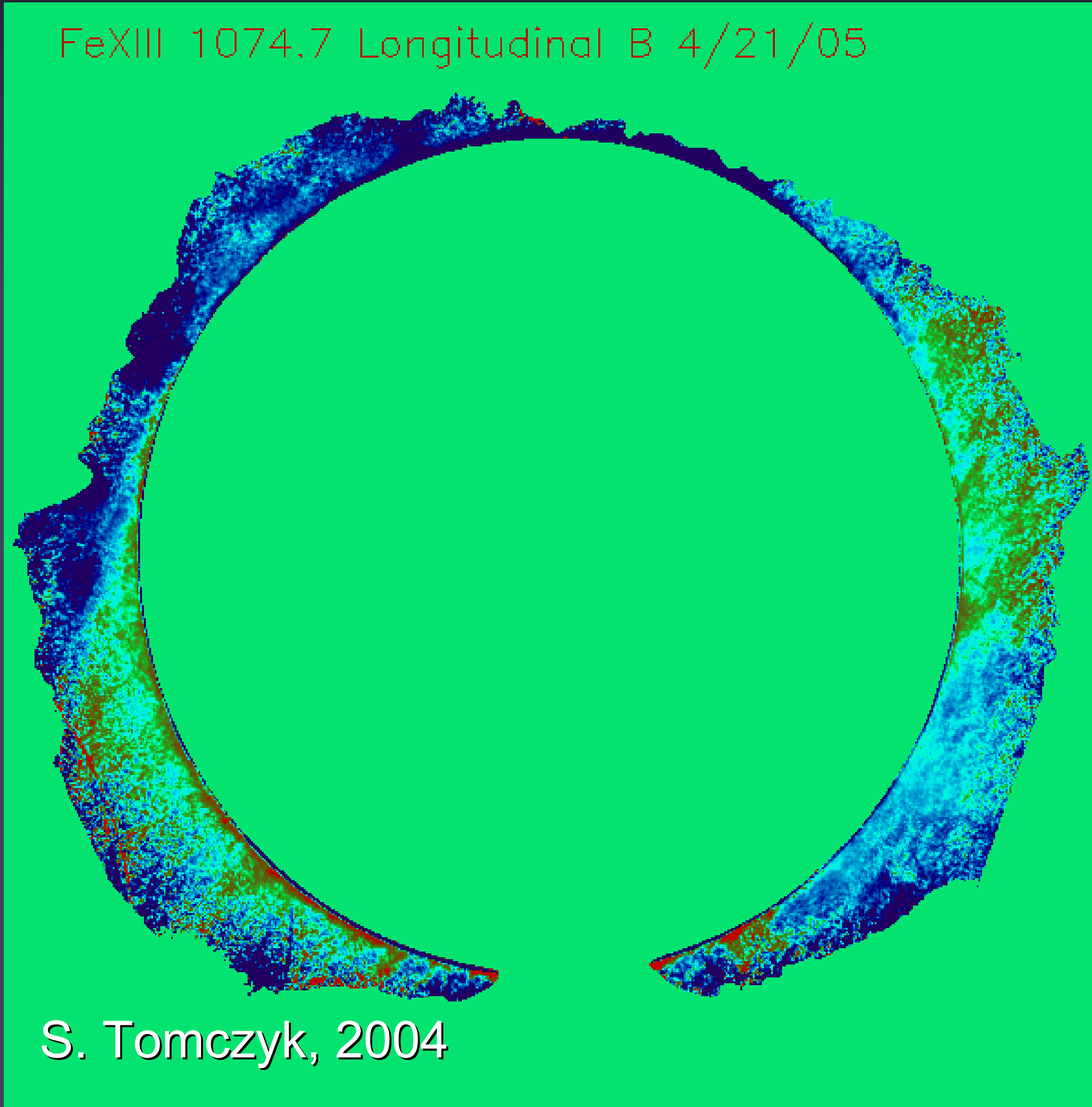

Radio measurements of coronal field

- Two main emission mechanisms compete in the solar corona at microwave frequencies:
  - free-free emission or bremsstrahlung: produced by collisional energy loss of non-thermal e^-. Present everywhere in corona. Dominates in regions of weaker field, e.g. active region plage, and at low frequencies ($\nu < 2$ GHz)
  - Gyroresonance emission or cyclotron emission or magneto-bremsstrahlung: produced by the gyration of e^- around magnetic field lines (Larmor orbit) due to Lorentz force. Sun: dominant in strong-field regions above sunspots, and generally at frequencies above a few GHz.
- Both mechanisms produce circular polarisation.

Active region at different radio frequencies

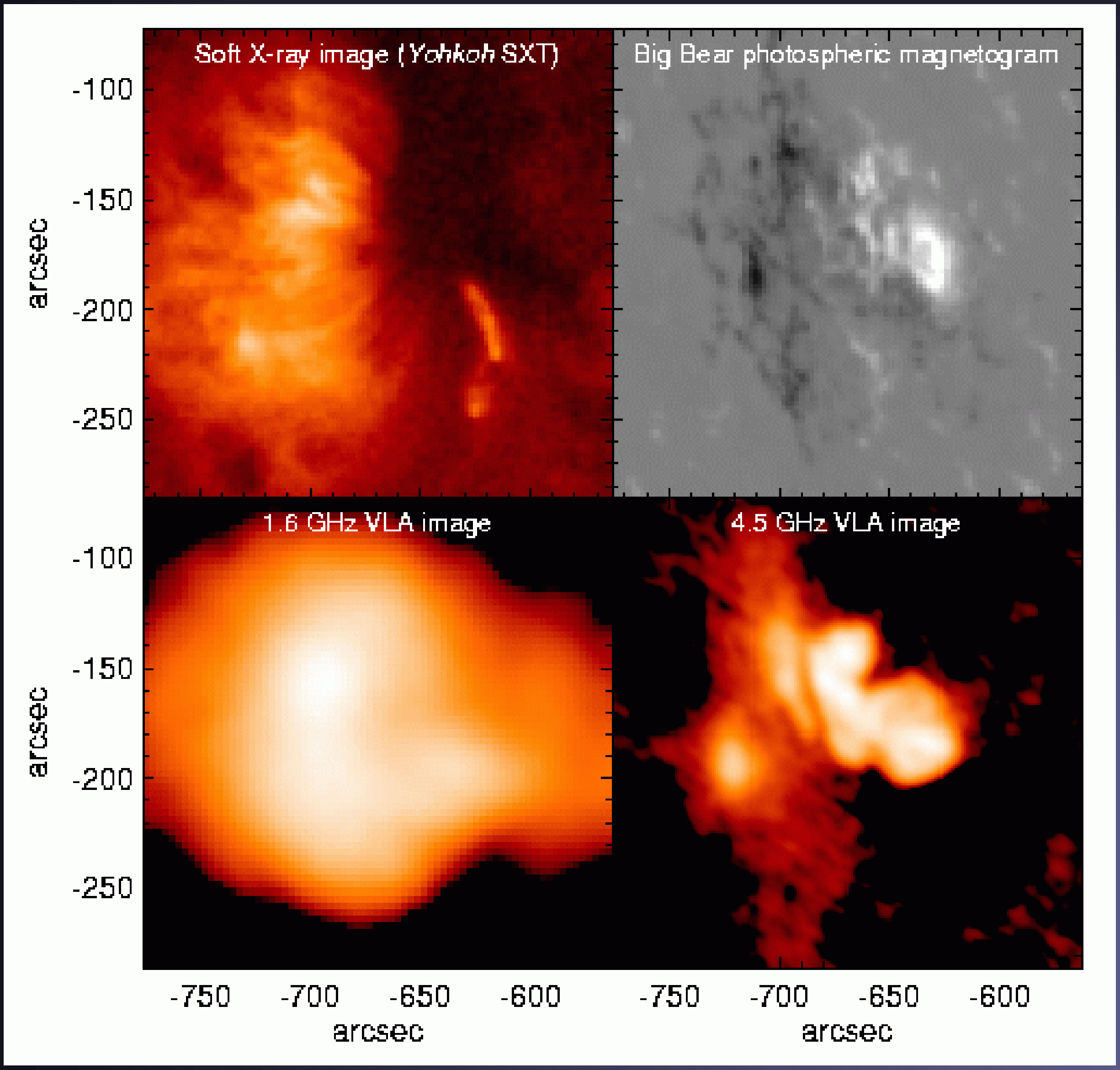

At low frequencies (lower left) bremsstrahlung (f-f) dominates radio emission. Maps resembles soft X-rays (upper left)

Above 2-3 GHz, gyro emission dominates radio maps. They resemble magnetograms (right)

Gyroresonance

- Produces emission peaks at multiples s of e^- gyrofrequency

$$\nu_B = \left(\frac{e\ B}{2\pi\ m_e c} \right) = 2.80 \times 10^6 B \qquad \text{[cgs units]}$$

- Gyrofrequency scales linearly with B
- Note: For strong fields of 10 MG, as found in magnetic WDs, the gyrofrequency reaches optical wavelengths; for $B > 10^{10}$ G (e.g. pulsars) it reaches X-ray & γ-ray wavelengths
- Opacity of gyroresonance emission for Maxwellian distribution of e^- velocities:

$$\propto \quad n_e B / (\partial B / \partial l)\ (\ T \sin^2\theta / mc^2\ )^{s\text{-}1}$$

where $s = 1, 2, 3, \ldots$ is the harmonic, θ is angle between $\mathbf{B}$ and line of sight (brighest for perpendicular fields)

Properties of gyroresonance emission

- Big difference in opacity of two polarizations of EM waves: extraordinary (x) mode interacts more with e$^-$ than ordinary (o) mode

- x and o modes → opposite circular polarizations (key to unlocking B)

- Looking on solar atmosphere from above, we only see down to highest optically thick layer at a given frequency and polarization, typically $s=3$ for x-mode, $s=2$ for o-mode

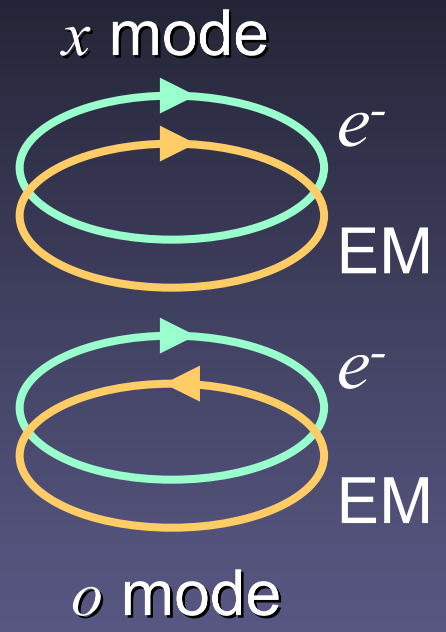

Calculated model sunspot gyroresonance layers

Gyro-resonance provides field strength B, but also gives some limited information on direction of field

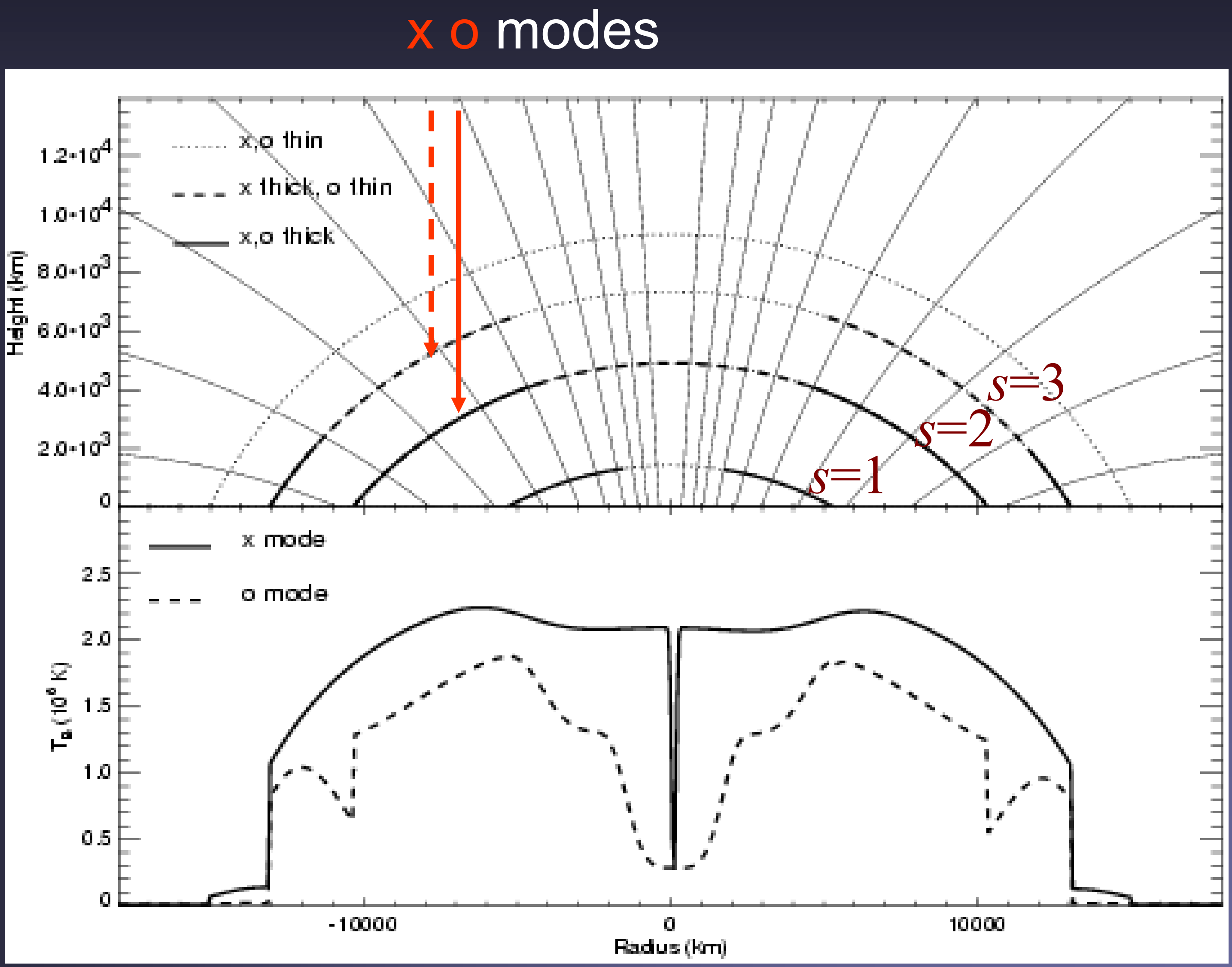

Gyroresonance layers

- Gyroresonance opacity is the only mechanism that makes corona optically thick at frequencies > 4 GHz
- Emission comes from a surface of constant B
- Microwaves are sensitive to fields in range 200–3000 G
- High levels of circular polarization also indicate presence of strong B and can be used to measure temperature gradients

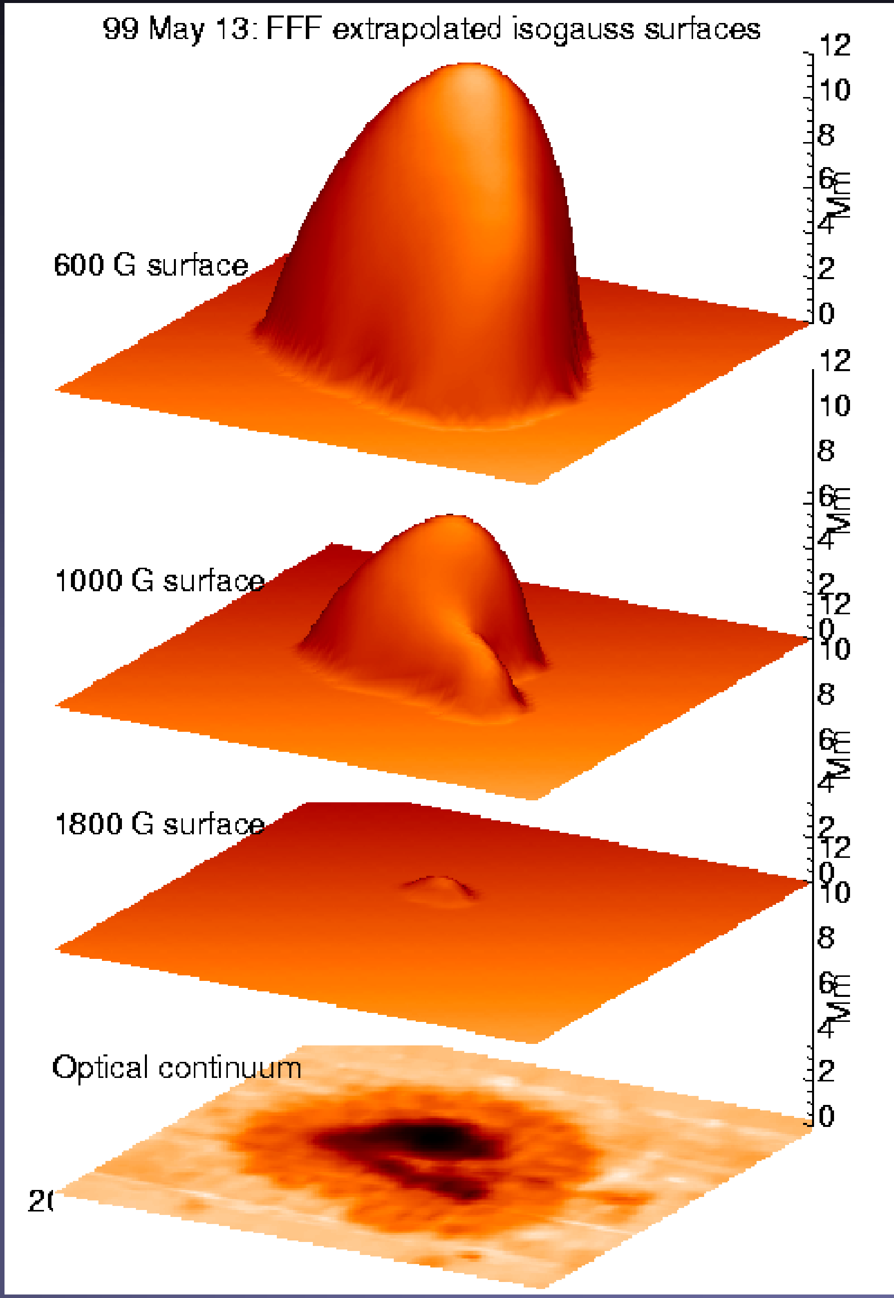

Radio Emission from Coronal Magnetic Fields

Region showing strong shear: radio images show high B and very high temperatures exactly where the magnetic field is non-potential

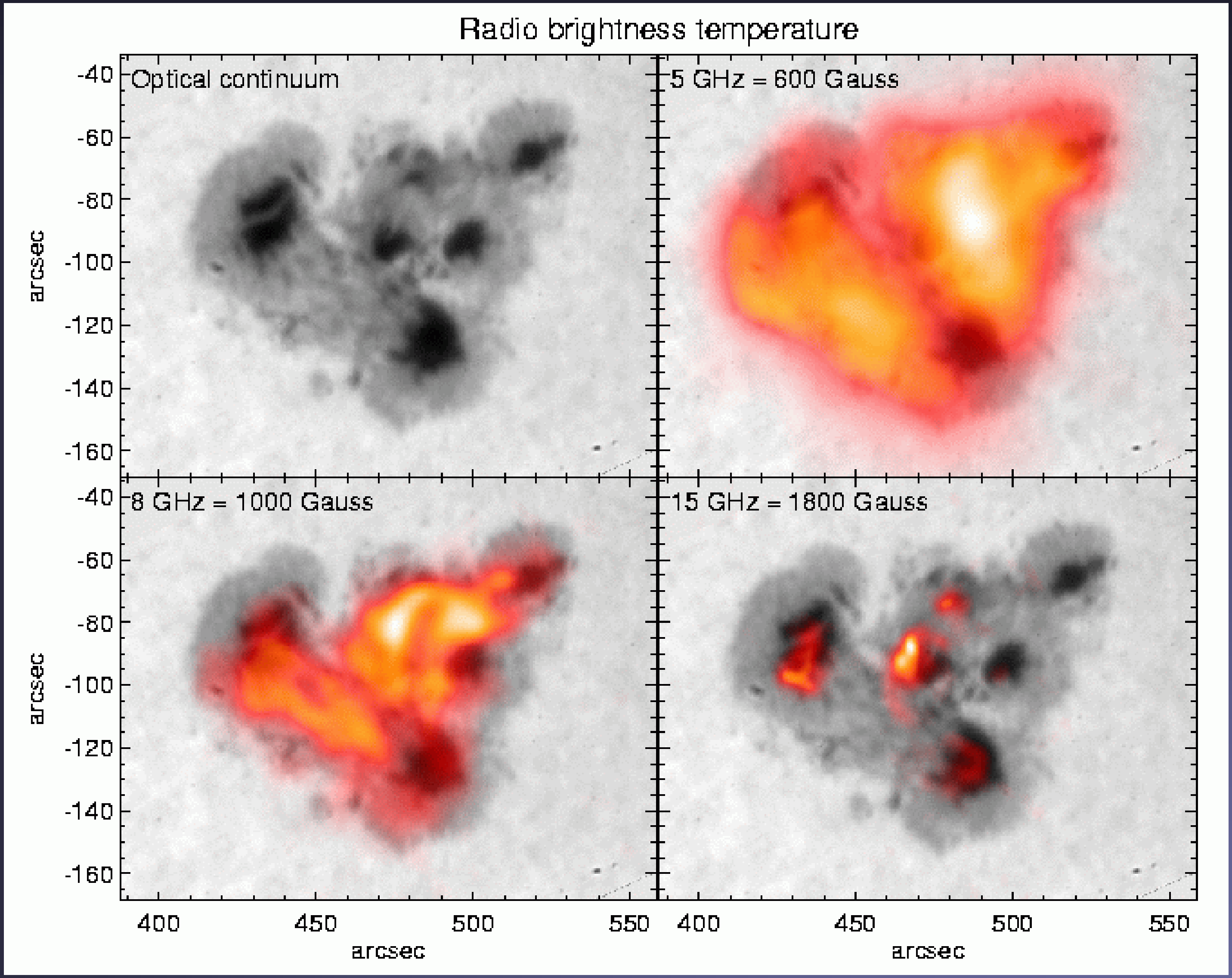

Radio Measurements: Faraday Rotation

- plane of linear polarization is rotated by magnetized plasma with density n_e (Nicholson 1983) :

$$\Delta\chi \propto \lambda^2 \int_{LOS} n_e \vec{B} \cdot d\vec{s}$$

→ measures product of n_e and B_{LOS}

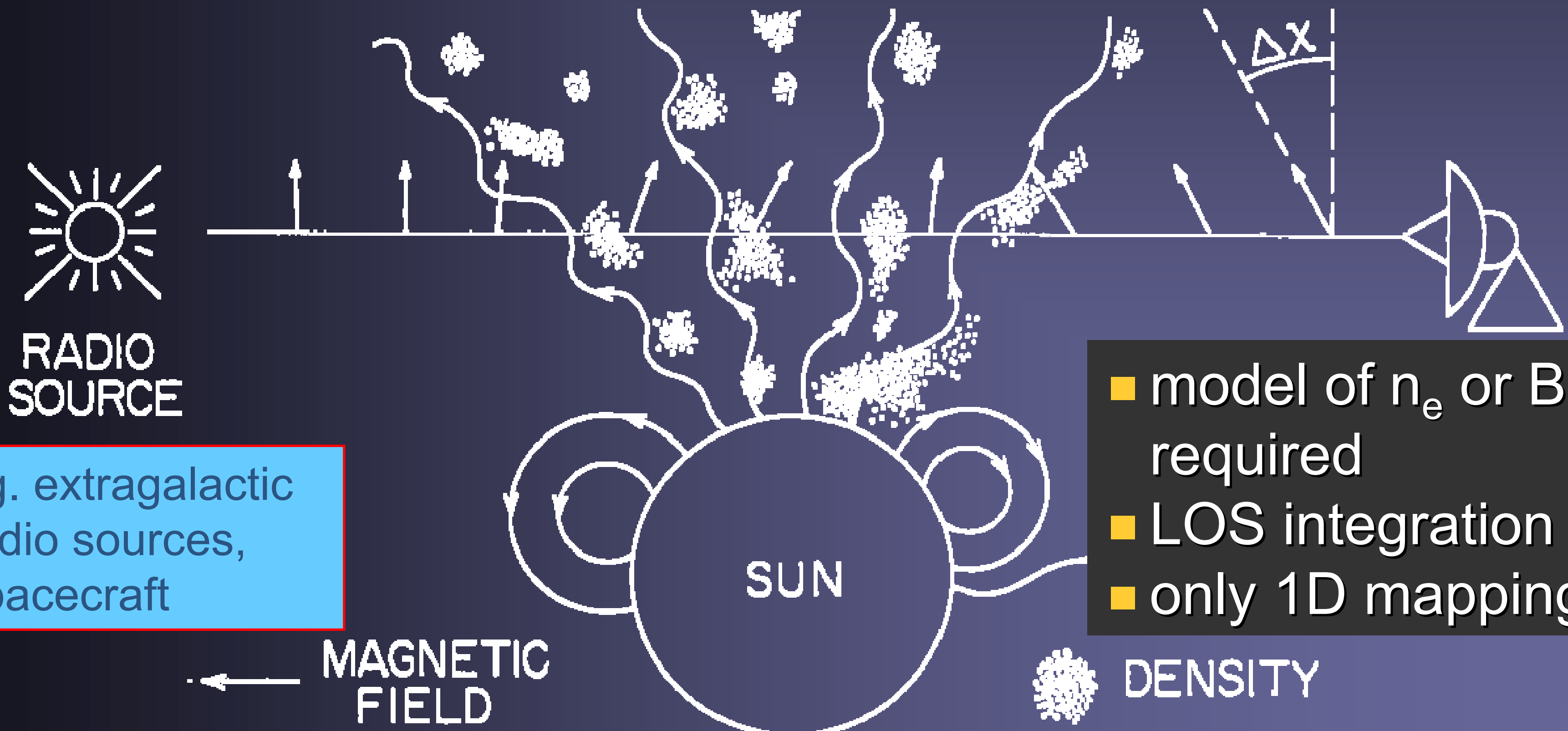

eg. extragalactic radio sources, spacecraft

- model of n_e or B required
- LOS integration
- only 1D mapping

Faraday rotation: results

- Measurements at 2 or more λ allow Δχ to be deduced without knowledge of initial polarisation angle
- Most Faraday rotation results refer to the outer corona, where the field is weaker & density is lower
- Easier for weak fields & low-density plasma: avoids multiple rotations

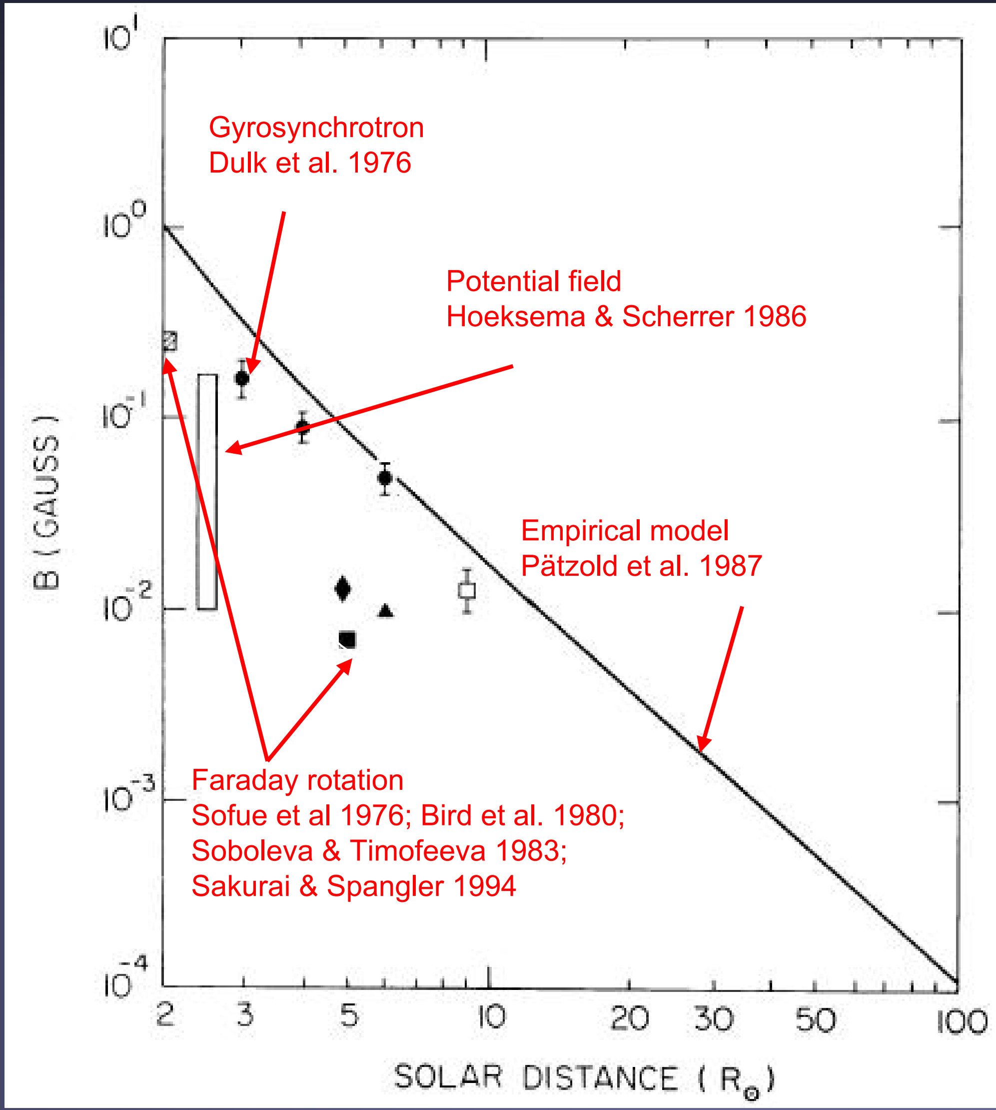

Heliospheric magnetic field from Ulysses

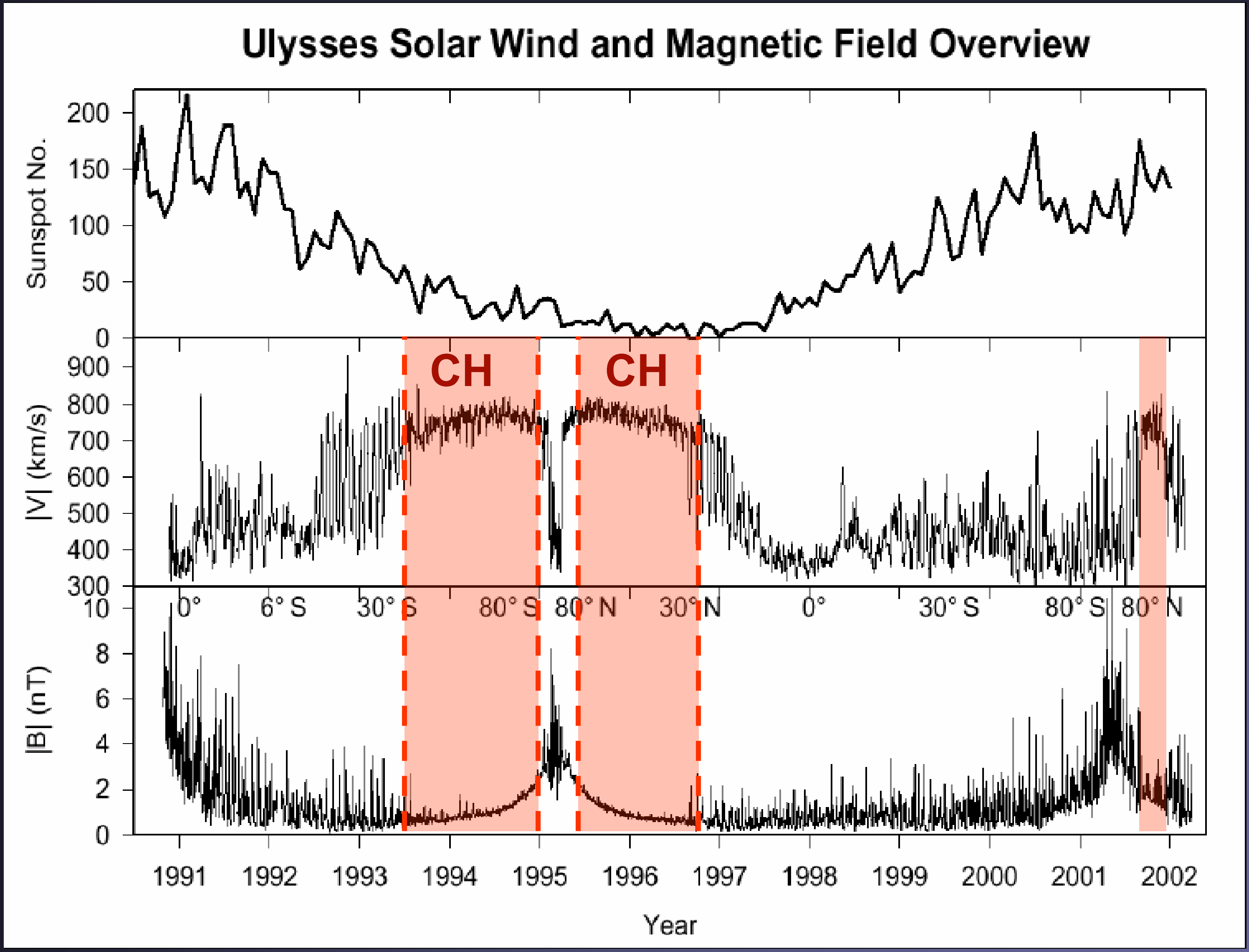

Making the Parker spiral visible

- Ulysses followed electron streams ejected from Sun on 25 & 30.10.1994 from above the south solar pole, with the help of the clouds' radio emission (dots)
- The e^- streams follow the Parker spiral as expected

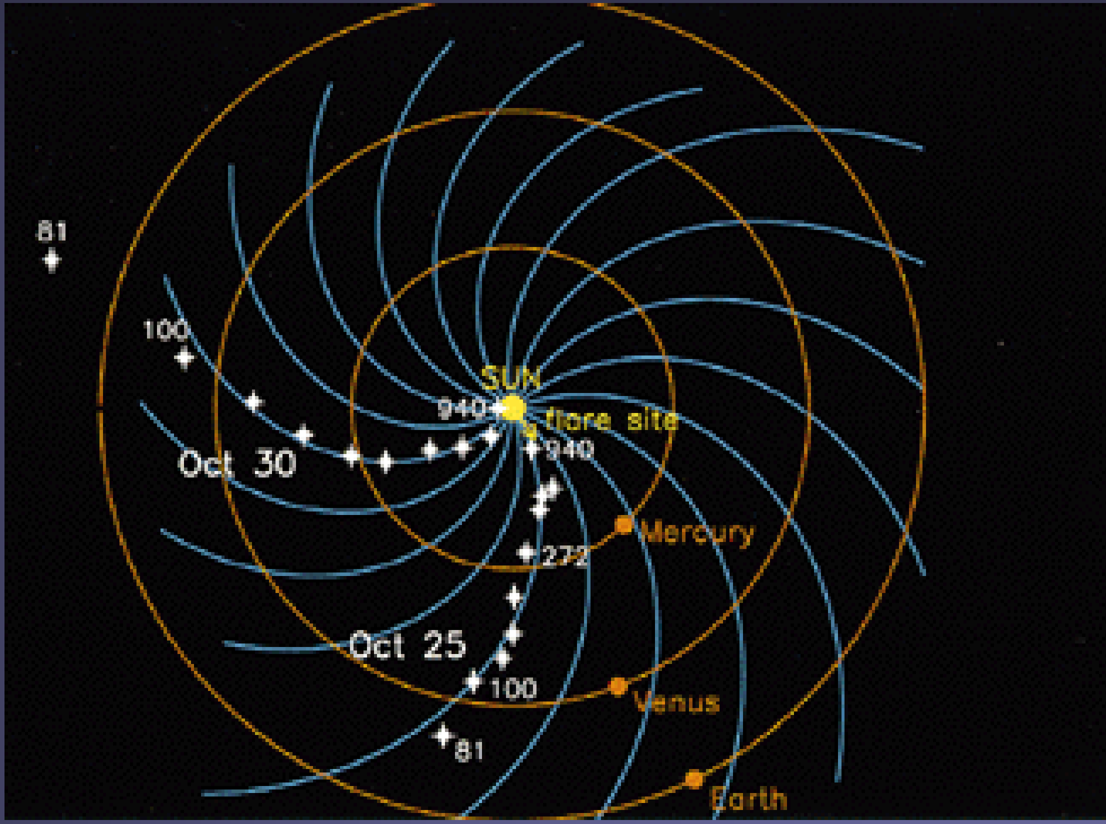

Techniques for stellar magnetic field measurements

From the Sun to the stars

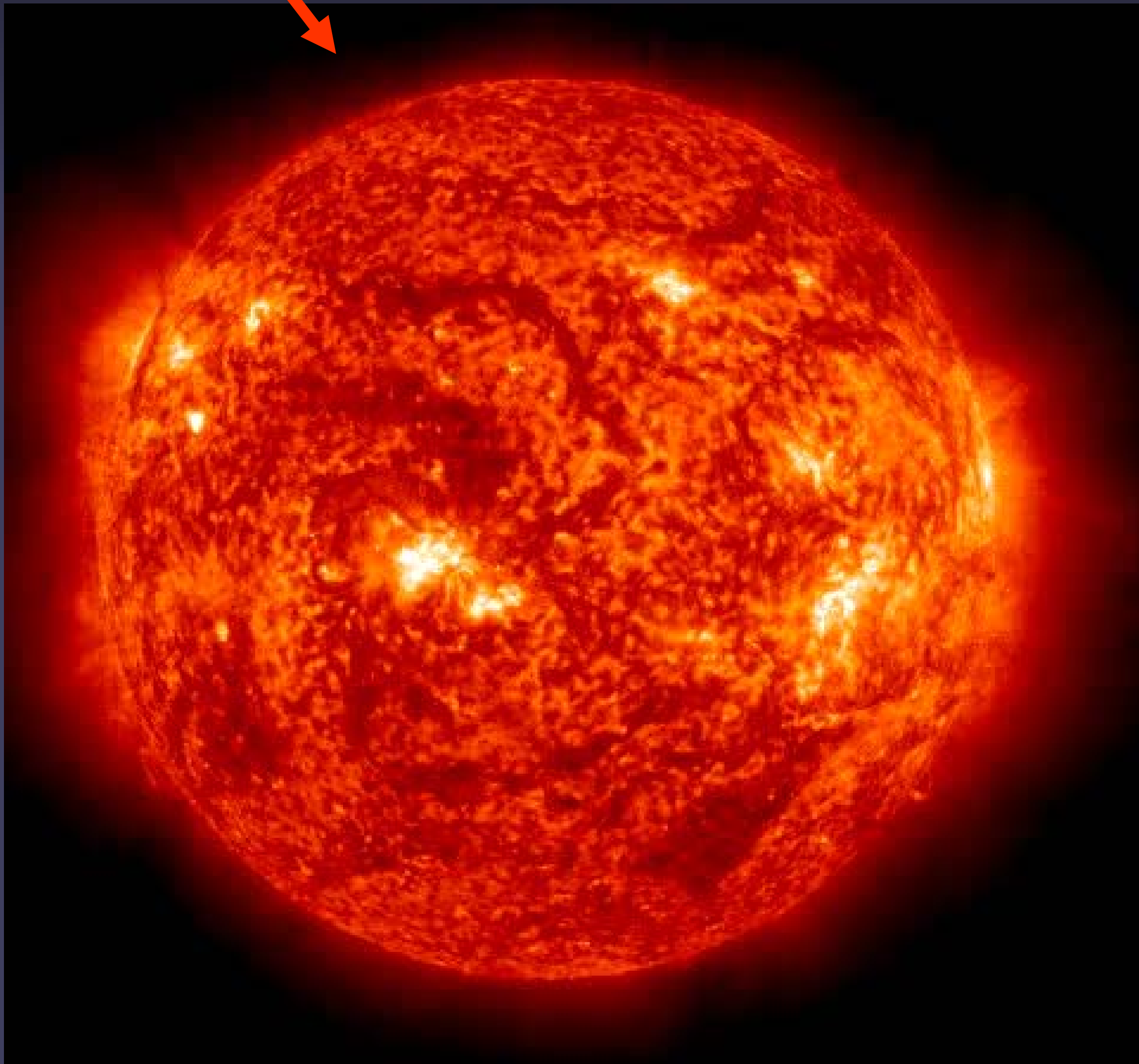

From the Sun to the stars

- Going from Sun to stars means **losing**
  - spatial resolution
  - photons and hence sensitivity
- & **gaining** in diversity of stars & parameters
  - Hot stars: different magnetic structure
  - Cool stars: how usual or unusual is today’s Sun
  - Probe non-solar parameter regimes
- Depending on the type of star different measurement techniques have to be applied

Stars with large-scale field: e.g. Ap stars

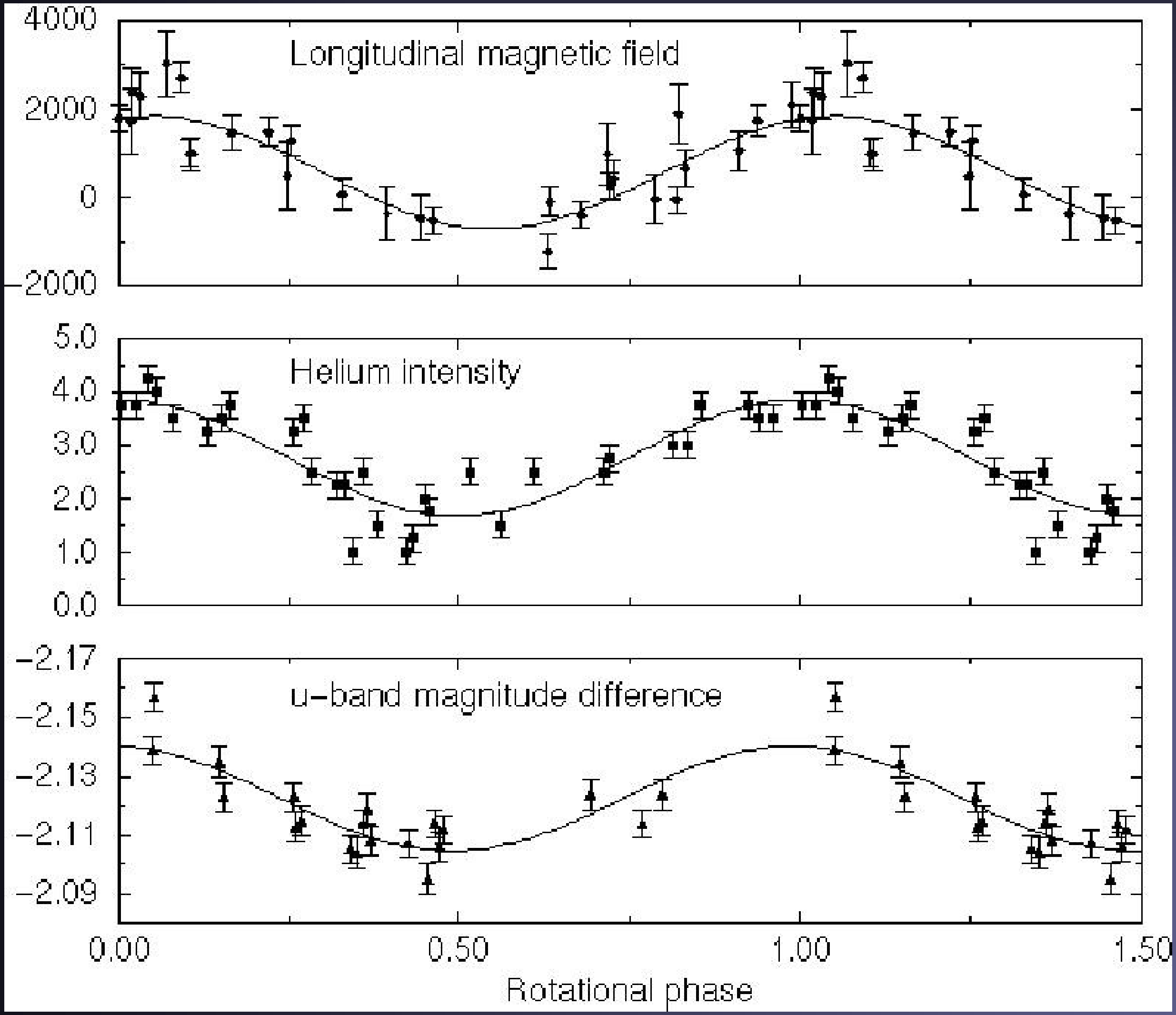

Field in early-type stars is dominated by low-order multipoles, e.g. dipoles.

A tilted dipole produces a roughly sinusoidal variation of Stokes V

Landstreet

Complex fields of cool stars and missing spatial resolution!

- Solar magnetogram
- Note complexity of the magnetic signal: magnetic polarities are mixed often on small scales!
- Average over the whole solar disk gives extremely small Stokes signals

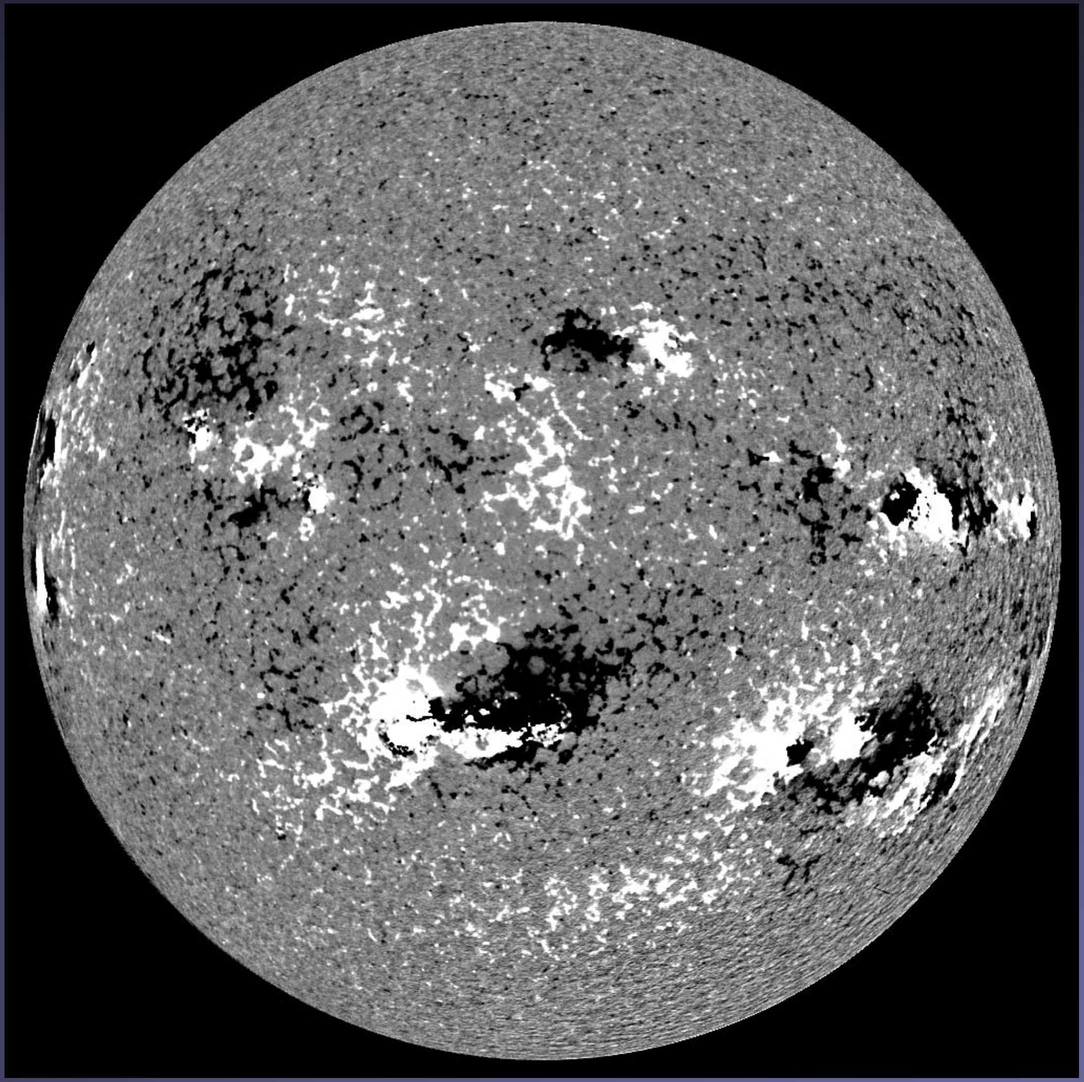

Cancellation of magnetic polarity

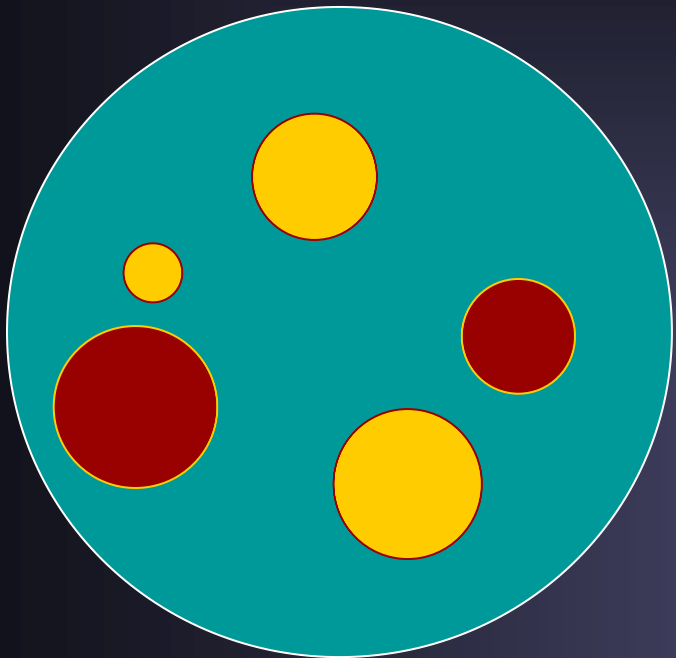

unresolved star with flux is distributed on small scales

= positive polarity magnetic field

= negative polarity magnetic field

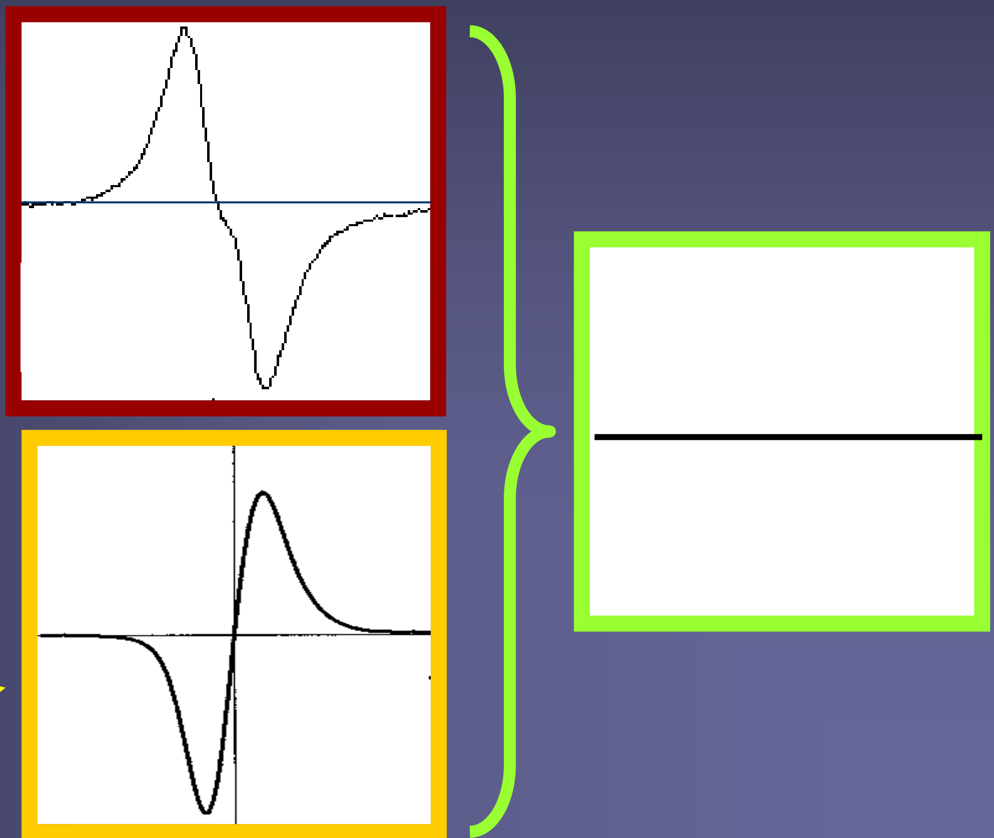

Measuring B on Sun-like stars

- For slowly rotating stars polarisation signal is strongly reduced by mixture of magnetic polarities on stellar surface. Detect field from its weak influence on intensity spectra.
- Example: Even ε Eri with $fB \approx 160$ G (outside starspots) needs high S/N for field to be visible

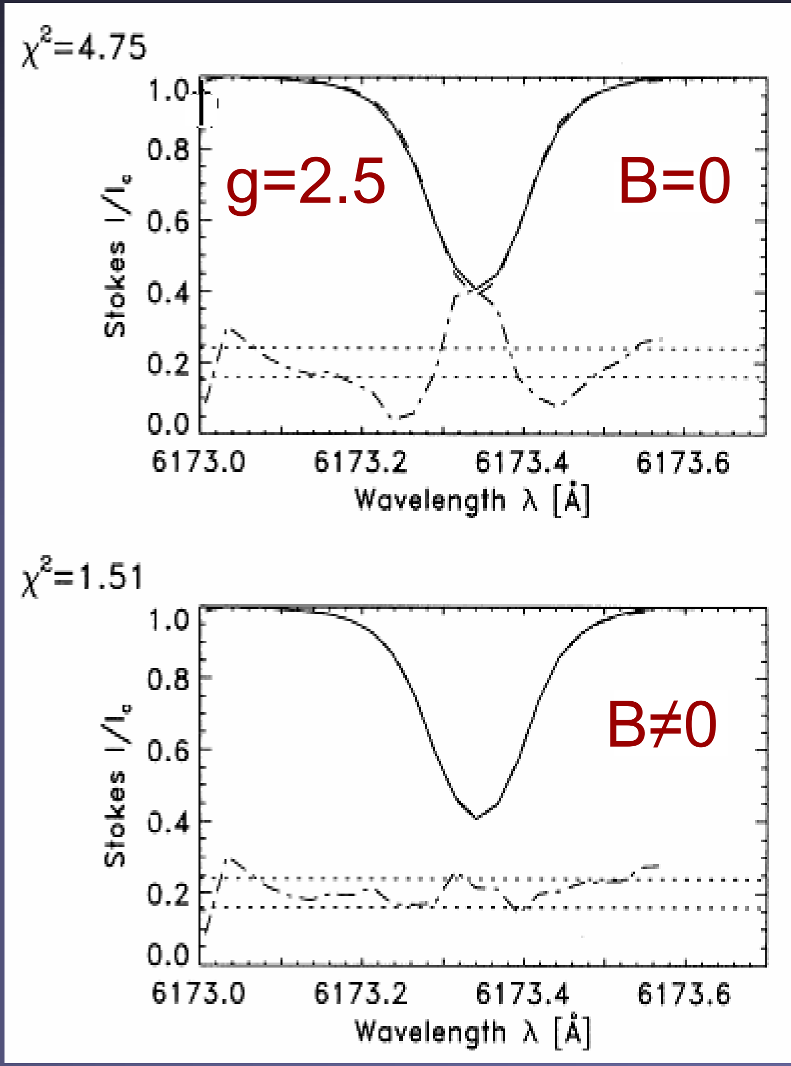

Rüedi et al. 1997

Rapid rotation: boon and bane

+ Rapid rotation produces more activity and larger magnetic flux (lecture 9) ➔ easier to measure

+ Larger activity ➔ larger magnetic features ➔ less mixing on small scales?

+ Zeeman degeneracy is reduced by rapid rotation: Zeeman Doppler Imaging can be used. Works for $v \sin i = 10\text{-}100$ km/s and $i = 20\text{-}70^{o}$

- With increasing vsini, S/N is reduced as line gets weakened. Reason for 100 km/s limit on ZDI

Doppler Imaging: the principle

- Brightness structures on surface of rapidly rotating star map onto shape of line profile & its variation with time

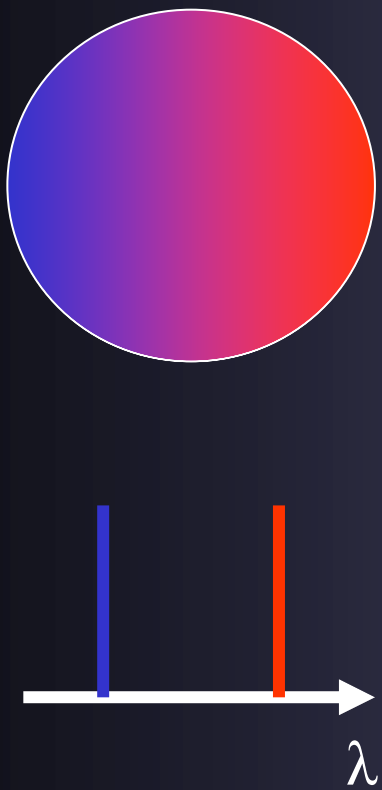

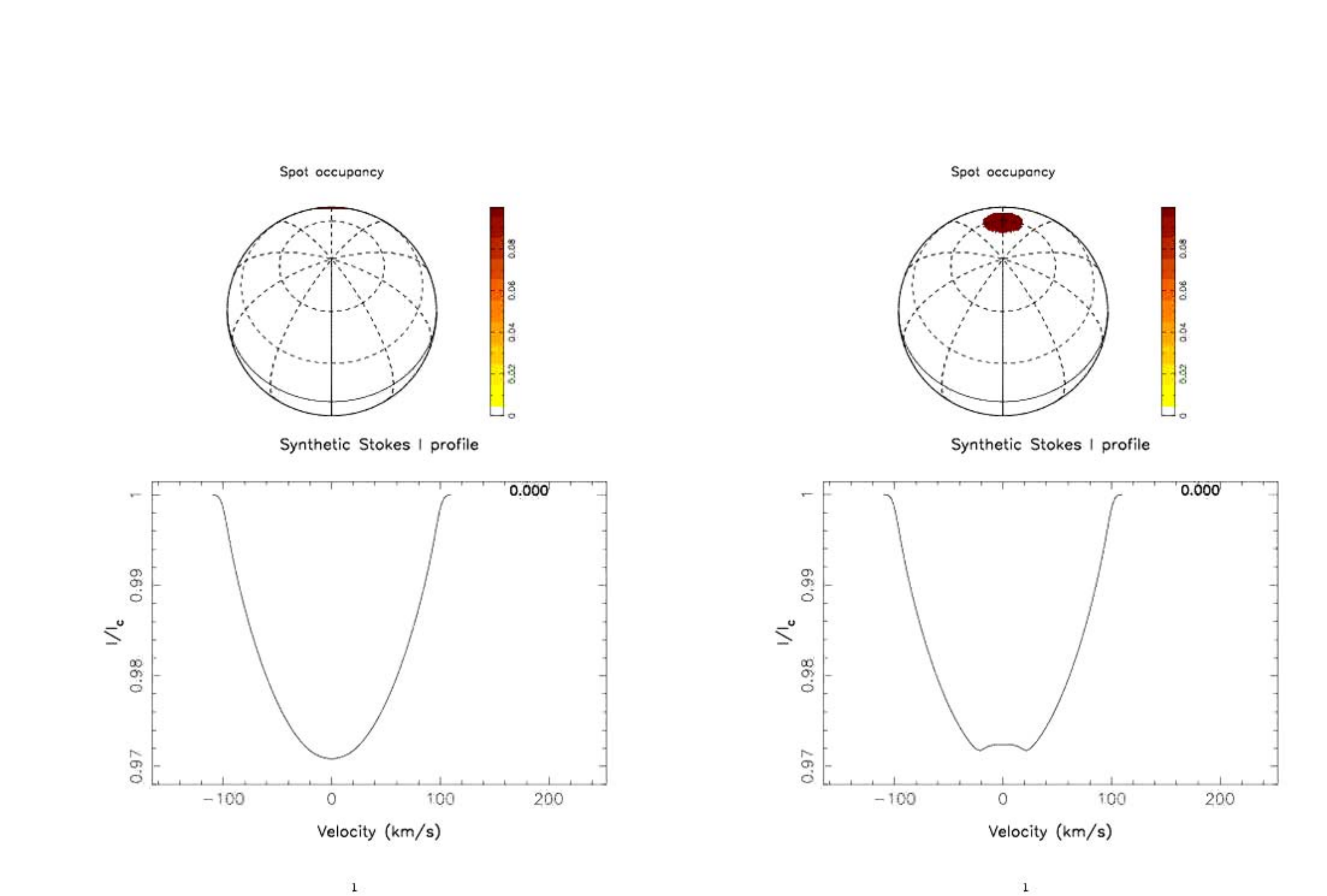

Doppler Imaging: does it work?

- Aim: recreate 2-D image of stellar surface
- Data: spectrum (1-D) + its variation (1-D)
- Ill-posed inverse problem. Soluble, but needs regularization (e.g. maximum entropy)
- Tests using synthetic stars have been successful

Original

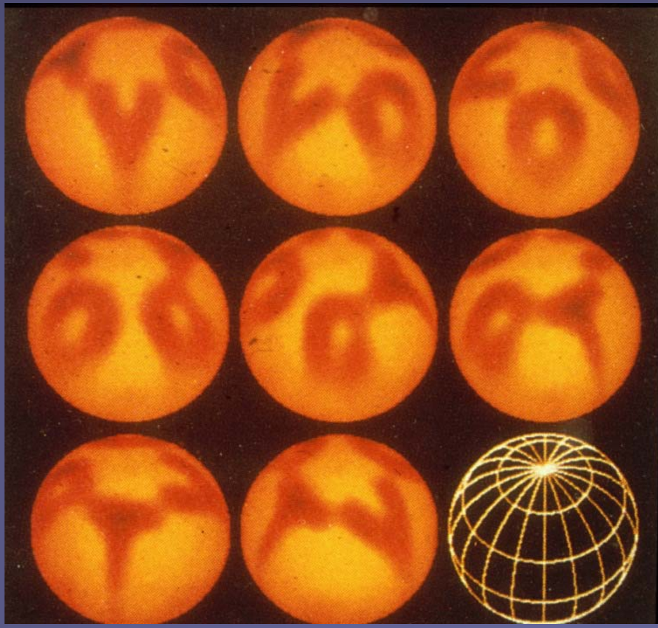

Reconstructed

Zeeman Doppler Imaging

Animations
P. Petit

Use Stokes spectra to determine distribution of field (Semel 1989)

Radial field Latitude of B: 30°	Azimuthal field 30°	Radial field 60°

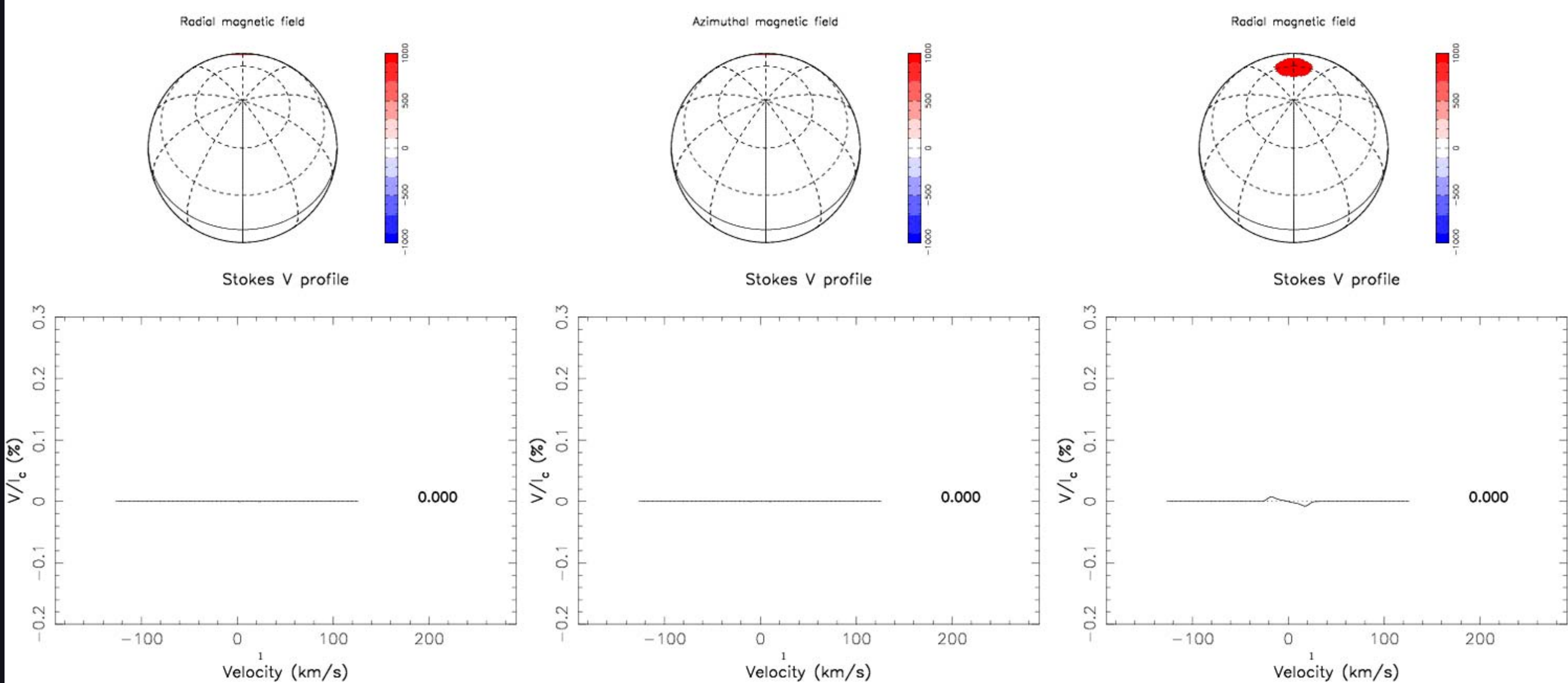

Limitations of ZDI

- Determining 2-D maps of full magnetic vector (3x2 = 6-dimensional data set) from just 2 Stokes parameters I and V is not trivial (Q and U are not measurable on cool stars: in Ap stars all 4 Stokes params can be used, Piskunov et al.)
- Misses a significant, in cool stars even dominant fraction of the field (since it is ordered on small scales)
- Is not sensitive to fields in dark features, e.g. starspots: strongest field regions in cool stars are not well covered
- S/N is an issue
- All limitations inherent to Doppler Imaging also apply

Least Squares Deconvolution (LSD)

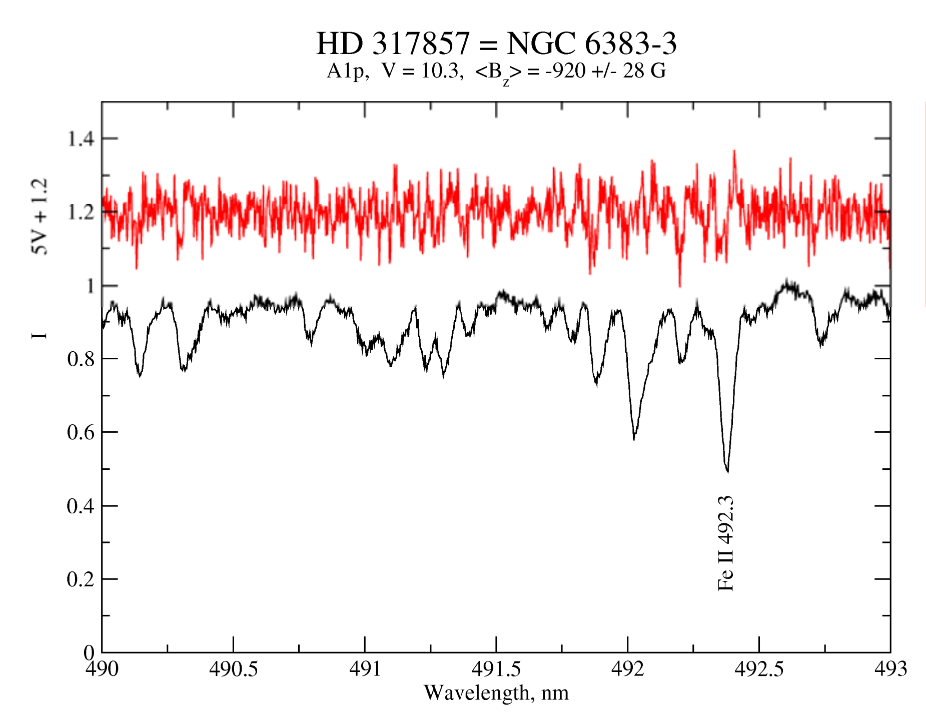

Part of observed spectrum.
Stokes V: red, Stokes I: black

LSD V and I profiles

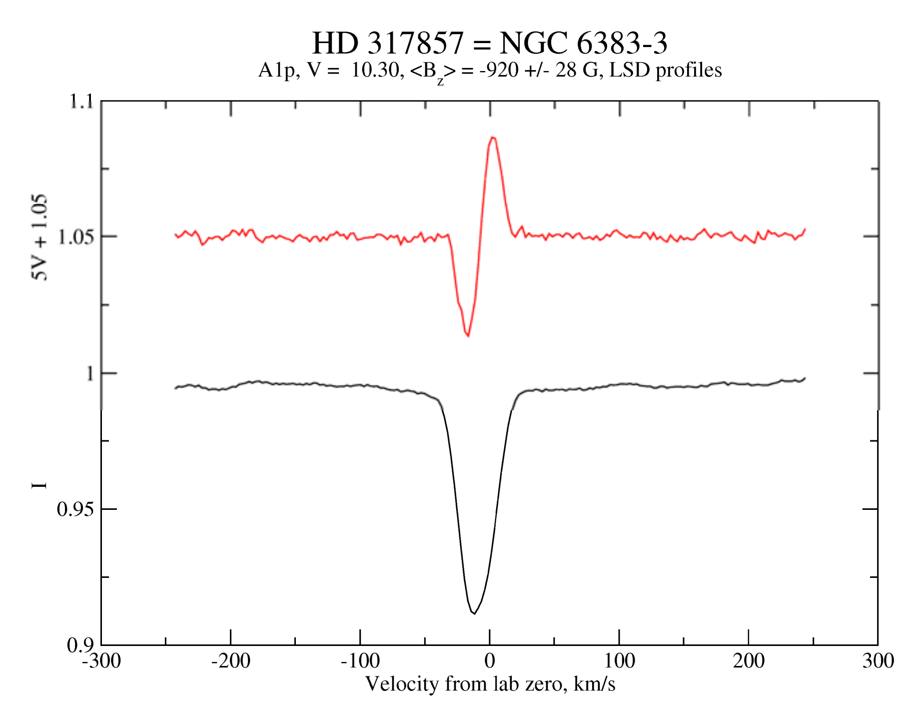

Proposed by Semel & Li (1992) named by Donati et al. (1997). Basically averages signal from 1000s of lines. Brings out signal hidden in noise. LSD V, but not Q & U, may be modelled as single line!

Magnetic field regimes: stronger fields

$$H = -\frac{\hbar}{2m}\nabla^2 + V(r) + \xi(r)\mathbf{L}\cdot\mathbf{S} + \left(-\frac{e}{2mc}\mathbf{B}\cdot(\mathbf{L}+2\mathbf{S}) + \frac{e^2}{8mc^2}(Br\sin\theta)^2\right)$$

- Perturbation theory regimes:
  - Quadratic magnetic term << linear term << spin-orbit term: (linear) Zeeman effect
  - Quadratic magnetic term << spin-orbit term << linear term: Paschen-Back effect
  - Spin-orbit term << linear term << quadratic magnetic term: quadratic Zeeman effect
  - Electronic binding term << quadratic magnetic term: needle atoms

Following J. Landstreet

B at which different regimes are reached

- May estimate size of magnetic terms by taking $L \sim \hbar$, $r \sim$ Bohr radius a_0, $V \sim Ze/r$. We find
  - For normal atoms and $B < 50$ kG (5 T), most atomic lines are in linear Zeeman regime
  - Above about 100 kG quadratic term becomes important. Quadratic Zeeman effect is observed in lines of H
  - Above about 10 MG magnetic terms become comparable to Coulomb term, perturbation methods no longer work. Must solve structure of atom in combined (external and internal) field

Following J. Landstreet

Zeeman and Paschen-Back effects

- In Paschen-Back regime, $\mathbf{L}$ and $\mathbf{S}$ decouple, so J is not a good quantum number. Now M_L and M_S good quantum numbers → perturbation energy $(e/2mc)\,B(M_L+2M_S)\,\hbar$

→ all lines are split by same amount. Only three line components ($\Delta M = -1,0,1$)

- Atomic PBE: main application WDs. Only few lines in non-degenerate stars. Molecular PBE: common, also in cool stars

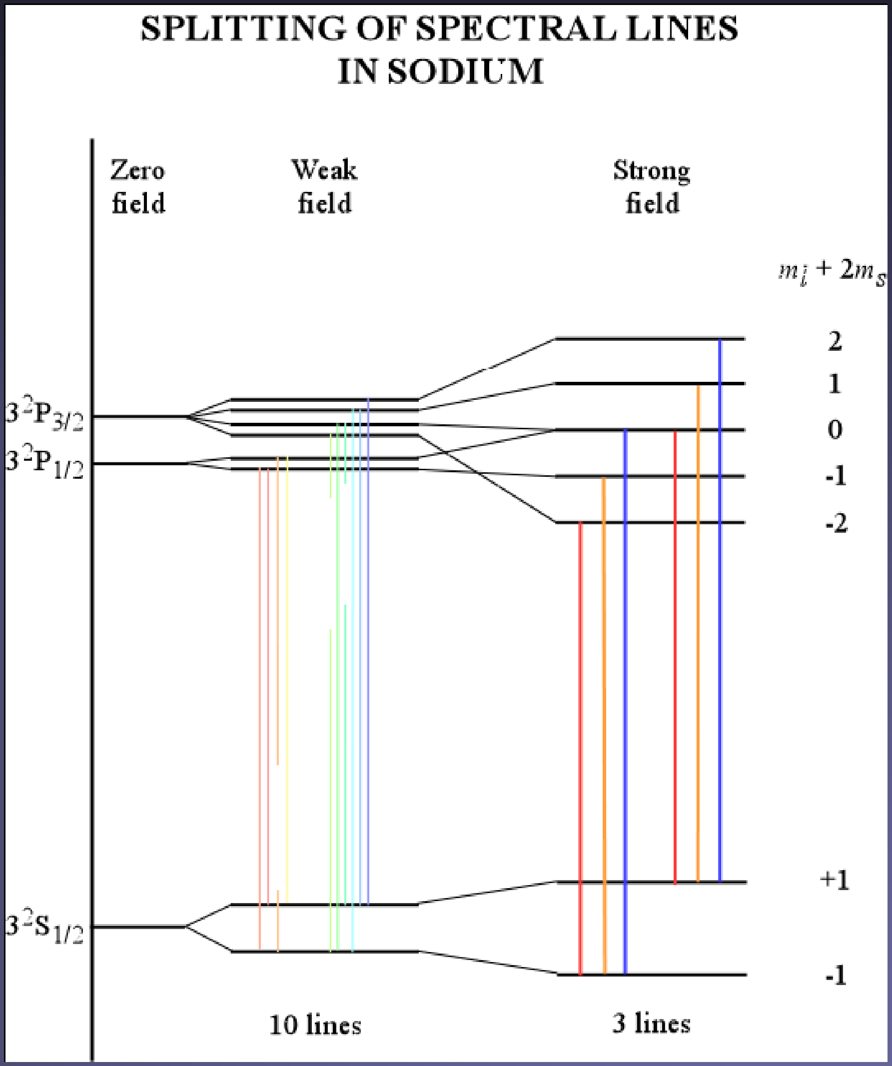

Follow J. Landstreet

Molecular Zeeman & PB effect

- Molecular lines are interesting for cool stars: cool stars or starspots (and sunspot umbrae) show strong molecular absorption features.
- Spectral lines of many diatomic molecules display Zeeman splitting. Molecular energy levels often lie close together, PBE takes place already at low field strengths (often a few 100 G) and must be included
- Full theory for arbitrary molecular electronic states
  - Zeeman and Paschen-Back effects: *Berdyugina & Solanki (2002), Berdyugina et al. (2003, 2005)*
  - Scattering & Hanle effect: *Berdyugina et al. (2002), Berdyugina & Fluri (2004), Shapiro et al. (2007,2008)*

Molecular Zeeman & PB effect

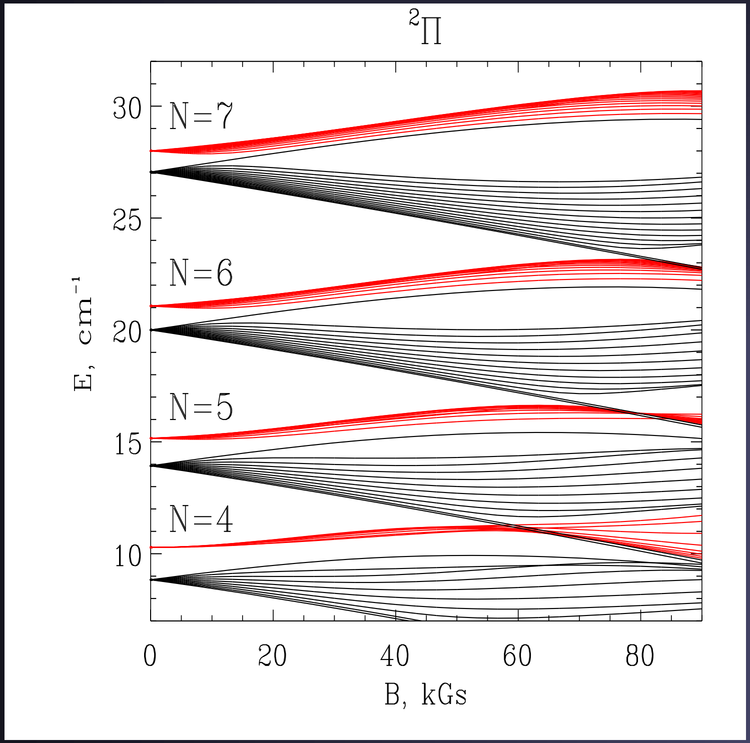

CN
FeH

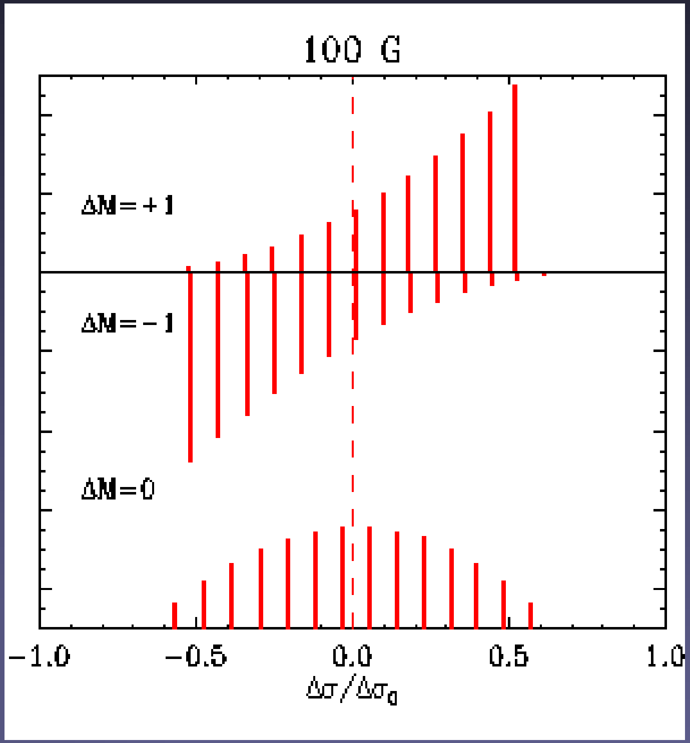

- Peculiarities due to the PBE ⇒ New diagnostics and higher sensitivity
  - Stokes profile asymmetries ⇒ Net polarization across line profiles
  - Wavelength shifts and polarization sign changes depending on B

Quadratic Zeeman effect

- The effect of the quadratic term in the Hamiltonian of an atom in a magnetic field is to shift all spectral line components in H to shorter wavelengths by about

  $$\Delta\lambda_Q \simeq (-e^2\, a_0^2 \,/\, 8mc^3h)\; \lambda^2\, n^4\, (1+M_L^2)\, B^2$$

  where λ is in Å, a_0 is the Bohr radius, and n and M_L are the principal and magnetic quantum numbers of the upper level

- Quadratic effect dominates for hydrogen H10 for B > 10 kG
- At 1 MG, H8 is shifted by about 350 km/s relative to Hα, an easily detectable effect (Preston 1970, ApJ 160, L143)
- Polarisation effects are similar to those of Zeeman effect, but components are not split symmetrically about unsplit line

Atomic structure in huge fields

- For fields above 10 MG the magnetic terms in the Hamiltonian are comparable to the Coulomb terms, and the structure of the combined system must be solved consistently
- Has been solved for H, and to a large extent for He (review: e.g. Becken & Schmelcher 2002, Phys Rev A, 65, 033416)
- Basically, each line component decouples from the others and moves about (in λ) in a dramatic way
- Absorption lines in stellar spectra for fields over about 50 MG are affected by fact that the line positions vary rapidly with B. If B is not constant over the stellar surface. Lines occur at wavelengths where for some range of B the absorption wavelength does *not* change rapidly

Splitting of H lines in strong fields

- Plotted are the λ of the Zeeman components of the lowest Ly, H, Paschen and Brackett lines of hydrogen vs. $\beta = 4.7 \cdot 10^9$ G
- Components move over large parts of spectrum.
- → Identifying them can be quite adventurous

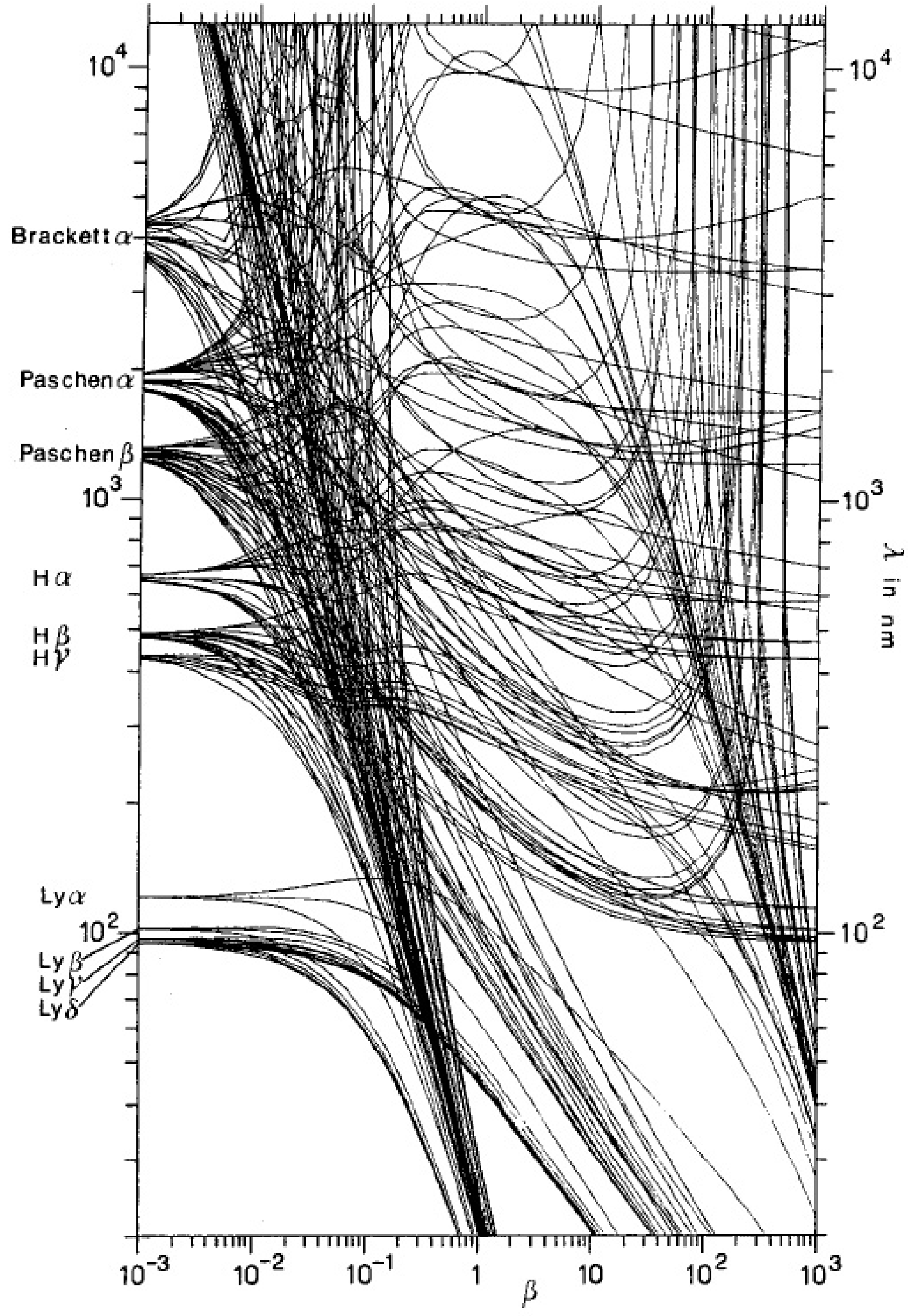

Wunner 1990

Splitting of H lines in strong fields (contd.)

- For large B values, the σ-components of spectral lines vary rapidly with wavelength. They are almost undetectable on stars where B varies by a factor of two.
- Some π-like transitions vary little over a range of B (“stationary components”). Such transitions can produce useful lines over a range of field strengths in the range of hundreds of MG

Wunner et al 1985, A&A 149, 102

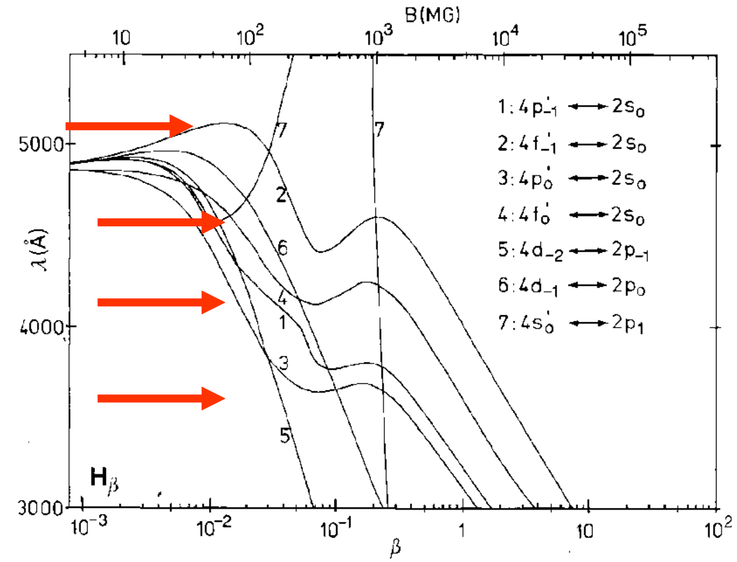

Fig. 3. The wavelengths of the 7 stationary Hβ components as functions of the magnetic field

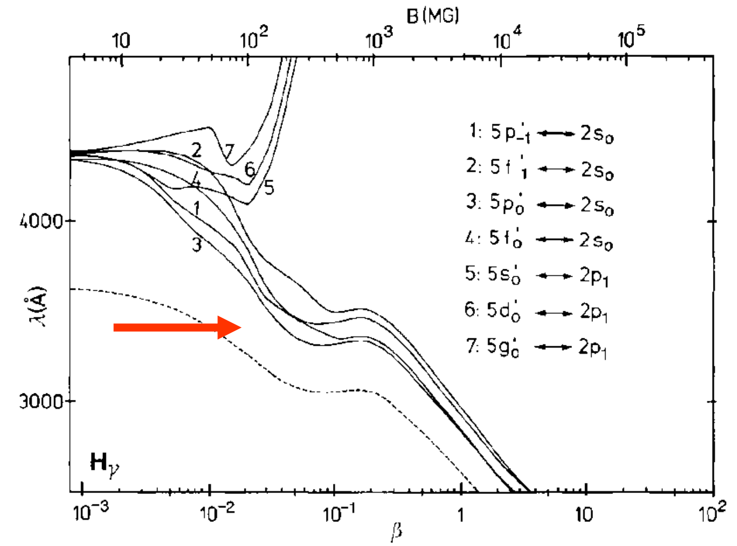

Fig. 4. The wavelengths of the 7 Hγ components stationary as functions of the magnetic field. Dashed curve: Balmer edge for transitions from 2*s* to the continuum

Techniques for measuring white dwarf magnetic fields

- Fields of white dwarfs are observed using several detection methods based on the behaviour of atoms & electrons in increasingly strong fields
  - For B below about 100 kG, the normal Zeeman effect (and perhaps the Paschen-Back effect in H) are used, as in non-degenerate stars
  - From 100 kG to about 10 MG, the linear Zeeman effect is overtaken by the quadratic Zeeman effect
  - Above 10 MG, even the spectrum of H is no longer easily recognised. It is greatly distorted, and continuum polarisation (circular and then linear) becomes detectable
  - In polars e^- cyclotron radiation is observed & employed

Measurement of field on Grw +70 8247

- Top panel: computed hydrogen line positions vs. B
- Middle panel: observed spectrum
- Bottom panel: H line positions computed by another group

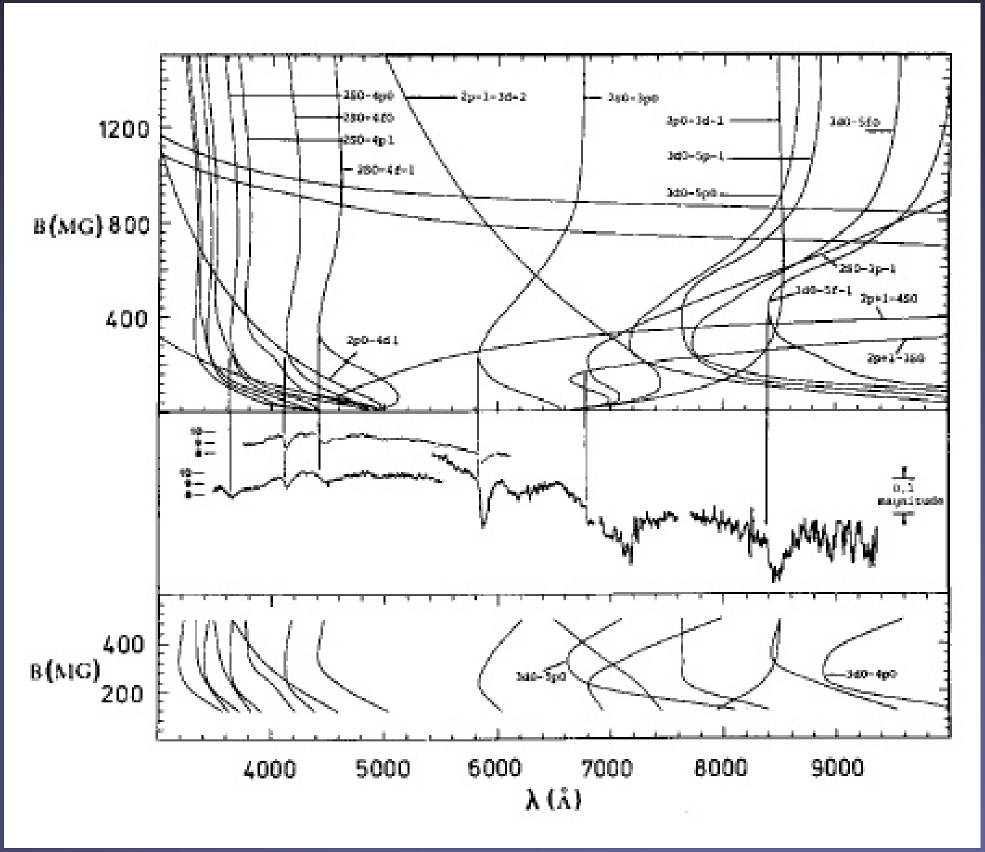

Continuum polarisation of white dwarf radiation in MG fields

- Free e⁻ spiral around field lines ➔ continuum absorption is *dichroic* (cyclotron radiation). Right & left circularly polarised light is absorbed *differently* ➔ continuum becomes circularly polarised by field with comp. along line of sight. In visible range this happens for $B > 10$ MG
- For $B \geq 100$ MG a similar effect gives continuum linear polarisation
- So far not possible to reproduce observed continuum polarisation spectra (cf. Koester & Chanmugam 1990, Rep. Prog. Phys., 53, 837, Sec 8)

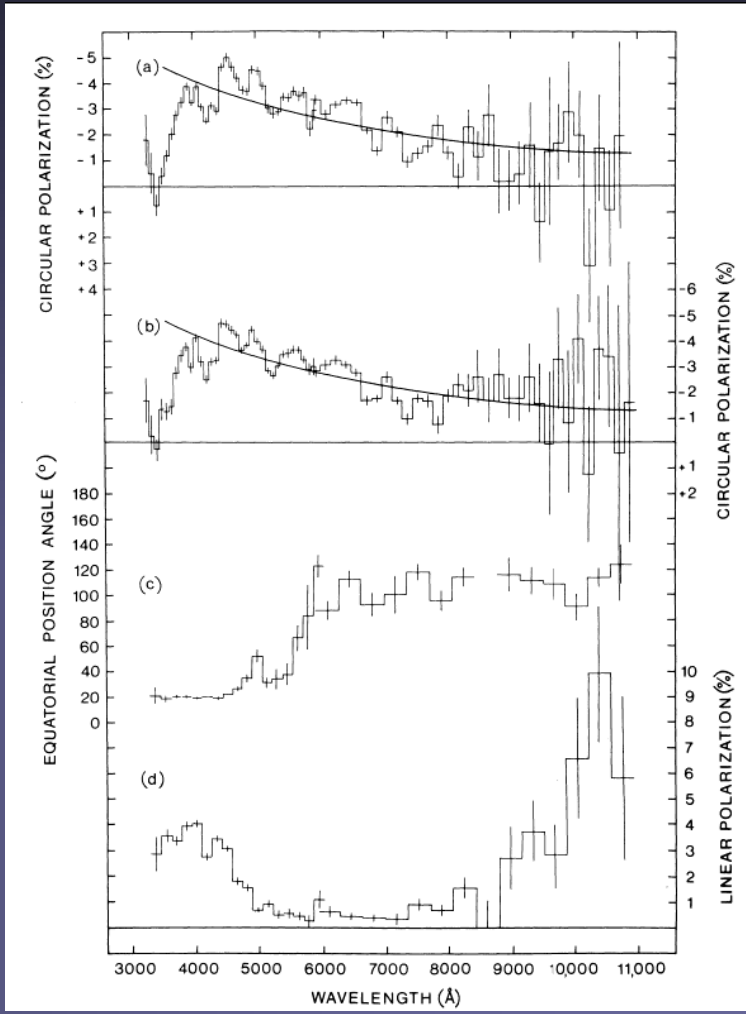

Grw +70 8247

Activity in stellar envelopes caused by the magnetic field

Which stars have magnetic fields or show magnetic activity?

- Best studied star: Sun
- F, G, K, M, L stars (outer or full convection zones) show magnetic activity & have <B> fields of G-kG.
- Early type stars: Ap, Bp, (kG-100kG), Ae,Be (100G), O,B (100 G)
- White dwarfs have B ≈ kG-10^9 G, no activity
- Not on diagram: pulsars

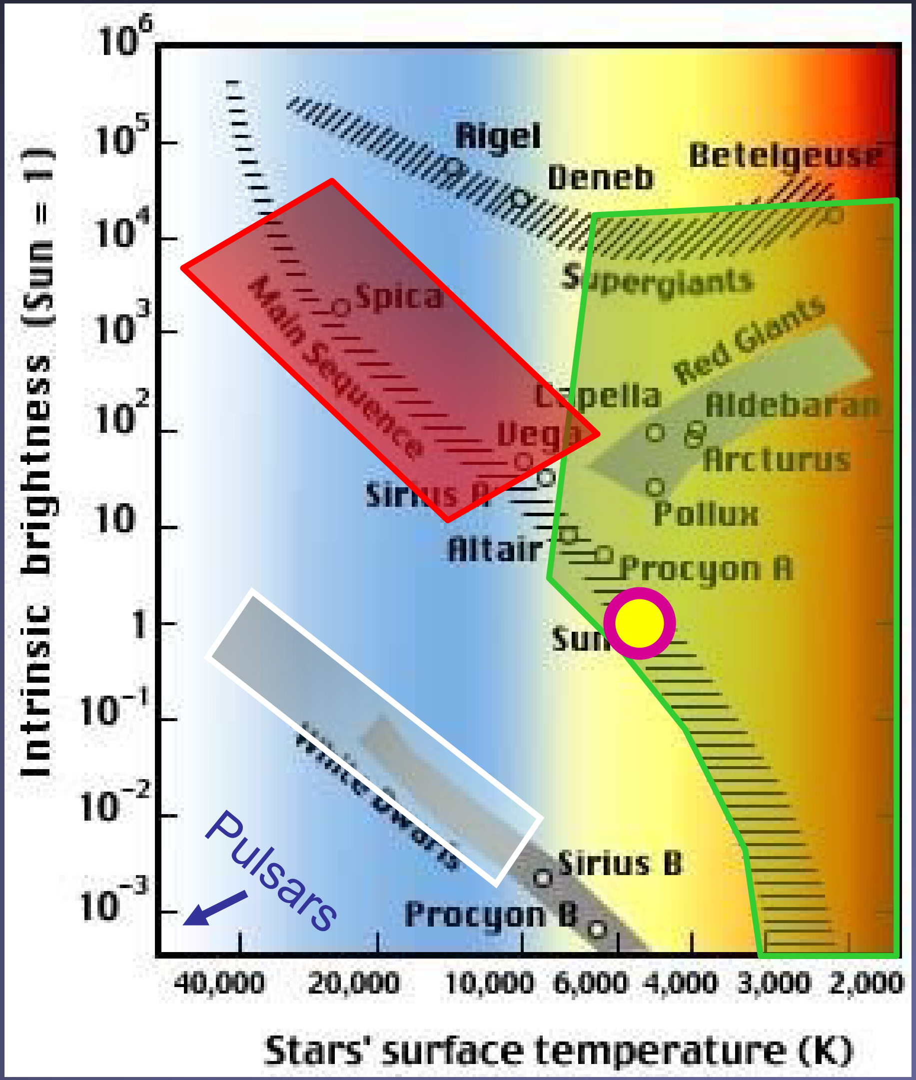

Stellar magnetic activity

- Magnetic activity: high energy radiation, e.g. X-rays, stellar wind, or stellar variability due to magnetic fields
- Stellar magnetic activity can be driven by:
  - interaction of magnetic field with convection in an outer convection zone (solar case) or in completely convective stars (dynamo driven fields). By far the most common
  - Modification of accretion of matter by magnetic fields (e.g. polars, i.e. AM Hercules systems) and/or interaction with an accretion disk as in classical T-Tauri stars
  - Interaction of magnetic field with turbulent wind in O, B stars

How is stellar magnetic activity measured ?

- X-ray emission
- Enhanced chromospheric emission and its variability
- Photospheric variability
- I'll concentrate mainly on cool stars, showing "solar-like" magnetic activity (although over a much larger range)

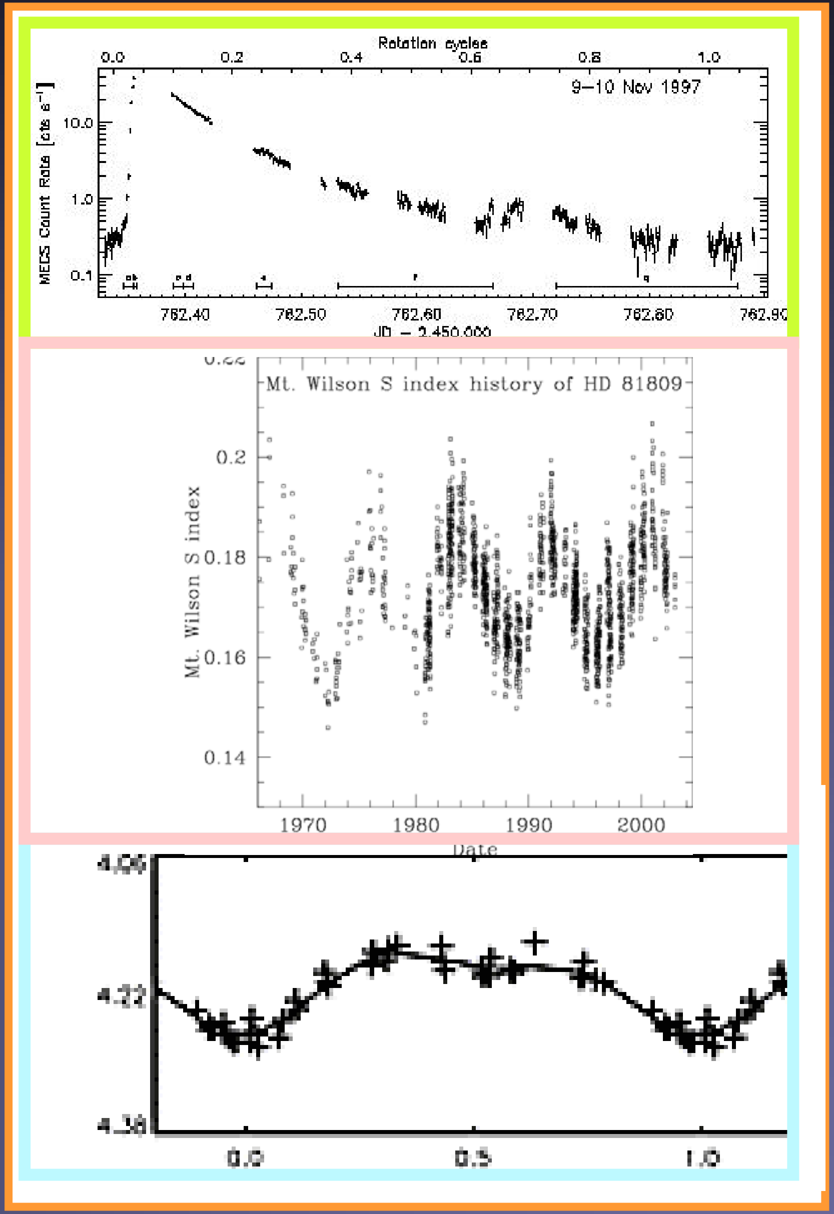

Which stars emit X-rays?

- Fraction of stars emitting X-rays vs. colour (i.e. temperature)
- Fraction increases at B-V=0.3
- Fraction decreases towards later types due to lower luminosity and sensitivity limit

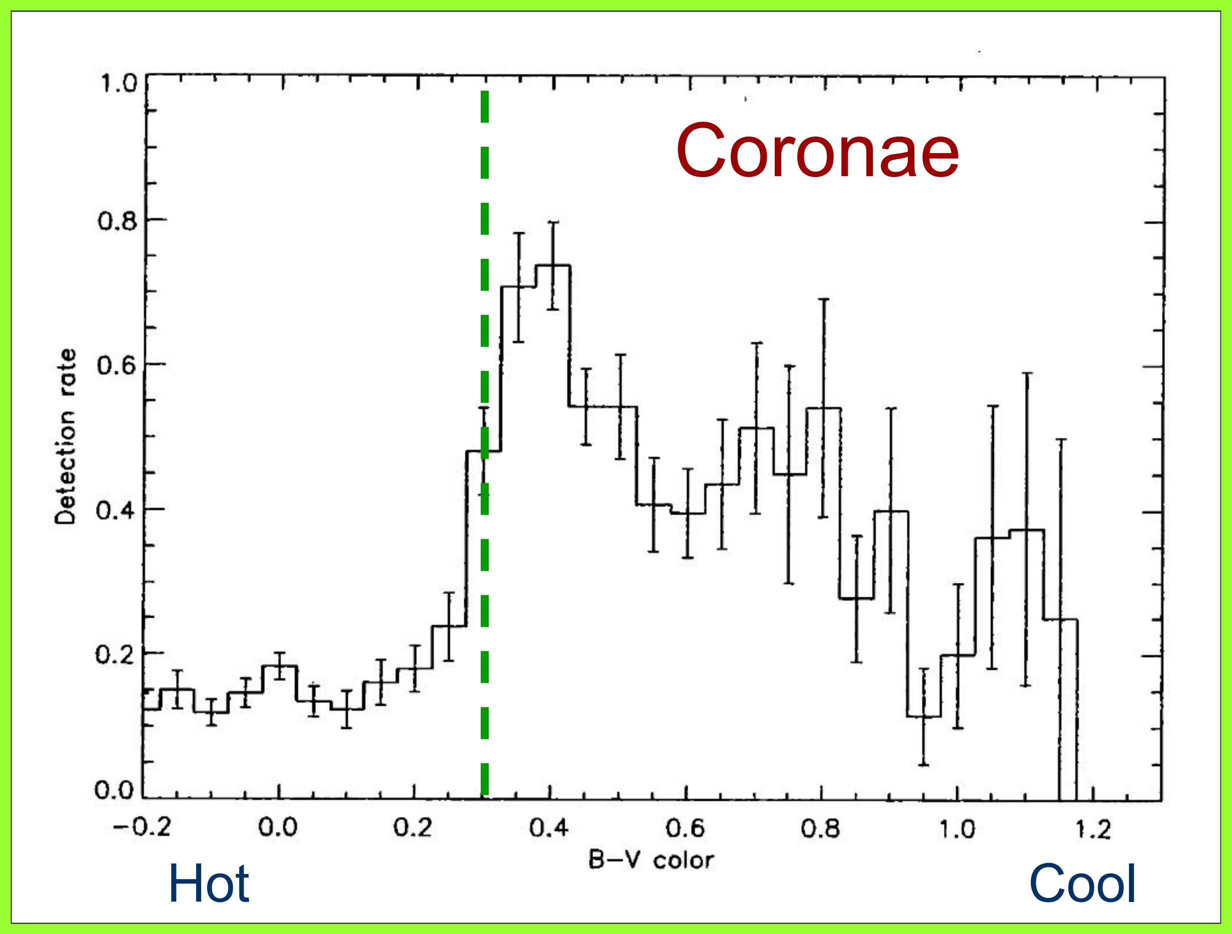

Rotational velocity vs. colour: evidence for rotational braking

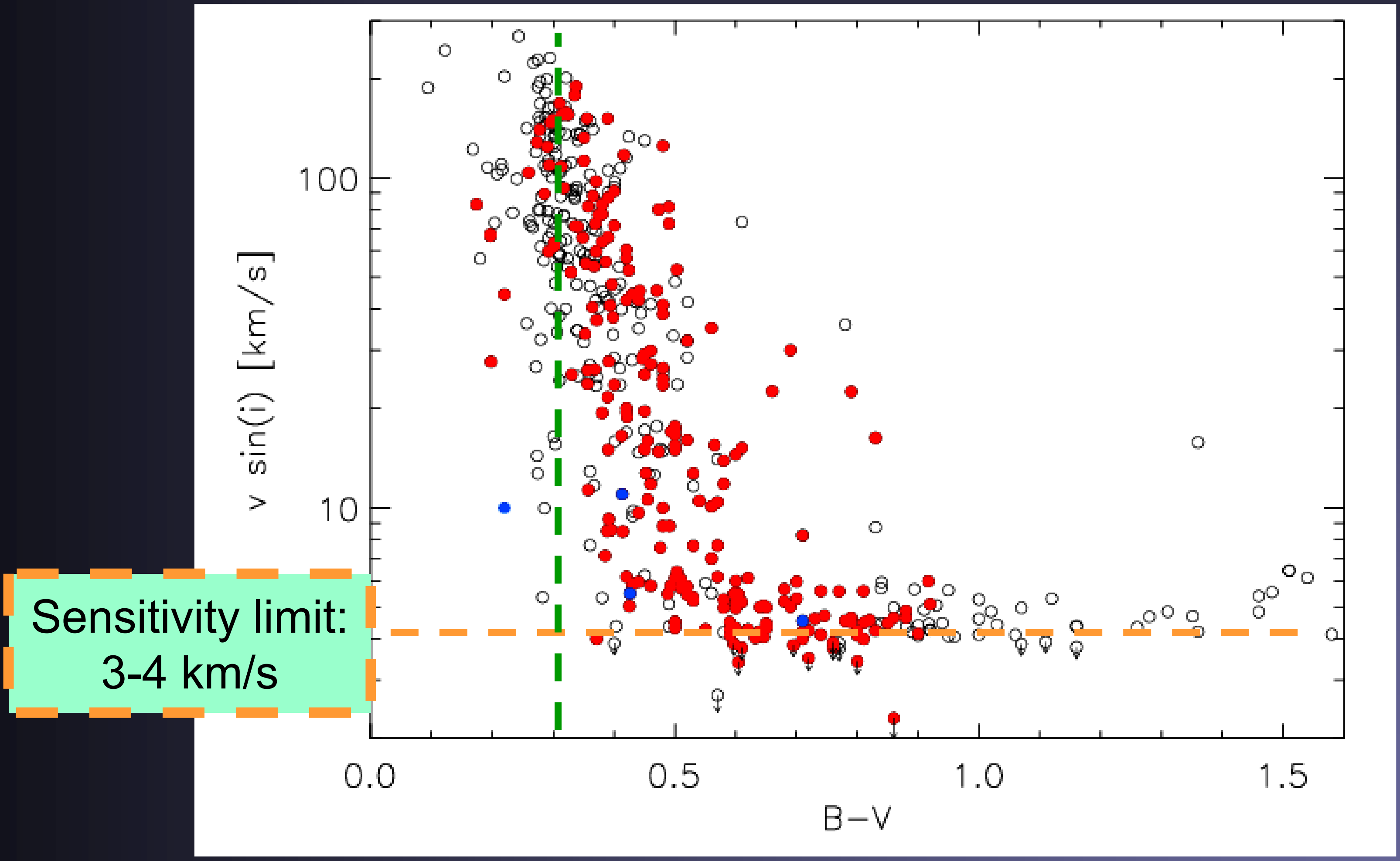

Ca II K as a magnetic activity indicator

- Ca II H and K: strongest lines in visible spectra of G and K stars
- $I_{core}/I_{wing} \sim \langle B \rangle^{0.6}$
- Ca lines are good tracers of stellar (chromospheric) magnetic activity
- Better S/N than X-rays. Can be observed from ground

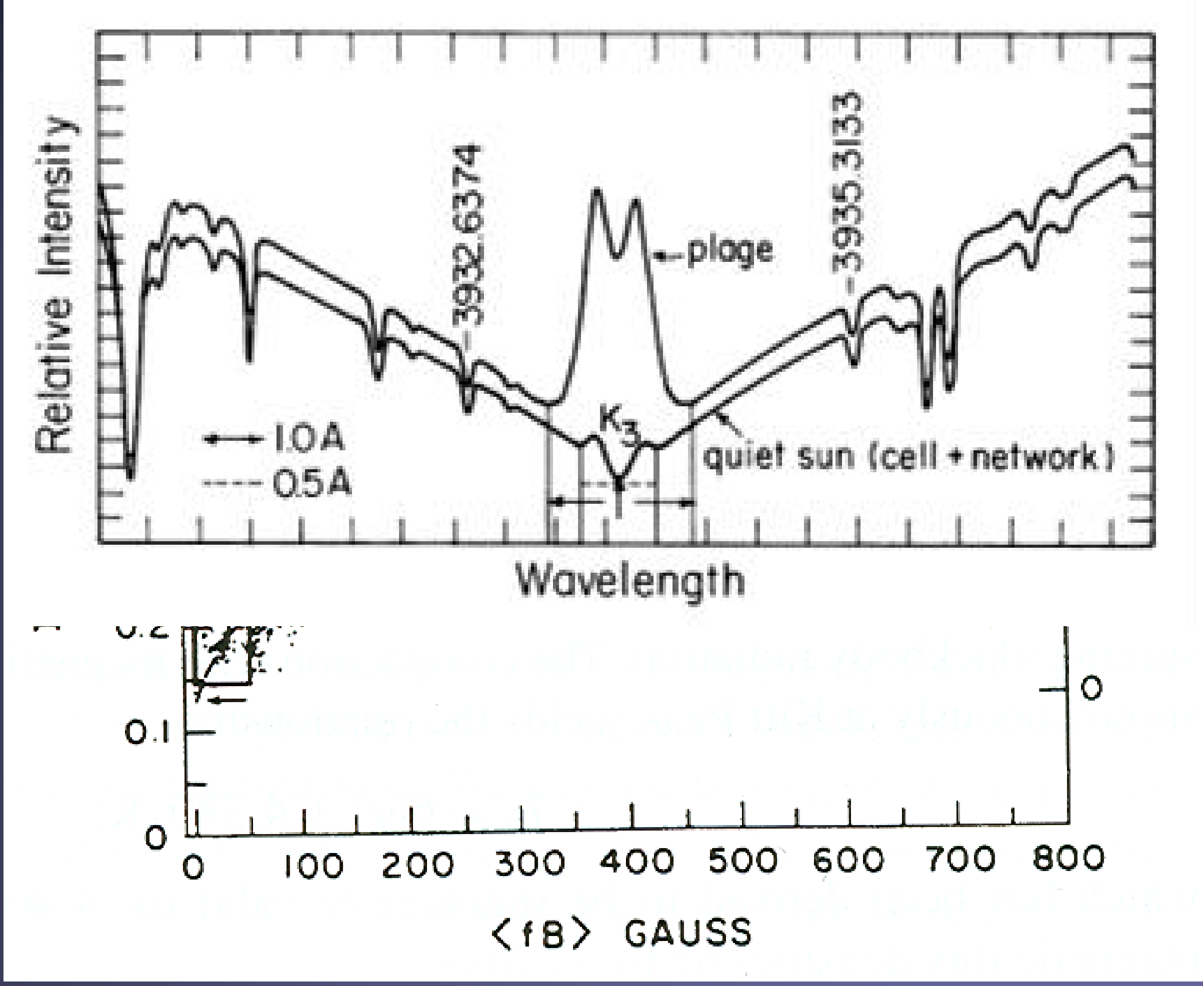

Activity-rotation relationship

- Typical: Activity increases with decreasing rotation period
- Scatter is reduced if L_x/L_{bol} is plotted (instead of just L_x)
- Also typical: below a certain rotation period there is a saturation. I.e. activity does not increase anymore

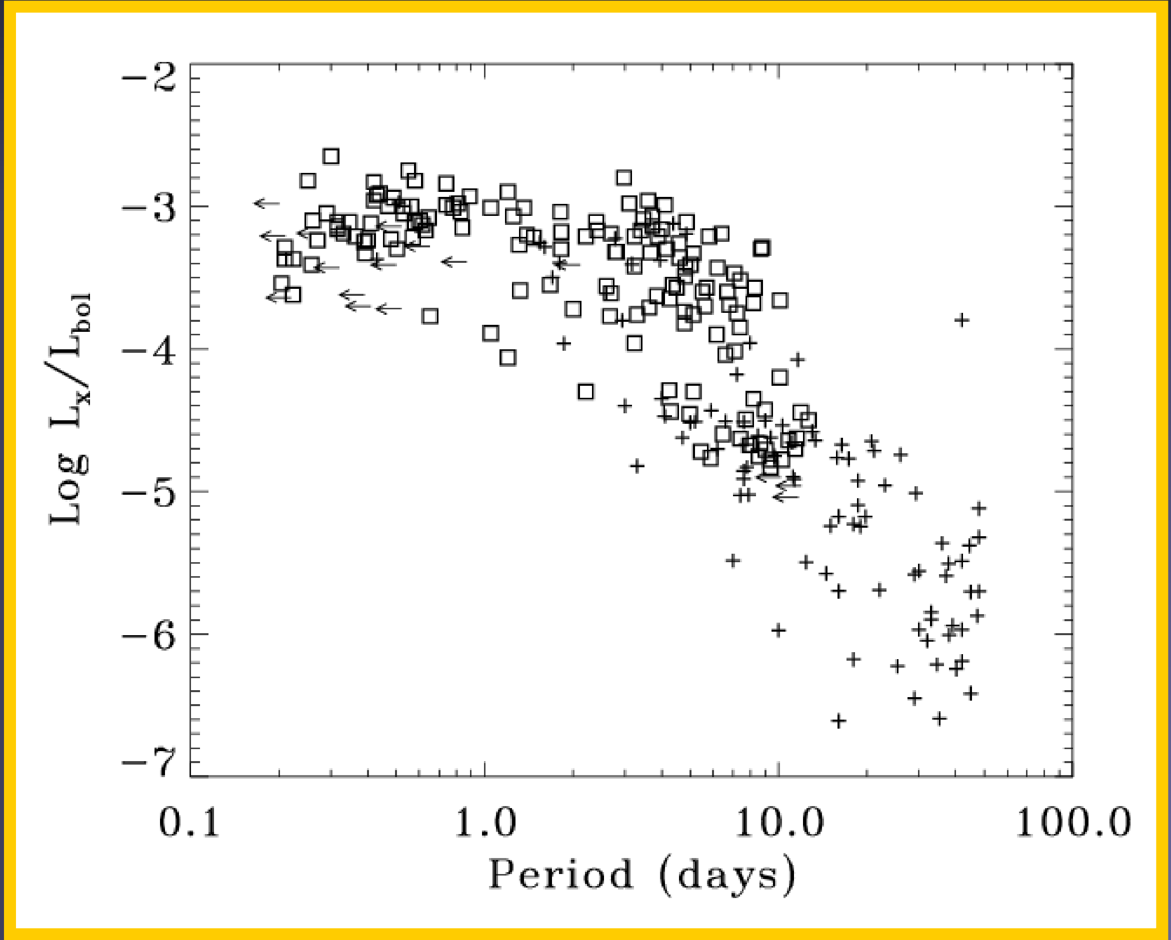

Pizzolato et al. 1993

Activity-rotation relationship

- Typical: scatter is further reduced if instead of rotation period the Rossby number is used.

$$Ro = \frac{v_c}{2H\Omega} \propto \frac{P_{\mathrm{rot}}}{\tau_{\mathrm{c}}}$$

- Rossby number: ratio of rotation time-scale to convective timescale
- It removes (or at least reduces) the stellar mass dependence

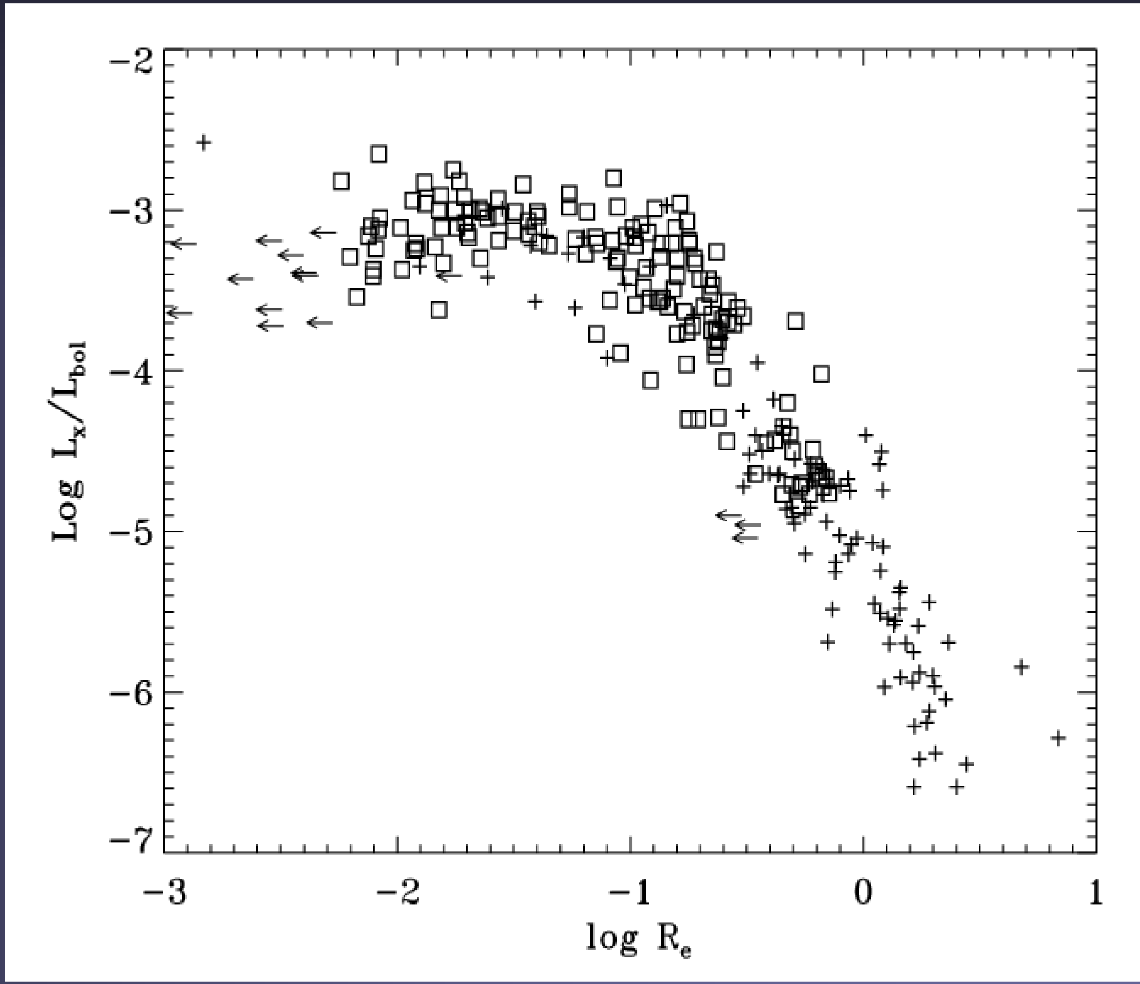

Pizzolato et al. 1993

Activity-rotation relationship

- Level at which L_x saturates depends on mass
- Mass dependence is reduced for L_x/L_{bol}
- Period at which saturation takes place P_{sat} also depends on stellar mass

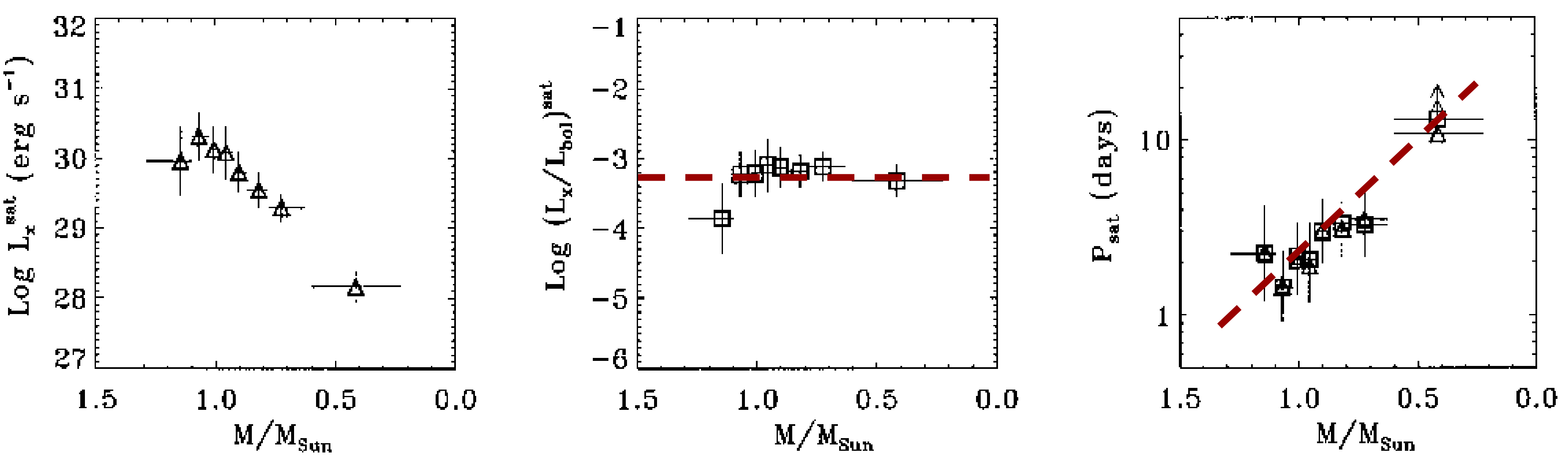

Pizzolato et al. 1993

Does the magnetic field saturate?

It really is the dynamo that saturates, not the heating!

Data for G, K, M stars. Saturation in magnetic flux seen mainly for the most rapidly rotating M stars

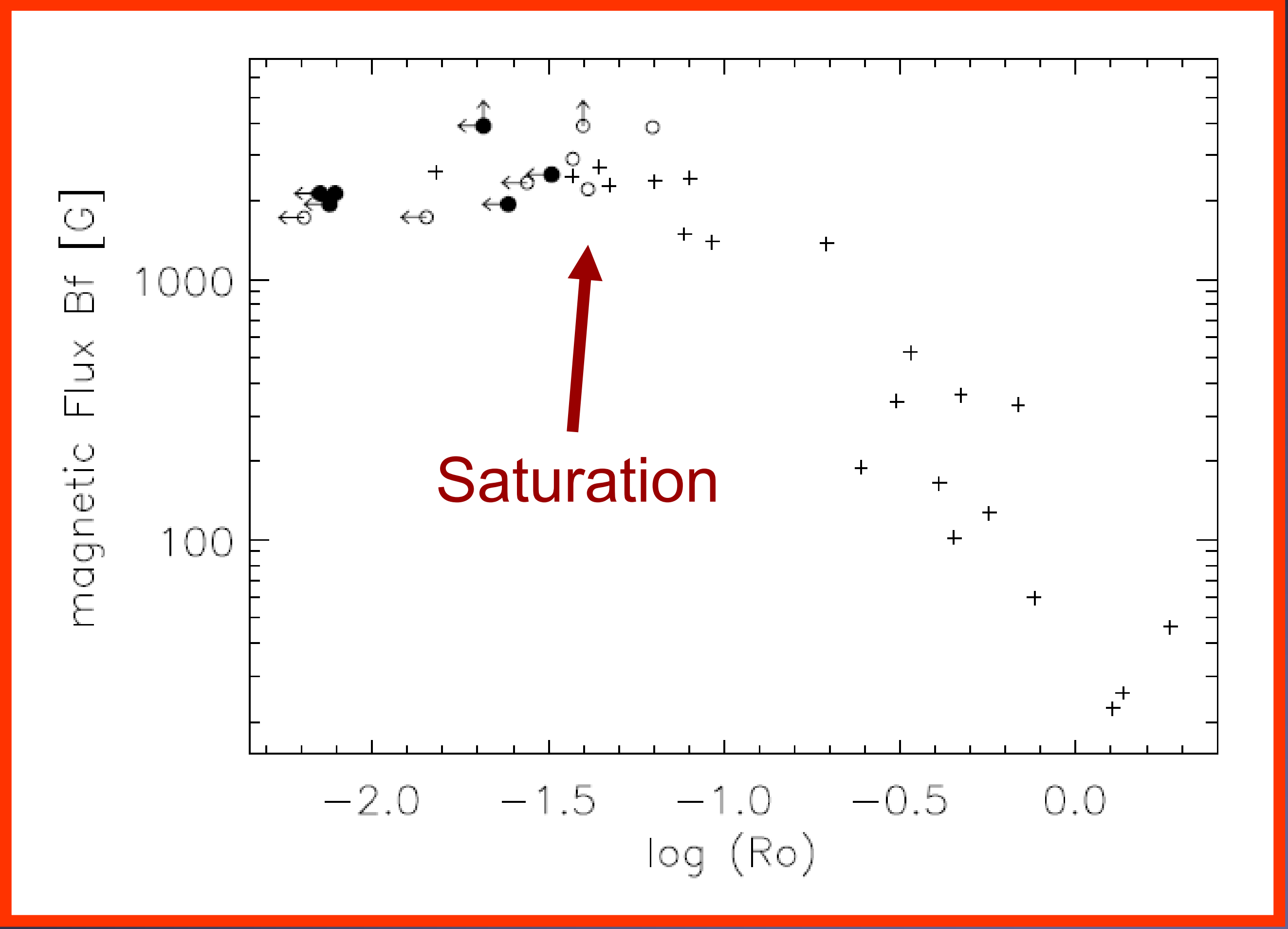

Reiners & Basri 2009

Combined solar-stellar L_x-Φ relationship

Almost linear relationship over 12 orders of magnitude of flux

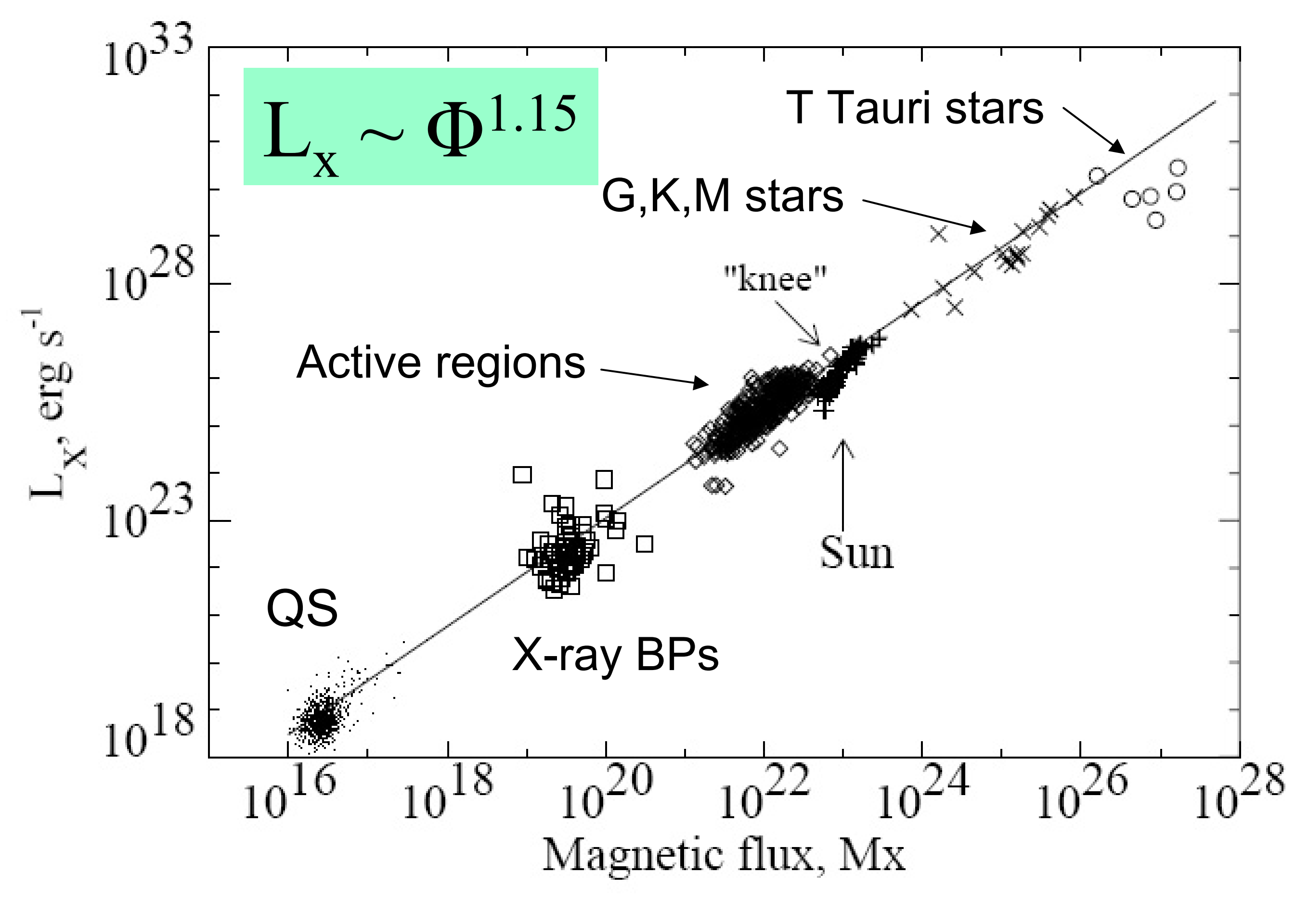

➔ universal (?) volumetric heating rate:

$Q \sim \underline{B}/L$

$\underline{B}$ = average field strength

L = length of field line between footpts

Pevtsov et al. 2003

L_x-Φ relationship: T Tauri stars

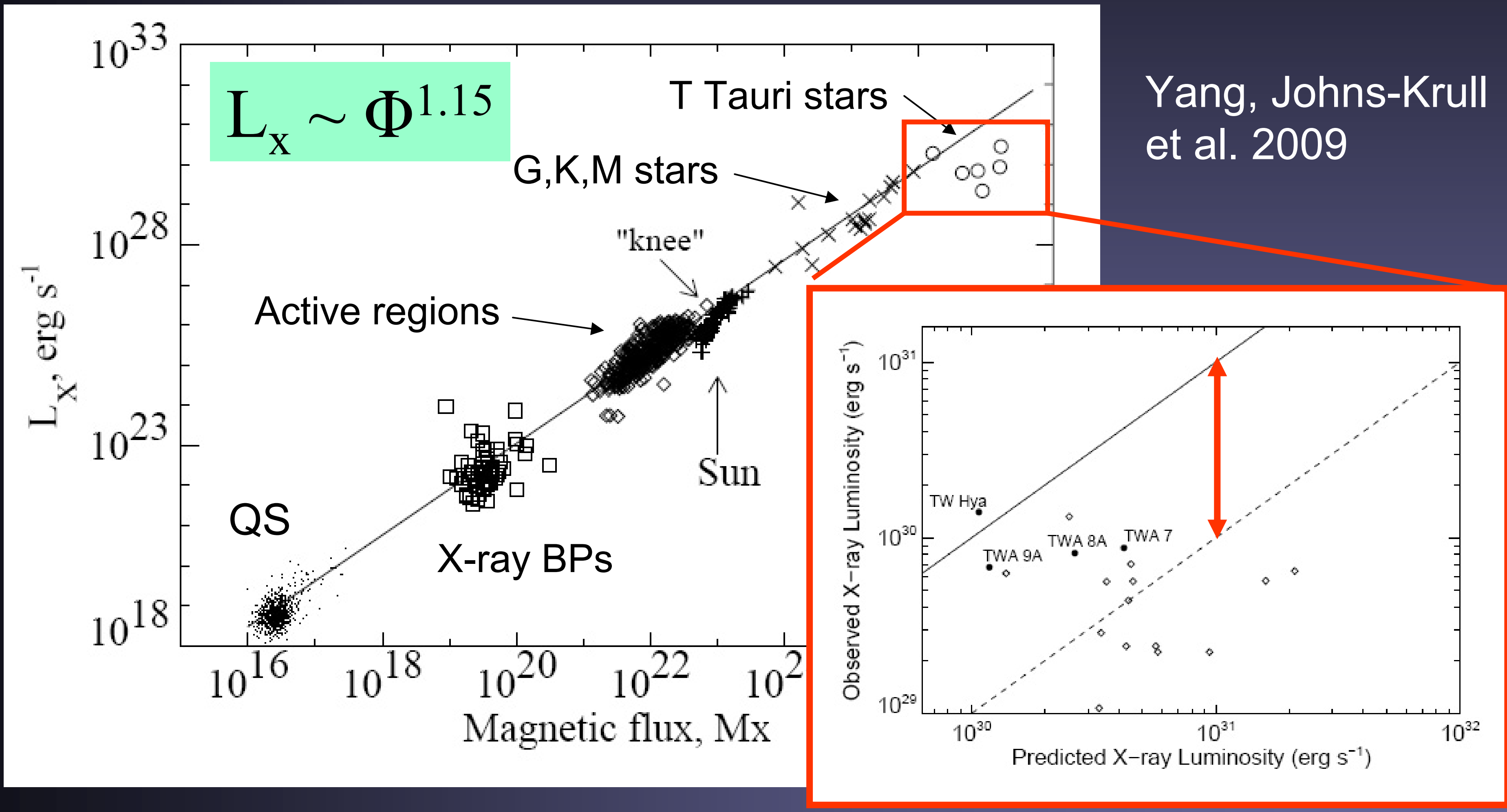

Yang, Johns-Krull et al. 2009

X-ray Coronal Dividing Line

- Giants hotter than the red line show strong X-ray emission and possess hot coronae
- Giants cooler than the red line show very little X-ray emission

Haisch & Linsky; Haisch et al.

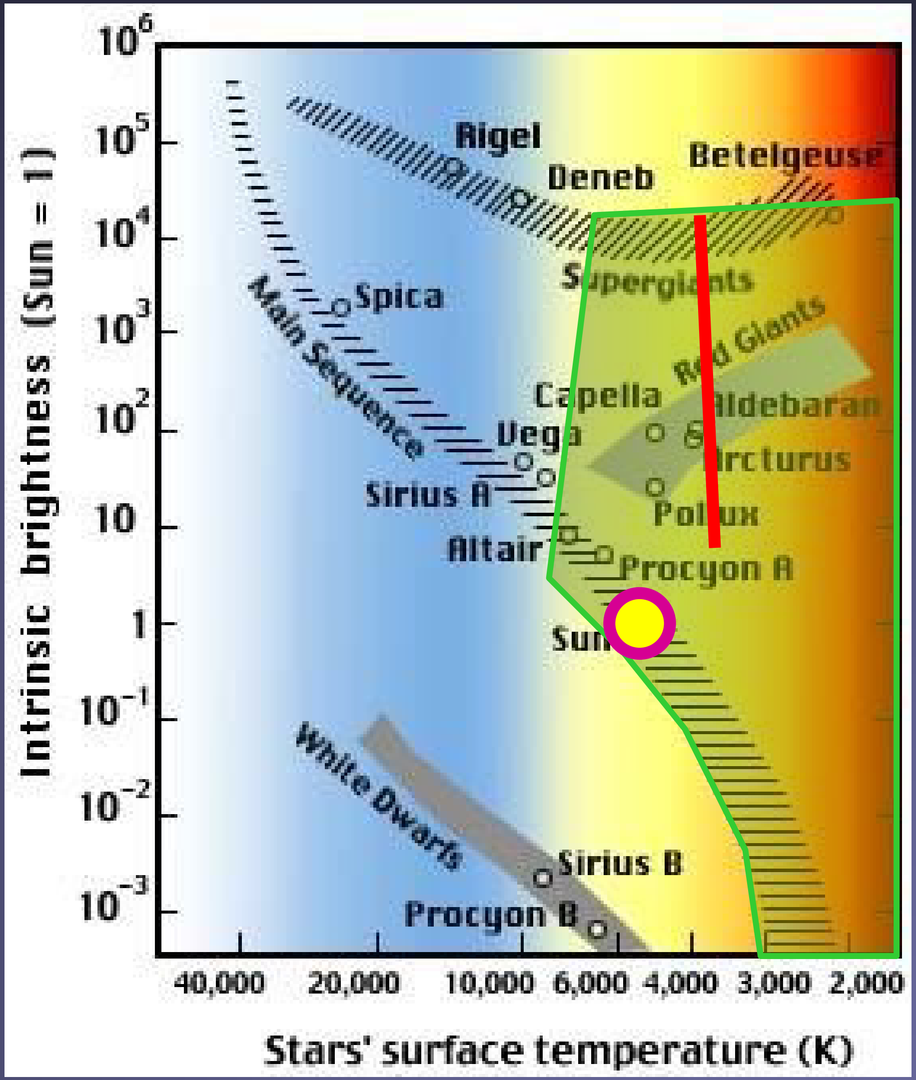

Magnetic topology across the X-ray Coronal Dividing Line

Leftward of the CDL:
- large-scale bipolar regions
- big coronal loops
- mostly closed field
- strong X-ray emission
- weak stellar wind

Rightward of the CDL:
- small-scale mixed polarity
- no large coronal loops
- mostly open field
- weak X-ray emission
- strong stellar wind

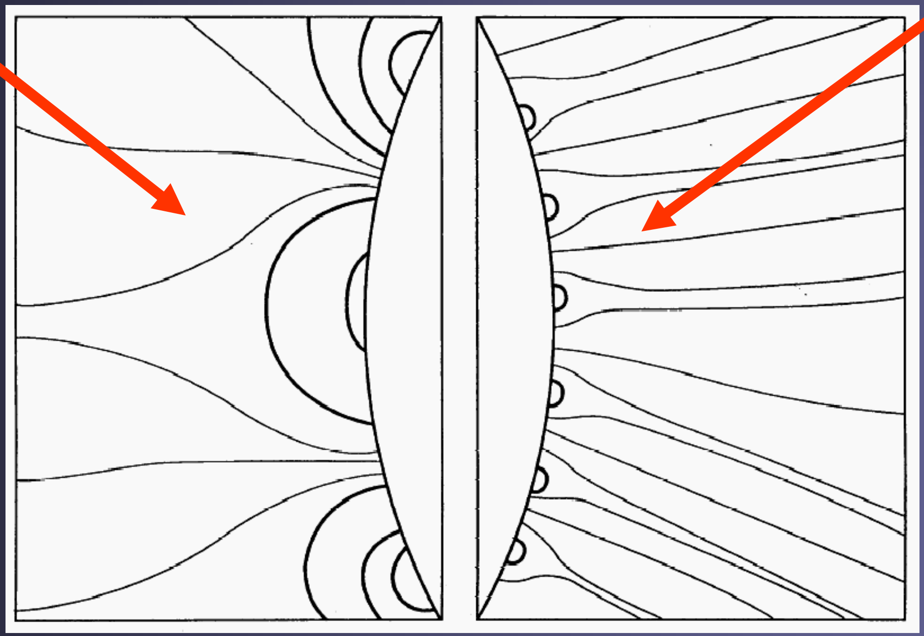

Rosner et al. (1995)

Eruption vs. trapping: buoyancy vs. curvature

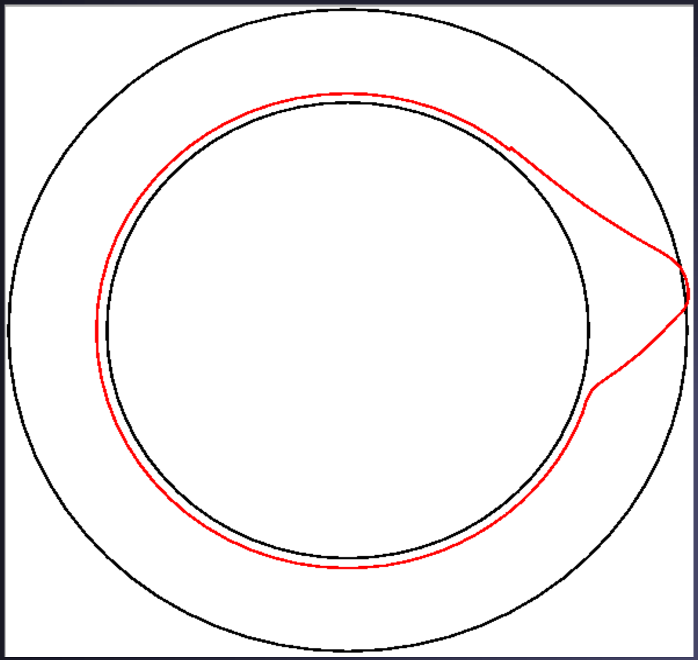

Main-sequence star

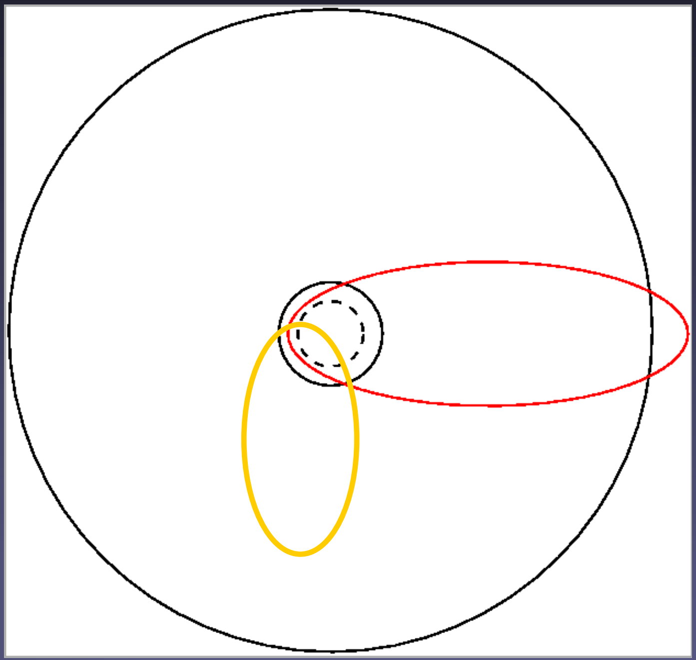

Giant

Sufficiently small initial radius:

➔ curvature force increases more rapidly than buoyancy force

➔ new equilibrium within the convection zone

$\boxed{\text{Trapping for } R_{tube} / R_{star} \lesssim 0.2}$

Magnetic topology across the X-ray Coronal Dividing Line

- **Leftward of the CDL:**
  - → large-scale bipolar regions
  - → big coronal loops
  - → mostly closed field
  - → strong X-ray emission
  - → weak stellar wind

- **Rightward of the CDL:**
  - → small-scale mixed polarity
  - → no large coronal loops
  - → mostly open field
  - → weak X-ray emission
  - → strong stellar wind

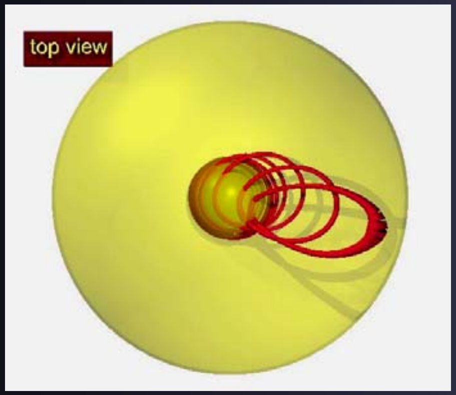

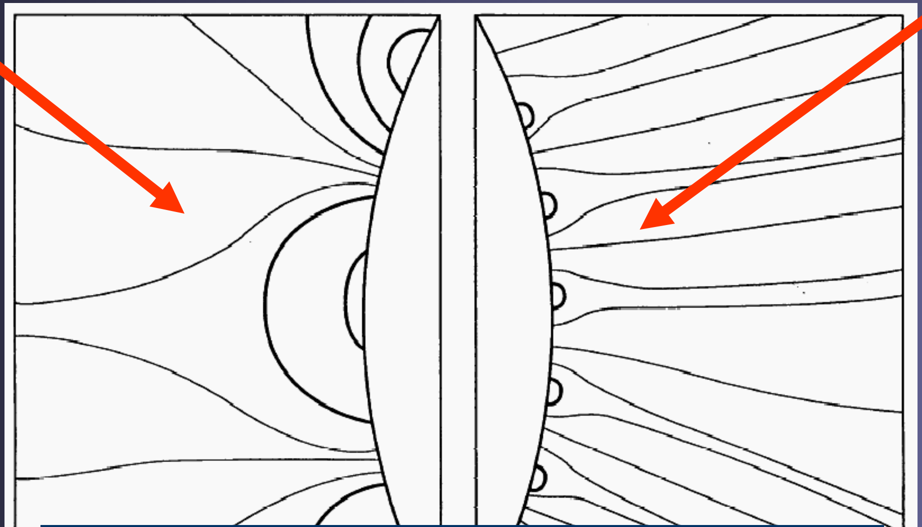

Holzwarth & Schüssler 2002

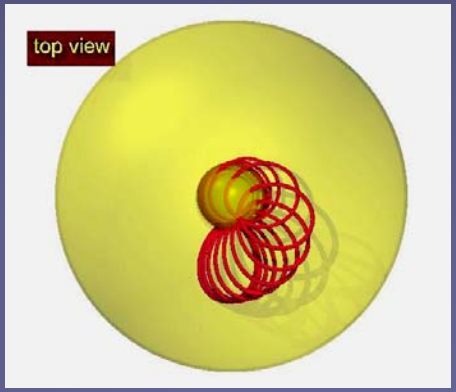

Rosner et al. (1995)

Spindown of cool stars

Spinup due to contraction

- Rotation rate evolves with stellar age on main sequence: $\Omega \sim t^{-1/2}$
- Ca II H+K flux (i.e. chromospheric activity) also decreases with $\Omega \sim t^{-1/2}$

Skumanich 1972

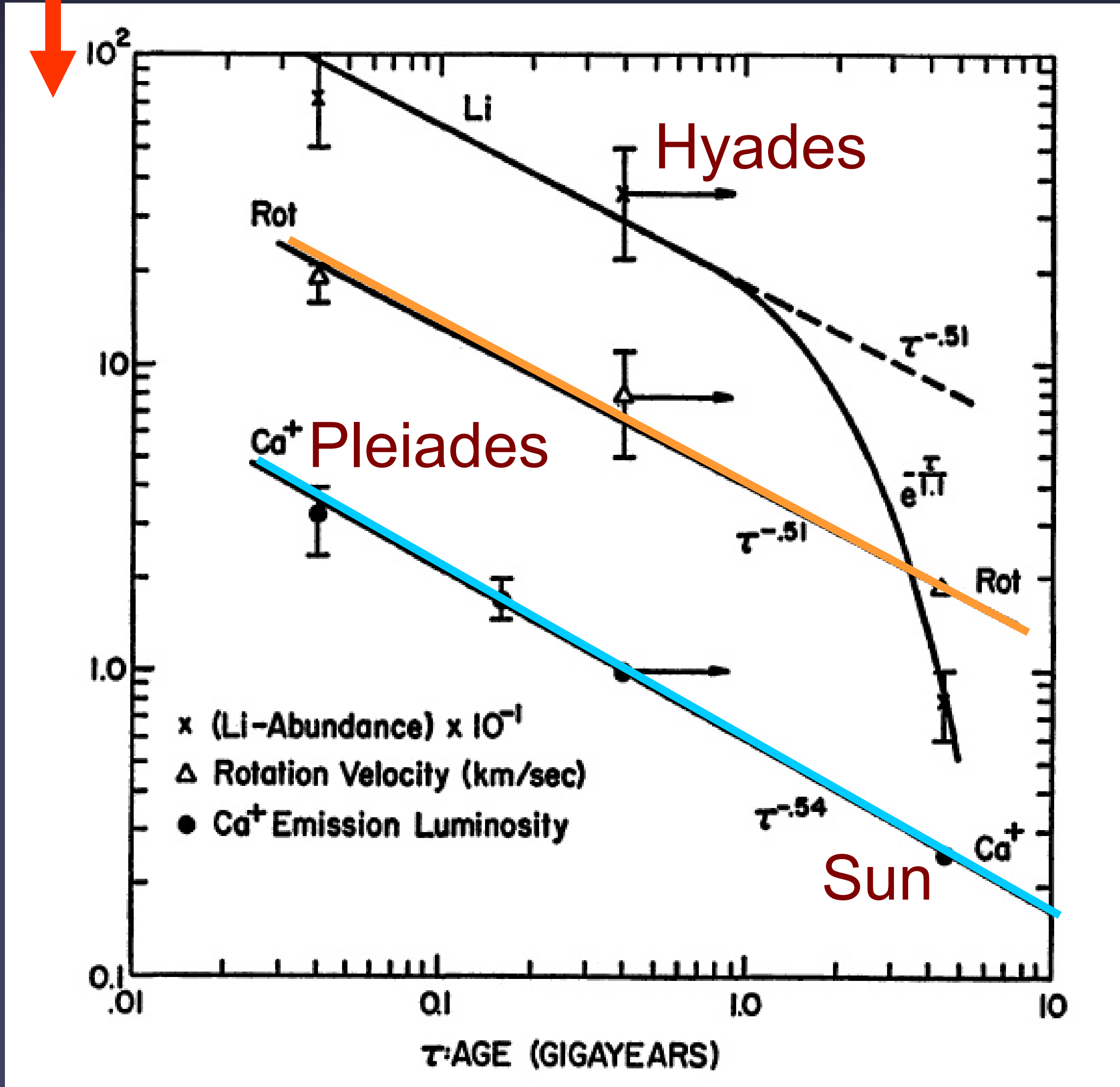

Stellar activity cycles

- Measurements of Ca II H and K flux over nearly 3 decades from Mt Wilson survey (started by Olin Wilson)
- Stars at different activity levels are seen. Some clearly display cycles

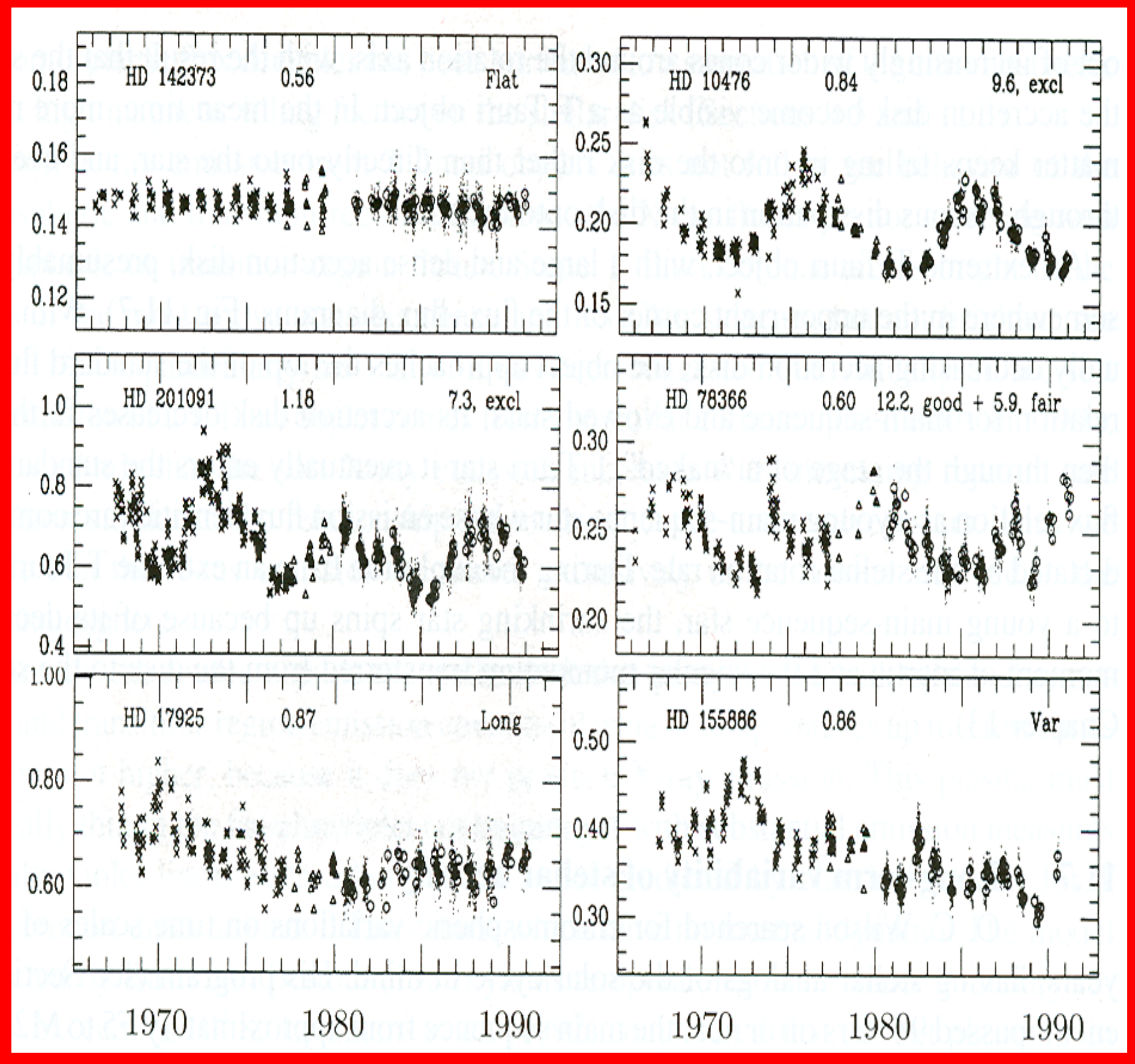

Activity cycles in chromosphere & corona

- Chromospheric activity cycle from Mt Wilson & Lowell Obs. (extension & continuation of Mt Wilson program)
- XMM/Newton shows parallel X-ray cycle

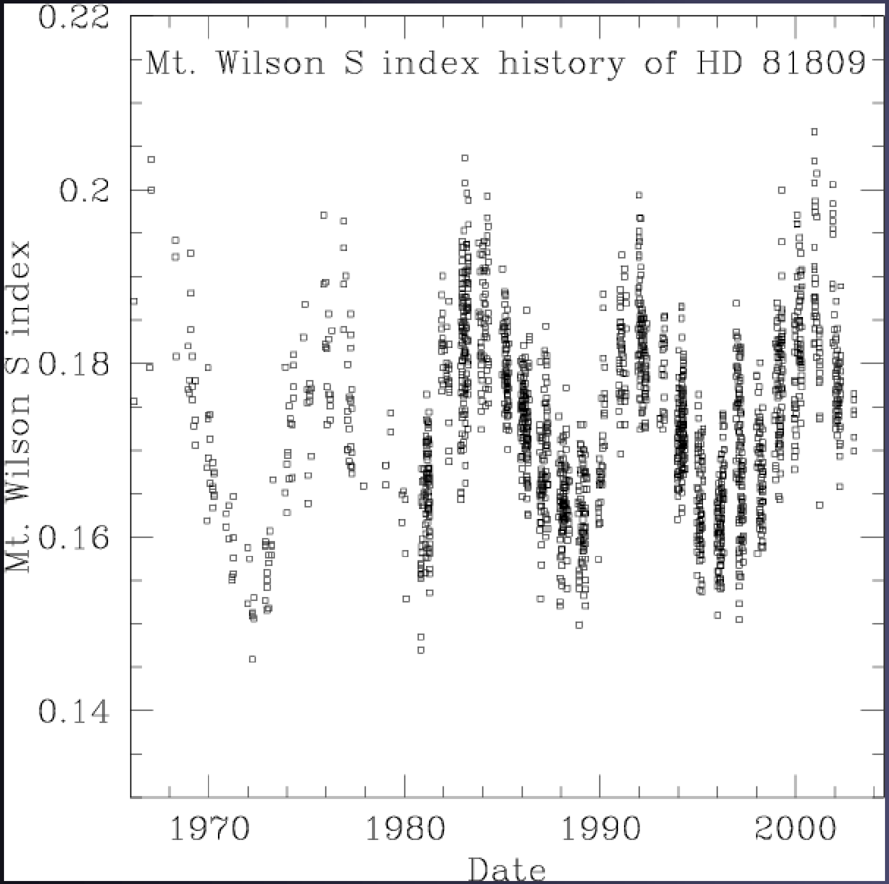

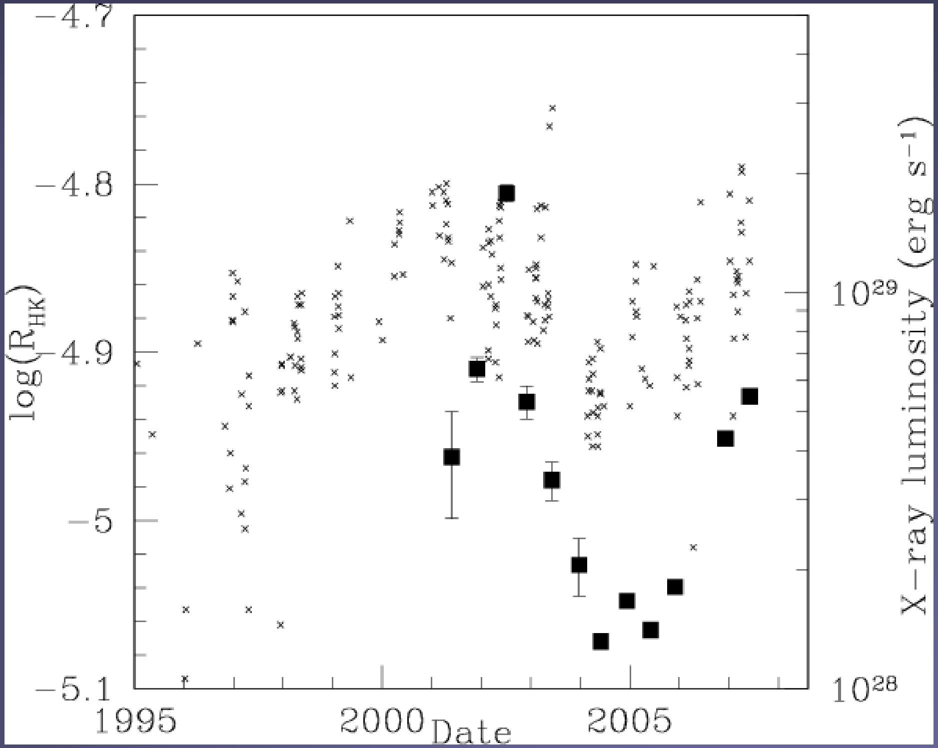

Cycle period vs. rotation period

- Cycle frequency ω_{cyc} scales with rotation rate Ω
- Two branches: inactive stars: I, active stars: A
- Active stars have shorter cycles (for given Ω)
- $\omega_{cyc} \sim \Omega^{1.15}$ for I stars
- $\omega_{cyc} \sim \Omega^{0.8}$ for A stars

Saar (2002)

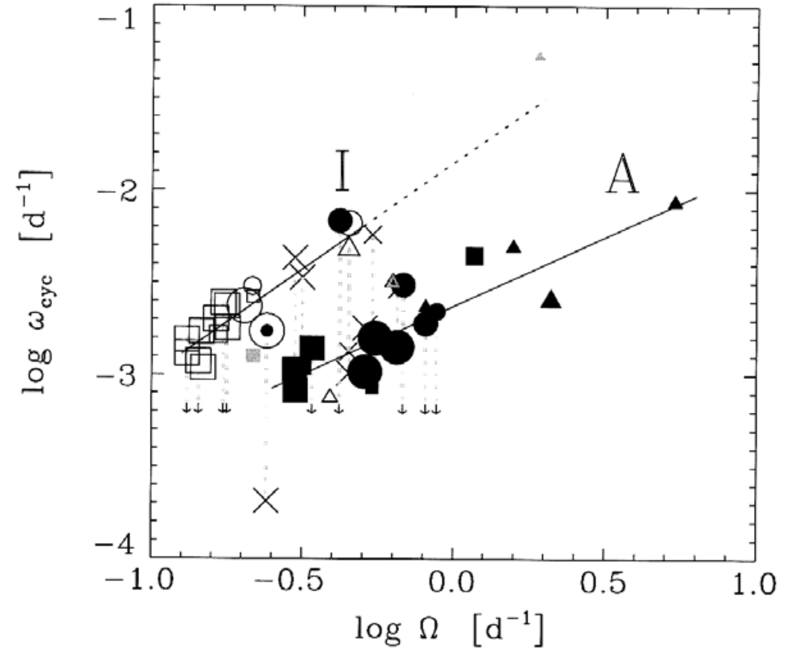

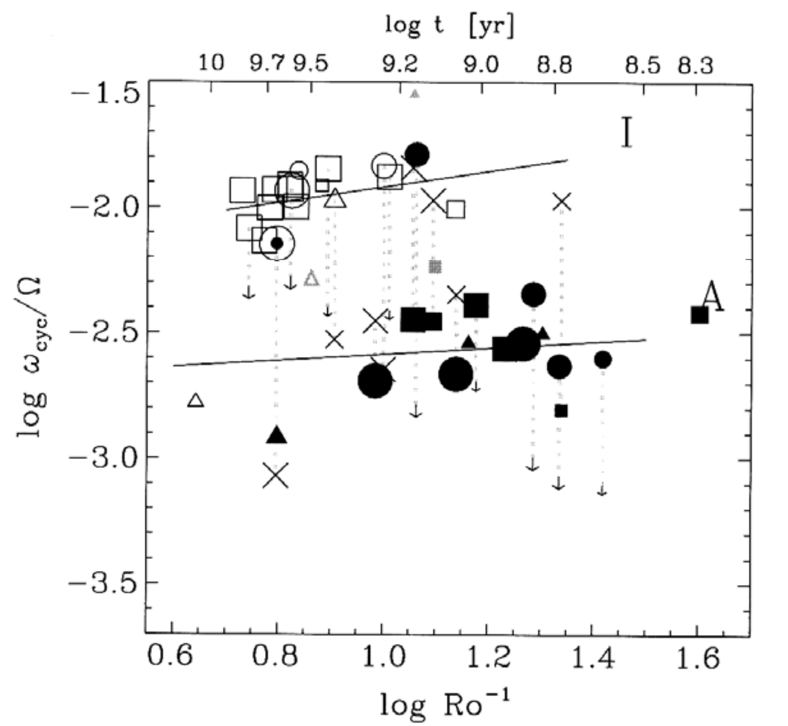

Stars leaving or entering a Grand Minimum?

- Some stars are seen to move into or out of a flat low-activity state → Interpreted as entering or leaving a Grand Minimum
- HD 3651: over 6 years in low activity state: GM candidate
- HD 140538: spent 2-3 years in low activity state: if that is a Grand Min, then Sun is now also in a Grand Min. since 2006

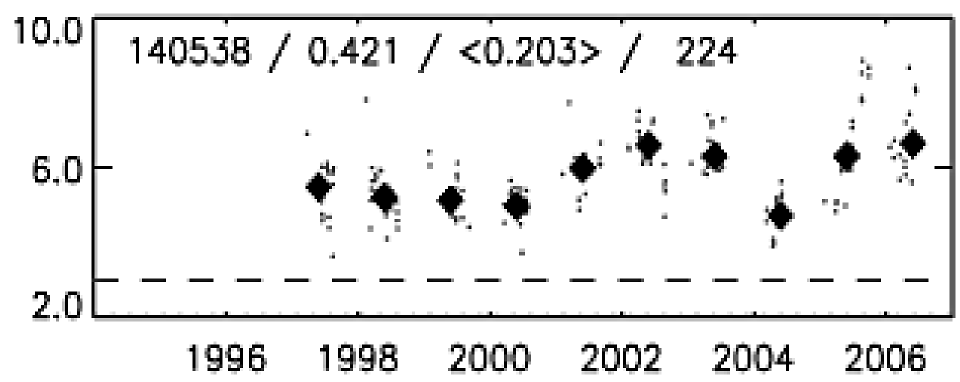

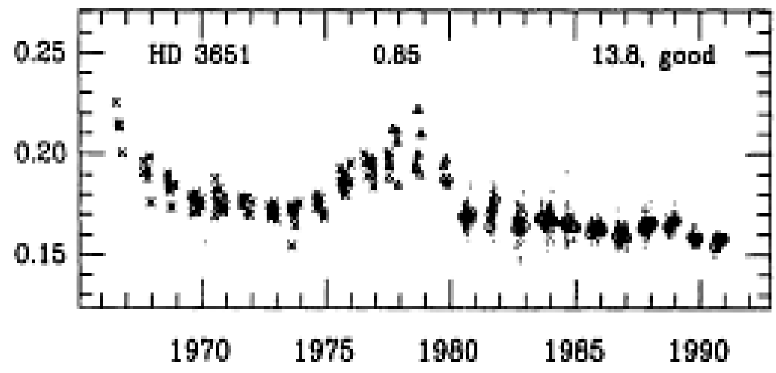

Baliunas et al. 1995, Hall et al. 2007

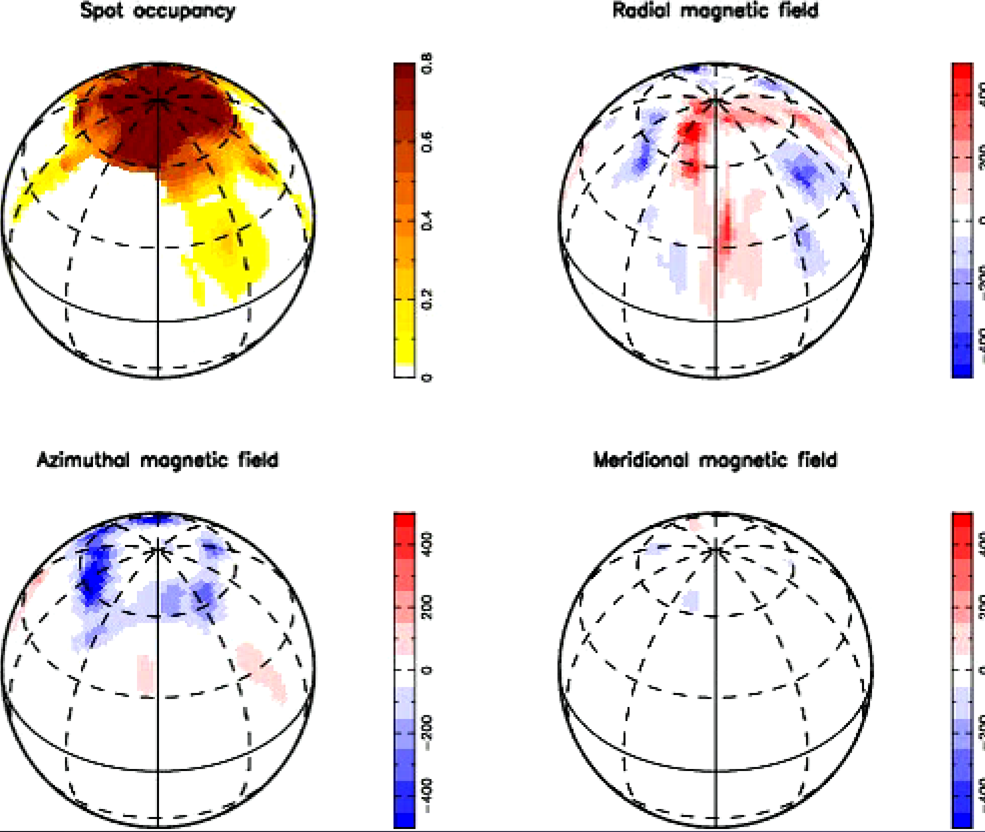

Sunspots - starspots

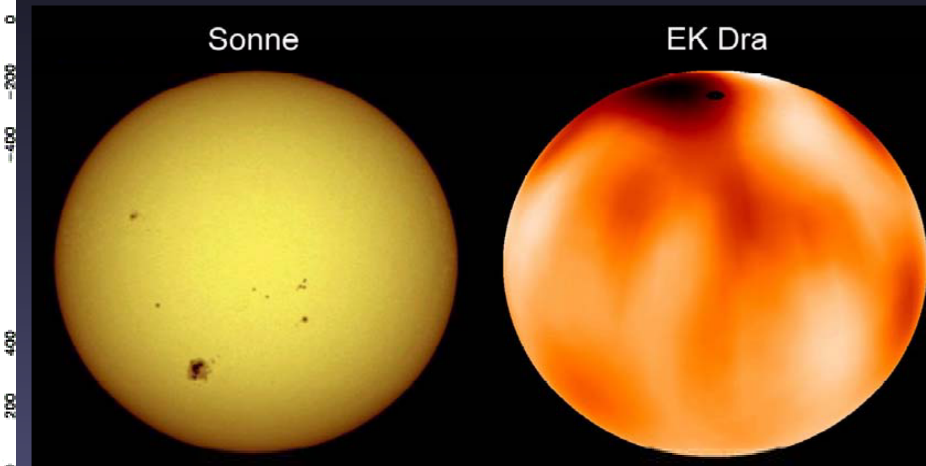

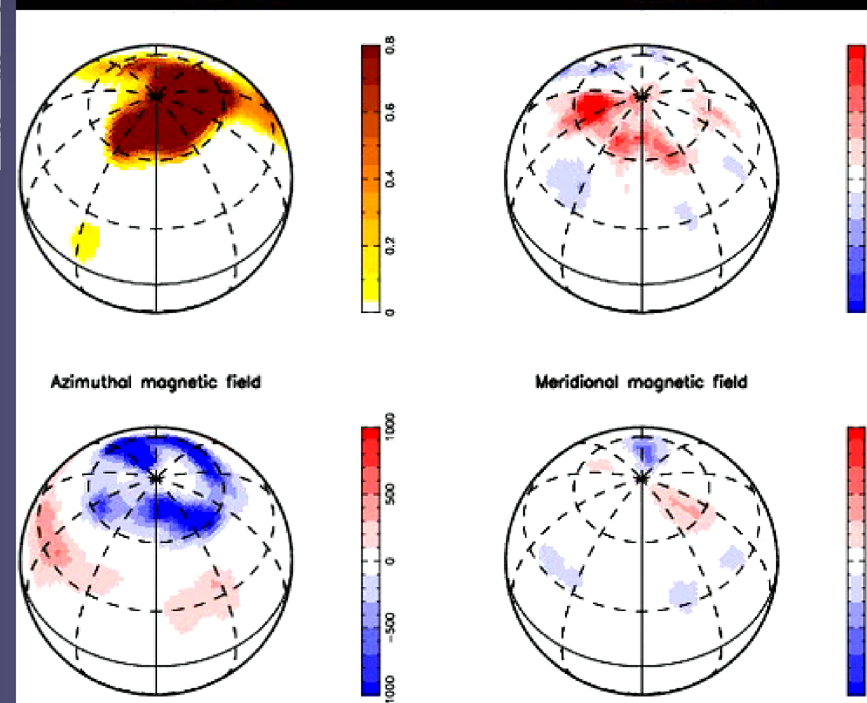

- Active binary stars, slightly evolved
- Display large spot coverage (10% or more of visible hemisphere)

Ratio of faculae to plage in active to inactive stars

- inactive star displays behaviour similar to Sun: at cycle phase with higher activity (chromospheric index) star is brighter
- active star displays opposite behaviour: star is darker during more active phase
- Ratio of faculae (plage) to spots chages with increasing activity

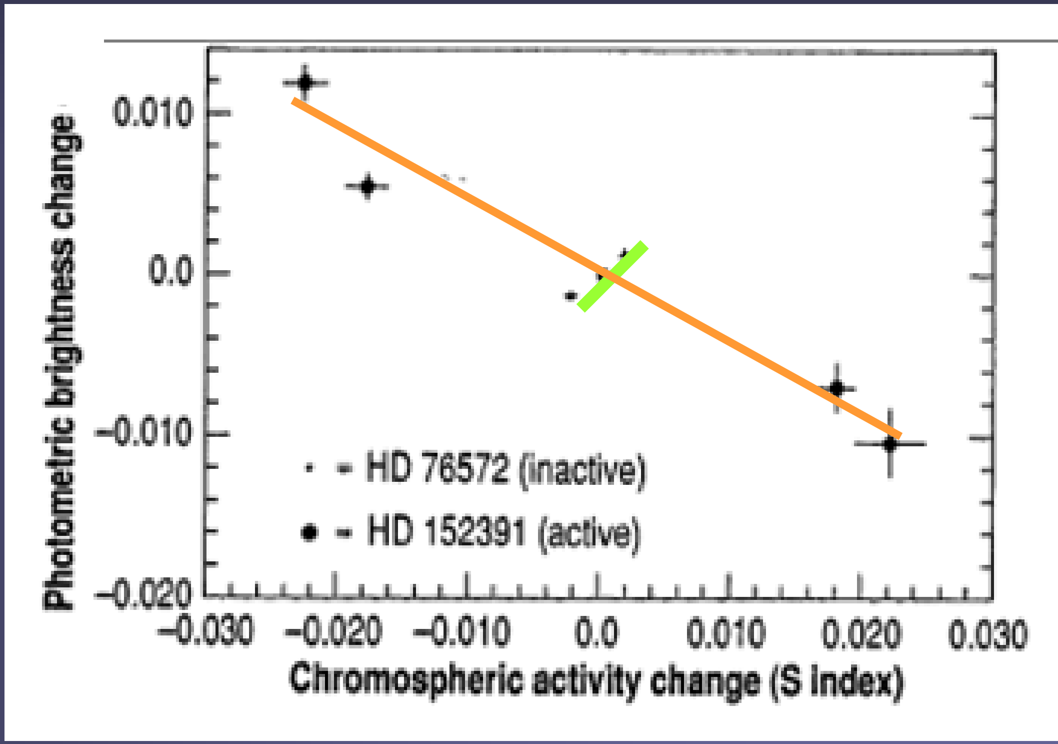

Radick et al. 1989

Extrapolation to active stars

- results of Lockwood et al. (1992); Radick et al. (1998, 2007): more active stars dark at high activity
- Extrapolation from Sun (Knaack et al. in prep.) roughly reproduces ➔Strengthens “solar paradigm” for stellar activity

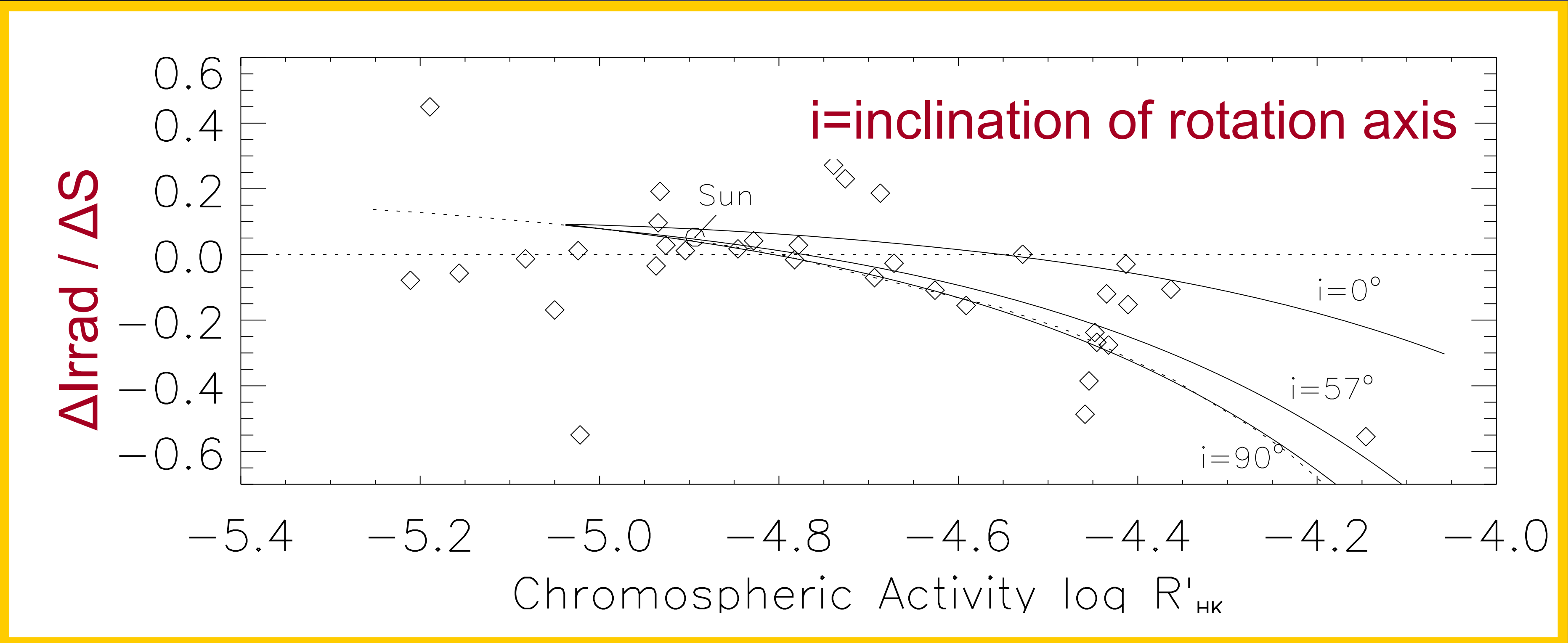

Is the Sun a sun-like star?

- Consider variability vs. activity
- Sun lies slighly (<1σ) above the relation for chromospheric variability
- Sun lies 2σ below the relation for photospheric variability